

A Thesis Submitted for the Degree of PhD at the University of Warwick

Permanent WRAP URL:

<http://wrap.warwick.ac.uk/106816>

Copyright and reuse:

This thesis is made available online and is protected by original copyright.

Please scroll down to view the document itself.

Please refer to the repository record for this item for information to help you to cite it.

Our policy information is available from the repository home page.

For more information, please contact the WRAP Team at: wrap@warwick.ac.uk

PARTS OF THE WORK CONTAINED IN THIS THESIS
WHICH HAVE BEEN PREPARED FOR PUBLICATION

Studies of Dioxamide and Dithio-oxamide Metal Complexes. Part 1. Crystal and Molecular Structures of $\text{SbCl}_3\text{L}_{1.5}$ ($\text{L} = \text{N,N}'$ -diethyldithiooxamide) and Uncomplexed L
M. G. B. Drew, J. M. Kisenyi and G. R. Willey
J. Chem. Soc., Dalton Trans., 1982, 1729

Studies of Dioxamide and Dithiooxamide Metal Complexes. Part 2. Synthesis and Spectral Characterisation of RHNCSNHR ($\text{R} = \text{alkyl, aryl}$) Complexes with SbX_3 ($\text{X} = \text{Cl, Br}$), BiCl_3 , SnX_4 ($\text{X} = \text{Cl, Br}$), and TiCl_4 Crystal and Molecular Structures of $\text{N,N}'$ -diisopropyldithiooxamide (DIPDIO) and $\text{SbCl}_3\text{DIPDIO}_{1.5}$
M. G. B. Drew, J. M. Kisenyi, G. R. Willey and S. O. Wandiga

Studies of Dioxamide and Dithiooxamide Metal Complexes. Part 3. Confirmation of $\text{N,N}'$ -Disubstituted Dithiooxamides as Bidentate (S,S)-Chelating Ligands. Crystal and Molecular Structures of the Six Coordinate Tin(IV) Complex $[\text{SnBr}_4(\text{C}_4\text{H}_9(\text{H})\text{NCSCSN}(\text{H})\text{C}_4\text{H}_9)]$ and the Seven Coordinate Bismuth(III) Complex $[\text{BiCl}_3(\text{C}_2\text{H}_5(\text{H})\text{NCSCSN}(\text{H})\text{C}_2\text{H}_5)_2]$
M. G. B. Drew, J. M. Kisenyi and G. R. Willey

$\text{N,N}'$ -Disubstituted Dithiomalonamide Complexes of Sb(III) . Crystal and Molecular Structure of $[\text{SbCl}_3(\text{C}_2\text{H}_5\text{NHCSCH}_2\text{CSNHC}_2\text{H}_5)]$ with Lone Pair Occupation of a Metal Coordination Site
M. G. B. Drew, J. M. Kisenyi and G. R. Willey

Unexpected Cyclisation of $\text{N,N}'$ -Diethyldithiomalonamide. The Crystal and Molecular Structure of $[\text{EtNHCSCHCSNHET}]_2[\text{SnCl}_6]$
M. G. B. Drew, J. M. Kisenyi and G. R. Willey

Toluene-3,4-dithiol Complexes of Group (VB) Halides. Observations of Lone Pair Stereochemical Activity and Redox Behaviour
J. M. Kisenyi, G. R. Willey, M. G. B. Drew and S. O. Wandiga

ABSTRACT

The coordination and structural chemistry of complexes of Groups (IVA), (IVB) and (VB) halides with neutral (S)-donor ligands has been investigated.

The N,N'-disubstituted dithiooxamides $\text{RHN}(\text{C}(\text{S})\text{C}(\text{S})\text{NHR})$ ($\text{R} = \text{CH}_3, -\text{C}_2\text{H}_5, i\text{-C}_3\text{H}_7, n\text{-C}_4\text{H}_9, -\text{C}_6\text{H}_{11}, -\text{CH}_2\text{-C}_6\text{H}_5$) and dithiomalonamides $\text{RHNC}(\text{S})\text{CH}_2\text{C}(\text{S})\text{NHR}$ ($\text{R} = -\text{CH}_3, -\text{C}_2\text{H}_5, n\text{-C}_3\text{H}_7, n\text{-C}_4\text{H}_9$) act as (S,S)-donors towards MX_3 ($\text{M} = \text{Sb, Bi, X} = \text{Cl, Br}$) and MX_4 ($\text{M} = \text{Ti, Sn, X} = \text{Cl, Br}$) to form adducts with the following stoichiometries: with $\text{L} =$ dithiooxamide ligand, we have $\text{SbCl}_3 \cdot \text{L}_{1.5}$, $\text{SbBr}_3 \cdot \text{L}_{1.5}$, $\text{BiCl}_3 \cdot \text{L}_2$, $\text{SnCl}_4 \cdot \text{L}$, $\text{SnBr}_4 \cdot \text{L}$, and $\text{TiCl}_4 \cdot \text{L}$, while with $\text{L}' =$ dithiomalonamide ligand, we have $\text{SbCl}_3 \cdot \text{L}'$ and $\text{SnCl}_4 \cdot \text{L}'$. Uncomplexed dithiooxamide ligands are (S,S)-*trans* as shown by the crystal structures of two examples: $\text{EtNHC}(\text{S})\text{C}(\text{S})\text{NHET}$ and $\text{Pr}^i\text{NHC}(\text{S})\text{C}(\text{S})\text{NHPr}^i$.

The crystal structures of the complexes $\text{SbCl}_3(\text{EtNHC}(\text{S})\text{C}(\text{S})\text{NHET})_{1.5}$ and $\text{SbCl}_3(\text{Pr}^i\text{NHC}(\text{S})\text{C}(\text{S})\text{NHPr}^i)_{1.5}$ show the ligands in an (S,S)-bridging bonding mode while the crystal structures of $\text{BiCl}_3(\text{EtNHC}(\text{S})\text{C}(\text{S})\text{NHET})_2$, $\text{SnBr}_4(\text{But}^n\text{NHC}(\text{S})\text{C}(\text{S})\text{NHBut}^n)$, and $\text{SbCl}_3(\text{EtNHC}(\text{S})\text{CH}_2\text{C}(\text{S})\text{NHET})$ show the (S,S)-chelate bonding mode. No evidence was found for the stereochemical involvement of the lone pair of electrons associated with M(III) in the structures of $\text{SbCl}_3(\text{EtNHC}(\text{S})\text{C}(\text{S})\text{NHET})_{1.5}$, $\text{SbCl}_3(\text{Pr}^i\text{NHC}(\text{S})\text{C}(\text{S})\text{NHPr}^i)_{1.5}$ and $\text{BiCl}_3(\text{EtNHC}(\text{S})\text{C}(\text{S})\text{NHET})_2$. However, evidence for stereochemical activity of the lone pair was observed in $\text{SbCl}_3(\text{EtNHC}(\text{S})\text{CH}_2\text{C}(\text{S})\text{NHET})$ as shown in its crystal structure. Recrystallisation of $\text{SnCl}_4(\text{EtNHC}(\text{S})\text{CH}_2\text{C}(\text{S})\text{NHET})$ from benzene gave an unexpected 'cyclisation' product $[\text{EtNHC}(\text{S})\text{CHC}(\text{S})\text{NHET}][\text{SnCl}_6]$. A plausible reaction scheme is presented.

The N,N'-disubstituted oxamide $\text{RHNC}(\text{O})\text{C}(\text{O})\text{NHR}$ ($\text{R} = -\text{CH}_3, -\text{C}_2\text{H}_5, n\text{-C}_3\text{H}_7, n\text{-C}_4\text{H}_9, t\text{-C}_4\text{H}_9, -\text{C}_6\text{H}_{11}$) and malonamides $\text{RHNC}(\text{O})\text{CH}_2\text{C}(\text{O})\text{NHR}$ ($\text{R} = -\text{CH}_3, -\text{C}_2\text{H}_5, n\text{-C}_3\text{H}_7, n\text{-C}_4\text{H}_9, t\text{-C}_4\text{H}_9, -\text{C}_6\text{H}_{11}$) act as (O,O)-donors towards SbCl_3 and SnCl_4 .

Toluene-3,4-dithiol (td) reacts with MCl_3 ($\text{M} = \text{As, Sb, Bi}$) with the expulsion of HCl to give 1:1 $\text{M}(\text{td})\text{Cl}$ complexes. The crystal structure of $\text{As}(\text{td})\text{Cl}$ shows three coordinate metal centres with the ligand acting as an (S,S)-chelate and a stereochemically active lone pair taking up one of the tetrahedral positions on the As. Toluene-3,4-dithiol also reacts with SbCl_3 and BiCl_3 to give $\text{Sb}(\text{td})_2$ and $\text{Bi}(\text{td})_2^-$ respectively. In the bismuth complex we have complete loss of all -SH protons on td to give the ionic species $\text{Bi}(\text{td})_2^-$ while in the antimony complex one of the -S-H protons is retained as evidenced by i.r. and ^1H n.m.r. data. Attempts to abstract this proton with base resulted in the oxidation of $\text{Sb}(\text{III})$ to form a 1:3 $\text{Sb}:\text{td}$ ionic complex featuring $\text{Sb}(\text{V})$. The crystal structure of this complex has been determined and it shows $\text{Sb}(\text{td})_3$ as a *trans* chelate with a distorted octahedral environment around the antimony.

Reactions of *d*- and *l*-penicillamine and dimercaptosuccinic acid (DMSA) with SbCl_3 , NaAsO_2 and a 'naked' Sb^{3+} solvate have been briefly studied in an effort to prepare (S)- and (O)-donor complexes with possible chemotherapeutic potential. Octahedral structures involving (S,N,O)-donors in the case of penicillamine, and (S,O)-donors in the case of DMSA are proposed.

ACKNOWLEDGEMENTS

I would like to express my thanks to Dr. G. R. Willey for his supervision, constant help, and encouragement during the course of this work.

I would like to especially thank Dr. M. G. B. Drew of the University of Reading for his invaluable aid and support of this work and for supervising me during a 10-week visit to Reading University when I was introduced to the technique of X-ray crystallography. I would also like to thank Mr. A. Jahans for his encouragement during my visit to Reading University and for teaching me some of the practical aspects of crystallography.

My heart felt thanks go to Dr. S. R. Wade for his friendship, continued help and encouragement all through the course of this work.

I thank the technical staff of the University of Warwick for their assistance, in particular, the glassblowing workshop under Mr E. Burgess for their readily available services, Miss J. Clarke and Mr. H. Beaton for experimental assistance and all the workshops.

I thank Mr. D. Gordon, Mr. M. Pennington, Mr P. Matejtschuk, Mr. M. Wood and Miss P. Slaich for help with proof reading this manuscript.

A studentship award from the European Economic Community is gratefully acknowledged.

MAY GOD BLESS YOU ALL

★★

CONTENTS

	Page
<i>Abstract</i>	
 <i>Chapter 1 Introduction</i>	
1.1 A Summary of the Bonding Theories in Coordination Complexes	4
1.2 Group (VB) Coordination Chemistry	27
1.3 Group (IVA) and (IVB) Coordination Chemistry	39
1.4 Crystal Structure Analysis	45
 <i>Chapter 2 Dithiooxamides</i>	
2.1 Introduction	59
2.2 The Crystal Structures of N,N'-Diethyl- and N,N'-Diisopropyl Dithiooxamide	66
2.3 Reactions of Dithiooxamides with Group (VB) Halides	75
2.4 The Crystal Structure of SbCl ₃ .DEDTO _{1.5}	85
2.5 The Crystal Structure of SbCl ₃ .DIPDTO _{1.5}	98
2.6 Reactions of Dithiooxamides with Group (IV) Halides	101
2.7 The Crystal Structure of BiCl ₃ .DEDTO ₂	107
2.8 The Crystal Structure of SnBr ₄ .DBDTO	116
2.9 Reactions of Dithiooxamides with Mo(CO) Species	123

		Page
2.10	Experimental	125
<i>Chapter 3</i>	<i>Dithiomalonamides</i>	
3.1	Introduction	130
3.2	Synthesis and Characterisation of Dithiomalonamides	135
3.3	Reactions of Dithiomalonamides with SbCl ₃	137
3.4	The Crystal Structure of SbCl ₃ .DEDTM	140
3.5	Complexes of SnCl ₄ with DEDTM, DPDTM, DBDTM	147
3.6	Crystal and Molecular Structure of [EtNHC(\overline{S})CHC(\overline{S})NHEt] ₂ [SnCl ₆]	150
3.7	Experimental	161
<i>Chapter 4</i>	<i>Oxamides, Malonamides, Succinamides and their Complexes with SbCl₃ and SnCl₄</i>	
4.1	Introduction	164
4.2	Complexes of SbCl ₃ and SnCl ₄ with N,N'-Disubstituted Oxamides and Malonamides	168
4.3	Experimental	175
<i>Chapter 5</i>	<i>Reactions of Group (VB) Halides with Toluene-3,4-dithiol</i>	
5.1	Introduction	177
5.2	Reactions of Toluene-3,4-dithiol with Post Transition Metals	180

	Page
5.3	1:1 Complexes of MCl_3 ($M = As, Sb, Bi$) with Toluene-3,4-dithiol
5.4	The Crystal Structure of $As(td)Cl$
5.5	1:2 Complexes of Sb and Bi with Toluene-3,4-dithiol
5.6	1:3 Complexes of $Sb(V)$ with Toluene- 3,4-dithiol
5.7	The Crystal Structure of $[Ph_4P][Sb(td)_3]$
5.8	Experimental
Chapter 6	<i>Complexes of Penicillamine and Dimercaptosuccinic Acid with Group (VB) Elements</i>
6.1	Introduction
6.2	Reactions Involving Penicillamine
6.3	Reactions Involving Dimercaptosuccinic Acid
6.4	Reactions Involving the 'Naked' Cationic Species Sb^{3+} Solvate
6.5	Experimental
	<i>Appendix</i>
	<i>References</i>

LIST OF TABLES

	Page
<i>Chapter 2</i>	
2.2.1 Crystal Data and Refinement Details for DEDTO and DIPDTO	71
2.2.2 Atomic Coordinates for DEDTO and DIPDTO	72
2.2.3 Bond lengths and Angles for DEDTO and DIPDTO	73
2.2.4 Torsion Angles for DEDTO	74
2.3.1 Principal i.r. Bands for Group (VB) Metal Complexes	77
2.3.2 ^1H n.m.r. Data for Group (VB) Metal Complexes	81
2.4.1 Crystal Data and Refinement Details for $\text{SbCl}_3\cdot\text{DEDTO}_{1.5}$ and $\text{SbCl}_3\cdot\text{DIPDTO}_{1.5}$	92
2.4.2 Atomic Parameters for $\text{SbCl}_3\cdot\text{DEDTO}_{1.5}$ and $\text{SbCl}_3\cdot\text{DIPDTO}_{1.5}$	93
2.4.3 Bond Lengths and Angles for $\text{SbCl}_3\cdot\text{DEDTO}_{1.5}$ and $\text{SbCl}_3\cdot\text{DIPDTO}_{1.5}$	94
2.4.4 Torsion Angles for $\text{SbCl}_3\cdot\text{DEDTO}_{1.5}$	97
2.6.1 Principal i.r. bands for Group (VB) Metal Complexes	102
2.6.2 ^1H n.m.r. data for Group (IVB) Metal Complexes	103
2.7.1 Crystal Data and Refinement Details for $\text{BiCl}_3\cdot\text{DEDTO}_2$ and $\text{SnBr}_4\cdot\text{DBDTO}$	109

		Page
2.7.2	Atomic positions for $\text{BiCl}_3 \cdot \text{DEDTO}_2$	110
2.7.3	Bond Lengths and Angles for $\text{BiCl}_3 \cdot \text{DEDTO}_2$	111
2.8.1	Atomic Positions for $\text{SnBr}_4 \cdot \text{DBDTO}$	119
2.8.2	Bond Lengths and Angles for $\text{SnBr}_4 \cdot \text{DBDTO}$	120

Chapter 3

3.3.1	Analytical data of SbCl_3 Dithio-malonamide Complexes	138
3.3.2	Principal i.r. Bands for Dithio-malonamides and their SbCl_3 Complexes	138
3.3.3	^1H n.m.r. Data for Dithiomalonamides and some SbCl_3 Complexes	138
3.4.1	Crystal Data for $\text{SbCl}_3 \cdot \text{DEDTM}$	142
3.4.2	Atomic Positions for $\text{SbCl}_3 \cdot \text{DEDTM}$	143
3.4.3	Bond Lengths and Angles for $\text{SbCl}_3 \cdot \text{DEDTM}$	144
3.5.1	Principal i.r. bands of some SnCl_4 Dithiomalonamide Complexes	147
3.6.1	Crystal Data and Refinement Details for $[\text{EtNHC}(\overline{\text{S}})\text{CHC}(\overline{\text{S}})\text{NHET}]_2[\text{SnCl}_6]$	152
3.6.2	Atomic Coordinates for $[\text{EtNHC}(\overline{\text{S}})\text{CHC}(\overline{\text{S}})\text{NHET}]_2[\text{SnCl}_6]$	153
3.6.3	Bond Lengths and Angles for $[\text{EtNHC}(\overline{\text{S}})\text{CHC}(\overline{\text{S}})\text{NHET}]_2[\text{SnCl}_6]$	154

Chapter 4

4.2.1	Analytical Data for Selected SbCl_3 Oxamide and Malonamide Complexes	169
4.2.2	Principal i.r. bands for SbCl_3 Oxamide and Malonamide Complexes	169

		Page
4.2.3	^1H n.m.r. Data for SbCl_3 Oxamide and Malonamide Complexes	170

Chapter 5

5.4.1	Crystal Data and Refinement Details for $\text{As}(\text{td})\text{Cl}$	188
5.4.2	Atomic Positions for $\text{As}(\text{td})\text{Cl}$	189
5.4.3	Bond Lengths and Angles for $\text{As}(\text{td})\text{Cl}$	190
5.4.4	Thermal Parameters and Calculated Hydrogen Atom Positions in $\text{As}(\text{td})\text{Cl}$	191
5.7.1	Crystal data and Refinement Details for $[\text{Ph}_4\text{P}][\text{Sb}(\text{td})_3]$	201
5.7.2	Atomic Coordinates for $[\text{Ph}_4\text{P}][\text{Sb}(\text{td})_3]$	202
5.7.3	Bond Lengths and Angles in $[\text{Ph}_4\text{P}][\text{Sb}(\text{td})_3]$	203

Chapter 6

6.5.1	Effect of pH on ^1H n.m.r. Spectrum of <i>d</i> -penicillamine	216
6.5.2	^1H n.m.r. Spectra of a Penicillamine Solution treated with Successive Quantities of NaAsO_2	216

LIST OF FIGURES

	Page
<i>Chapter 2</i>	
2.2.1 Molecular Geometry of DEDTO	70
2.2.2 Molecular Geometry of DIPDTO	70
2.4.1 Crystal Structure of $\text{SbCl}_3 \cdot \text{DEDTO}_{1.5}$	91
2.4.2 $\text{SbCl}_3 (\text{S}_2\text{C}_5\text{H}_{10})$	87
2.5.1 Crystal Structure of $\text{SbCl}_3 \cdot \text{DIPDTO}_{1.5}$	99
2.5.2 (a) The Two-Dimensional Polymer in $\text{SbCl}_3 \cdot \text{DEDTO}_{1.5}$	100
(b) The Three-Dimensional Polymer in $\text{SbCl}_3 \cdot \text{DIPDTO}_{1.5}$	100
2.7.1 Crystal Structure of $\text{BiCl}_3 \text{DEDTO}_2$	108
2.7.2 Structures $\text{BiCl}_3 \text{DEDTO}_2$ Showing (a) Hydrogen Bonding, and (b) Equatorial Plane Respectively	108
2.8.1 Crystal Structure of $\text{SnBr}_4 \cdot \text{DBDTO}$	118
<i>Chapter 3</i>	
3.4.1 Crystal Structure of $\text{SbCl}_3 \cdot \text{DEDTM}$	141
3.6.1 Crystal Structure of $[\text{EtNHC}(\overline{\text{S}})\text{CHC}(\overline{\text{S}}) - \text{NHET}]^+$	151
3.6.2 Molecular Arrangement in $[\text{EtNHC}(\overline{\text{S}})\text{CHC}(\overline{\text{S}}) - \text{NHET}]_2 [\text{SnCl}_6]$	151

	Page
Chapter 4	
4.2.1	Crystal Structure of <i>cis</i> -SnCl ₄ (DMSO) ₂ 173
Chapter 5	
5.4.1	Crystal Structure of As(td)Cl 187
5.4.2	Molecular Arrangement in As(td)Cl 187
5.7.1	Crystal Structure of the [Sb(td) ₃] ⁻ Ion 200
Appendix	
A.1	The Vacuum Line 233
A.2	Solvent Still 233
A.3	A 'Pig' 233
A.4	Washing at the Vacuum Line 234
A.5	Conductivity Cell 234

ABBREVIATIONS

DMDTO	N,N'-dimethyldithiooxamide
DEDTO	N,N'-diethyldithiooxamide
DIPDTO	N,N'-diisopropyldithiooxamide
DBDTO	N,N'-di-n-butyl dithiooxamide
DCXDTO	N,N'-dicyclohexyldithiooxamide
DBZDTO	N,N'-Dibenzyl dithiooxamide
DMDTM	N,N'-dimethyldithiomalonamide
DEDTM	N,N'-diethyldithiomalonamide
DPDTM	N,N'-di-n-propyldithiomalonamide
DBDTM	N,N'-di-n-butyl dithiomalonamide
DCXDTM	N,N'-dicyclohexyldithiomalonamide
DMO	N,N'-dimethyloxamide
DEO	N,N'-diethyloxamide
DPO	N,N'-di-n-propyloxamide
DBO	N,N'-di-n-butyl oxamide
DTBO	N,N'-ditertiarybutyloxamide
DCXO	N,N'-dicyclohexyloxamide
DMM	N,N'-dimethylmalonamide
DEM	N,N'-diethylmalonamide
DPM	N,N'-di-n-propylmalonamide
DBM	N,N'-di-n-butylmalonamide
DTBM	N,N'-ditertiarybutylmalonamide
DCXM	N,N'-dicyclohexylmalonamide
DES	N,N'-diethylsuccinamide
tu	thiourea
py	pyridine
mn	maleonitrile

td	toluene-3,4-dithiol
pen	penicillamine
DMSA	<i>meso</i> -2,3-dimercaptosuccinic acid
THF	tetrahydrofuran
DMF	N,N-dimethylformamide
DMSO	dimethylsulphoxide
diars	O-phenylenebisdimethylarsine
tbp	trigonal bipyramid

Abbreviations used in the description of
i.r. spectra

s	strong
w	weak
vs	very strong
br	broad
sh	shoulder
m	medium

Abbreviations used in the description of
n.m.r. spectra

s	singlet
d	doublet
t	triplet
q	quartet
m	multiplet

On some of the diagrams

me denotes a -CH₃ group

On X-ray crystal structure diagrams

(a) bond lengths are given in (Å)

(b) bond angles are in (°)

CHAPTER 1
INTRODUCTION

CHAPTER 1
INTRODUCTION

This work is mainly concerned with the general Lewis acid behaviour of the M(III) series As, Sb, and Bi (principally the halides) and their reactions with various donor systems. This coordination behaviour of Group (VB) elements is silhouetted against that of Group (IVA) and Group (IVB) by making direct comparisons with the analogous systems of Ti(IV) and Sn(IV) respectively. For simplicity the chlorides and in some cases the bromides of Ti(IV) and Sn(IV) are considered as representative members of their respective groups.

One important facet of antimony chemistry concerns the use of antimony(III) complexes in the control of Bilharzia (Schistosomiasis). Interest in Bilharzia arises from a collaboration with Professor S. O. Wandiga of the University of Nairobi. Bilharzia remains a major disease in developing countries with a wet warm climate. The precise number of infected persons throughout the world is difficult to monitor but the figure could be as high as 300 million.

Bilharzia is caused by a blood fluke worm that lives in the abdominal veins where it causes damage to the liver, spleen, walls of the intestinal tract and the circulatory system. It is extremely difficult to combat especially in those areas of the world where sanitation levels and conditions are somewhat primitive.

Symptoms may include a prickly skin rash, diarrhoea, abdominal pains, dizziness, headaches and loss of appetite. In critical stages the central nervous system becomes involved producing neurological symptoms.

Schistosoma means split body and refers to the deep ventral groove in the body of the parasite with which the male enfolds the female during copulation and throughout the long periods of oviposition. In the egg laying process, the paired worms which are usually located in the pelvic and abdominal veins proceed down to the terminal venules where the female lays her eggs without leaving the gyneacophoral canal of the male. These eggs lodge in the liver, spleen or they pass through wall tissue and penetrate into the bladder and intestines. Those that are entrapped locally pass into faeces and urine to ultimately reach the exterior of the body. Once outside, the eggs are ready to hatch when they reach fresh water.

Once hatched, the larvae attack a suitable mollusc by burrowing through its soft underbelly, if unsuccessful in this endeavour, they die within 24 hours. Inside this snail, further changes occur which result in a second larvae-type cercaria. When mature, the cercaria emerge from the host snail and are ready to penetrate into a human host either through the skin (which may take about 10 minutes) or by ingestion (drinking water). Again, those that are unsuccessful die within 48 hours. Once in the human host, passage through the tissues takes about 24 hours to reach a venule from which it is carried

by venous circulation to the heart where they can circulate to all parts of the body. Those which survive to reach the arteries of abdominal viscera and are able to reach the mesenteric veins commence their real development and will ultimately reach maturity.

Antimony compounds have dominated the scene in the treatment of schistosomiasis and Leishmaniasis for over fifty years despite their toxic side effects and the fact that the drug is unpleasant and has to be administered over quite lengthy periods (4-6 weeks). There is now evidence that modification of the functional groups which bind Sb(III) will go a long way towards reducing or better still eliminating the toxic side effects of antimonials. In general, the toxicity of drugs containing antimony bound to sulphur is much less than that of drugs in which the antimony is bound to oxygen. To augment that, it has been reported¹ that addition of penicillamine (3,3-dimethyl-cysteine) to tartar emetic (potassium bis tartrato-diantimonate(III)) produces a dramatic decrease in toxicity with no loss in effectiveness. Alternative antimonial compounds which possess the same therapeutic efficiency but with much reduced toxicity levels must be found.

Our contribution here is three-fold:

- (a) To prepare further antimony compounds with Sb-A bonds (A = O, N, S) especially those with Sb-S bonds that may be potential schistosomides.
- (b) To carry out a full spectroscopic (i.r., ¹H n.m.r.) and X-ray structural characterisation of these new compounds.

- (c) To investigate the coordination and reactivity properties of M(III) systems especially the stereochemical activity or otherwise of the lone pair of electrons associated with each metal ion.

Such is the diversity of the systems investigated that a detailed review of each is inappropriate here. Rather each chapter will have a short introduction of its own giving the relevant background. In this first chapter we include a broad discussion of the underlying principles on which coordination chemistry is built.

1.1 A SUMMARY OF THE BONDING THEORIES IN
COORDINATION COMPLEXES

The three main bonding theories are: the valence bond (V.B.) approximation, the crystal-field theory (C.F.T.), and the molecular orbital (M.O.) theory.

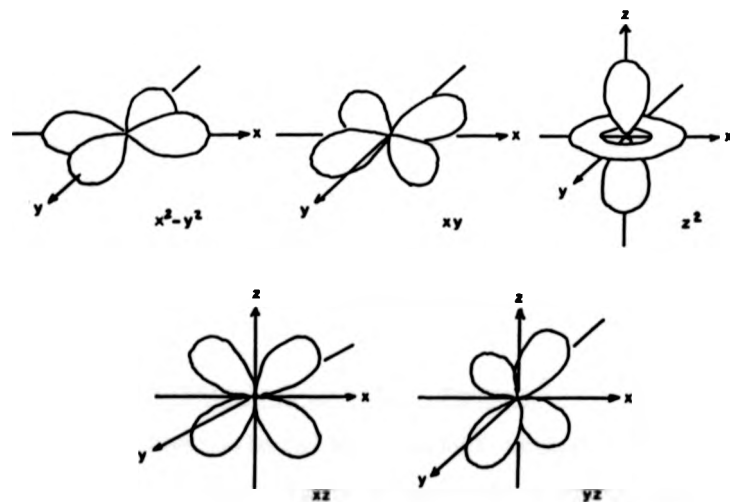
(a) Valence Bond Theory²

According to V.B. a Lewis acid (in most cases metal or metal ion) reacts with a Lewis base (ligand) forming a coordinate covalent (or dative) bond between the ligand and the metal. The bond formed is treated as a pairing of electron spins and the maximum overlapping of atomic orbitals containing these electrons to give a region of common electron density to the two atoms involved. In coordination compounds the orbitals should be of suitable energy and symmetry. The strongest

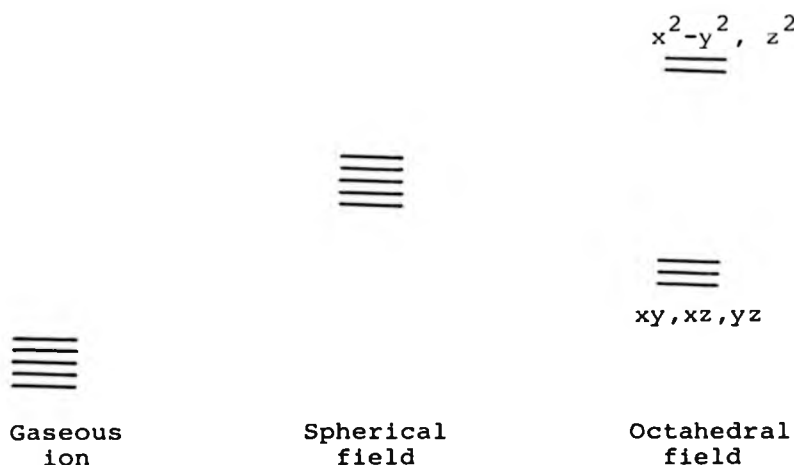
bonds are formed when maximum interaction of electron density is effected. Bond formation may involve more than one orbital from each atom (hybridisation). The hybrid orbitals are formed by the mixing of atomic orbitals and they have characteristic directions in space depending on the metal coordination number (C.N.). For C.N. = 2 the stereochemistry is linear, for C.N. = 3, trigonal planar; C.N. = 4 could be either square planar or tetrahedral C.N. = 5 is trigonal bipyramidal and C.N. = 6 is octahedral.

(b) Crystal Field Theory³

Crystal field theory assumes that interaction between the ligand and the metal is purely electrostatic (ionic). The five d-orbitals in an isolated gaseous metal ion are degenerate and an appreciation of their spatial arrangement is necessary viz.:



For the formation of an ML_6 complex, if all the six ligands approach the metal along the axes, x , y , z , the d orbitals directed towards the ligands will be raised in energy as a result of the negative electrons of the orbitals and the negative field generated by the ligands. The energy of the orbitals not directed towards the ligands will also increase but not as much as the others, hence the degeneracy will be split.

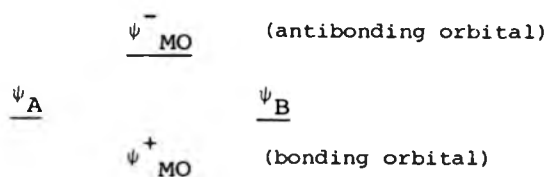


Splitting for fields of other symmetries can be similarly derived. s - and p -orbitals are also affected by approaching ligands but these effects are much less important in C.F.T. terms.

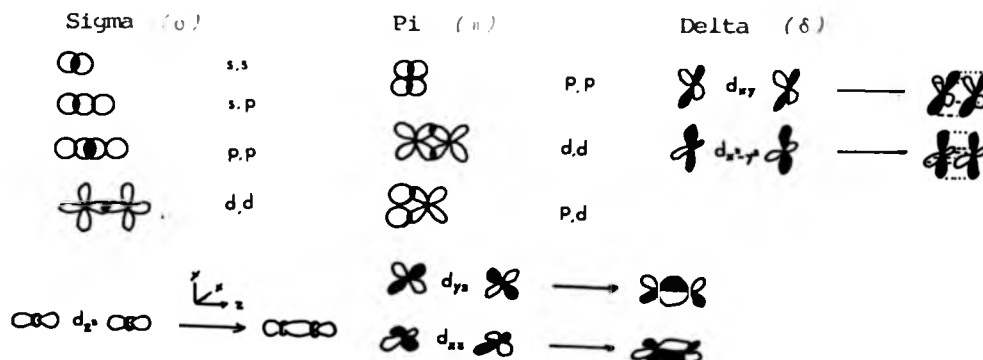
(c) Molecular Orbital Theory⁴

The molecular orbital theory takes into consideration all the electrons of the combined atoms and considers them to be jointly held together by the

molecule in a set of polynuclear molecular orbitals. Approximations concerning the form of the wave function for molecular orbitals are made by using linear combinations of atomic orbitals. A combination of two atomic orbitals results in the formation of two molecular orbitals, their difference in energy is related to the effective overlap between the two atomic orbitals.



The common types of atomic orbital overlap are diagrammatically presented below.



The σ valence orbitals of the ligand will vary from ligand to ligand but they are normally composed of s and p orbitals hence they will be lower in energy than the metal valence orbitals.

The Valence Shell Electron Pair Repulsion Model (VSEPR)

This theory is sometimes called the Sidgwick-Powell—Gillespie-Nyholm Theory in honour of those who initiated the work⁵. It aims at predicting molecular structure and suggesting explanations for the observed structures. The predictions are not valid for transition metal systems with d-orbitals. The model is presented as a set of rules. It should be kept in mind that in different molecules, different energy factors will be responsible in varying degrees for the structure of the resulting molecule, hence the rules must be treated with necessary caution.

Rule 1

Pairs of electrons in a valence shell adopt that arrangement which maximises their distance apart, i.e. electron pairs behave as if they repel one another.

Two important considerations to note:

- (a) Electron pairs occupy some definite volume in space and once they do, they repel all other electrons from it.
- (b) Pairs in the same valence shell have to adopt arrangements that maximise their distances apart.

Rule 2

A non-bonding pair of electrons takes up more room on the surface of an atom than a bonding pair.

Rule 3

The size of a bonding electron pair decreases with increasing electronegativity of the ligand.

Rule 4

The two electron pairs of a double bond or the three electron pairs of a triple bond take up more room than does the one electron pair of a single bond.

Rule 1 can be used to provide the idealised orientations of electron pairs about an atom. The electron pairs are assumed to have equal stereochemical significance.

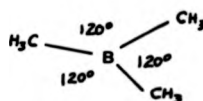
Table 1 Idealised orientations of electron pairs about an atom

Number of Electron Pairs	Idealised Structure of Electron pairs
2	linear
3	trigonal plane
4	tetrahedron
5	trigonal bipyramid
6	octahedron
7	pentagonal bipyramid
	* capped octahedron
	* capped trigonal prism

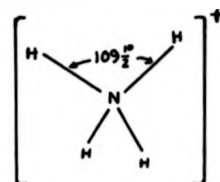
If all electrons from the central atom form equivalent bonding pairs, then the observed geometries are in excellent agreement with the idealised structure. The following examples serve as an illustration:



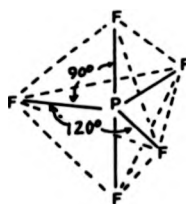
Linear
two sp σ -bonds



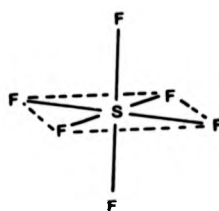
Trigonal planar
three sp^2 σ -bonds



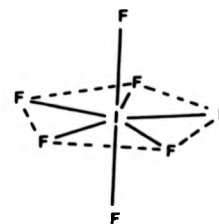
Tetrahedral
four sp^3 σ -bonds



Trigonal
bipyramidal
five sp^3d
 σ -bonds



Octahedral
six sp^3d^2
 σ -bonds



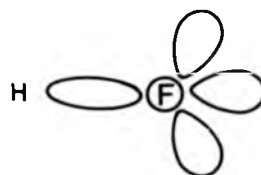
Pentagonal
bipyramid
seven sp^3d^3
 σ -bonds

For molecules with a lone pair, the lone pair is under the attraction of only one nucleus while bonding pairs experience attraction from two nuclei; the lone pair also represents the charge of two electrons near the core of the atom while the bonding pair represents one electron hence the order of repulsion between electron pairs is:

lone pair - lone pair \gg lone pair - bond pair $>$ bond pair - bond pair.

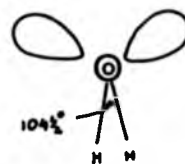
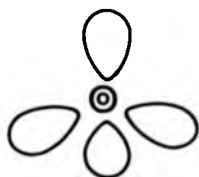
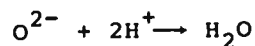
For Four Electron Pairs

Consider a central atom with four equivalent electron pairs tetrahedrally arranged around the atom as predicted by Rule 1. If a proton interacts with one of them, that pair will be polarised between the proton and the atom, e.g. $F^- + H^+ \rightarrow HF$.



This is an ABE_3 system.

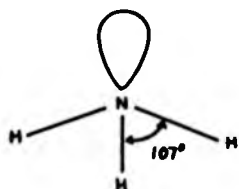
If the interaction involves two protons:



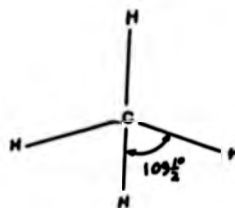
AB_2E_2

This approach can be extended to N^{3-} and C^{4-} to provide

NH_3 and CH_4



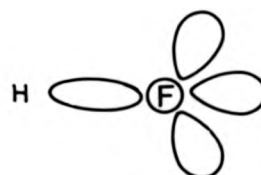
AB_3E



AB_4

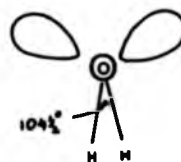
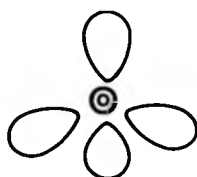
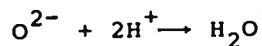
For Four Electron Pairs

Consider a central atom with four equivalent electron pairs tetrahedrally arranged around the atom as predicted by Rule 1. If a proton interacts with one of them, that pair will be polarised between the proton and the atom, e.g. $F^- + H^+ \rightarrow HF$.



This is an ABE_3 system.

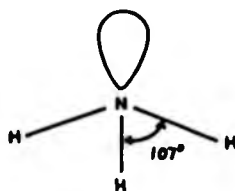
If the interaction involves two protons:



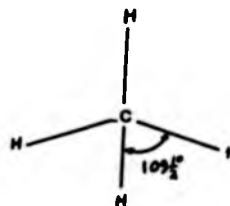
AB_2E_2

This approach can be extended to N^{3-} and C^{4-} to provide

NH_3 and CH_4



AB_3E

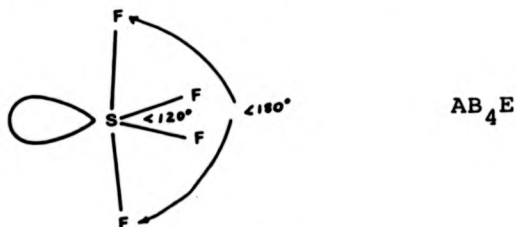


AB_4

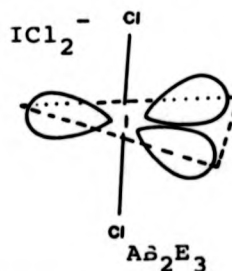
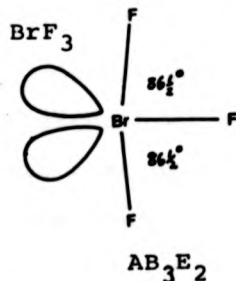
The reduction in the HAH bond angle for the series $A = C, N, O$ is an illustration of the effects of the lone pair in an isoelectronic series.

For Five Electron Pairs

Idealised geometry has already been presented in the structure of PF_5 which has trigonal bipyramidal geometry with two sets of equivalent sites: two Axial and three Equatorial sites. If one of the electron pairs is a non-bonded pair then from considerations of lone pair-bond pair repulsion, an equatorial position would be predicted for the lone pair as observed in SF_4 :



Similarly, lone pairs take up equatorial positions in systems with two and three non-bonded pairs:

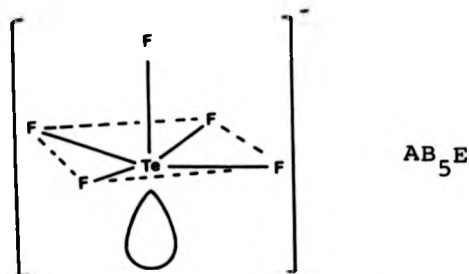


Although trigonal bipyramidal geometry provides a base for explaining the shapes of most five electron-pair systems, it is possible to have square pyramidal geometry. These two geometries are energetically

similar and they readily inter-convert (trigonal bipyramidal \rightleftharpoons square pyramidal).

For Six Electron Pairs

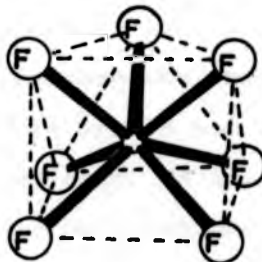
Octahedral geometry is expected for equivalent pairs. A single lone pair may take up one of the octahedral positions as in TeF_5^- .



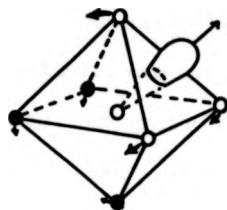
For two lone pairs, there is the question of whether the lone pairs occupy 'cis' or 'trans' positions. In the structure of ICl_4^- , they are *trans*.

For Seven Electron Pairs

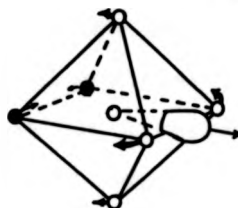
There are three possible structures viz. pentagonal bipyramid, capped octahedron and capped trigonal prism, which are all very similar energetically. The structures of IF_7 and ReF_7 ⁶ are pentagonal bipyramid while that of the NbF_7^{2-} ion in K_2NbF_7 is a capped trigonal prism⁷:



Considering XeF_6 as an AB_6E system, the basic octahedron is distorted by the presence of a lone pair⁸ which may operate through the centre of one of the faces (C_{3v} distortion) or through one of the edges (C_{2v} distortion).



(C_{3v})



(C_{2v})

There is no uniquely favoured geometrical arrangement, the system is stereochemically non-rigid. Stereochemical non-rigidity is operative in systems with fewer than six electron pairs but it becomes even more so in systems with more than six electron pairs.

Classification of Donor and Acceptor Atoms

A wide variety of complexes are formed by direct reactions between simple molecules or ions and ligands. This makes it desirable to have some form of classification whereby the relative reactivities of such compounds may be predicted.

Historically, the first attempt at such a classification was made by G N Lewis⁹. According to Lewis an acid molecule or ion is one in which the normal electron grouping surrounding some atom is incomplete and thus the molecule or ion can accept an electron pair from some other atom. A base, on the other hand has an electron pair which it can share with an acid.

Thus, a Lewis acid is an electron acceptor and a Lewis base an electron donor.

All metal ions may act as Lewis acids; ligands therefore become part of a more general term, Lewis base. Because of its simplicity and wide applicability, Lewis's definition of the acid and base and the concept of the electron pair bond has had a strong impact throughout all chemistry. Much as that may be, the theory has certain limitations. One notable deficiency lies in Lewis's definition of the relative nature of acidity and basicity, e.g. a compound can act as both Lewis acid and Lewis base in two different conditions. The commonly quoted example is ethylacetate which will accept OH^- to its carbonyl group thus acting as a Lewis acid and can also act as a Lewis base by 'complexing' with a proton *via* an oxygen donor site. This vaguery may be compared with one of the limitations of the Lowry-Brønsted definition of acids and bases¹⁰. In this case an acid is a substance that has a tendency to release a proton and a base is characterised by its tendency to accept a proton. Once again, both the relative acidity and borderline cases are hard to define.

Water is capable of acting as a proton donor towards ammonia



and as a proton acceptor towards substances like acetic acid



We can also have autoionisation



In 1939, a Russian chemist, Usanovich¹¹, proposed an all embracing definition of acids and bases. He described an acid as any chemical species which reacts with bases, gives up cations or accepts anions or electrons; likewise a base is any chemical species which reacts with acids, gives up anions or electrons, or combines with cations.

Bjerrum¹² in his study of the reactions between metal ions and halide ions, observed that metal ions can be grouped into two categories: those which favour small unpolarisable bases such as fluoride and those which favour large polarisable bases such as iodide. These categories were labelled as class (A) acceptors and class (B) acceptors respectively by Swarzenbach¹³ who carried out further studies in this field. A slightly different method of classification was introduced by Ahrland, Chatt and Davies¹⁴, viz., class (a) acceptors are those which form more stable complexes with ligands whose donor atoms are first row elements (N, O, and F) while class (b) acceptors are those that prefer to bond to ligands with second row elements as donor atoms (P, S and Cl).

[illegible]

7

Q

• • • • •

17

For ligand atoms, the relative coordinating affinities are represented by the stability series for class (a) and class (b) acids (acceptors).

Class (a)	Class (b)
N >> P > As > Sb > Bi	N << P > As > Sb > Bi
O >> S > Se > Te	O << S ~ Se ~ Te
F >> Cl > Br > I	F < Cl < Br << I

Since classification into class (a) or class (b) is derived in the main from free energy data for metal ligand interactions, it has limitations. An improvement of the classification was necessary to cover a wide range of acids and bases including many examples from organic chemistry. The search for a better system led to the terminology "hard" and "soft" acids and bases¹⁵. This classification was based on both thermodynamic and kinetic data. The new terms 'hard' and 'soft' arise from considering the general properties of the acids and bases concerned. Donors (bases) having high electronegativity, low polarisability, and high resistance to oxidation are described as hard while donors having low electronegativity, high polarisability and which are readily oxidised are described as soft. The acids are then classified simply according to whether they prefer hard or soft bases. Thus, the principle of hard and soft acids and bases (HSAB) classifies species by stating that hard acids

prefer to associate with and readily react with hard bases and similarly for soft acids and soft bases. In his later papers, Pearson^{15b} tried to quantify the HSAB principle and tried to establish a series of the relative hardness or softness of an acid base. However, the HSAB is best treated as a qualitative rather than a quantitative theory.

An attempt to explain acid-base interactions using a molecular orbital approach has been introduced by Klopman *et al.*¹⁶ with considerable success. According to Klopman, the initial change in the energy (ΔE) of the system upon an early stage of complex formation may be approximated by the following equation:

$$\Delta E = \frac{-q_B \cdot q_A}{r_{AB} \cdot e_c} + 2 \sum_{mB} \sum_{nA} \frac{(C_B^m \cdot C_A^n B_{AB})^2}{(E_m^* - E_n^*)}$$

where q_A and q_B = total net charge densities at the acceptor and donor atoms respectively

r_{AB} = the distance between donor and acceptor atoms

e_c = dielectric constant of the solvent

C_B^m = coefficient of the donor orbital m at the donor atom

C_A^n = coefficient of the acceptor orbital n at the acceptor atom

B_{AB} = resonance integral between the donor and acceptor atoms at distance r_{AB}

E_m^* = energy of the donor orbital m in the field of acid A corrected for any solvation or desolvation accompanying the removal of an electron from the orbital

E_n^* = energy of the acceptor orbital n in the field of base B corrected for any solvation or desolvation accompanying the addition of an electron to the orbital

\sum_{mB} = summation over all the occupied orbitals m of species B

\sum_{nA} = summation over all the occupied orbitals n of species A

For a strong interaction ΔE should be large and negative. In this equation, the first term is clearly electrostatic and is dependent on the net charge densities and distance between donor and acceptor atoms as well as the dielectric constant of the intervening medium. The second term represents the covalent interaction which depends on the overlap, symmetry and energies of the donor and acceptor orbitals (m and n) as modified by the solvent in which the reaction is occurring. The two terms are essentially independent as the first term is influenced by properties independent of those which influence the second term. Obviously, one should expect a strong interaction to be brought about between acids that have large net positive charge densities at their acceptor sites and bases that have large negative charge densities at their donor sites, thus maximising the first term. Alternatively, the corresponding donor and acceptor orbitals should have the appropriate symmetries to ensure good overlap and thus maximise the second term. With this in mind, Klopman has suggested that donor-acceptor interactions can be subdivided into 'charge controlled' (dominated by the first term) and 'orbital controlled' (dominated by the second term). It is worth noting that the donor orbital on the base is usually the highest occupied molecular orbital (HOMO) and the acceptor orbital is the lowest

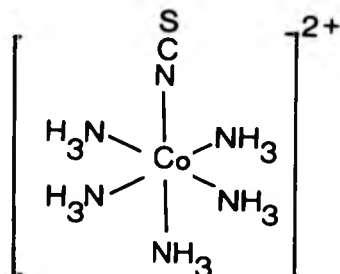
unoccupied molecular orbital (LUMO). For metal ligand interactions, metal orbitals are generally higher than ligand orbitals. For an acid (A) with a high net positive charge density at its acceptor atom and a high lying LUMO, its interaction with a series of bases will be charge controlled and the apparent base strength order established corresponds to the order of net negative charge (electron) density of the donor atoms of those bases. In contrast, for an acid (B) with a low net positive charge density at its acceptor atom and a low lying LUMO, such an interaction will be orbital controlled and the apparent base strength order corresponds to the order of HOMO energies of the bases. The acids A and B correspond to hard and soft respectively.

Ambidentate Behaviour in Ligands

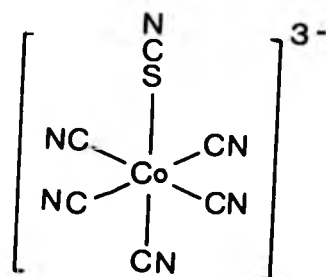
With the exception of NO_2^- and CN^- , ambidentate ligands possess one donor atom from the second row of the periodic table and one from the third row. Bonding through either site will depend on the kind of metal ion acceptor. As an example, the ligand SCN^- forms its most stable complex with Pd(II) , a class (b) ion, through the S atom in $[\text{Pd}(\text{SCN})_4]^{2-}$. With Cd(II) , an ion classed as being on the border between class (a) and class (b), N- and S-bonded ligands are observed while the class (a) metal ion Co(III) form the N-bonded complex ion $[\text{Co}(\text{NH}_3)_5\text{NCS}]^{2+}$.

Effect of a Ligand on the further Coordinating Ability of the Metal (Symbiosis and Antisymbiosis)

Some of the factors which influence the acceptor properties of the metal stem from steric and electronic effects of the other ligands already attached to the metal. For example, in contrast with the N-bonded complex $[\text{Co}(\text{NH}_3)_5\text{NCS}]^{2+}$ (I) the analogous complex $[\text{Co}(\text{CN})_5\text{SCN}]^{3-}$ (II) is S-bonded.

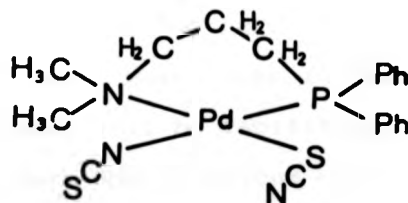


I



II

Interestingly, both bonding modes are observed in $[\text{Pd}(\text{Ph}_2\text{PC}_3\text{H}_6\text{NMe}_2)(\text{SCN})(\text{NCS})]$ (III)

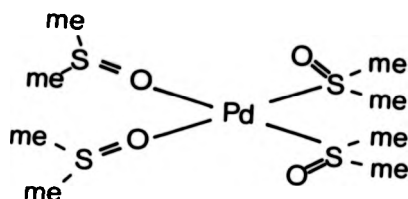


III

The concept of chemical symbiosis was first introduced by Jørgensen¹⁷ and is best illustrated by some cobalt (III) complexes. $[\text{Co}(\text{NH}_3)_5\text{X}]^{2+}$ is more stable for $\text{X} = \text{F}$ than I showing hard acid characteristics whereas $[\text{Co}(\text{CN})_5\text{X}]^{3-}$ is more stable for $\text{X} = \text{I}$ and the complex with $\text{X} = \text{F}$ is not known. Jørgensen characterised this as symbiosis. In symbiosis, hard bases (electro-negative donor atoms) retain their valence electrons when coordinated to a given acid (which is bound to be hard), hence the positive charge on the acid is unaffected and the acid remains hard. In contrast, soft bases (donor atoms of low electronegativity tend to give up a considerable amount of their valence electrons to the acid, so reducing the positive charge and making it a softer Lewis acid. So, in a stepwise formation of a complex AB_n , if the initial interaction of B and A results in a complex AB whose outer orbitals represent a species with hard rather than soft characteristics, further addition of hard rather than soft bases is favoured. On the other hand if a stepwise formation of AB_n involves a gradual reduction of the hard character due to charge donation by the soft bases then further coordination of similar soft bases will be facilitated.

Although the behaviour of many metal ions is in accord with symbiosis, many class (b) or soft metal ions behave in an antisymbiotic manner¹⁸. A soft base coordinated to a soft Lewis acid sometimes lowers the affinity of the 'trans' site to the point of exclusion of other soft bases. Antisymbiosis arises because two

mutually *trans* soft bases compete with each other for the same metal orbitals thus it does not matter whether they are purely σ -donors or σ -donors and π -acceptors. Davies and Hartley¹⁹ have pointed out that since antisymbiosis operates through the metal orbitals, the interactions should be orbital controlled, this antisymbiotic effect should therefore be more important with soft acids. Antisymbiosis is well illustrated by the palladium complex with $(\text{CH}_3)_2\text{SO}$ (DMSO) in which two sulphur and two oxygen bonded DMSO ligands are in a *cis* configuration²⁰.



Antisymbiosis predicts this *cis* arrangement as a consequence of the factors responsible for the *trans* influence. Each sulphur is bonded *trans* to the oxygen. Likewise in the thiocyanate complex of palladium(II) with diphenylphosphine-3-dimethylamino propane, $[\text{Pd}(\text{Ph}_2\text{P}(\text{CH}_2)_3\text{NMe}_2)(\text{SCN})(\text{NCS})]$ (III) antisymbiosis is illustrated by the fact that the hard N-bonded thiocyanate is *trans* to the softer P while the soft S-bonded thiocyanate is *trans* to the harder N of the bidentate ligand²¹.

Chelate Effect²²

When unidentate ligands are replaced by chelating ligands in a substitution reaction, the

product formed having the same number of donor atoms, will be more stable than the complex with unidentate ligands. This phenomenon known as the *chelate effect* has been known for a long time. For example, $[\text{Ni}(\text{en})_3]^{2+}$ is more stable than $[\text{Ni}(\text{NH}_3)_6]^{2+}$ although the number of nitrogen atoms present is the same for each species. It is thus expected that the following reaction is favourable.



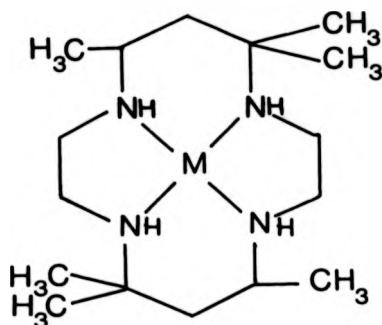
Both entropy and enthalpy contribute to the extra stability of the chelate complex but the former appears to make the major contribution. The substitution reaction leads to an increase in the number of free molecules which in turn increases the randomness of the system and consequently there is an increase in entropy. The relation between entropy and stability can be seen more clearly by referring to the following equations:

$$\Delta G^\ominus = \Delta H^\ominus - T\Delta S^\ominus \quad ; \quad \Delta G^\ominus = -|RT \ln K^\ominus|$$

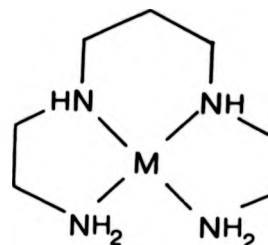
In summary, a positive contribution of entropy (ΔS^\ominus) results in a negative contribution to the free energy (ΔG^\ominus) and hence a positive contribution to the equilibrium constant (K^\ominus).

Macrocyclic Effect

The kinetic and thermodynamic stability of an M(II) complex formed with a 14-membered cyclic tetramine ligand is considerably greater than that formed by the same metal and an open chain tetramine ligand.



is 10^4 and 10^6
more stable than
for M = Cu(II)
and Ni(II)
respectively



Margerum and coworkers²³ have termed this the *macrocyclic effect*. This effect is characterised by slow rates of formation and usually large stability constants of macrocyclic complexes compared with corresponding open chain ligands. This phenomenon is best summarised as all the properties that cause enhanced stability of the macrocyclic complex. As with the chelate effect, both entropy and enthalpy considerations are important in the explanation of the macrocyclic effect. There is less configurational change in the ligand on complex formation and thus less loss in configurational entropy. The size of the "hole" in the macrocycle may favour particular metal-donor distances and any small deviations in optimum

$$\frac{\text{radius of hole}}{\text{radius of metal}}$$

ratio may be accommodated by the flexibility of the ring. The metal acceptor may have stereochemical requirements on chelating with the macrocyclic ligand. This is especially true for ions with unfilled d-orbitals and for P-block elements with a lone pair of electrons.

Though these factors are clearly important, they only play a minor role in the case of the tetramine ligands above. The dominant factor responsible for the macrocyclic effect in this case is the lower degree of solvation of the macrocycle.

1.2 GROUP VB COORDINATION CHEMISTRY

Oxidation State 3

The Trihalides

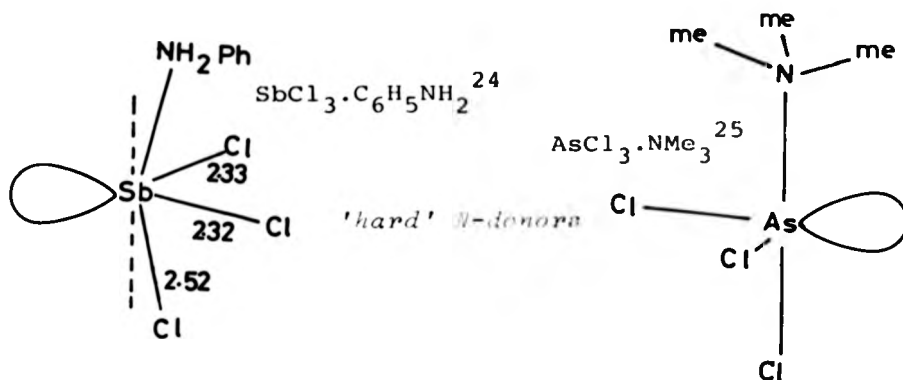
AsCl_3 is a clear colourless liquid that may be readily distilled. Both AsBr_3 and AsI_3 are solids. SbCl_3 , SbBr_3 , SbI_3 and all bismuth trihalides are solids that will sublime at low pressures. The trihalides are all hydrolysed by water and are best kept under strictly anhydrous conditions.

Coordination Chemistry

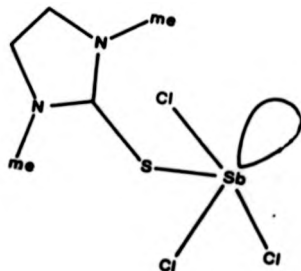
Our interest in coordination compounds lies in their stoichiometry, the variety of coordination numbers and coordination geometry, and the possible positions on the coordination sphere for both monodentate and bidentate ligands.

Coordination Number 4

This is mainly found in 1:1 adducts of Group (VB) trihalides. In the majority of examples, the observed geometry corresponds to a distorted sp^3d trigonal bipyramid with the lone pair taking up one of the equatorial positions as predicted by VSEPR. Examples:

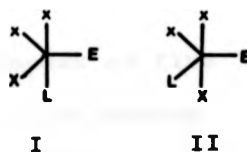


and $SbCl_3 \cdot dmit$ ²⁶ (dmit = 1,3-dimethyl-2-(3H)-imidazolethione)



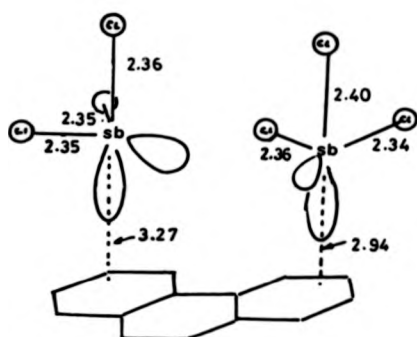
'soft' S-donor

These structures also demonstrate the energetically favourable isomeric possibilities for an AX_3LE system (A-central atom, X-halogen, L-donor atom, E-lone pair) where the ligand may occupy either an axial I or equatorial II.

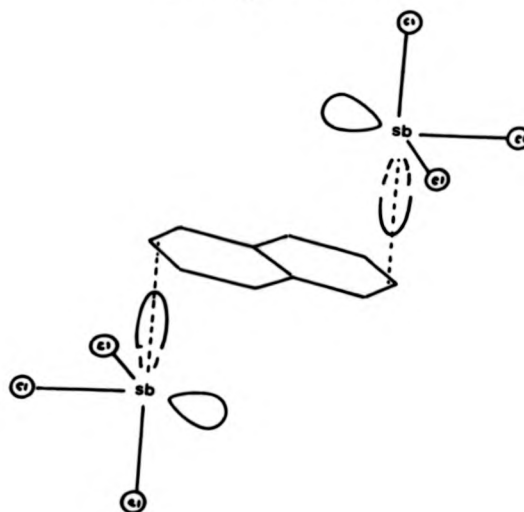


In the 2:1 complexes formed between SbCl_3 and various aromatic systems, antimony still adopts the pseudo trigonal bipyramidal structure with the lone pair in the equatorial position, e.g.

$2\text{SbCl}_3 \cdot \text{Phenanthrene}^{27}$

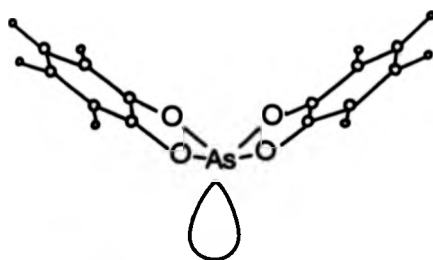


$2\text{SbCl}_3 \cdot \text{Naphthalene}^{28}$



and xylene²⁹.

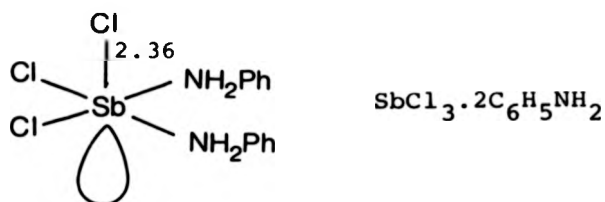
Four coordination has also been observed in complexes where all halogen atoms have been replaced, e.g. $\sim\text{K}[\text{As}(\text{C}_6\text{H}_4\text{O}_2)_2]^{30}$



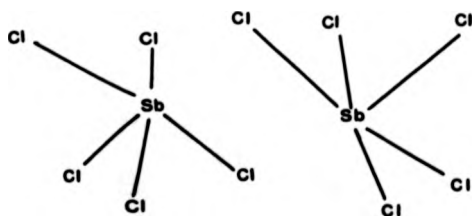
Coordination Number 5

There are relatively few examples of five coordination, usually 1:1 complexes with bidentate ligands or 1:2 (M:L) complexes with monodentate

ligands. In $\text{SbCl}_3 \cdot 2\text{C}_6\text{H}_5\text{NH}_2$ ³¹, the Sb atom is situated below the basal plane of a distorted square pyramid, so the structure is derived from an octahedral coordination in which one position is occupied by the lone pair.

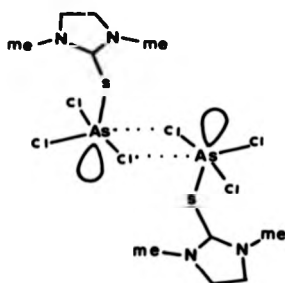


The effect of the lone pair seems to be comparatively diminished in the structure of potassium pentachloro antimonate(III) (K_2SbCl_5)³². The arrangement of chlorine atoms around each antimony could readily be described in terms of an octahedron with the lone pair occupying the sixth position but the Sb-Sb distance is much shorter than would be expected under the usual influence of active lone pairs.



Molecular arrangement of the two SbCl_5^{2-} units

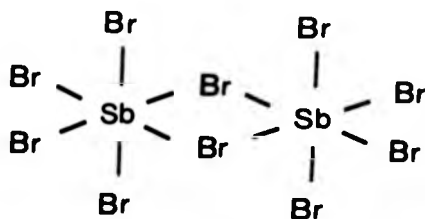
Although Williams and coworkers³³ first described the structure of $\text{AsCl}_3 \cdot \text{dmit}$ complex in terms of pseudo-trigonal bipyramid in order to emphasise the variety of isomeric possibilities, this dimeric system linked by long As---Cl bridges is best described as two distorted square pyramids sharing a common edge:



The $\text{AsCl}_3 \cdot \text{dmit}$ dimer

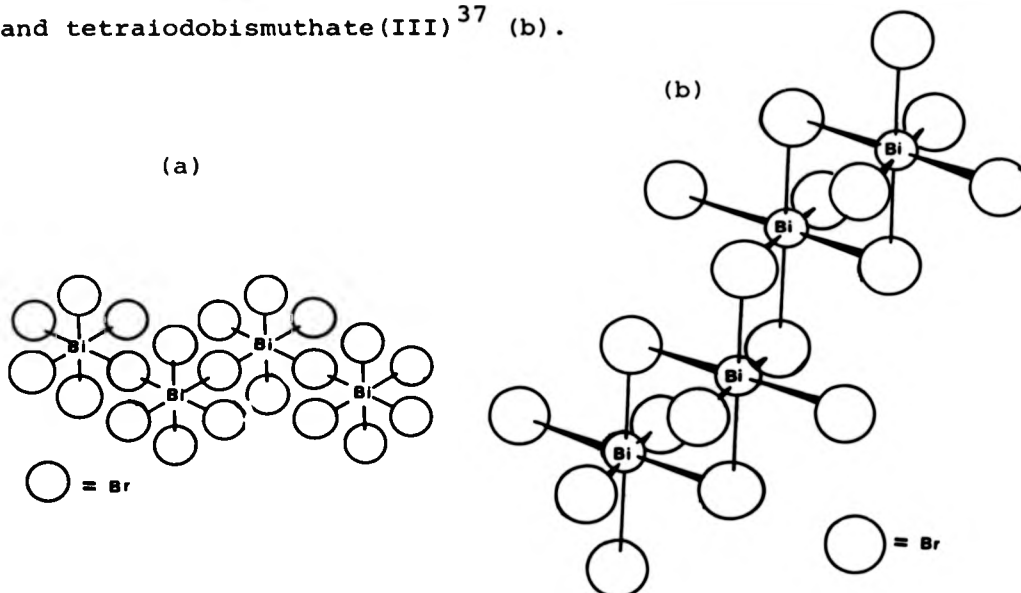
Coordination Number 6

This is probably the most popular coordination for complexes of Group (VB) trivalent elements. There are numerous examples of halogen bridged complex anions with octahedral geometry around each antimony, e.g.

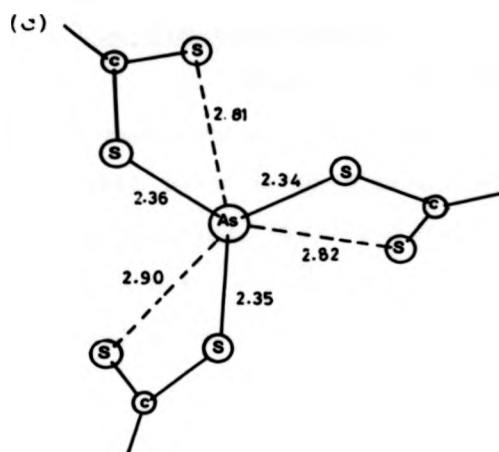


A portion of the anion chain in
 $(\text{pyH})\text{SbBr}_4$ ³⁴

Notable work by Meyers and coworkers on the structures of bismuth complexes shows that many of them are halogen bridged. In tris(dimethylammonium)hexachlorobismuthate(III) $[(CH_3)_2NH_2]_3BiBr_6$ ³⁵, the $BiBr_6^{3-}$ ions are independent octahedra, the dimethyl ammonium groups are also independent. The $BiBr_5$ ions in bispiperidinium-pentabromobismuthate(III) (a) are bromine bridged³⁶ like the $BiBr_4^-$ anions in 2-picolinium tetrabromobismuthate(III) and tetraiodobismuthate(III)³⁷ (b).

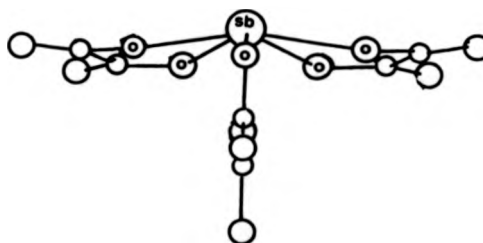


In these systems, the lone pair does not show any marked stereochemical activity. AX_6E systems with an active lone pair involve ligands associated with a narrow bite. The diethyldithiocarbamate complexes $As(S_2CNEt_2)_3$ ³⁸ (c), $Sb(S_2CNEt_2)_3$ and $Bi(S_2CNEt_2)_3$ ³⁹ are all examples of AX_6E systems which are based on an octahedron with the lone pair acting through the centre of one of the faces (C_{3v} distortion) resulting into a set of three long M-S bonds and three shorter ones.

 C_{3v}

There are many other examples of this type of structure, the more recent ones being $Sb[S_2P(OR)_2]_3$ $R = Me$ and Pr^{140} .

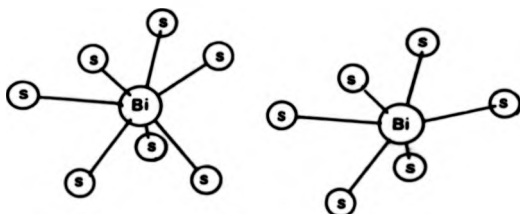
The six coordination-number story is incomplete without the AX_6E system where the influence of the lone pair is dramatised, i.e. the structure of the $Sb(C_2O_4)_3^{3-}$ ion⁴¹.

 D_{5h}

The coordination geometry is based on a pentagonal bipyramid with the lone pair taking up one of the axial positions.

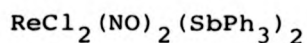
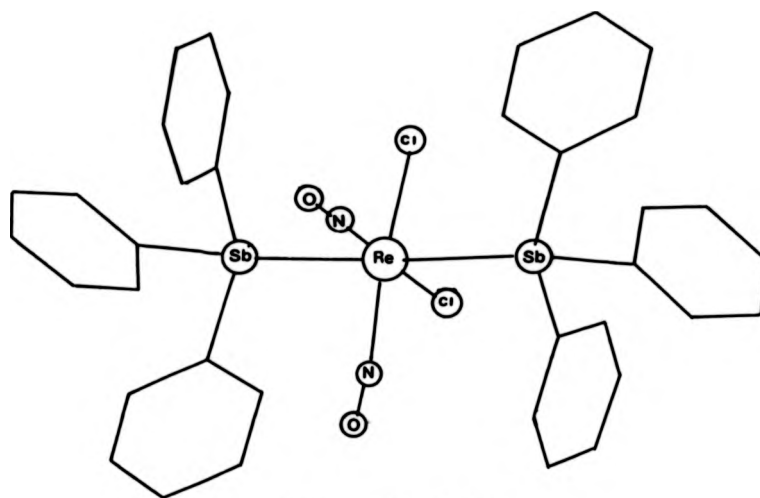
Coordination Number 7

There are not many examples of group (VB) compounds with coordination number seven, a few compounds with Bi-O or Bi-S bonds will be considered. The structure of bismuth (2:1) borate ($2\text{BiO}_3 \cdot \text{B}_2\text{O}_3$) shows both C.N. = 6 and C.N. = 7⁴², this is also true for bismuth indium sulphide ($\text{Bi}_2\text{In}_4\text{S}_9$)⁴³.



The two BiS_6 coordination polyhedra in
 $\text{Bi}_2\text{In}_4\text{S}_9$

Reactions involving ligands where nitrogen, phosphorous, arsenic, and antimony are the donor-centres are well documented. We shall just consider one representative example. The reaction between SbPh_3 and $\text{ReCl}_2(\text{NO})_2$ ⁴⁴ results in a complex with C.N. = 4, and with antimony(III) in a distorted tetrahedral environment. Such Lewis base character decreases down the group, bismuth does not exhibit this property.



Oxidation State 5

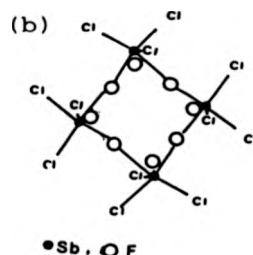
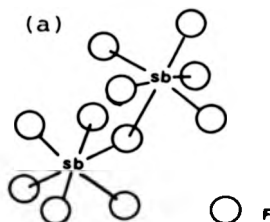
The compounds of Group (VB) in oxidation state 5 play a less important role in terms of the subject matter of this thesis and only merit a brief examination.

Group (VB) Pentahalides

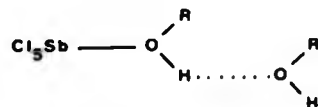
SbCl_5 is a colourless liquid which is a well known chlorinating agent and also a powerful electron acceptor⁴⁵. Bismuth pentafluoride is a white crystalline solid and an extremely powerful fluorinating agent. Although the pentachlorides of antimony and arsenic are well known, bismuth does not form a pentachloride. The relative stabilities are $\text{PCl}_5 \gg \text{AsCl}_5 \ll \text{SbCl}_5$, so in Group (VB) only antimony pentahalides have some appreciable coordination chemistry.

Coordination Chemistry

SbF_5 and AsF_5 are very strong Lewis acids⁴⁶. There are many examples of complexes of PF_5 , AsF_5 , SbF_5 with fluoride ions to give MF_6^- . Likewise SbCl_5 forms the anion SbCl_6^- . More complex anions such as As_2F_{11} and Sb_2F_{11} (a) have also been isolated⁴⁷. Mixed halides such as SbCl_4F are well known and there is now structural evidence for the mixed halide SbCl_3F_2 which is obtained from SbCl_4F and SbF_5 in sulphur dioxide⁴⁸. The analysis shows that SbCl_3F_2 exists as a *cis*-fluorine bridged tetramer giving a distorted octahedral arrangement of halogen atoms around each antimony atom (b).

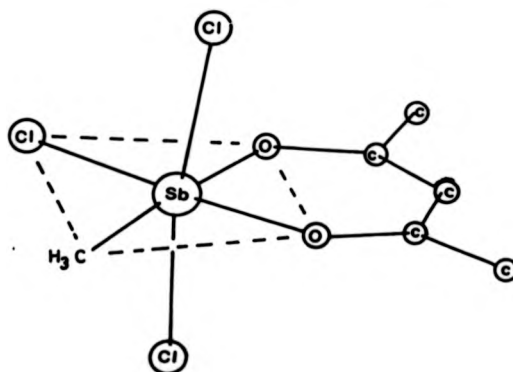


SbF_5 forms 1:1 and 1:2 complexes with IF_5 ⁴⁹. The 1:2 complex can be formulated as $\text{IF}_4^+ \text{Sb}_2\text{F}_{11}^-$ with strong fluorine bridging to the iodine. SbCl_5 forms a 1:1 addition compound with methanol which reacts with further alcohol to produce compounds with stoichiometries $\text{SbCl}_5(\text{MeOH})_n$, $n = 2, 3, 4$ ⁵⁰. The suggested structure as supported by i.r. data is:



The ionic formulation $\text{H}^+ [(\text{CH}_3\text{OH})_n \text{SbCl}_5 \text{OCH}_3]^-$ is seemingly preferred for $n > 3$.

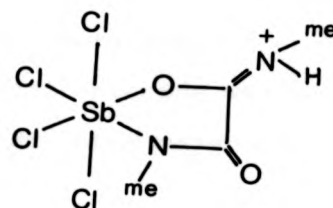
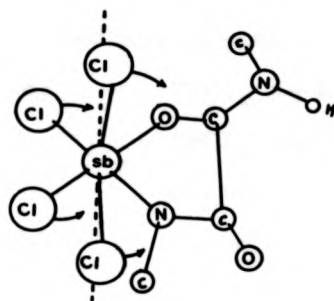
In Sb(V) compounds, important coordination numbers are 5 and 6. The idealised geometry in five coordination is either trigonal bipyramidal or square pyramidal. A distorted trigonal bipyramidal structure is observed for both SbBr_3Ph_2 and SbBr_2PhCl ⁵¹, and a distorted square pyramidal is seen in bis(triphenylantimony catecholate) hydrate⁵². Coordination number six is quite common and in the majority of cases, octahedral geometry is observed, e.g. methyltrichloro(acetyl acetonato)antimony(V) ($\text{CH}_3\text{SbCl}_3(\text{C}_5\text{H}_7\text{O}_2)$), I⁵³, and diphenyl antimony(V) dichloride acetylacetonate⁵⁴.



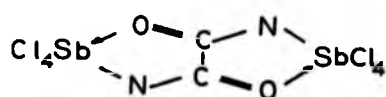
I: The molecular structure of $\text{CH}_3\text{SbCl}_3(\text{C}_5\text{H}_7\text{O}_2)$

The 1:1 product obtained from the reaction between N,N'-dimethyloxamide and antimony(V) pentachloride in 1,2-dichloroethane or chloroform with the elimination of HCl ⁵⁵, has been the subject of a structural investigation⁵⁶. Here again antimony(V) is in an octahedral environment but the N,N'-dimethyloxamido ligand being N,O-bonded is of great interest. Sb-Cl distances fall between 2.301 and 2.355 Å. The C-N bond lengths 1.274 and 1.495 Å are consistent with some degree of double bond character

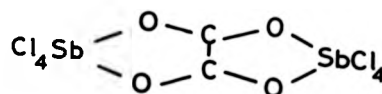
for the former as shown:



Similar structures have been proposed for the 2:1 compound I⁵⁷ and the related bis[tetrachloro antimony(V)] oxalate II⁵⁸.

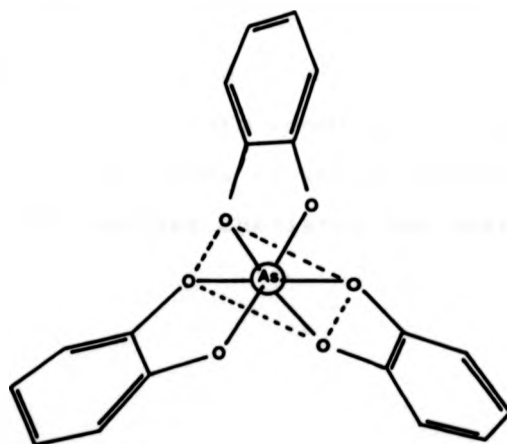


I



II

Another structure of interest is the distorted octahedral tris(benzene 1,2-diolato)arsenate(V) anion in $\text{K Sb}(\text{C}_6\text{H}_4\text{O}_2)_3$ ⁵⁹.



For comparison, we now turn to the Ti(IV) and Sn(IV) halides as representatives of Groups (IVA) and (IVB) respectively with the following considerations:

- (a) TiCl_4 is a transition metal chloride while SnCl_4 and SnBr_4 are halides of a main group element.
- (b) There is no lone pair of electrons associated with Group (IV) tetrahalides to be correlated with any irregularities or deviations from perfect symmetry shown by their complexes.
- (c) Such an investigation provides more chemical information about the reactivity of the ligands of interest.

1.3 GROUPS (IVA) AND (IVB) COORDINATION CHEMISTRY

In looking at the coordination chemistry of Groups (IVA) and (IVB), we shall only concern ourselves with oxidation state (IV). Furthermore, for simplicity we shall restrict ourselves to the specific compounds TiCl_4 , SnCl_4 and SnBr_4 . These tetrahalides are liquids that may be readily distilled. They all fume strongly in moist air, are readily hydrolysed by water, and have to be kept under strictly anhydrous conditions. Most of the earlier chemistry has been reviewed by Beattie⁶⁰.

For comparison, we now turn to the Ti(IV) and Sn(IV) halides as representatives of Groups (IVA) and (IVB) respectively with the following considerations:

- (a) TiCl_4 is a transition metal chloride while SnCl_4 and SnBr_4 are halides of a main group element.
- (b) There is no lone pair of electrons associated with Group (IV) tetrahalides to be correlated with any irregularities or deviations from perfect symmetry shown by their complexes.
- (c) Such an investigation provides more chemical information about the reactivity of the ligands of interest.

1.3 GROUPS (IVA) AND (IVB) COORDINATION CHEMISTRY

In looking at the coordination chemistry of Groups (IVA) and (IVB), we shall only concern ourselves with oxidation state (IV). Furthermore, for simplicity we shall restrict ourselves to the specific compounds TiCl_4 , SnCl_4 and SnBr_4 . These tetrahalides are liquids that may be readily distilled. They all fume strongly in moist air, are readily hydrolysed by water, and have to be kept under strictly anhydrous conditions. Most of the earlier chemistry has been reviewed by Beattie⁶⁰.

For comparison, we now turn to the Ti(IV) and Sn(IV) halides as representatives of Groups (IVA) and (IVB) respectively with the following considerations:

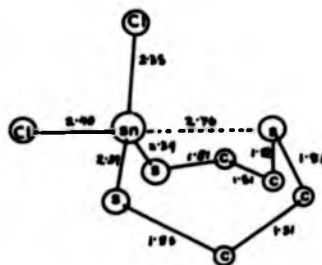
- (a) TiCl_4 is a transition metal chloride while SnCl_4 and SnBr_4 are halides of a main group element.
- (b) There is no lone pair of electrons associated with Group (IV) tetrahalides to be correlated with any irregularities or deviations from perfect symmetry shown by their complexes.
- (c) Such an investigation provides more chemical information about the reactivity of the ligands of interest.

1.3 GROUPS (IVA) AND (IVB) COORDINATION CHEMISTRY

In looking at the coordination chemistry of Groups (IVA) and (IVB), we shall only concern ourselves with oxidation state (IV). Furthermore, for simplicity we shall restrict ourselves to the specific compounds TiCl_4 , SnCl_4 and SnBr_4 . These tetrahalides are liquids that may be readily distilled. They all fume strongly in moist air, are readily hydrolysed by water, and have to be kept under strictly anhydrous conditions. Most of the earlier chemistry has been reviewed by Beattie⁶⁰.

Coordination Number 5

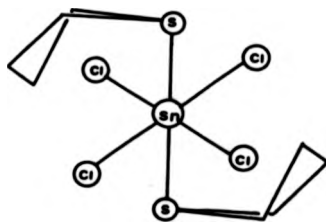
Evidence for five coordination in titanium tetrahalides was first obtained by Antler and Laubengayer⁶¹ in their study of $\text{Me}_3\text{N} \cdot \text{TiCl}_4$, $\text{Me}_2\text{NH} \cdot \text{TiCl}_4$, $\text{MeNH}_2 \cdot \text{TiCl}_4$ and $\text{NH}_3 \cdot \text{TiCl}_4$ systems. This work was extended by Fowles and coworkers⁶² who noticed that titanium tetrachlorides do not only form 1:1 adducts with tertiary amines but that tetravalent titanium is reduced to titanium(III) species in the presence of excess amine. So with trimethylamine, five coordinate species $\text{TiX}_4 \cdot \text{NMe}_3$ and $\text{TiX}_3(\text{NMe}_3)_2$ are obtained. A trigonal bipyramidal geometry is proposed for both compounds. The trivalent compound may also be prepared by direct reaction of NMe_3 with Ti(III) halides. TiCl_4 also forms 1:2 adducts with pyridine, but with excess pyridine Ti(IV) is reduced to Ti(III)⁶³. In their work on heterocyclic ring systems containing metals, Dräger and coworkers have investigated five coordinate Sn(IV) systems⁶⁴ which make excellent structural comparison with their As(III) and Sb(III) analogues⁶⁵. All these are eight membered ring systems with 1,5-transannular M---S or M---O interactions. The metal is in a pseudo trigonal bipyramid environment as illustrated by the structure of 2,2-dichloro-1,3,6,2-trithiastannaoctane:⁶⁴



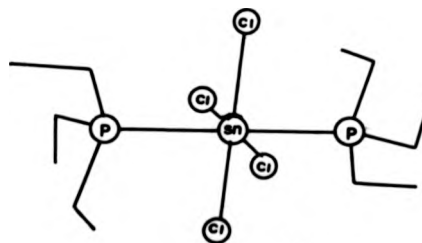
Trigonalbipyramidal (tbp) coordination is otherwise rare in Sn(IV) halides and their derivatives. The SnCl_5^- ion in $[(\text{C}_6\text{H}_5)_4\text{C}_4\text{Cl}]\text{SnCl}_5^{66}$ represents one of the simplest examples available. There are numerous examples of organotin(IV) complexes, e.g. the Ph_3PO complex with trimethyltin nitrate $(\text{C}_6\text{H}_5)_3\text{SnNO}_3 \cdot (\text{C}_6\text{H}_5)_3\text{PO}^{67}$ where the tbp arrangement is again observed.

Coordination Number 6

Tin(IV) chloride forms adducts of the type $\text{SnCl}_4 \cdot 2\text{L}$ and $\text{SnCl}_4 \cdot \text{L-L}$ (L = monodentate, L-L = bidentate). With octahedral 1:2 adducts, there is the possibility of either *cis* or *trans* isomers. The complexes $\text{SnX}_4(\text{Py})_2^{68}$, X = Cl, Br; $\text{SnCl}_4(\text{THT})_2(\text{I})^{69}$ THT = tetrahydrothiophene, and $\text{SnCl}_4(\text{PET}_3)_2^{70}$ (II) provide examples of *trans*-octahedral geometry.

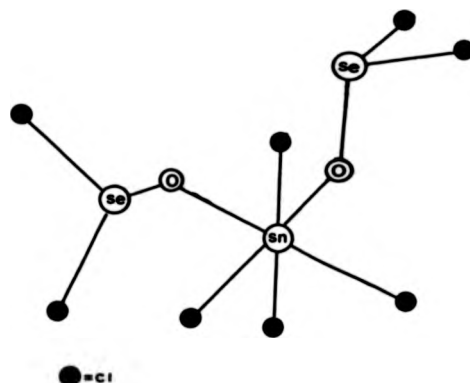


I



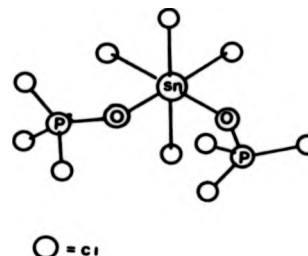
II

Complexes of $\text{SnCl}_4(\text{SeOCl}_2)_2$ III⁷¹, $\text{SnCl}_4(\text{POCl}_3)_2$ IV⁷², $\text{SnCl}_4(\text{DMSO})_2^{73}$, $\text{SnCl}_4(\text{CH}_3\text{CN})_2^{74}$ and the ligand bridged $\text{SnCl}_4\text{NC}(\text{CH}_2)_3\text{CN}^{75}$ are among those with *cis*-octahedral geometry.



III

The molecule of $\text{SnCl}_4 \cdot 2\text{SeOCl}_2$



IV

The molecule of $\text{SnCl}_4 \cdot 2\text{POCl}_3$

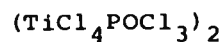
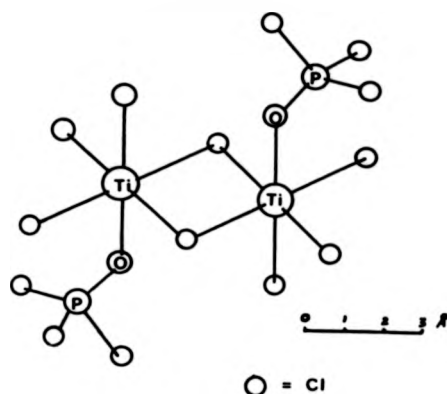
Many other *cis* or *trans* 1:2 adducts have been prepared and characterised by their ^{35}Cl n.q.r. spectra⁷⁶ where two resonances are expected for a *cis* adduct (two distinct types of chlorine atoms, axial and equatorial) and one resonance for a *trans* adduct.

In their study of the effects of various donor atoms on *cis-trans* isomerisation in 1:2 SnX_4 adducts, Harrison, Lane and Zuckerman⁷⁷ concluded that for monodentate ligands:

- (a) All Group (VB) donors give *trans*-isomers (triphenylarsine is the exception).
- (b) Oxygen donors give predominantly *cis*-isomers.

With bidentate ligands, octahedral *cis* $\text{SnX}_4 \cdot \text{L-L}$ chelates dominate the stereochemistry⁷⁸ examples being the complexes formed with 2,2-bipyridine and 1,10-phenanthroline.

1:1 Adducts of TiCl_4 are mostly octahedral with halogen bridging, e.g. $(\text{TiCl}_4 \cdot \text{POCl}_3)_2$ ⁷⁹, the ethylacetate adduct⁸⁰, and the CH_3NO_2 adduct⁸¹.

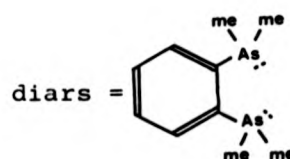
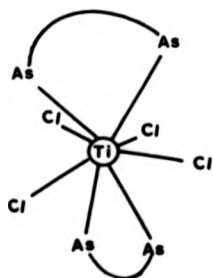


The 1:2 adduct of TiCl_4 and POCl_3 is isostructural with the *cis*-octahedral $\text{SnCl}_4 \cdot 2\text{POCl}_3$.⁸²

Coordination Numbers 7 and 8

Coordination numbers 7 and 8 are very rare in simple inorganic tin(IV) and titanium(IV) complexes.

Notable examples are the eight coordinate $\text{TiCl}_4(\text{diars})_2$ ⁸³ complexes.



There are many examples of seven coordinate complexes with pseudo pentagonal bipyramidal geometry but they are outside the scope of this work because they involve the replacement of all or most of the halogen atoms with O, S, N, or even C.

One of the problems we have experienced with our dithiooxamide complexes is the limited information that is provided by the 'normal' spectroscopic methods. This is indeed true for many coordination complexes. In the earlier stages of this work, we had conflicting analyses for some of the compounds (e.g. $\text{SbCl}_3 \cdot \text{DEDTO}_2$ and $(\text{SbCl}_3)_2 \text{DIPDTO}$) and the information provided by i.r. and ^1H n.m.r. was inconclusive. It was decided to use X-ray crystallography as a technique in order to fully understand the apparent structural complexities.

Rather than simply have samples analysed by an external source, it was decided that I should spend some time learning the basics of this technique. Accordingly, I spent 10 weeks at Reading University with Dr. M. G. B. Drew.

The following section represents a brief introduction to an X-ray crystal structure analysis.

1.4 CRYSTAL STRUCTURE ANALYSIS

The analysis of a crystal structure may be summarised as comprising the stages:

- (1) Experimental measurement of the unit cell dimensions and of the intensities of a large fraction of the diffracted beams from the crystal. These intensities depend only on the nature of atoms present and their relative positions within the unit cell. Data inferred from measurements on the diffraction pattern include:
 - (a) The relative positions of the diffracted beams which can be used to measure the size and shape of the unit cell.
 - (b) Intensities of the diffracted beams which may be analysed to give positions of the atoms within the unit cell.
- (2) The deduction, by some method, of a suggested atomic arrangement (a trial structure). Intensities of the diffraction maxima corresponding to this arrangement can then be calculated and compared with those observed.
- (3) Modification of this suggested arrangement (refinement) of scattering material until the agreement between calculated and observed intensities is within the limits of error of the observations.

General Experimental Procedure in Structural Determinations
in this Thesis

Space groups and cell dimensions were determined from precession photographs taken on a STOE-BUERGER precession X-ray goniometer. The data for crystal structures were collected on a STOE-STADI-2-diffractometer. Zirconium filtered Mo-K $_{\alpha}$ radiation was used. The crystal was set up to rotate around an axis and the appropriate cell dimensions were fed into the instrument's mini-computer. Cell dimensions were refined using high angle measurements. Intensity data was collected semi-automatically in the ω -scan mode with a scan rate of $0.033^{\circ} \text{ s}^{-1}$ that was applied to the scan width ($\Delta\omega$) of $(1.5 + \sin \mu / \tan \theta)$. Background counts at each end of the scan were 20 sec. The intensity data output was in the form of punched paper tapes. During data collection, one intense reflection was chosen as a standard for each set of measurements and the intensity of this reflection checked at intervals throughout the data collection. No significant decomposition of any crystal was observed and no correction was applied.

To illustrate the main principles, the crystal structure analysis of AsCl(td) (see Chapter 5) is outlined as an example:

The compound was recrystallised from a methanol/dichloromethane solution as very light yellow crystals. Its density was measured by suspending a chosen crystal in a mixture of carbon tetrachloride and diiodomethane such that the crystal neither sank to the bottom nor floated

General Experimental Procedure in Structural Determinations
in this Thesis

Space groups and cell dimensions were determined from precession photographs taken on a STOE-BUERGER precession X-ray goniometer. The data for crystal structures were collected on a STOE-STADI-2-diffractometer. Zirconium filtered Mo-K $_{\alpha}$ radiation was used. The crystal was set up to rotate around an axis and the appropriate cell dimensions were fed into the instrument's mini-computer. Cell dimensions were refined using high angle measurements. Intensity data was collected semi-automatically in the ω -scan mode with a scan rate of $0.033^{\circ} \text{ s}^{-1}$ that was applied to the scan width ($\Delta\omega$) of $(1.5 + \sin \mu / \tan \theta)$. Background counts at each end of the scan were 20 sec. The intensity data output was in the form of punched paper tapes. During data collection, one intense reflection was chosen as a standard for each set of measurements and the intensity of this reflection checked at intervals throughout the data collection. No significant decomposition of any crystal was observed and no correction was applied.

To illustrate the main principles, the crystal structure analysis of AsCl(td) (see Chapter 5) is outlined as an example:

The compound was recrystallised from a methanol/dichloromethane solution as very light yellow crystals. Its density was measured by suspending a chosen crystal in a mixture of carbon tetrachloride and diiodomethane such that the crystal neither sank to the bottom nor floated

to the surface. The density was obtained by weighing accurately 5.0 cm³ of the mixture.

Density (ρ measured) = 1.84.

(A) Selection of the Crystal

A few crystals of AsCl(td) were sprinkled on a microscope slide and placed under a polarising microscope. The sample was rotated while being viewed in plane polarised light. Our objective was an individual crystal of suitable size (approximate dimensions 0.1 mm-0.5 mm). The selected crystal was one that changed relief between 'bright' and 'dark' every 90°. This observation is an indication that the material is crystalline in nature and is unlikely to be "twinned", i.e. a combination of two or more lattices. The crystal chosen for X-ray studies had approximate dimensions 0.40, 0.10 and 1.25 mm.

(B) Setting the Crystal

The crystal of choice was then placed in a Lindemann tube along its most prominent axis. A small amount of high vacuum grease was introduced into the tube to prevent the crystal altering position during further investigation. The tube was sealed at both ends and mounted on a goniometer head using "soft Beeswax". The head was affixed to the precession camera and aligned by making both arc and lateral adjustments until the crystal was centred just below the crosswires in the telescope and finally in the X-ray beam, so that it would be bathed in radiation. The crystal was then

rotated so that the X-ray beam was perpendicular to a prominent face and therefore possibly coaxial with a crystal axis.

With the following settings: $\mu = 7.5^\circ$, $F = 0$, no filter, no screen [(in this case the reciprocal lattice is precessed through $\mu = 7.5^\circ$ so that reflections, which can only occur when reciprocal lattice points cross the Ewald sphere, may be obtained) $60-F = \text{distance (in mm) from the crystal to the film}$] the precession camera was set in motion and X-rays fired at the crystal for fifteen minutes. After this time the photographic film was developed. This process was repeated with a few adjustments on the crystal settings and after several attempts, a 'circle' was obtained. The circle indicates that the crystal has been aligned so that an axis is coincident with the X-ray beam. Rotating the crystal by 90° fortunately gave another circle indicating two axes at right angles.

(C) Obtaining Precession Photographs

With the settings for the zero layer: $\mu = 25^\circ$, $F = 0$, screen with annular slit diameter of 40 mm, Mo K_α radiation and $S = 42.8$ (S is the distance from the screen to the crystal) the crystal was set for each axis in turn and layer photographs obtained over 16 hours.

(D) Using Precession Photographs

(i) From the symmetry of the reciprocal lattice it was adjudged that the crystal is monoclinic with β equal to 91° .

rotated so that the X-ray beam was perpendicular to a prominent face and therefore possibly coaxial with a crystal axis.

With the following settings: $\mu = 7.5^\circ$, $F = 0$, no filter, no screen [(in this case the reciprocal lattice is precessed through $\mu = 7.5^\circ$ so that reflections, which can only occur when reciprocal lattice points cross the Ewald sphere, may be obtained) $60-F = \text{distance (in mm) from the crystal to the film}$] the precession camera was set in motion and X-rays fired at the crystal for fifteen minutes. After this time the photographic film was developed. This process was repeated with a few adjustments on the crystal settings and after several attempts, a 'circle' was obtained. The circle indicates that the crystal has been aligned so that an axis is coincident with the X-ray beam. Rotating the crystal by 90° fortunately gave another circle indicating two axes at right angles.

(C) Obtaining Precession Photographs

With the settings for the zero layer: $\mu = 25^\circ$, $F = 0$, screen with annular slit diameter of 40 mm, Mo K_α radiation and $S = 42.8$ (S is the distance from the screen to the crystal) the crystal was set for each axis in turn and layer photographs obtained over 16 hours.

(D) Using Precession Photographs

(1) From the symmetry of the reciprocal lattice it was adjudged that the crystal is monoclinic with β equal to 91° .

(ii) From the spacings between the spots on the photographs, cell dimensions of the real cell lattice were worked out.

$$\text{Dimension in } \text{\AA} = \left(\frac{\text{spacings in mm}}{60 \times 0.7107} \right)^{-1}$$

The volume of the unit cell was obtained from the dimensions

$$\begin{aligned} V_c &= a \times b \times c \sin \beta \\ &= \left(\frac{69.5}{10 \times 60 \times 0.7107} \right)^{-1} \times \left(\frac{54.2}{20 \times 60 \times 0.7107} \right)^{-1} \times \left(\frac{78.5}{18 \times 60 \times 0.7107} \right)^{-1} \\ &= 849.76 \text{ \AA} \end{aligned}$$

(iii) The contents of a crystal were checked by calculating a value of density from the mass of the contents of the unit cell divided by the volume of the unit cell. This is given by the formula:

$$\rho = \frac{\text{M.W.} \times 1.66 \times Z}{V_c}$$

where ρ = density of crystal

M.W. = Molecular Weight

Z = number of molecules in the unit cell
(an integer)

(Z is checked for consistency with the spacegroups)

Calculated density ($\rho_{\text{calc.}}$) for AsCl(td) = 1.86.

(iv) Examination of the photographs for systematic

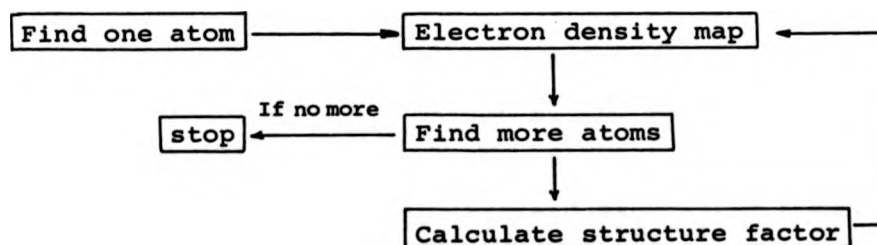
absences revealed no systematic absences for hkl reflections so that the unit cell is primitive (p) but systematic absences were observed for hol with l odd and for oko with k odd. These observations confirmed the monoclinic symmetry and the systematic absences lead unambiguously to space group $P2_1/c$ (No. 14) after consulting international tables for X-ray crystallography (Vol. 1)⁸⁴.

(E) Intensity Measurements

The intensities of 1690 symmetry independent reflections were measured on the diffractometer and corrections applied to take account of polarisation and Lorentz effects. An absorption correction was also made.

(F) Data Analysis

A schematic representation



Relative structure factors ($|F_r|$) were calculated from intensity measurements (I) using a data reduction program which applied the formula:

$$|F_{hkl}| = \left(\frac{k I_{hkl}}{L_p} \right)^{\frac{1}{2}}$$

k is a scale factor
proportional to
(a) crystal size
(b) beam intensity
(c) a number of
fundamental
constants

$$p = \left(\frac{1 + \cos^2 2\theta}{2} \right) \quad (\text{polarisation factor})$$

$$L = \frac{1}{\sin 2\theta} \quad (\text{Lorentz factor})$$

The atomic coordinates were found by the heavy atom method. This was achieved by computing the Patterson function of the crystal. This is a Fourier series for which only the indices and the $|F|^2$ value of each diffracted beam are required:

$$P_{uvw} = \frac{1}{V_c} \sum_h \sum_k \sum_l |F_{hkl}|^2 \cos 2\pi (hu + kv + lw)$$

proportional to I_{hkl}

P is evaluated at every point (u, v, w) of a three dimensional grid which fills a space that has the size and shape of the unit cell. This function gives a map of interatomic vectors. A peak in the Patterson function at a position related to the origin of the map by a vector (U, V, W) implies that there are two atoms in the crystal structure at positions (x_1, y_1, z_1) and (x_2, y_2, z_2) such that $x_2 - x_1 = U$, $y_2 - y_1 = V$ and $z_2 - z_1 = W$. The height of the peak will be proportional to the product of the number of electrons in each of the two atoms involved. It is these two properties that facilitate the location of the heavy atom. From the data for $P2_{1/c}^{84}$. The coordinates of vectors between symmetry related positions of any atom in terms of its atomic position parameters were derived as follows:

(a) Atomic positions

1.	x	y	z
2.	\bar{x}	\bar{y}	\bar{z}
3.	\bar{x}	$\frac{1}{2} + y$	$\frac{1}{2} - z$
4.	x	$\frac{1}{2} - y$	$\frac{1}{2} + z$

(b) Interatomic vectors between symmetry related atoms are expected at positions corresponding to the differences in coordinates of the various atomic positions

(1 - 2)	2x	2y	2z
(1 - 3)	2x	$\frac{1}{2}$	$\frac{1}{2} + 2z$
(1 - 4)	0	$\frac{1}{2} + 2y$	$\frac{1}{2}$

The vector between any other positions, e.g. 2 - 4 or 4 - 3 is either identical to one of these or related by a mirror-plane or rotation axis.

(c) The Patterson map for AsCl(td) shows peaks at the following positions:

	x	y	z
peak 1	0	0	0
3	0	0	0.5
4	0.46	0.5	0.1873
9	0.4556	0.5	0.6845

Direct comparison of these with the general expected positions in (b) above showed the consistent set of coordinates for the As atom to be

$$x = 0.23 \quad y = 0.25 \quad \text{and } z = 0.34.$$

Once the heavy atom has been located the assumption is then made that it dominates the diffraction pattern and the phase angle for each diffracted beam for the whole structure is approximated by that for the heavy atom. From the position and intensity of the heavy atom the structure factor and the phase of the diffracted beam from the heavy atom (As) were worked out using the following formulae:

$$|F_{hkl}| = \sum_{r=1}^N f_r \exp 2\pi i (hx_r + ky_r + lz_r)$$

f_r - obtained from international tables,
proportional to the number of
electrons at

$$\frac{\sin \theta}{\lambda} = 0$$

$$F_{hkl_{obs}} \approx F_{calc} = \underbrace{\sum_{r=1}^N f_r \cos 2\pi (hx_r + ky_r + lz_r)}_A + \underbrace{i \sum_{r=1}^N f_r \sin 2\pi (hx_r + ky_r + lz_r)}_{iB}$$

$$= A + iB$$

$$|F_{hkl}| = \sqrt{A^2 + B^2}$$

$$\alpha = \tan^{-1} \left[\frac{B_{hkl}}{A_{hkl}} \right]; \quad \cos \alpha = \frac{A}{|F_{calc}|}; \quad \sin \alpha = \frac{B}{|F_{calc}|}$$

where α is the phase angle

Once F_{calc} and α had been obtained, another Fourier Series, from which the electron density $\rho(x, y, z)$ at any point (x, y, z) in the cell can be obtained, was computed using the formula:

$$\rho(x, y, z) = \frac{1}{V} \sum_h \sum_k \sum_l F_{hkl} \exp(-2\pi i (hx + ky + lz))$$

F_{hkl} - not merely the moduli of structure factors which are available as $|F_o|$ but rather the moduli plus the unobservable phases
 $F_{hkl} = |F_{hkl}| e^{i\alpha}$; $F_{hkl} = |F_{hkl}| \cos \alpha + i |F_{hkl}| \sin \alpha$
 or $F_{hkl} = A_{hkl} + i B_{hkl}$

Evaluation of ρ at all points (x, y, z) provided an electron density map and more atoms, in this case two S and one Cl were located by assuming that the function ρ is maximum at a point where there is an atom. The coordinates of the two S and Cl atoms were used along with those of As to calculate a slightly more accurate value of F_{calc} and the value of α obtained, as expected, is closer to the actual value of α for the cell. These 'new' values were used to provide an improved electron density map from which all the carbon atoms were located. In a general case, the process can be repeated until all the atoms have been located.

Final positional and thermal parameters were refined by full-matrix least squares analysis until convergence occurred, i.e. minimum Q where

$$Q = \sum_{hkl} w \left(\underbrace{|F_o| - \frac{1}{k} |F_c|}_{\Delta F} \right)^2$$

k is a scale factor

A weighting scheme was chosen to give similar values of $w(\Delta F)^2$ with ranges of F_o and $\frac{\sin \theta}{\lambda}$; the weighting scheme used on the STOE diffractometer was

$$\rho(x, y, z) = \frac{1}{V} \sum_h \sum_k \sum_l F_{hkl} \exp(-2\pi i (hx + ky + lz))$$

F_{hkl} - not merely the moduli of structure factors which are available as $|F_o|$ but rather the moduli plus the unobservable phases
 $F_{hkl} = |F_{hkl}| e^{i\alpha}$; $F_{hkl} = |F_{hkl}| \cos \alpha + i |F_{hkl}| \sin \alpha$
 or $F_{hkl} = A_{hkl} + i B_{hkl}$

Evaluation of ρ at all points (x, y, z) provided an electron density map and more atoms, in this case two S and one Cl were located by assuming that the function ρ is maximum at a point where there is an atom. The coordinates of the two S and Cl atoms were used along with those of As to calculate a slightly more accurate value of F_{calc} and the value of α obtained, as expected, is closer to the actual value of α for the cell. These 'new' values were used to provide an improved electron density map from which all the carbon atoms were located. In a general case, the process can be repeated until all the atoms have been located.

Final positional and thermal parameters were refined by full-matrix least squares analysis until convergence occurred, i.e. minimum Q where

$$Q = \sum_{hkl} \omega \underbrace{(|F_o| - \frac{1}{k}|F_c|)}_{\Delta F}^2$$

k is a scale factor

A weighting scheme was chosen to give similar values of $\omega(\Delta F)^2$ with ranges of F_o and $\frac{\sin \theta}{\lambda}$; the weighting scheme used on the STOE diffractometer was

$$\omega = \frac{1}{(\sigma F + .003(F)^2)}$$

where $\sigma(F)$ was taken from counting statistics

σ was a variable (usually 2 or 3).

A final residual index (R) was obtained by the formula

$$R = \frac{\sum_{hkl} |F_o| - k|F_c|}{\sum |F_o|}$$

($F_o = k\sqrt{I_{\text{corr}}}$ where k is chosen to give $\sum |F_o| = \sum |F_c|$)

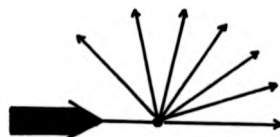
Where F_o - observed structure factor

F_c - calculated structure factor

k - overall scale factor

Scattering Factors

When light is scattered by particles that are very small relative to the wavelength of the light, scattered light has the same intensity in all directions.



For larger particles, radiation from different regions will still be in phase in the forward direction but at higher angles, there is interference between radiation scattered from various parts of the particle. Therefore the intensity of radiation scattered at higher angles is less than that of radiation scattered in the forward direction.

$$\omega = \frac{1}{(\sigma F + .003(F)^2)}$$

where $\sigma(F)$ was taken from counting statistics

σ was a variable (usually 2 or 3).

A final residual index (R) was obtained by the formula

$$R = \frac{\sum |F_o| - k \sum |F_c|}{\sum |F_o|}$$

($F_o = k \sqrt{I_{\text{corr}}}$ where k is chosen to give $\sum |F_o| = \sum |F_c|$)

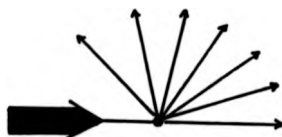
Where F_o - observed structure factor

F_c - calculated structure factor

k - overall scale factor

Scattering Factors

When light is scattered by particles that are very small relative to the wavelength of the light, scattered light has the same intensity in all directions.



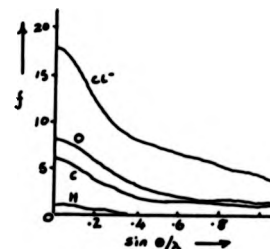
For larger particles, radiation from different regions will still be in phase in the forward direction but at higher angles, there is interference between radiation scattered from various parts of the particle. Therefore the intensity of radiation scattered at higher angles is less than that of radiation scattered in the forward direction.



This effect is greater the larger the particle relative to the wavelength. The scattering factor of an atom (f_{atom}) is given by:

$$f_{\text{atom}} = \frac{\text{Amplitude of wave scattered by the atom}}{\text{Amplitude of wave scattered by a single electron}}$$

note that f_{atom} decreases as $\frac{\sin \theta}{\lambda}$ increases



Temperature Factor

Atoms in a crystal are not stationary objects. They are vibrating about their mean positions. This increases their effective size leading to a more rapid decline of atomic scattering factors than would be expected for stationary atoms. Mean vibration amplitudes tend to increase with temperature so the reduction of scattering factor at large scattering angles becomes more pronounced at high temperatures. The simplest assumption we can make is that the motion of each atom is the same in all directions, i.e. ISOTROPIC. Such

motion results in an exponential decrease in atomic scattering factors as the scattering angle (2θ) increases. The scattering factor of an atom at rest (f) is then replaced by $f e^{-\frac{B \sin^2 \theta}{\lambda^2}}$ where $B = 8\pi^2 \langle u^2 \rangle$. Here $\langle u^2 \rangle$ is the mean square vibrational amplitude and is known as the Debye factor. If the atom vibrates ANISOTROPICALLY (as most atoms do because of their different atomic environments) the next simplest approximation is the assumption that the motion is ellipsoidal, i.e. it can be described by the six parameters of a general ellipsoid rather than the single parameter characteristic of a sphere. Three of these parameters are considered to define lengths of three mutually perpendicular axes describing the amount of motion in these directions and the remaining three to define the orientation of these ellipsoidal axes relative to the crystal axes. The usual way of taking this kind of ellipsoidal motion into account in structure factor equations is by means of an exponential factor analogous to that of the isotropic case but with six anisotropic temperature factors, U_{ij} , as multipliers of the indices for each reflection hkl in the exponent e^{-T} where

$$T = 2\pi^2 (U_{11}h^2a^{*2} + U_{22}k^2b^{*2} + U_{33}l^2c^{*2} + U_{12}hka^*b^* + U_{23}klb^*c^* + U_{13}hla^*c^*)$$

For this work, metal, chlorine and sulphur atoms were refined anisotropically. Wherever possible, oxygen, nitrogen and carbon atoms were also refined anisotropically.

Hydrogen atoms bonded to carbon were placed in the appropriate trigonal or tetrahedral positions and given individual thermal parameters. Hydrogens on the same carbon atom were constrained to be equivalent. Hydrogen atoms on amine-nitrogen atoms were located from difference Fourier maps and their parameters allowed to refine. Scattering factors were taken from International tables⁸⁵. Calculations were made using the CDC 7600 computers at the Regional computer centre at the University of Manchester or London using the SHELX 76 system of programs⁸⁶. The University of Reading ICL 1904 computer was also used for initial treatment of intensity data from the diffractometer and for the plotting of the final structures. The programmes used were either written and/or adapted for the machines by Dr. M. G. B. Drew.

CHAPTER 2
DITHIOOXAMIDES

CHAPTER 2

DITHIOOXAMIDES

2.1 INTRODUCTION

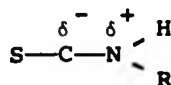
Dithiooxamides have been known for a long time and utilised in a wide range of applications. They were seen as potential metal deactivators in petroleum products⁸⁷, vulcanisation accelerators⁸⁸, and they were found to possess inhibitory properties against certain bacteria⁸⁹; they also found use in the synthesis of 2,2'-dithiazoles⁹⁰. Dithiooxamides readily form metal complexes some of which have been used as colour sources in the photographic industry⁹¹; N,N'-disubstituted dithiooxamide complexes with copper(II) show electric behaviour of semiconductors⁹².

Numerous metal complexes of dithiooxamide and its N-substituted derivatives have been reported⁹³ and so we now outline some trends in this area of chemistry. The reasons for our interest in dithiooxamides will be stated later.

Factors Governing Metal Complex Formation with Dithiooxamides

(a) Dithiooxamides possess four centres that are strong Lewis bases: two sulphurs and two nitrogens. There are lone pairs of electrons on each, available for donation although the lone pair on the nitrogen is partially delocalised to give an

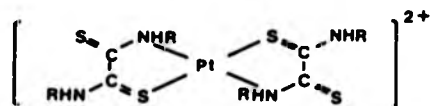
system.



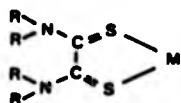
Persson and Sandström⁹⁴ have calculated π -electron densities and π -bond orders in the ground and excited states for *inter alia* N,N'-tetrasubstituted dithiooxamides. The choice of donor sites therefore often leads to great controversy.

In the HSAB classification, (N)-donors are usually classified as hard bases while (S)-donors are usually soft bases. If HSAB and class (a) - class (b) considerations are the dominant factors influencing complex formation, then depending on the metal centre, only one donor type, (S) or (N) will be involved in coordination for these dithiooxamides.

(b) Chelate formation is quite common with various metal centres. In many cases, involvement of both (N)- and (S)-centres is proposed. One such complex is the platinum(II) ion with substituted dithiooxamide⁹⁵.

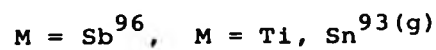
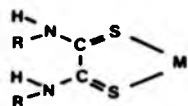


In their work on tetraalkyldithiooxamides with Group (VB) metals, Peyronel and coworkers^{93(f)} propose structures where only (S)-donation to the metal is involved:



M = As, Sb, Bi, R = Me, Et

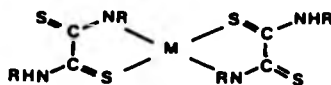
This view is supported by work in these laboratories with N,N'-disubstituted dithiooxamide complexes of Group (VB) and Group (IV) halides.



Chelate formation is dictated by the size of the ligand 'bite' in relation to the size of metal centre and is therefore less likely in some ligands associated with a narrow bite.

(c) Reaction conditions:

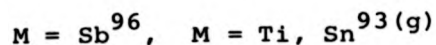
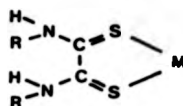
In neutral or alkaline media: Dithioamides and their partially N-substituted derivatives are known to lose the amidic proton and form (N,S)-bonded non-electrolytic $M(\text{LH})_2$ complexes (I) $M = \text{Po}(\text{II}), \text{Pt}(\text{II})^{97}$. With nickel, polymeric complexes have been observed⁹⁸⁻¹⁰⁰.



(I)

When it was first observed, proton loss was thought to be a necessary prerequisite for complex formation but the preparation of dithioamide complexes in acid media soon proved this not to be the case.

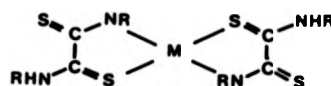
In acid media: Dithioamide and its partially substituted derivatives react with divalent transition metals to form monomeric complexes of the general formula $M^{(\text{II})}(\text{LH}_2)_2\text{X}_2$ with no incipient proton loss ($M = \text{Pd}, \text{Pt}^{93(b)}$ and $\text{Ni}^{93(a)}$) presumably with the following (N,S)-bonded structure:.



Chelate formation is dictated by the size of the ligand 'bite' in relation to the size of metal centre and is therefore less likely in some ligands associated with a narrow bite.

(c) Reaction conditions:

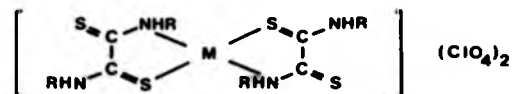
In neutral or alkaline media: Dithioamides and their partially N-substituted derivatives are known to lose the amidic proton and form (N,S)-bonded non-electrolytic $M(\text{LH})_2$ complexes (I) $M = \text{Po(II)}, \text{Pt(II)}$ ⁹⁷. With nickel, polymeric complexes have been observed⁹⁸⁻¹⁰⁰.



(I)

When it was first observed, proton loss was thought to be a necessary prerequisite for complex formation but the preparation of dithioamide complexes in acid media soon proved this not to be the case.

In acid media: Dithioamide and its partially substituted derivatives react with divalent transition metals to form monomeric complexes of the general formula $M^{(II)}(\text{LH}_2)_2X_2$ with no incipient proton loss ($M = \text{Pd}, \text{Pt}$ ^{93(b)} and Ni ^{93(a)}) presumably with the following (N,S)-bonded structure:.



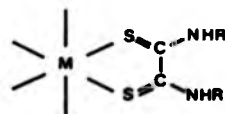
M = Ni(II), Cu(II)

With Co(III), tris(S,N)-chelates with a general formula $\text{Co}(\text{LH}_2)_3$ have been formed ($\text{LH}_2 = \text{MeHNC}(\text{S})\text{C}(\text{S})\text{NHMe}$, $\text{C}_6\text{H}_{11}\text{HNC}(\text{S})\text{C}(\text{S})\text{NHC}_6\text{H}_{11}$)¹⁰¹ and there is great interest in their stereochemistry.

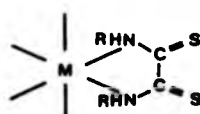
Neutral complexes $\text{M}(\text{LH}_2)_2$ of planar dithiooxamides such as $\text{H}_2\text{NC}(\text{S})\text{C}(\text{S})\text{NH}_2$, $\text{RHNC}(\text{S})\text{C}(\text{S})\text{NH}_2$ and $\text{RHNC}(\text{S})\text{C}(\text{S})\text{NHR}$ have also been prepared by reacting *solid* $\text{M}(\text{LH}_2)_2$ complexes with *solid* NaF (M = Ni, Pd, Pt)¹⁰²

(d) Possible ligand bonding modes:

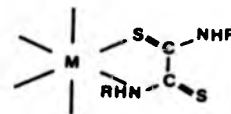
The bonding arrangement in dithiooxamide complexes is in many ways dictated by the choice of donor sites. Examples of *cis*-(S,S)-(I) and (N,S)-chelates(II) have been described above



I



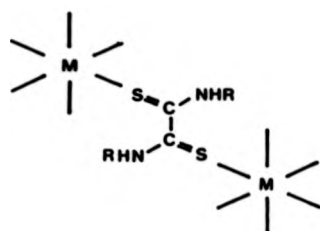
III



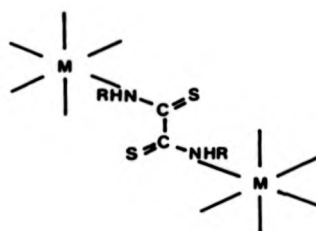
II

It is possible to have chlorine bridged structures involving *cis*-chelates.

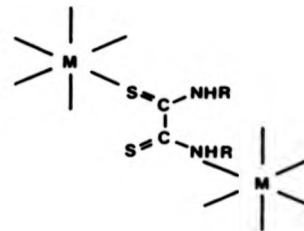
Trans-(S,S)-(IV), (N,N)-(V), and (S,N)-(VI) bridging structures where the ligand forms a bridge to two different metal centres, rather like the bridging role of the ligand in the antimony(III) complex with 1,4-dithiane¹⁰³ are other possibilities. Similar *cis*-(S,S)-, (N,N)-, bridges can be constructed.



IV

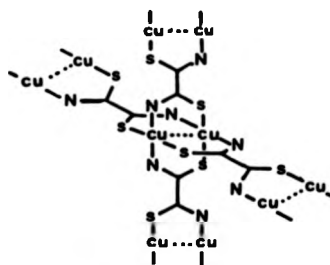


V

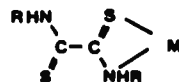


VI

An extension of the *trans* (S,S)- and *trans* (N,N)-bridging modes where the ligand uses all its donor atoms to bridge different metal centres has been suggested by Girerd and coworkers⁹²



One last bonding mode that has not been observed to date is that where the ligand bonds 'endo' to one metal centre.



Our interest in the coordination chemistry of dithiooxamide ligands is centred on the following considerations:

- (a) Since most of the complexes prepared so far

have been with transition metals, there is a natural extension of dithiooxamide chemistry to main-Group elements. A comparison between Group (VB) (As, Sb, Bi) halides in their trivalent state and Group (IV) halides of Ti and Sn seems most appropriate.

(b) Unusual (N,N)-bonded systems have been observed in complexes of Group (IV) halides¹⁰⁴ with dithiooxamide or thiourea whereas oxamides give predominantly (O,O)-bonded complexes with the same acceptors. An investigation of the products formed with N,N'-disubstituted dithiooxamides would furnish not only information regarding the effects of substitution at the amine centre on the nature of complex formed but also information on the interesting variety of donor schemes that might be expected.

(c) Again it would be useful to make a comparison between the donor properties of similar (S)- and (O)-bonded systems in terms of 'HSAB' and 'class (A)-class (B)' theories. Titanium(IV) which is normally described as a hard (class (A)) acid is a better electron acceptor towards sulphur (soft, class (B)) than oxygen in thioxan¹⁰⁵.

(d) Most of the complexes in the literature have been characterised on the basis of their spectroscopic properties. We sought to augment spectral assignments with some structural characterisation of both the ligands and the complexes.

(e) There is wide coverage of the reactions of dithiooxamide and related ligands in aqueous systems where deprotonation is a reality. An investigation of similar reactions in totally

anhydrous conditions would contribute to the evaluation of deprotonation and its influences on complex formation.

In this chapter we describe the syntheses and reactions of RHNC(S)C(S)NHR [$\text{R} = -\text{CH}_3$ (DMDTO), $-\text{C}_2\text{H}_5$ (DEDTO), $i\text{-C}_3\text{H}_7$ (DIPDTO), $n\text{-C}_4\text{H}_9$ (DBDTO), $-\text{C}_6\text{H}_{11}$ (DCXDTO), $-\text{CH}_2\text{C}_6\text{H}_5$ (DBZDTO)] with various Sb(III) , Bi(III) , Sn(IV) , and Ti(IV) halides. We also describe the crystal structures of two of the ligands namely: DEDTO and DIPDTO and those of the complexes $\text{SbCl}_3 \cdot \text{DEDTO}_{1.5}$, $\text{SbCl}_3 \cdot \text{DIPDTO}_{1.5}$, $\text{BiCl}_3 \cdot \text{DEDTO}_2$ and $\text{SnBr}_4 \cdot \text{DBDTO}$.

Synthesis and Characterisation of Dithiooxamides

Two general synthetic routes have been employed in the synthesis of dithiooxamide ligands:

(a) Preparation of the relevant oxamide from diethyloxalate followed by treatment with phosphorous pentasulphide¹⁰⁶. Only one of the dithiooxamide ligands namely $\text{N,N'$ -dimethyldithiooxamide has been successfully isolated following this route.

(b) As an alternative, many ligands were prepared by the modified Wallach reaction¹⁰⁷ as described by Woodburn and Scroog¹⁰⁸ where primary aliphatic amines are condensed with dithiooxamide. Spectroscopic data are listed in Tables 2.3.1 and 2.3.2.

2.2 THE CRYSTAL STRUCTURES OF N,N'-DIETHYL
DITHIOOXAMIDE (DETO) AND N,N'-DIISOPROPYL-
DITHIOOXAMIDE (DIPDIO)

The two ligands crystallise in the space group $P2_1/C$ as monomeric molecular units. Details of cell constants, data collection and refinement are given in Table 2.2.1. Atomic coordinates, bond distances and bond angles, and torsion angles (DETO) are presented in Tables 2.2.2, 2.2.3 and 2.2.4 respectively. Figure 2.2.1 shows the molecular geometry of DETO and Figure 2.2.2 that of DIPDIO. In both ligands the sulphur atoms are *trans* to one another. For DETO, there are two centrosymmetric ligands in the unit cell, similarly, centrosymmetric symmetry is crystallographically imposed in DIPDIO.

For DETO, the S-C-C-S torsion angle is 180° which shows that the ligand is completely planar. This planarity with a *trans* geometry is exhibited by dithiooxamide¹⁰⁹, and N,N'-bis(trimethyl silyl)dithiooxamide¹¹⁰. It is interesting that in all the structures investigated so far, N,N'-disubstitution does not alter the planar *trans* centrosymmetric structure observed in the parent dithiooxamide. Planarity favours the delocalisation of π -electron density along the SCCN moiety. The extent to which this occurs in the free ligand is indicated by the C-C bond length as compared to that of carbon-carbon single and double bonds. The value of 1.542 Å for DETO and similar values for dithiooxamide¹⁰⁹, N,N'-bis(trimethyl silyl)dithiooxamide¹¹⁰,

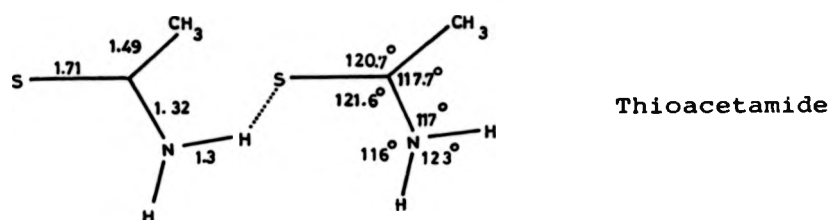
and DIPDTO suggest that there is hardly any delocalisation along the S-C-C-S part of the molecule. It is still curious that these molecules should be so accurately planar and yet have the central bond with the length of a single bond. As already stated, N,N-dimethyl substitution results in a non-planar cisoid structure¹¹¹. The C-C bond length (1.518 Å) in this molecule is surprisingly shorter than the corresponding C-C bond lengths in planar N,N'-disubstituted dithiooxamides but it still corresponds to the value of a single bond.

Turning to the S-C-N fragment of the molecule, the three molecular positions obviously describe a plane and hence possible charge delocalisation. Values for C-N and C-S bond lengths are intermediate between those expected for formal single and double bonds. For DEDTO, the C-S bond length (1.664 Å) is significantly shorter than the C-S single bond (1.88 Å) found in 1,4-dithiane¹⁰³ and the C-N bond length (1.305 Å) is shorter than the C-N single bond (1.472 Å) found in the same ligand. This decrease in C-S and C-N bond length values of the S-C-N moiety has been observed in structures of thiourea¹¹², ethylene-thiourea¹¹³, thioacetamide¹¹⁴, dithiooxamide¹⁰⁹, and its N,N'-disubstituted derivatives of which DIPDTO is no exception. The decrease has been explained in terms of delocalisation of electron density in the N-C-S moiety. This phenomenon is not unique to sulphur systems, it is also common to oxygen analogues, i.e. there is delocalisation in the NCO fragment as well. For DEDTO, the S-C-N_H^C torsion angle is close to zero

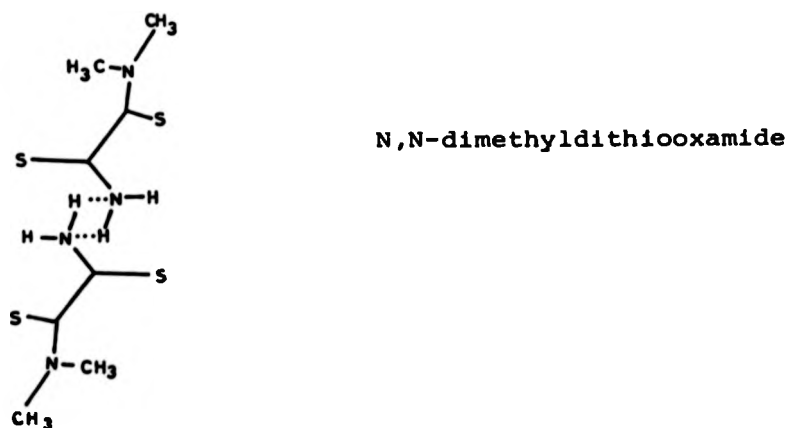
at 1.8° , however the C-N-C torsion angle is 83.7° . Such a wide variation of "C(4)" is not unexpected and can be ascribed to packing effects.

Hydrogen bonding has been a dominant feature of all the structures in this family of compounds.

In thioacetamide¹¹⁴ the structure consists of two molecules held together by hydrogen bonds:



Thiourea and ethylthiourea also exist as two molecules held together by hydrogen bonding; in dithiooxamide the packing arrangement is influenced by considerable hydrogen bonding; and in N,N-dimethyldithiooxamide¹¹¹ the $-NH_2$ ends of the two molecules are linked by hydrogen-bonds:



For DEDTO, there is only one N---S intermolecular contact that could represent a hydrogen bond, namely S(1)---N(3) of 3.50 Å with an S---H distance of 2.85 Å but this does seem rather long. There are no other intra-molecular distances of note less than the sum of van der Waal's radii. This is true for DIPDTO as well. It seems that partial substitution at the nitrogen centre greatly reduces the possibility of hydrogen bonding in the ligand as evidenced by its absence in N,N'-bis-(trimethylsilyl)dithiooxamide¹¹⁰, DEDTO, and DIPDTO, although all three structures have this curious habit of two molecules in the unit cell.

For DEDTO, there is only one N---S intermolecular contact that could represent a hydrogen bond, namely S(1)---N(3) of 3.50 Å with an S---H distance of 2.85 Å but this does seem rather long. There are no other intra-molecular distances of note less than the sum of van der Waal's radii. This is true for DIPDTO as well. It seems that partial substitution at the nitrogen centre greatly reduces the possibility of hydrogen bonding in the ligand as evidenced by its absence in N,N'-bis-(trimethylsilyl)dithiooxamide¹¹⁰, DEDTO, and DIPDTO, although all three structures have this curious habit of two molecules in the unit cell.

Figure 2.2.1 Molecular Geometry of DEDTO

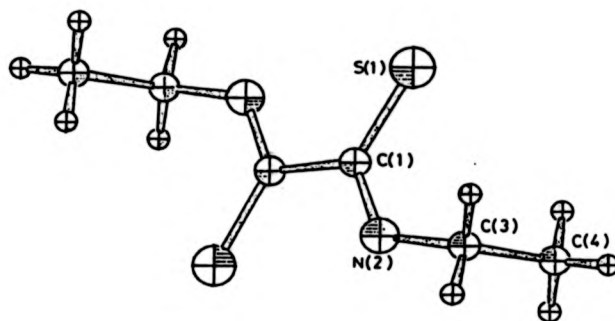


Figure 2.2.2 Molecular Geometry of DIPDTO

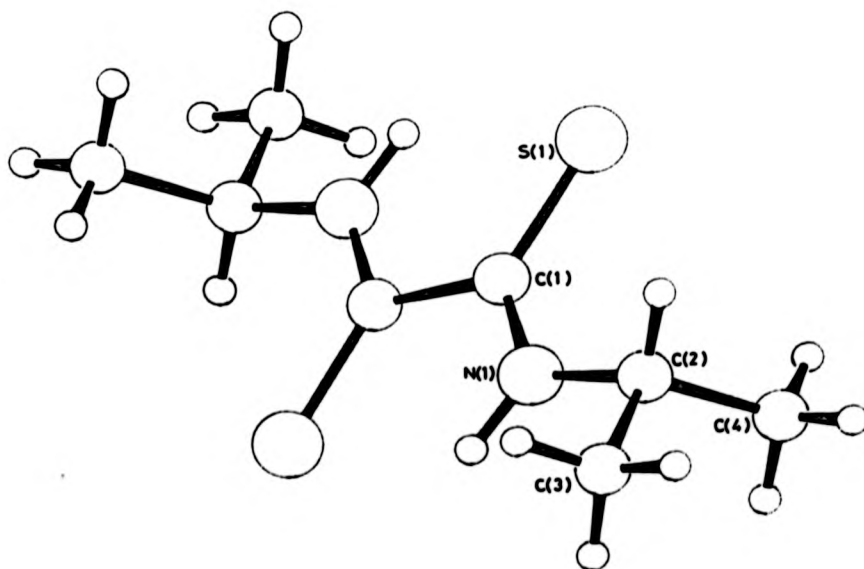


Table 2.2.1 Crystal Data and Refinement Details for DEDTO and DIPDTO

Compound	DEDTO	DIPDTO
Formula	$C_6H_{12}N_2S_2$	$C_8H_{16}N_2S_2$
M	176.2	204
Crystal class	Monoclinic	Monoclinic
Space group	$P2_1/c$	$P2_1/c$
Absences	$(h,0,l), l = 2n + 1$ $(0,k,0), k = 2n + 1$	$(h,0,l), l = 2n + 1$ $(0,k,0), k = 2n + 1$
$a(\text{\AA})$	4.502(7)	6.226(7)
$b(\text{\AA})$	6.024(9)	8.067(11)
$c(\text{\AA})$	16.425(11)	11.187(12)
$\beta(^{\circ})$	91.3(1)	91.0(1)
$V(\text{\AA}^3)$	445.3	561.8
Z	2	2
μ (cm^{-1})	5.13	4.16
D_m (g cm^{-3})	1.33	not done
D_c (g cm^{-3})	1.32	1.21
$\lambda(\text{\AA})$	0.7107	0.7107
F(000)	188	220
Crystal size (mm)	0.8 x 0.2 x 0.5	1.8 x 0.5 x 0.25
Rotation axis	a	a
$2\theta_{\text{max}}$ ($^{\circ}$)	50	50
No. of data	750	1028
Criterion for data inclusion	$> 3\sigma(I)$	$> 2\sigma(I)$
No. of data in refinement	495	630
R	0.061	0.077

Table 2.2.2 Atomic Coordinates ($\times 10^4$) for DEDTO
and DIPDTO with Estimated Standard
Deviations in Parentheses

DEDTO

ATOM	X	Y	Z
C(1)	1067(10)	125(9)	371(3)
S(1)	1506(4)	2546(2)	846(1)
N(2)	2378(9)	-1719(7)	592(3)
C(3)	2904(15)	-2329(10)	2068(4)
C(4)	4453(12)	-1979(10)	1291(3)

DIPDTO

ATOM	X	Y	Z
S(1)	2477(3)	1825(3)	365(2)
N(1)	8600(10)	1069(8)	1122(5)
C(2)	8526(12)	2412(10)	2003(7)
C(3)	6972(14)	1880(14)	2996(7)
C(1)	10175(11)	742(9)	400(6)
C(4)	7873(14)	4033(11)	1396(8)

Table 2.2.3 Bond lengths (\AA) and Angles ($^\circ$) in
DEDTO and DIPDTO

DEDTO

S (1)	-	C (1)		1.664 (5)	
C (1)	-	N (2)		1.305 (6)	
C (1)	-	C (1***)		1.542 (6)	
N (2)	-	C (3)		1.472 (6)	
C (3)	-	C (4)		1.483 (8)	
S (1)	-	C (1)	-	C (1***)	121.4 (3)
N (2)	-	C (1)	-	C (1***)	114.0 (4)
C (1)	-	N (2)	-	C (3)	125.6 (4)
N (2)	-	C (3)	-	C (4)	112.6 (4)

Equivalent Positions

***-x, -y, -z

DIPDTO

S(1)	-	C(1)	1.680(7)		
N(1)	-	C(2)	1.466(9)		
N(1)	-	C(1)	1.308(8)		
C(2)	-	C(3)	1.546(10)		
C(2)	-	C(4)	1.526(11)		
C(1)	-	C(1***)	1.508(14)		
C(2)	-	N(1)	-	C(1)	126.7(6)
N(1)	-	C(2)	-	C(3)	107.8(6)
N(1)	-	C(2)	-	C(4)	110.2(6)
C(3)	-	C(2)	-	C(4)	113.1(7)

DIPDTO (Continued)

S(1)	-	C(1)	-	N(1)	124.0(5)
S(1)	-	C(1)	-	C(1***)	121.3(5)
C(1***)	-	C(1)	-	N(1)	115.0(6)

Equivalent Positions

***2-x,-y,-z

Table 2.2.4 Torsion Angles ($^{\circ}$) for DEDTO

S(1)	-	C(1)	-	N(2)	-	C(3)	1.8
S(1)	-	C(1)	-	C(1 ^{III})	-	S(1 ^{III})	180.0
C(1)	-	N(2)	-	C(3)	-	C(4)	83.7

2.3 REACTIONS OF DITHIOOXAMIDES WITH GROUP (VB) HALIDES

Preparation of the complexes follows direct equimolar addition of the appropriate N,N'-disubstituted dithiooxamide (L) and covalent metal halide. This leads to complexes of the following types: $\text{MX}_3\text{L}_{1.5}$ (M = Sb; X = Cl, Br) and BiCl_3L_2 . These stoichiometries appear to be unaffected by either conditions of mixing or the quantities of reactants. These reactions were carried out in neutral conditions; benzene was the solvent of choice for antimony(III) complexes while solubility made acetone a better solvent for bismuth(III) complexes. The antimony(III) adducts were purified by washing with n-hexane and pumping *in vacuo*. They were all handled in strict seclusion of air and moisture because antimony trichloride is known to easily hydrolyse. Solubility of antimony complexes is limited to polar organic solvents. They are all insoluble in non-coordinating solvents. Conductivity data in MeCN solutions showed, over a range of concentrations that the complexes were essentially non-conducting.

All complexes are listed in Table 2.3.1. Although several attempts were made, no arsenic(III) complexes could be isolated to complete the As, Sb, Bi "trio" of Group (VB) metals. This was rather disappointing because the N,N'-tetrasubstituted dithiooxamides $\text{R}_2\text{NCSCSNR}_2$ (R = Me, Et) have been reported to form complexes with AsX_3 (X = Cl, Br) as well as SbX_3 and

BiX_3 , ($\text{X} = \text{Cl}, \text{Br}, \text{I}$) in very strong acid conditions^{93(f)}. The adducts are hydrolytically unstable. Addition of water resulted in hydrolysis in every case. As a general rule, Sb(III) and Bi(III) complexes show a greater thermal and hydrolytic stability than their As(III) counterparts. In solution, as well as in the solid state, bismuth complexes with dithiooxamides are much less stable than those of antimony; decomposition, even when sealed under vacuum, was a constant feature of all solid bismuth adducts.

Principal i.r. bands are listed in Table 2.3.1. Assignments are based on those used by Desseyne and Herman¹¹⁵⁻¹¹⁷. Of particular interest are the changes in $\nu(\text{CS})$ and $\nu(\text{CN})$ bands on complexation. Conclusions reached on the question of possible donor sites are based on these changes in i.r. spectra. [N.B. The bands rarely represent pure vibrational modes and assignments are only indicative of the major constituent of a particular band.] A shift to lower frequency of the composite thioamide IV band* ($\sim 870 \text{ cm}^{-1}$ and with a high $\nu(\text{CS})$ contribution) accompanied by a corresponding shift to higher frequency of the thioamide I band ($\sim 1520 \text{ cm}^{-1}$ and with a major $\nu(\text{CN})$ contribution) is a confirmation of the donor role of (S)-atoms. The shift to higher frequency of the thioamide I band may be accompanied by a shift to higher frequency of the $\nu(\text{NH})$ band ($\sim 3160 \text{ cm}^{-1}$). In the spectra of the free ligands, the $\nu(\text{CN})$ band ($\sim 1520 \text{ cm}^{-1}$) is a mass-sensitive band which shifts to lower frequency with increasing substitution at the nitrogen centres. This

*The terms 'Thioamide I Band' and 'Thioamide IV Band' are borrowed from Desseyne and Herman¹¹⁵.

Table 2.3.1 Principal i.r. bands (cm^{-1}) for Metal Complexes

Compound	$\nu(\text{NH})$ (s)	i.r. (Nujol)		(MS/MX) (m)	(C=O) (s,br)
		Thioamide I $\nu(\text{CN})(\text{s})$	Thioamide IV $\nu(\text{CS})(\text{m})$		
DMDTO	3179	1540	872		
$\text{SbCl}_3(\text{DMDTO})_{1.5}$	3250, 3266	1571	851	330, 287, 264	
$\text{SbBr}_3(\text{DMDTO})_{1.5}$	3222	1563	853	305, 226	
$\text{BiCl}_3(\text{DMDTO})_2(\text{Me}_2\text{CO})$	3190	1570	861	290, 245	1695
DEDTO	3166	1523	840		
$\text{SbCl}_3(\text{DEDTO})_{1.5}$	3210, 3180	1570, 1543	820	325, 301, 262	
$\text{SbBr}_3(\text{DEDTO})_{1.5}$	3200, 3175	1566, 1542	823	325, 208	
$\text{BiCl}_3(\text{DEDTO})_2(\text{Me}_2\text{CO})$	3180	1550	801, 820	240	1695
DIPDTO	3147	1513	890		
$\text{SbCl}_3(\text{DIPDTO})_{1.5}$	3160	1542	852	351, 314, 290, 241	
$\text{SbBr}_3(\text{DIPDTO})_{1.5}$	3163	1528	850	372, 210	
$\text{BiCl}_3(\text{DIPDTO})_2(\text{Me}_2\text{CO})$	3160	1540	846	240	1680
DBDTO	3180	1520	888		
$\text{SbCl}_3(\text{DBDTO})_{1.5}$	3182	1539	849	313, 295	
$\text{SbBr}_3(\text{DBDTO})_{1.5}$	3181	1525	845	-	
$\text{BiCl}_3(\text{DBDTO})_2(\text{Me}_2\text{CO})$	3172	1545	825	240	1695
DCXDTO	3150	1507	872		
$\text{SbCl}_3(\text{DCXDTO})_{1.5}$	3158	1545	859, 835	349, 328, 287	
$\text{SbBr}_3(\text{DCXDTO})_{1.5}$	3159	1530	859, 831	-	
DBZDTO	3170	1519	874		
$\text{SbCl}_3(\text{DBZDTO})_{1.5}$	3172	1534	859	350, 308, 220	
$\text{SbBr}_3(\text{DBZDTO})_{1.5}$	3160	1532, 1520	855	280, 225	
$\text{BiCl}_3(\text{DBZDTO})_2$	3165	1522	850		1680

band appears at even lower frequencies in the N,N'-tetrasubstituted ligand^{93(f)}.

Table 2.3.1 shows that for all antimony(III) and bismuth(III) complexes there is a shift, to higher energy, of the thioamide I [$\nu(\text{CN})$] band, indicative of increased C-N bond order; this is accompanied by a corresponding shift to lower frequencies, of the thioamide IV [$\nu(\text{CS})$] band, indicative of decreased C-S double bond character. This decrease in double bond character implies an electron drain from the sulphur to the metal centre hence the conclusion that ligand binding is *via* sulphur.

The shift to higher frequency of $\nu(\text{CN})$ is much greater than the respective decrease of $\nu(\text{CS})$, i.e. the increase in double bond character of $\nu(\text{CN})$ is not compensated by the decrease in that of $\nu(\text{CS})$. The implication is that bond order in the C-N bond is maintained mainly by delocalisation from the NHR group and is thus little affected by changes in $\text{C}=\text{S}$. In the i.r. spectra of dithiooxamides and their substituted derivatives, a band at 1430 cm^{-1} has been assigned in the past to $\nu(\text{C}=\text{S})$ as compared to $\nu(\text{C}=\text{O})$ at 1660 cm^{-1} 104,118. If this assignment was correct, then this band ($\sim 1430\text{ cm}^{-1}$) would be expected to shift to lower frequency upon sulphur coordination, no such shift has been observed with Group (VB) complexes so if there is a $\nu(\text{C}=\text{S})$ contribution to this band at all, it is very small.

For BiCl_3 complexes, there is a consistent band at 1695 cm^{-1} due to inclusion of a molecule of acetone in

the crystal lattice as supported by X-ray crystallography.

Assigning peaks in the low energy region of the spectrum is made very difficult by the range and multiplicity of modes. $\nu(\text{Sb-Cl})$ bands appear in the region $320\text{--}350\text{ cm}^{-1}$ ^{93(f)} while those of Sb-Br appear at $210\text{--}230\text{ cm}^{-1}$. $\nu(\text{Bi-Cl})$ bands appear in the region below 190 cm^{-1} which was not investigated. Bands assignable to the ring vibrational frequency of $\begin{array}{c} \text{C} \text{---} \text{S} \\ | \quad \diagup \\ \text{C} \text{---} \text{S} \end{array} \text{M}$ have not been looked into for the same reason. Sb-S bands are expected to appear in the region $280\text{--}300\text{ cm}^{-1}$ while Bi-S bands are expected at $240\text{--}245\text{ cm}^{-1}$. M-S bands are generally mass-sensitive, so their position is generally affected by the metal centre as well as its other substituents. In general, bands observed in the region below 400 cm^{-1} comprise metal-halide, metal-ligand [$\nu(\text{M-S})$] and perhaps some ring deformational vibration components (where chelate rings are formed) with no clear delineation possible.

For complexes of N,N' -disubstituted dithiooxamides the presence of strong $\nu(\text{N-H})$ bands at $3100\text{--}3280\text{ cm}^{-1}$ is a clear indication that complex formation in neutral, non-aqueous solutions does not call for deprotonation at the amine centre. This observation is augmented by both ^1H n.m.r. and X-ray crystallographic findings. From i.r. evidence we can therefore make the following two conclusions:

- (a) there is no deprotonation of the amine centre of dithiooxamides on complexation;
- (b) for Group (VB) halides, the ligand binds

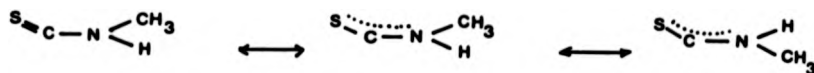
the metal through the sulphur.

Once sulphur coordination has been established, chemical intuition backed by considerations of the chelate stabilisation effect has led to the assumption that *cis* (S,S)-chelate formation rather than (S,S)-bridging would be the preferred bonding mode. The structural resolution of some of these Group (V) complexes namely $\text{SbCl}_3 \cdot \text{DEDTO}_{1.5}$; $\text{SbCl}_3 \cdot \text{DIPDTO}_{1.5}$ and $\text{BiCl}_3 \cdot \text{DEDTO}_2$ shows that both bonding modes are possible depending on the particular metal centre.

^1H n.m.r. spectra are given in Table 2.3.2.

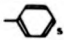
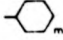
^1H n.m.r. Spectra of the Ligands:

The spectrum of DMDTO ($\text{R} = -\text{CH}_3$) shows a broad, 2H singlet at δ 10.47 for the amide protons indicating an exchange process and hence no coupling is expected for -N-H with the CH_3 protons. In CDCl_3 , the 6H peak for - CH_3 protons centred at δ 3.30 appears as a doublet and not a singlet because of the restricted rotation along the amide $[\text{SC}-\text{N}(\text{H})\text{CH}_3]$ bond caused by the partial double bond character.



It appears that the two $\text{SCN}(\text{H})\text{CH}_3$ moieties are 'equivalent' in CDCl_3 . The spectrum of this ligand in d^6 -acetone shows further splitting of these peaks into a quartet. The spectrum of DEDTO shows the broad, amide, 2H singlet at δ 10.28, a 4H multiplet for the - CH_2 - protons due to spin-spin coupling with the - CH_3 protons further

Table 2.3.2 ^1H n.m.r. Data δ ppm with reference to TMS ($\tau = 0$)

Compound	NH s,br	CH m	CH ₂	CH ₂ m	CH ₂ m	CH ₃		
DMDTO	10.47					3.30 d		
SbCl ₃ (DMDTO) _{1.5}	10.47					3.27 d		
SbBr ₃ (DMDTO) _{1.5}	10.29					3.30 d		
BiCl ₃ (DMDTO) ₂	10.28					3.30 d		
DEDTO	10.28		3.76 m			1.39 t		
SbCl ₃ (DEDTO) _{1.5}	10.24		3.76 m			1.39 t		
SbBr ₃ (DEDTO) _{1.5}	10.24		3.74 m			1.37 t		
BiCl ₃ (DEDTO) ₂	10.40		3.79 m			1.32 t		
DIPDTO	10.17	4.48				1.37 d		
SbCl ₃ (DIPDTO) _{1.5}	10.19	4.49				1.38 d		
SbBr ₃ (DIPDTO) _{1.5}	10.20	4.48				1.37 d		
BiCl ₃ (DIPDTO) ₂	10.19	4.50				1.36 d		
DBDTO	10.27		3.72 m	1.74	1.47	1.00 t		
SbCl ₃ (DBDTO) _{1.5}	10.31		3.37 m	1.76	1.47	0.98 t		
SbBr ₃ (DBDTO) _{1.5}	10.31		3.73 m	1.74	1.46	0.98 t		
BiCl ₃ (DBDTO) ₂	10.34		3.70 m	1.73	1.46	0.97 t		
DBZDTO	10.44		4.85 d				7.35	
SbCl ₃ (DBZDTO) _{1.5}	10.56		4.91 d				7.38	
SbBr ₃ (DBZDTO) _{1.5}	10.50		4.91 d				7.39	
BiCl ₃ (DBZDTO) _{1.5}	10.44		4.89 d				7.36	
DCXDTO	10.34							4.26-1.46
SbCl ₃ (DCXDTO) _{1.5}	10.27							4.21-1.45
SbBr ₃ (DCXDTO) _{1.5}	10.32							4.25-1.46

complicated by 'amide rotation' as discussed above; and a 6H triplet at δ 1.39 which is fairly well resolved presumably because the $-\text{CH}_3$ protons are at least two bondlengths away from the S-CN moiety and are much less affected by any changes in amide double bond character. The isopropyl species DIPDTO shows a 12H doublet for the $-\text{CH}_3$ protons at δ 1.37 due to spin-spin coupling with the $-\text{CH}$ proton; the 2H resonance ($-\text{C}-\text{H}$) at δ 4.48 is a multiplet complicated by both spin-spin coupling with the methyl groups as well as amide rotation. The spectrum of the n-butyl derivative follows the classic pattern: a 6H triplet at δ 1.00 for the $-\text{CH}_3$, a 4H sextet at δ 1.47 for the adjacent $-\text{CH}_2-$, a 4H pentaplet at δ 1.74 for the next $-\text{CH}_2-$, and a 4H quartet at δ 3.72 for the $-\text{CH}_2-$ closest to the NH. The benzyl derivative shows a 10H singlet at δ 7.35, indicating magnetic equivalence of all the aromatic protons, and a 4H doublet at δ 4.85 for the $-\text{CH}_2-$ due to amide rotation. The cyclohexyl derivative shows the characteristic cyclohexyl multiplet. The N-H proton appears as a broad singlet in all the ligands.

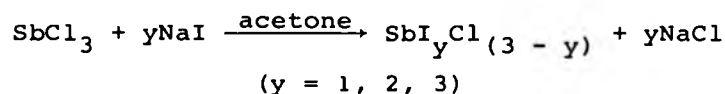
¹H n.m.r. Spectra of the Complexes:

As is evident from Table 2.3.2, there are no conspicuous changes in chemical shift values for N(H)R groups following complexation. This is not surprising since the sort of changes we are anticipating are on protons that are at least four bond distances away from the metal centre. Also there are no changes in multiplicity. There is evidence that in solution, there is only weak binding of ligand to metal (hence minimal effect on chemical shift

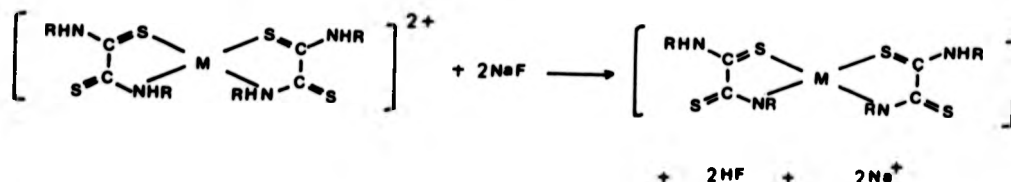
values of the alkyl groups). Results from cryoscopic molecular weight determinations of some of the antimony(III) complexes in benzene, suggest some degree of dissociation in solution.

Halide Exchange

SbCl_3 complexes with dithiooxamides attack CsI infrared plates on exposure to air. In a preliminary investigation, an acetone solution of SbCl_3 was added to a solution of NaI in acetone to give insoluble NaCl and an intensely coloured reddish brown powder which was not characterised any further. This is a recognised method for $\text{Cl} \rightleftharpoons \text{I}$ exchange¹¹⁹. We therefore propose the following reaction:



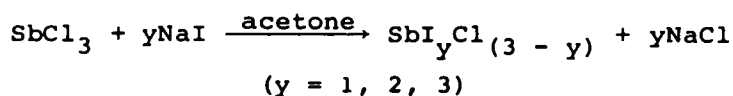
This reaction occurs even in the solid state; all SbCl_3 complexes give this brown powder when ground with NaI . This could be a means of preparing mixed halide $\text{SbI}_y\text{Cl}_{(3-y)}$ N,N' -disubstituted dithiooxamide complexes. The recent publication of the reaction between complexes of $\text{M}^{(\text{II})}(\text{LH}_2)_2$ ($\text{M} = \text{Ni}, \text{Pd}, \text{Pt}$) with NaF in the solid state to give $\text{M}^{(\text{II})}(\text{LH})_2$ ¹⁰², provides a useful comparison; here the apparent reaction is:



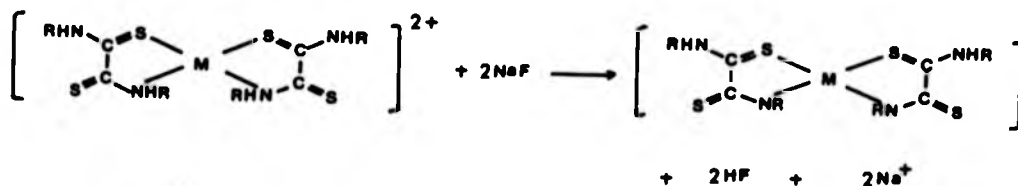
values of the alkyl groups). Results from cryoscopic molecular weight determinations of some of the antimony(III) complexes in benzene, suggest some degree of dissociation in solution.

Halide Exchange

SbCl_3 complexes with dithiooxamides attack CsI infrared plates on exposure to air. In a preliminary investigation, an acetone solution of SbCl_3 was added to a solution of NaI in acetone to give insoluble NaCl and an intensely coloured reddish brown powder which was not characterised any further. This is a recognised method for $\text{Cl} \rightleftharpoons \text{I}$ exchange¹¹⁹. We therefore propose the following reaction:



This reaction occurs even in the solid state; all SbCl_3 complexes give this brown powder when ground with NaI . This could be a means of preparing mixed halide $\text{SbI}_y\text{Cl}_{(3-y)}$ N,N'-disubstituted dithiooxamide complexes. The recent publication of the reaction between complexes of $\text{M}^{(\text{II})}(\text{LH}_2)_2$ ($\text{M} = \text{Ni}, \text{Pd}, \text{Pt}$) with NaI in the solid state to give $\text{M}^{(\text{II})}(\text{LH})_2$ ¹⁰², provides a useful comparison; here the apparent reaction is:



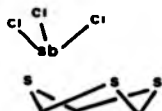
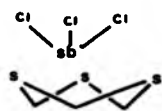
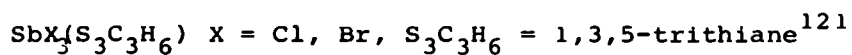
It is unlikely that the reaction between SbCl_3 dithiooxamide complexes and NaI or CsI will result in the deprotonation of the amine centre; but it is likely to be accompanied by loss of the ligand since SbI_3 is a poorer acceptor than SbCl_3 .

2.4 THE CRYSTAL STRUCTURE OF $\text{SbCl}_3(\text{DEDTO})_{1.5}$

The bright orange crystals of $\text{SbCl}_3(\text{DEDTO})_{1.5}$ belong to the C2/c space group. Crystal data and refinement details are given in Table 2.4.1 while atomic parameters, bond lengths and angles, and torsion angles ($\text{SbCl}_3.\text{DEDTO}_{1.5}$) are given in Tables 2.4.2, 2.4.3 and 2.4.4 respectively. The structure is polymeric (Figure 2.4.1) with SbCl_3 units connected by ligand molecules which form bidentate bridges to separate Sb atoms. In the unit cell, each antimony assumes a distorted octahedral environment with bonds to three chlorine and three sulphur atoms. The Sb-Cl bond distances of 2.340(s), 2.388(3) and 2.381(3) Å are virtually unchanged from those of pure crystalline SbCl_3 (2.38 Å)³¹. The Cl-Sb-Cl angles lie in the range 92.4(1)-95.8(2)° as compared with those in the starting SbCl_3 (94.2-95.7°). Three sulphur atoms approach to the metal octahedral positions for a *fac*-isomer with Sb-S distances 3.212(3), 3.396(3) and 3.165(3) Å reflecting very weak Sb---S interactions. This is consistent with the spectral changes observed in i.r. and ¹H n.m.r. This loose Sb---S association is only significant in the solid state since we cannot rule out dissociation to free ligand and antimony trichloride in solution.

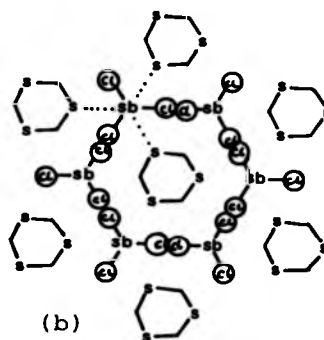
It has been suggested¹²⁰ that the strength of the M-S bond formed will be reflected by the change in S-C bond length. For a strong M-S bond, C-S should

get longer on complexation. There is hardly any significant change in C-S bond length on complexation in the present instance. This again underlines the fact that only a very weak bond is formed between DEDTO and SbCl_3 . Complexes with cyclic thioethers form a good comparison:



(a)

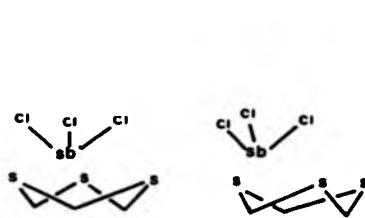
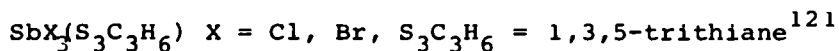
Molecular arrangement
in $\text{SbCl}_3(\text{S}_3\text{C}_3\text{H}_6)$



(b)

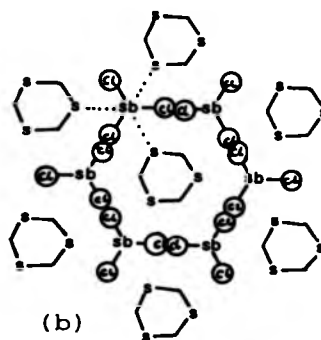
In this structure, the Sb atom possesses the particular six coordination similar to that observed in $\text{SbCl}_3 \cdot \text{DEDTO}_{1.5}$. Antimony is bound to three chlorine (Br) atoms at 2.375 \AA (2.521 \AA) in a plane above the antimony forming a trigonal pyramid with Sb at the apex, and to three symmetrically equivalent sulphur atoms with bond distances of 3.258 \AA (3.347 \AA); all three sulphur atoms are again in a plane below the antimony forming a trigonal pyramid with Sb at the apex. This six-coordinate arrangement is also observed in $\text{SbCl}_3(\text{S}_2\text{C}_5\text{H}_{10})^{122}$ ($\text{S}_2\text{C}_5\text{H}_{10}$ - 1,4-dithiacycloheptane).

get longer on complexation. There is hardly any significant change in C-S bond length on complexation in the present instance. This again underlines the fact that only a very weak bond is formed between DEDTO and SbCl_3 . Complexes with cyclic thioethers form a good comparison:



(a)

Molecular arrangement
in $\text{SbCl}_3(\text{S}_3\text{C}_3\text{H}_6)$



(b)

In this structure, the Sb atom possesses the particular six coordination similar to that observed in $\text{SbCl}_3 \cdot \text{DEDTO}_{1.5}$. Antimony is bound to three chlorine (Br) atoms at 2.375 \AA (2.521 \AA) in a plane above the antimony forming a trigonal pyramid with Sb at the apex, and to three symmetrically equivalent sulphur atoms with bond distances of 3.258 \AA (3.347 \AA); all three sulphur atoms are again in a plane below the antimony forming a trigonal pyramid with Sb at the apex. This six-coordinate arrangement is also observed in $\text{SbCl}_3(\text{S}_2\text{C}_5\text{H}_{10})^{122}$ ($\text{S}_2\text{C}_5\text{H}_{10}$ - 1,4-dithiacycloheptane).

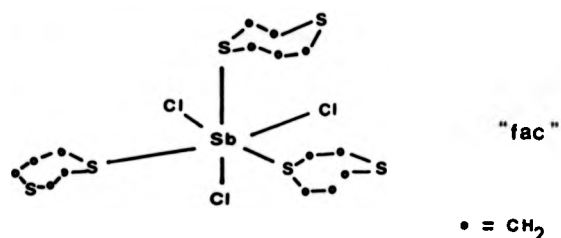
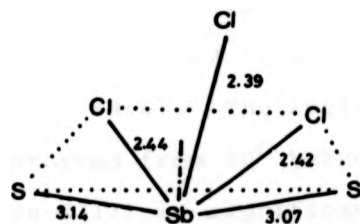


Figure 2.4.2 $\text{SbCl}_3(\text{S}_2\text{C}_5\text{H}_{10})$
 Sb-S 3.13, 3.23, and 3.40 Å

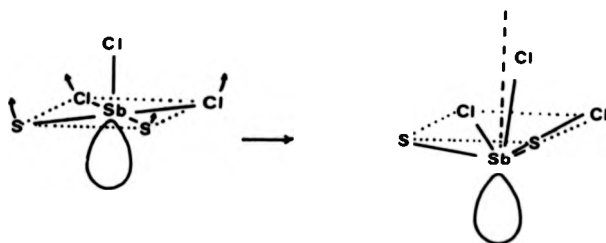
These complexes are referred to as 'weak' in respect of their Sb-S bond lengths and their instability other than in the solid state. This description may be extended to $\text{SbCl}_3(\text{S}_2\text{C}_4\text{H}_8)$ $\text{S}_2\text{C}_4\text{H}_8 = 1,4\text{-dithiane}$ (Sb-S = 3.135, 3.065 Å)¹⁰³. Here we observe an interesting structure where the antimony is in a five coordinate geometrical environment. Each antimony is bonded to three chlorine and two sulphur atoms from separate 1,4-dithiane molecules.

The arrangement of atoms has been interestingly described as an extremely distorted octahedron whose apexes are occupied by one antimony atom and one chlorine atom. The two other chlorines and the two sulphur atoms form a plane; the apex-chlorine lies 2.071 Å above this plane with Sb at 0.273 Å below.



The metal environment
 in $\text{SbCl}_3(\text{S}_2\text{C}_4\text{H}_8)$

The above description does not take into consideration the structural influences of the lone pair of electrons associated with antimony (III). We would favour a description in terms of an octahedral environment around the five coordinate antimony with the lone pair occupying the sixth position of the octahedron.



The observed distortions in bond angles are consistent with the effects of the lone pair as predicted by Rule 2 of VSEPR.

With reference to the six-coordinate structure of $\text{SbCl}_3(\text{DEDT})_{1.5}$ (Figure 2.4.1), the bond angles show a definite distortion from a regular octahedron as might be expected given the varied bond lengths. The atom S(11) is significantly further away ($3.396(3) \text{ \AA}$) from the metal centre than the other two sulphur atoms Sb-S (mean) 3.186 \AA . We will therefore define an equatorial plane with atoms Sb, S(5), S(1¹), Cl(3) and Cl(1) which is almost planar (maximum deviation 0.08 and mean deviation 0.05 \AA). In this plane the inter ligand angles S-Sb-S 92.2° , and Cl-Sb-Cl 92.4° are greater than those for Cl-Sb-S 86.5° , 88.8° . The angles involving S(11) are far more distorted from 90° being 85.9 , 95.3 , 70.5 and 105.0° . Thus S(11) is significantly tilted from the axial position

towards S(1¹) and away from Cl(1). This could suggest that the lone pair is operative between Cl(1) and S(11) but this seems unlikely as it does not fit any obvious mode of deformation from O_h symmetry observed when the lone pair is stereochemically active. A trigonal distortion (C_{3v}) with the lone pair located in the face defined by Cl(1), S(11), S(5) and assuming full stereochemical activity would constitute a seven-coordinate system on the VSEPR model⁵. The resulting molecule would have C_{3v} symmetry. The structure of $SbCl_3(S_2C_5H_{10})$ (Figure 2.4.2), is an analogous structure, wherein the antimony does coordinate preferentially with two of its three nearest sulphur neighbours. This preferential bonding is not the rule because the structure of $SbCl_3(S_3C_3H_6)$ shows three symmetrically equivalent sulphur atoms. The rationale by Schmidt *et al.*¹²² that Sb(III) can achieve an enhanced bonding situation *via* a coordination increase from five to six to form linked distorted octahedra at the expense of stereochemical involvement of the lone pair of electrons seems equally applicable to the $SbCl_3 \cdot (DEDTO)_{1.5}$ case. Because of steric interactions between the ligands and the general bulkiness of DEDTO and other similar ligands, significant crowding of the Sb(III) environment might reasonably be expected should the ligand be more closely attached. As it is, there are no significant intermolecular contacts between the ligands and the $SbCl_3$ unit.

As is apparent in Figure 2.4.1 there are two polymeric chains of $(SbCl_3L)_n$ which are connected by an additional

ligand over centres of symmetry. It is probably significant that this additional ligand is more weakly bound than the other two although we cannot find any non-bonded contacts to account directly for this increased value.

It is interesting that the Sb-S-C angles are $100.8(4)$, $90.4(3)$ and $102.8(3)^\circ$, roughly what one might expect if the Sb-S bonds were far shorter. This supports our view that the Sb-S interactions represent bonding even though it may be of a very weak nature. The conformations of the two ligands are very similar in that they are both *trans* with S-C-C-S torsion angles of $-173.3(1)$ and 180° . Also the S-C-N-C angles are *ca.* 0° , being -1.2 and -3.7° . (So the ligand maintains its planar structure within the complex.) This should bring the -NHR proton fairly close to the other sulphur atom in the ligand; however, the geometry is still not suitable for a hydrogen bond, despite S---N, S---H distances of 2.9 and 2.4 Å, since the angles C-S---H and N-H---S are 71.1 and 115.7° respectively. The only difference in conformation between the two ligands involves the position of the last carbon atom C(4). Torsion angles C(5)-N(6)-C(7)-C(8) and C(11)-N(12)-C(13)-C(14) are 167.8 and 117.0° respectively.

Figure 2.4.1 The Crystal Structure of $\text{SbCl}_3 \cdot \text{DEDTO}_{1.5}$

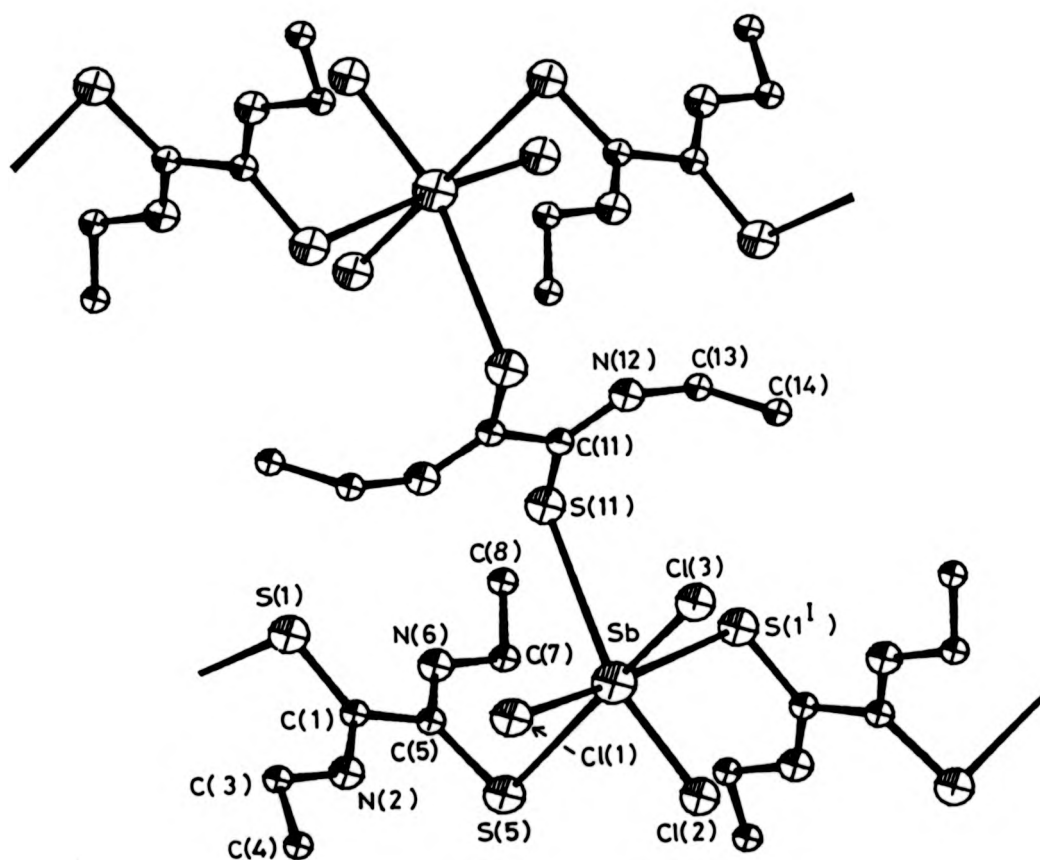


Table 2.4.1 Crystal Data and Refinement Details for $\text{SbCl}_3 \cdot \text{DEDTO}_{1.5}$ and $\text{SbCl}_3 \cdot \text{DIPDPO}_{1.5}$

Compound	$\text{SbCl}_3 \cdot \text{DEDTO}_{1.5}$	$\text{SbCl}_3 \cdot \text{DIPDPO}_{1.5}$
Formula	$\text{C}_9\text{H}_{18}\text{Cl}_3\text{N}_3\text{S}_3\text{Sb}$	$\text{C}_{12}\text{H}_{24}\text{Cl}_3\text{N}_3\text{S}_3\text{Sb}$
M	492.4	534.13
Crystal class	Monoclinic	Rhombohedral
Space group	C2/c	$R\bar{3}$
Absences	$(h,0,l), l = 2n + 1$ $(h,k,l), h + k = 2n + 1$	None
a (Å)	30.84 (1)	11.80 (1)
b (Å)	9.37 (1)	11.80 (1)
c (Å)	13.96 (1)	11.80 (1)
α (°)	(90)	60.1 (1)
β (°)	107.0 (1)	60.1 (1)
γ (°)	(90)	60.1 (1)
V (Å ³)	3857.8	1164.4
Z	8	2
ρ (cm ⁻¹)	21.6	17.96
D_m (g cm ⁻³)	1.70	not possible
D_c (g cm ⁻³)	1.70	1.53
μ (Å)	0.7107	0.7107
F(000)	1944	534
Crystal size (mm)	0.5 x 0.5 x 0.55	0.5 x 0.7 x 0.35
Rotation axis	C	(110)
$2\theta_{\text{max}}$ (°)	50	50
Number of data measured	3,783	3,618
Number of data used in refinement	1,991	1,089
Criterion for data inclusion	2σ (1)	3σ (1)
Final R value	0.055	0.068

Table 2.4.2 (a) Atomic Coordinates ($\times 10^4$) for $\text{SbCl}_3 \cdot \text{DEDTO}_{1.5}$ with Estimated Standard Deviations in Parentheses

ATOM	X	Y	Z
SB	1109 (0)	1952 (1)	-1853 (0)
S(1)	1311 (1)	524 (3)	1938 (2)
S(5)	490 (1)	-178 (3)	-1012 (2)
C(1)	962 (3)	618 (9)	927 (7)
N(2)	630 (3)	1514 (9)	813 (6)
C(3)	600 (5)	262 (13)	1558 (10)
C(4)	224 (5)	3577 (14)	1098 (13)
C(5)	912 (3)	-392 (9)	49 (6)
N(6)	1222 (3)	-1358 (9)	191 (6)
C(7)	1258 (5)	-2456 (12)	-504 (9)
C(8)	1687 (5)	-3191 (13)	-253 (11)
S(11)	2113 (1)	575 (3)	-454 (2)
C(11)	2471 (3)	1919 (10)	-398 (6)
N(12)	2728 (3)	2094 (9)	-993 (6)
C(13)	2767 (7)	1120 (15)	-1769 (11)
C(14)	2619 (5)	1704 (14)	-2750 (9)
CL(2)	462 (1)	2281 (3)	-3214 (2)
CL(3)	1555 (1)	3579 (3)	-2487 (3)
CL(1)	922 (2)	3728 (4)	-821 (3)

(b) Atomic Coordinates ($\times 10^5$ for Sb, $\times 10^4$ for other atoms) for $\text{SbCl}_3 \cdot \text{DIPDIO}_{1.5}$ with Estimated Standard Deviations in Parentheses

ATOM	X	Y	Z
SB(1)	23335 (7)	23335 (7)	23335 (7)
S(1)	5259 (2)	520 (3)	2829 (2)
CL(1)	3685 (3)	1613 (3)	3121 (3)
C(1)	5373 (8)	425 (8)	4279 (9)
N(1)	6095 (8)	1019 (8)	4297 (8)
C(2)	6883 (10)	1930 (10)	3072 (10)
C(3)	8371 (11)	1052 (11)	2456 (11)
C(4)	6869 (14)	2988 (13)	3497 (14)

Table 2.4.1 Bond Lengths (\AA) and angles ($^\circ$) in $\text{SbCl}_3 \cdot \text{DEDTO}_{1.5}$ (a) and $\text{SbCl}_3 \cdot \text{DIPDIO}_{1.5}$ (b)

(a) Metal Coordination Sphere in $\text{SbCl}_3 \cdot \text{DEDTO}_{1.5}$

SB	-	CL(2)	2.340 (3)		
SB	-	CL(3)	2.388 (3)		
SB	-	CL(1)	2.381 (3)		
SB	-	S (5)	3.212 (3)		
SB	-	S (11)	3.393 (3)		
SB	-	S (1*)	3.165 (3)		
CL(2)	-	SB	-	CL(3)	93.50 (13)
CL(2)	-	SB	-	CL(1)	95.79 (17)
CL(3)	-	SB	-	CL(1)	92.41 (12)
CL(2)	-	SB	-	S (1*)	88.73 (10)
CL(1)	-	SB	-	S (5)	86.46 (14)
CL(3)	-	SB	-	S (5)	178.59 (10)
CL(2)	-	SB	-	S (5)	85.51 (10)
S (5)	-	SB	-	S (11)	95.34 (07)
S (5)	-	SB	-	S (1*)	92.20 (07)
CL(2)	-	SB	-	S (11)	159.27 (10)
CL(3)	-	SB	-	S (11)	85.92 (10)
S (11)	-	SB	-	CL(1)	104.99 (12)
S (11)	-	SB	-	S (1*)	70.54 (07)
CL(1)	-	SB	-	S (1*)	175.22 (11)
CL(3)	-	SB	-	S (1*)	88.82 (10)

LIGAND DIMENSIONS IN $\text{SbCl}_3 \cdot \text{DEDTO}_{1.5}$

S(1)	-	C(1)	1.668(9)
S(5)	-	C(5)	1.673(9)
C(1)	-	N(2)	1.289(11)
C(1)	-	C(5)	1.523(13)
N(2)	-	C(3)	1.493(14)
C(3)	-	C(4)	1.470(17)
C(5)	-	N(6)	1.293(11)
N(6)	-	C(7)	1.462(13)
C(7)	-	C(8)	1.464(17)
S(11)	-	C(11)	1.660(10)
C(11)	-	N(12)	1.323(11)
C(11)	-	C(11**)	1.529(13)
N(12)	-	C(13)	1.428(15)
C(13)	-	C(14)	1.426(19)

(a) Metal Coordination Sphere in $\text{SbCl}_3 \cdot \text{DEDTO}_{1.5}$ (continued)

SB	-	S(1)	-	C(1)	100.8(4)
SB	-	S(5)	-	C(5)	90.4(3)
SB	-	S(11)	-	C(11)	102.8(3)
S(1)	-	C(1)	-	C(5)	120.6(6)
N(2)	-	C(1)	-	C(5)	114.4(7)
C(1)	-	N(2)	-	C(3)	124.6(8)
N(2)	-	C(3)	-	C(4)	109.4(11)
S(5)	-	C(5)	-	C(1)	120.4(6)
S(5)	-	C(5)	-	N(6)	124.7(6)
C(1)	-	C(5)	-	N(6)	113.9(7)
C(5)	-	N(6)	-	C(7)	125.1(8)
N(6)	-	C(7)	-	C(8)	112.6(9)
S(11)	-	C(11)	-	N(12)	125.6(7)
C(11)	-	N(12)	-	C(13)	125.1(10)
N(12)	-	C(13)	-	C(14)	113.3(11)
S(11)	-	C(11)	-	C(11**)	120.5(7)
C(11**)	-	C(11)	-	N(12)	114.1(8)

*,** refer to the following symmetry elements:

* $x, -y, \frac{1}{2} + z$

** $\frac{1}{2} - x, \frac{1}{2} - y, -z$

(b) $\text{SbCl}_3 \cdot \text{DIPDPO}_{1.5}$

SB(1)	-	CL(1)		2.413(2)	
SB(1)	-	S(1)		3.197(5)	
S(1)	-	C(1)		1.726(9)	
C(1)	-	N(1)		1.359(12)	
C(1*)	-	C(1)		1.537(16)	
N(1)	-	C(2)		1.488(12)	
C(2)	-	C(3)		1.533(14)	
C(2)	-	C(4)		1.552(16)	
S(1)	-	SB	-	CL(1)	79.2(18)
S(1)	-	SB	-	CL(1**)	89.6(18)
S(1)	-	SB	-	CL(1***)	171.5(16)
S(1)	-	SB	-	S(1*)	98.6(14)
CL(1)	-	SB	-	CL(1**)	92.5(2)
S(1)	-	C(1)	-	N(1)	126.5(6)

(b) $\text{SbCl}_3 \cdot \text{DIPDTQ}_{1,5}$ (Continued)

S (1)	-	C (1)	-	C (1*)	119.0 (6)
N (1)	-	C (1)	-	C (1*)	113.9 (6)
C (1)	-	N (1)	-	C (2)	126.3 (8)
N (1)	-	C (2)	-	C (3)	110.1 (7)
N (1)	-	C (2)	-	C (4)	109.8 (8)
C (3)	-	C (2)	-	C (4)	111.0 (9)

Table 2.4.4 Torsion Angles ($^{\circ}$) for $\text{SbCl}_3 \cdot \text{DEDTO}_{1.5}$

S(1)	-	C(1)	-	N(2)	-	C(3)	1.0
S(1)	-	C(1)	-	C(5)	-	C(5)	-173.3
S(1)	-	C(1)	-	C(5)	-	N(6)	4.8
N(2)	-	C(1)	-	C(5)	-	N(6)	-174.7
N(2)	-	C(1)	-	C(5)	-	S(5)	7.2
S(5)	-	C(5)	-	N(6)	-	C(7)	-1.2
C(1)	-	N(2)	-	C(3)	-	C(4)	170.1
C(5)	-	N(6)	-	C(7)	-	C(8)	167.8
S(11**)	-	C(11**)	-	C(11)	-	S(11)	180.0
S(11)	-	C(11)	-	N(12)	-	C(13)	-3.7
C(11)	-	N(12)	-	C(13)	-	C(14)	117.0

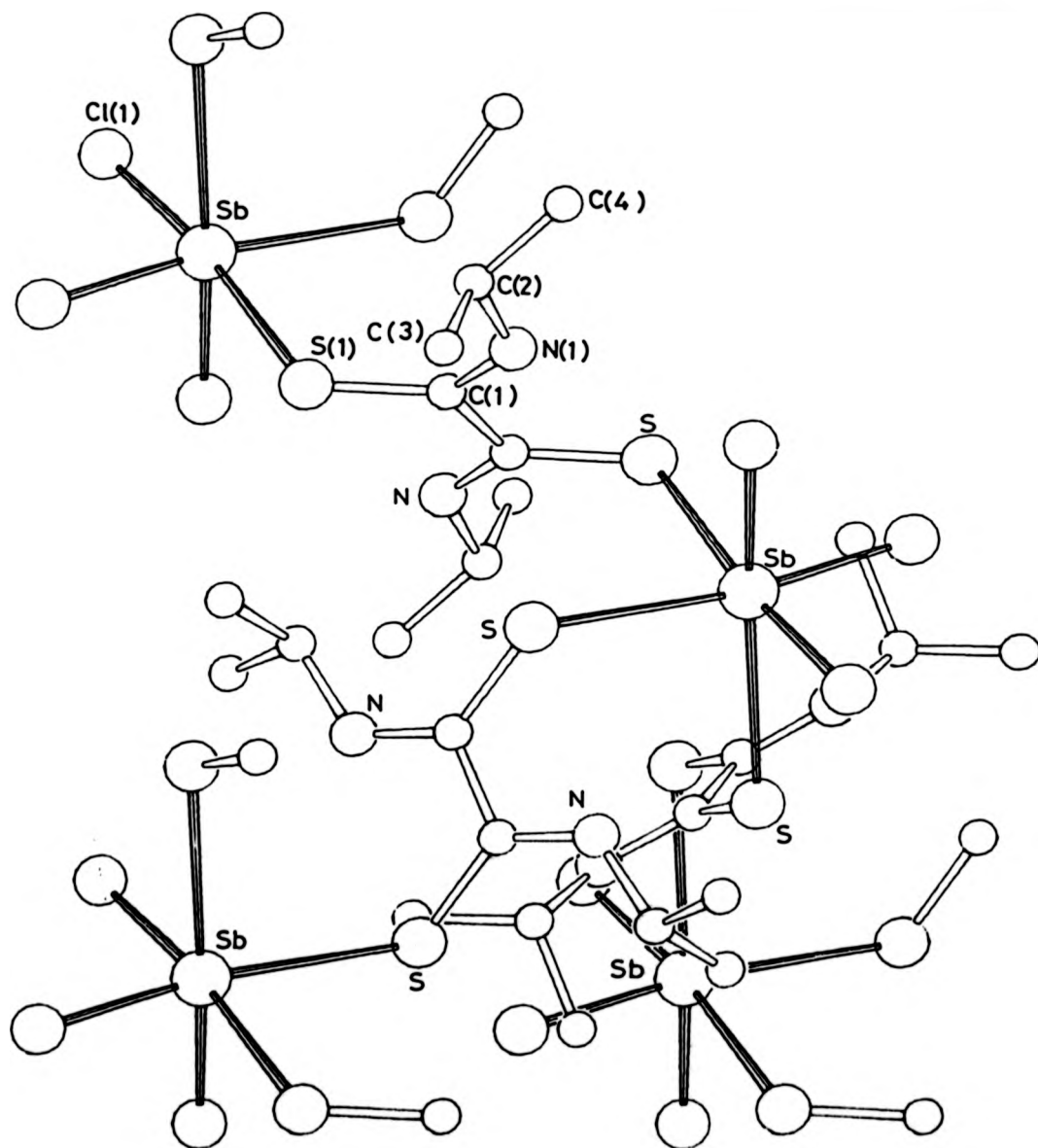
2.5 THE CRYSTAL STRUCTURE OF $\text{SbCl}_3(\text{DIPDTO})_{1.5}$

Figure 2.5.1 shows a portion of the molecular structure of $\text{SbCl}_3(\text{DIPDTO})_{1.5}$, Tables 2.4.2(b) and 2.4.3(b) show the atomic positions, and bond lengths and angles, respectively. The structure is polymeric and the metal atom has crystallographically imposed three-fold symmetry. The unique Sb-Cl distance (2.413(2) Å) is a little longer than those found in either pure SbCl_3 (2.38 Å)¹²⁰ or $\text{SbCl}_3\text{DEDTO}_{1.5}$ (2.340, 2.388, 2.381 Å) but comparable to Sb-Cl distances in the five coordinate structure of $\text{SbCl}_3(\text{dmit})$ ²⁶. The three Cl-Sb-Cl angles are all 92.5(2)°.

Considering the geometry around the metal centre, three sulphur atoms approach to the metal octahedral positions for a fac isomer. The unique Sb-S distance (3.197(5) Å) reflects very weak Sb---S interactions similar to those found in adducts of SbCl_3 with cyclic thioethers already described, and $\text{SbCl}_3\text{DEDTO}_{1.5}$ (Sb-S distances 3.1-3.4 Å). There is no indication that the lone pair is stereochemically active. The C-S bond in $\text{SbCl}_3\text{DIPDTO}_{1.5}$ (1.726(9) Å) is a little longer than the corresponding bond in the free ligand (1.680 Å). Since the lengthening of a C-S bond has been interpreted to indicate greater Sb-S interaction, it is not unreasonable to suggest that the Sb-S bonds in $\text{SbCl}_3\text{DIPDTO}_{1.5}$ may be stronger than in $\text{SbCl}_3\text{DEDTO}_{1.5}$.

The polymeric nature of $\text{SbCl}_3\text{DIPDTO}_{1.5}$ is unique for this type of Sb(III) adduct. Starting off the description from one antimony atom; then the metal is bonded to three sulphurs from three different ligands.

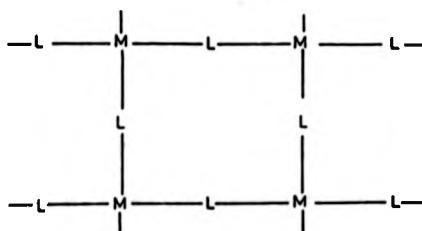
Figure 2.5.1 The Crystal Structure of $\text{SbCl}_3 \cdot \text{DIPDTO}_{1.5}$



Each ligand has a crystallographically imposed centre of symmetry and each symmetry related sulphur is then bonded to a different SbCl_3 moiety. The resulting polymer is three dimensional. The structure is in sharp contrast with that of $\text{SbCl}_3 \cdot \text{DEDTO}_{1.5}$ where two polymeric chains are connected by an additional ligand over centres of symmetry (Figure 2.5.2).

The Sb-S-C angles ($117.1(5)^\circ$) are rather longer than those found in $\text{SbCl}_3 \cdot \text{DEDTO}_{1.5}$ $110.8(4)^\circ$, $90.4(3)^\circ$, $102.8(3)^\circ$ but still roughly what would be expected if the Sb-S bonds were far shorter. We suspect that these variations are due to the steric requirements of the polymer chains and do not indicate any difference in the bonding. The ligand retains its *trans*-conformation.

Figure 2.5.2 (a) The two dimensional polymer in $\text{SbCl}_3 \cdot \text{DEDTO}_{1.5}$



(b) The three dimensional polymer in $\text{SbCl}_3 \cdot \text{DIPDTO}_{1.5}$



2.6

REACTIONS OF DITHIOOXAMIDES WITH
GROUP IV HALIDES



As with their Group (VB) counterparts, the TiCl_4 and SnX_4 ($\text{X} = \text{Cl}, \text{Br}$) complexes were all prepared by dropwise addition of the N,N'-disubstituted dithiooxamide ligand to the metal halide in benzene. The resulting 1:1 adducts were purified by successive washing with benzene and pumping *in vacuo*. All adducts were extremely air/moisture sensitive, the titanium ones being perhaps more so than their tin counterparts, and had to be handled either under nitrogen or under vacuum. Decomposition to black or brown solids without melting was observed for all complexes on heating under nitrogen. The complexes were generally insoluble in most non-polar solvents. Poor solubility in non-coordinating solvents greatly limited solution studies. Conductivity measurements in MeCN solutions over a range of concentrations, showed that the complexes were non-conducting.

The complexes are listed with their principal i.r. bands in Table 2.6.1 with assignments following those of Dessyn and Herman^{98,115}. The thioamide I band ($\approx 1540 \text{ cm}^{-1}$ and with a high $\nu(\text{CN})$ contribution) shifts to higher frequencies by $30\text{-}50 \text{ cm}^{-1}$. This is accompanied by a smaller shift in the thioamide IV band ($\sim 870 \text{ cm}^{-1}$ and with a high $\nu(\text{CS})$ contribution) to lower frequencies. This, as previously discussed, is consistent with sulphur coordination to the metal. The one notable difference between i.r. spectra of dithiooxamide

Table 2.6.1 Principal i.r. Bands (cm^{-1}) for Metal Complexes

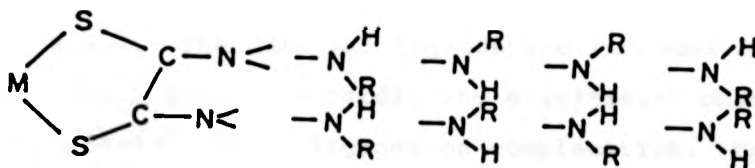
Compound	$\nu(\text{NH})_{(s)}$	Thioamide I $\nu(\text{CN})_{(s)}$	Thioamide IV $\nu(\text{CS})_{(m)}$	(MS) / (MX) (m)
DMDTO	3179	1540	872	
SnCl_4 (DMDTO)	3239	1583, 1570	865	311
SnBr_4 (DMDTO)	3205	1588, 1571	858	220
TiCl_4 (DMDTO)	3255, 3140	1566, 1553	802	400, 371, 340
DEDTO	3166	1523	840	
SnCl_4 (DEDTO)	3240, 3201	1573, 1558	803, 821	310
SnBr_4 (DEDTO)	3150	1558	800, 821	322, 210
DIPDTO	3147	1513	890	
SnCl_4 (DIPDTO)	3245, 3178	1550, 1538	844	328, 297
SnBr_4 (DIPDTO)	3195	1540	846	-
TiCl_4 (DIPDTO)	3235	1550, 1535	851	390, 344
DBDTO	3180	1520	890	
SnCl_4 (DBDTO)	3230, 3181	1575, 1550	861	346, 307
SnBr_4 (DBDTO)	3170	1564	865	-
TiCl_4 (DBDTO)	3258, 3180	1578	868	400, 353 314, 255
DCXDTO	3150	1507	872	
SnCl_4 (DCXDTO)	3160	1545	835	310, 286, 247
SnBr_4 (DCXDTO)	3200	1545, 1530	836	-
TiCl_4 (DCXDTO)	3178	1556, 1540	835	391, 348, 319
DBZDTO	3170	1519	874	
SnCl_4 (DBZDTO)	3140	1542	847	335, 320, 286
SnBr_4 (DBZDTO)	3140	1540, 1520	820	-
TiCl_4 (DBZDTO)	3170	1545	844	392, 371, 322

Table 2.6.2 ^1H n.m.r. Data CDCl_3 Solutions
 (ppm) with respect to TMS ($\delta = 0$)

Compound	NH s, br	CH m	CH ₂	CH ₂ m	CH ₂ m	CH ₃		
DMDTO	10.47					3.30 d		
SnCl_4 .DMDTO	-					3.46 d		
SnBr_4 .DMDTO	-					3.29 d		
TiCl_4 .DMDTO	10.33					3.30 d		
DEDTO	10.28		3.76 m			1.39 t		
SnCl_4 .DEDTO	10.07		3.90 m			1.42 t		
SnBr_4 .DEDTO	10.27		3.74 m			1.37 t		
DIPDTO	10.17	4.48				1.37 t		
SnCl_4 .DIPDTO	9.71	4.57				1.50 t		
SnBr_4 .DIPDTO	10.10	4.49				1.36 t		
TiCl_4 .DIPDTO	10.12	4.46				1.36 t		
DBDTO	10.27		3.72 m	1.74	1.47	1.00 t		
SnCl_4 .DBDTO	9.94		3.93 m	1.87	1.48	1.00 t		
SnBr_4 .DBDTO	10.31		3.71 m	1.74	1.47	0.28 t		
TiCl_4 .DBDTO	10.28		3.70 m	1.74	1.47	0.98 t		
DBCDTO	10.44		4.85 d				7.35	
SnCl_4 .DBCDTO	10.33		5.04 d				7.42, 7.32	
SnBr_4 .DBCDTO	10.49		4.86 d				7.36	
TiCl_4 .DBCDTO	10.42		4.85 d				7.33	
DCXDTO	10.34							4.26-1.46
SnCl_4 .DCXDTO	9.64							4.25-1.44
SnBr_4 .DCXDTO	10.31							4.26-1.44
TiCl_4 .DCXDTO	10.27							4.14-1.44

complexes of Group (IV) and those of Group (VB) is that the former show multiple character in the $\nu(\text{NH})$ 3000-3200 cm^{-1} , $\nu(\text{CN})$ 1560 cm^{-1} and $\nu(\text{CS})$ 800-870 cm^{-1} regions. The observation that $\nu(\text{CN})$ and $\nu(\text{CS})$ bands are split has been used previously as the basis for assigning complexes to a *cis*-(S,N)-chelate bonding mode^{98,100,123-125}. The X-ray crystallographic resolution of the (S,S)-chelate, $\text{SnBr}_4\text{DBDTO}$, which will be described in the next section, has shown that this is not necessarily the case. It is interesting to note that despite the splitting, MX_4 complexes show $\nu(\text{CN})$ and $\nu(\text{CS})$ shifts which are consistent with (S,S)-coordination. The splitting of these bands is perhaps best attributed to some lattice effects which result in changes in local site symmetry.

An interesting feature of the N-H bands of the MX_4 complexes is that all are split into two or three characteristic peaks. From the crystal structure of $\text{SnBr}_4(\text{C}_4\text{H}_9(\text{H})\text{NCSCSN}(\text{H})\text{C}_4\text{H}_9)$, we know that the ligand adopts a *cis*-(S,S)-chelate bonding mode in the complex. This makes it possible to have geometric isomers:



Geometrical isomerism has been previously suggested as one of the possible reasons for the splitting of the $\nu(\text{NH})$ bands. If this was the case, then all *cis*-(S,S)-complexes of dithiooxamides would be expected to feature multiple character in the $\nu(\text{N-H})$ region. The i.r. spectrum of the (S,S)-chelate, $\text{BiCl}_3(\text{DEDTO})_2$, does not show this feature. Indeed none of the other Bismuth(III) dithiooxamide chelates have this feature. I.r. spectra of TiCl_4 and SnCl_4 chelates with the oxygen analogues of dithiooxamide, also exhibit single intense $\nu(\text{NH})$ bands. It is therefore unlikely that the split in the N-H stretching frequency is due to geometrical isomerism and an explanation in terms of lattice packing effects is favoured.

In the low energy region of the spectrum ($400\text{--}200\text{ cm}^{-1}$), a series of strong M-X stretches are observed. For an octahedral arrangement of atoms around the metal involving ligand (S,S)-chelation, four $\nu(\text{M-X})$ bands are expected. M-S bands are also expected to appear in this region. Therefore, although a number of bands are observed, it is not clear as to what the major contributing groups are.

^1H n.m.r. spectra of the complexes are presented in Table 2.6.2. The data for ligands are included for comparison. There are hardly any significant changes in the spectra of the ligands on complexation. From the relative shifts of $\nu(\text{CN})$ and $\nu(\text{CS})$ in i.r. spectra it is not unreasonable to conclude that changes in the C-S bond do not affect the C-N bond very much and thus electronic changes in the N-H proton environment are expected

to be minimal which is what we observe. Any protons on the alkyl substituents of the nitrogen are not likely to be much affected by complex formation.

2.7 THE CRYSTAL STRUCTURE OF $\text{BiCl}_3 \cdot \text{DEDTO}_2$

Figures 2.7.1 and 2.7.2 show the molecular architecture of $\text{BiCl}_3 \cdot \text{DEDTO}_2$. Crystal data and refinement details of $\text{BiCl}_3 \cdot \text{DEDTO}_2$ and $\text{SnCl}_4 \cdot \text{DBDTO}$ are given in Table 2.7.1. Atomic positions, and bond lengths and angles, are given in Tables 2.7.2 and 2.7.3 respectively. The structure is monomeric containing discrete molecules of $\text{BiCl}_3 \cdot \text{L}_2$ and solvent (acetone) in the lattice. The two ligands are bound as (S,S)-bidentate chelates to the metal.

The bismuth atoms are seven-coordinate being bonded to three chlorine atoms and two bidentate DEDTO ligands. The metal environment is almost ideal pentagonal bipyramidal with two chlorines in the axial positions and one chlorine and the two bidentate DEDTO ligands in the equatorial plane. The metal atom and the five donor atoms are closely planar (deviations Bi -0.04, Cl(3) 0.04, S(4) 0.12, S(5) -0.08, S(6) 0.05, S(7) -0.10 Å). The largest deviations, those of S(4) and S(7) are concomitant with the smallest equatorial angle S(7)-Bi-S(4) $66.5(3)^\circ$, and are clearly required to increase the S(4)---S(7) non-bonded contact to a reasonable value. The Bi-S bonds for these atoms are longer (Bi-S(4) 3.042(11), Bi-S(7) 2.977(10) Å) than those for the sulphurs *cis* to Cl(3), viz. Bi-Cl(5) 2.818(13), Bi-Cl(6) 2.910(12) Å. The Bi-S-C angles also fall into two groups with Bi-S(4)-C(41), Bi-S(7)-C(71) considerably smaller at $91.1(12)$, $95.8(15)^\circ$ than the other two (Bi-S(5)-C(51), $106.1(14)$, Bi-S(6)-C(61) $106.8(12)$).

Figure 2.7.1 The Crystal Structure of $\text{BiCl}_3 \cdot \text{DEDTO}_2$

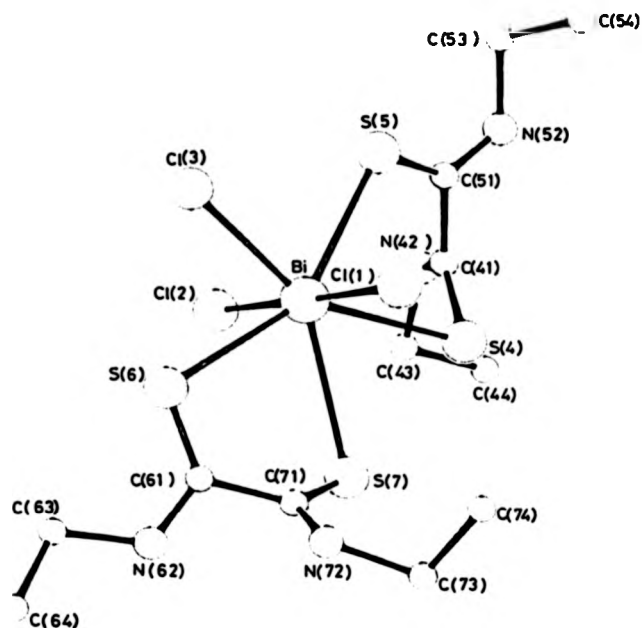


Figure 2.7.2 The Structure of $\text{BiCl}_3 \cdot \text{DEDTO}_2$ showing

(a) Hydrogen bonding to acetone (b) The equatorial plane

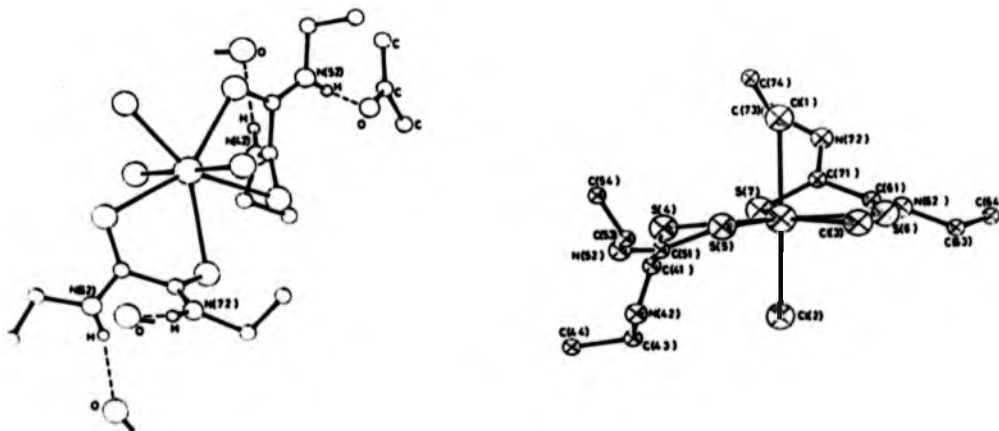


Table 2.7.1 Crystal Data and Refinement Details for $\text{SnBr}_4 \cdot \text{DBDO}$ and $\text{BiCl}_3 \cdot \text{DEDTO}_2$

Compound	(I)	(II)
Formula	$\text{SnBr}_4 \cdot \text{L}^1, 1/3 \text{C}_6\text{H}_6$ $\text{C}_{12}\text{H}_{22}\text{N}_2\text{S}_2\text{SnBr}_4$	$\text{BiCl}_3(\text{L}^2)_2 \cdot (\text{CH}_3)_2\text{O}$ $\text{C}_{15}\text{H}_{30}\text{N}_4\text{S}_4\text{BiCl}_3\text{O}$
M	696.33	725.8
Crystal Class	Monoclinic	Monoclinic
Space group	$\text{C}2/c$	$\text{P}2_1/c$
Absences	$hkl, h+k=2n+1$ $h0l, l=2n+1$ $0k0, k=2n+1$	$h0l, l=2n+1$ $0k0, k=2n+1$
a (Å)	20.766 (15)	10.568 (9)
b (Å)	21.245 (15)	8.780 (9)
c (Å)	14.835 (9)	30.086 (15)
β (°)	91.4 (1)	101.2 (1)
V (Å ³)	6542.9	2737.9
$F(000)$	3792	1416
Z	12	4
D_m	2.09	1.76
D_c	2.04	1.76
μ (cm ⁻¹)	91.1	67.2
λ	0.7107	0.7107
Crystal Size (mm)	8.5*0.65*0.5	0.6*0.6*0.5
Rotation Axis	a	(110) planes
2 θ max (°)	40	50
Number of data measured	3210	8687 (2 quadrants)
Number of data used in refinement	1247	2341
Criterion for data		
Inclusion	$I > 2\sigma(I)$	$I > 3\sigma(I)$
Final R value	0.10	0.08

Table 2.7.2 Atomic Coordinates ($\times 10^4$) for $\text{BaCl}_2 \cdot 4\text{H}_2\text{O}$, with estimated Standard Deviations in Parentheses

ATOM	X	Y	Z
B1	10 (1)	1894 (2)	1726 (0)
CL(1)	-1292 (13)	2055 (19)	4387 (4)
CL(2)	1387 (11)	1673 (17)	3054 (3)
CL(3)	-1619 (13)	-213 (15)	3327 (4)
S(4)	2324 (12)	2724 (15)	4458 (4)
S(5)	1126 (13)	-838 (16)	4109 (4)
S(6)	-2050 (11)	3465 (13)	3114 (4)
S(7)	560 (10)	5220 (12)	3786 (3)
C(41)	2029 (34)	1241 (46)	4780 (12)
N(42)	1710 (33)	1324 (42)	5185 (10)
C(43)	1500 (61)	2763 (63)	5362 (18)
C(44)	2575 (56)	3280 (75)	5747 (20)
C(51)	2104 (35)	-342 (50)	4620 (12)
N(52)	2905 (38)	-1206 (46)	4843 (12)
C(53)	3023 (54)	-2889 (66)	4729 (15)
C(54)	4168 (96)	-3300 (**)	4639 (52)
C(61)	-1615 (33)	5200 (48)	3095 (10)
N(62)	-2338 (31)	6368 (39)	2978 (10)
C(63)	-3718 (41)	6170 (63)	2813 (22)
C(64)	-4311 (45)	7541 (65)	2541 (21)
C(71)	-221 (71)	5638 (50)	3254 (11)
N(72)	243 (30)	6433 (43)	2955 (12)
C(73)	1622 (57)	7040 (69)	3058 (16)
C(74)	2473 (59)	5864 (63)	2963 (18)
O(1)	5445 (32)	310 (46)	4348 (11)
C(81)	5074 (50)	946 (102)	3961 (19)
C(82)	5191 (79)	2593 (84)	3861 (23)
C(83)	4662 (76)	-137 (99)	3612 (26)

Table 2.7.3 Bond Lengths (\AA) and Angles ($^\circ$) for $\text{BiCl}_3 \cdot 5\text{H}_2\text{O}$

BI	-		CL(1)		2.636(10)	
BI	-		CL(2)		2.717(10)	
BI	-		CL(3)		2.649(12)	
BI	-		S(4)		3.044(12)	
BI	-		S(5)		2.819(13)	
BI	-		S(6)		2.909(12)	
BI	-		S(7)		2.976(10)	
CL(1)	-	BI	-	CL(2)		178.6(4)
CL(1)	-	BI	-	CL(3)		89.4(4)
CL(2)	-	BI	-	CL(3)		90.5(4)
CL(1)	-	BI	-	S(4)		84.5(3)
CL(2)	-	BI	-	S(4)		94.8(3)
CL(3)	-	BI	-	S(4)		148.7(3)
CL(1)	-	BI	-	S(5)		88.6(4)
CL(2)	-	BI	-	S(5)		90.1(4)
CL(3)	-	BI	-	S(5)		76.9(4)
S(4)	-	BI	-	S(5)		72.2(3)
CL(1)	-	BI	-	S(6)		90.2(3)
CL(2)	-	BI	-	S(6)		90.4(3)
CL(3)	-	BI	-	S(6)		72.8(3)
S(4)	-	BI	-	S(6)		137.8(3)
S(5)	-	BI	-	S(6)		149.8(3)
CL(1)	-	BI	-	S(7)		91.5(4)
CL(2)	-	BI	-	S(7)		89.3(3)
CL(3)	-	BI	-	S(7)		144.6(3)
S(4)	-	BI	-	S(7)		66.5(3)
S(5)	-	BI	-	S(7)		138.5(3)
S(6)	-	BI	-	S(7)		71.72(29)

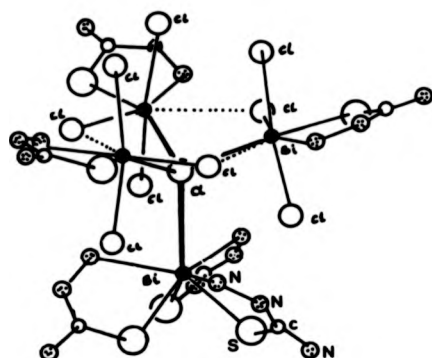
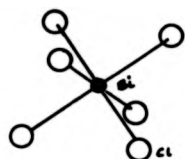
These variations are caused by steric strain in the pentagonal girdle.

This pentagonal bipyramid fits in well with predictions for seven coordinate molecules of the type MA_3B_2 , A = monodentate, B = bidentate^{5,126}. This geometry is favoured for ligands with relatively large bites (defined as $L---L/M-L$, L = donor atom), of about 1.15. This allows S-Bi-S angles of *ca.* 72° as required for a pentagonal bipyramid.

There is no obvious vacancy in the bismuth(III) coordination sphere for a stereochemically active lone pair of electrons. It has been suggested¹²⁷ that this lone pair is active when the ligand contains 'hard' donor atoms and/or 'narrow bite' bidentate ligands such as dithiocarbamates. Thus, the structures of some dithiophosphate systems^{39,128,129} feature a stereochemically active lone pair with the "small bite" bidentate ligands leaving space in the coordination sphere. The resulting compounds are also pseudo-seven-coordinate AX_6E (X = ligand, E = lone pair).

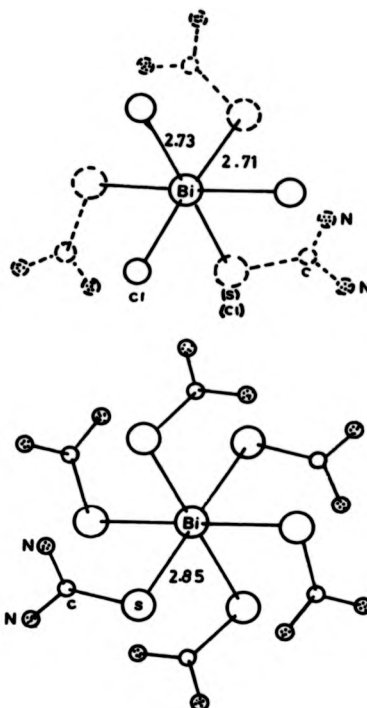
On the other hand, in μ -chloro{tris[trichloro(thiosemicarbazide)-bismuth(III)]}[tris(thiosemicarbazide)bismuth(III)]-hexachlorobismuthate(III)chloride(I)¹³⁰, the ligands form five membered rings with Bi(III); the metal atoms are both six- and seven-coordinate with no evidence for lone pair spatial activity. Other examples of octahedral geometry with no evidence for lone pair activity may be found in cationic and anionic bismuth(III) chlorothiourea complexes such as $[Bi(tu)_6][Bi((tu)_{1.5}Cl_{1.5})Cl_3]_2$, tu = thiourea, (II), and di- μ -chlorobis[chlorotri(thiourea)bismuth(III)]-

I



○ cl

II

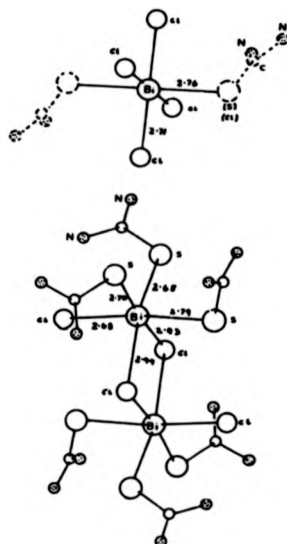


pentachlorothioureabismuthate(III) (III)¹³¹.

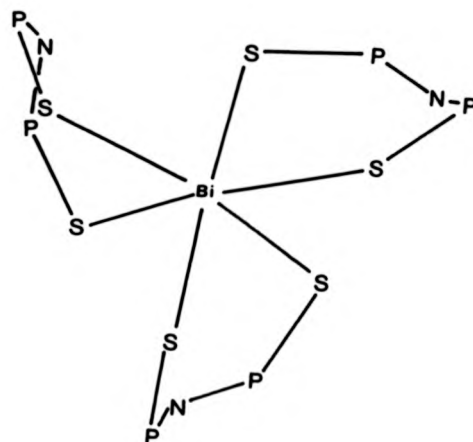
In tris-[P,P,P',P'-tetraphenylamidobis(phosphine sulfido)-S,S']bismuth(III) (IV)¹²⁷. The bidentate (S)-donor ligands (soft) form three six-membered rings with central atom and leave no space for a stereochemically active lone pair. Wyne¹³² noted that the lone pair is stereoinactive in complexes where the ligand is a 'soft' donor.

The present structure then would not be considered likely to have an active lone pair on two grounds: (1) the large bidentate 'bite' and (2) the 'soft' nature of the donor sulphur atoms. Interestingly, the thiosemicarbazide

III



IV



structure is one in which the ligands coordinate through both hard (N)- and soft (S)-donors. In this case the lone pair is not active but this is by no means a definitive case.

All four N-H groups in $\text{BiCl}_3 \cdot \text{DEDTO}$ are involved in hydrogen bonds. Distances are $\text{N}(42) \cdots \text{Cl}(1)$ 3.34, $\text{N}(52) \cdots \text{O}(1)$ 2.85, $\text{N}(62) \cdots \text{Cl}(3)$ 3.26, and $\text{N}(72) \cdots \text{Cl}(2)$ 3.23 Å. The angles at hydrogen are 168, 171, 152, 169°.

As discussed in the $\text{SnBr}_4 \cdot \text{DBDTO}$ structure, ring puckering is probably caused by intramolecular hydrogen bonding. S-C-C-S torsion angles are -57.2 and -56.7°. The bonding around the carbon atoms retains its planar structure. It may well be that the formation of hydrogen bonds also effects in the Bi-Cl distances. For example of the two axial chlorine atoms, that involved in the shorter contact to nitrogen forms a longer bond to the metal than

the other (Bi-Cl(2) 2.717(10), VS Bi-Cl(1) 2.636(10) Å).

2.8 THE CRYSTAL STRUCTURE OF $\text{SnBr}_4 \cdot \text{DBDTO}$

$\text{SnBr}_4 \cdot \text{DBDTO}$ is monoclinic and crystallises in the C2/c spacegroup. Crystal data and refinement details are given in Table 2.7.1. Atomic positions, bond lengths and angles are given in Tables 2.8.1 and 2.8.2 respectively. Figure 2.8.1 shows the molecular geometry around the tin. The structure contains discrete monomers together with benzene solvent in the lattice. The ligand is bidentate S,S-chelated to the metal.

There are two independent molecules of $\text{SnBr}_4 \cdot \text{DBDTO}$ in the structure one of them (A) in a general position but the other (B) is in a special position with the metal atom sitting on a two-fold axis which goes through the metal atom and the midpoint of the chelate C-C bond.

In both molecules the tin environment is octahedral and Sn-Br bond length *trans* to the sulphur are shorter (A, 2.527(11), 2.545(13); B, 2.544(11) Å) than those *trans* to bromine (A, 2.565(12), 2.625(13); B, 2.605(26) Å). The Sn-S bond lengths are equivalent to within experimental error (2.565(28), 2.551(24), 2.609(25) Å).

The S-Sn-S angles vary from 82.6(6) to 83.6(7)° thus the bite of the ligand is sufficiently large and only distorts the octahedron slightly. The angle subtended by the bromines *trans* to the sulphur, Br(1A)-Sn-Br(4A), is 101.8(4)° in A and the equivalent angle in B, Br(2B)-Sn-Br(2B*), is 102.7(5)°. This is extended to compensate for the narrower chelate angle.

The ligands are puckered in that the two S-C-C-S torsion angles are -44.3 and -40.7°. This is somewhat

surprising as the two carbon atoms retain their sp^2 character; the three angles subtended at the carbon adding up to 360° . This ring puckering contrasts with the planar conformation observed in the $MX_3L_{1.5}$ complexes where the ligand forms a weak S-bonded link between metal atoms. Perhaps the reason is that the puckering increases the distance between the two hydrogen atoms on the nitrogen and thus permits the formation of intermolecular hydrogen bonds. If there were no puckering it would be impossible to form such bonds because of steric hindrance.

All the N-H bonds are involved in hydrogen bonding to bromine atoms, viz. Br(3A)---N(3A) 3.66 Å; Br(2A)---N(3B) 3.40 Å; Br(1B)---N(10A) 3.56 Å. Using the calculated hydrogen positions, the Br---H-N angles are 155, 165, 156 respectively.

The structure may be compared with that of the 1:2 adduct of $SnCl_4 \cdot L_2$, L-1,3-dimethyldithiourea where the ligands are also *cis* (S,S)-coordinated to the metal¹³³ rather than through the nitrogen as suggested earlier¹³⁴.

Apart from the distances mentioned above, there are no close contacts less than the sum of van der Waals radii involving the benzene ring or the tin molecules.

Figure 2.8.1 The Crystal Structure of $\text{SnBr}_4 \cdot \text{DBDTO}$

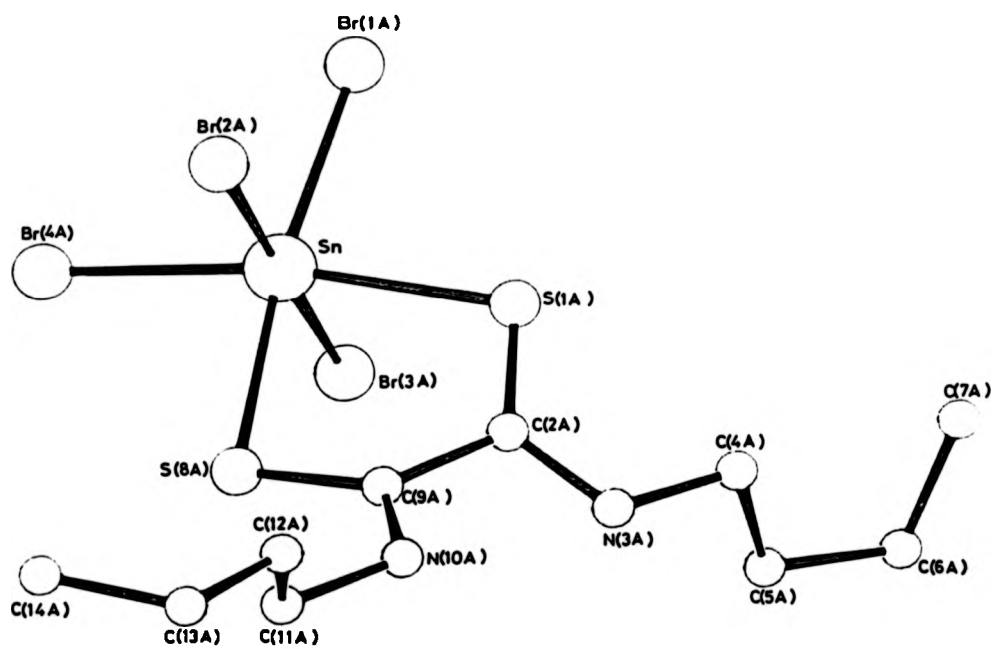


Table 2.8.1 Atomic Coordinate ($\times 10^4$) for $\text{SnBr}_4 \cdot \text{DBDTO}$ with Estimated Standard Deviations in Parentheses

ATOM	X	Y	Z
SN(1A)	532(3)	3025(3)	-1454(4)
BR(1A)	921(5)	2641(5)	51(6)
BR(2A)	1599(5)	2727(5)	-2253(7)
BR(3A)	-576(5)	3310(6)	-668(7)
BR(4A)	881(6)	4172(5)	-1441(7)
S(1A)	148(14)	1897(12)	-1763(16)
C(2A)	-91(39)	1947(30)	-2724(51)
N(3A)	-209(31)	1442(29)	-3315(39)
C(4A)	70(44)	833(31)	-3056(56)
C(5A)	611(78)	707(68)	-3789(75)
C(6A)	1005(56)	56(74)	-3673(115)
C(7A)	838(70)	-243(60)	-2708(89)
S(8A)	28(14)	3260(11)	-2970(15)
C(9A)	-352(30)	2558(28)	-3110(40)
N(10A)	-890(30)	2468(27)	-3654(42)
C(11A)	-1181(38)	3056(36)	-3983(52)
C(12A)	-1880(43)	3052(42)	-3601(74)
C(13A)	-2371(41)	3524(52)	-3978(81)
C(14A)	-2307(70)	4220(48)	-3724(88)
SN(1B)	7500(0)	1053(4)	7500(0)
BR(1B)	6704(6)	3977(5)	3885(7)
BR(2B)	6746(5)	3198(5)	1700(7)
S(1B)	8093(12)	4868(11)	3290(16)
C(2B)	7706(34)	5465(30)	3004(39)
N(3B)	7693(40)	6080(31)	3400(40)
C(4B)	7991(33)	6121(34)	4270(46)
C(5B)	7392(37)	6230(49)	4936(49)
C(6B)	7572(53)	6328(63)	5935(50)
C(7B)	8192(44)	5978(41)	6216(52)
C(41)	5605(62)	5287(58)	716(79)
C(42)	4949(121)	4339(74)	-113(98)
C(43)	5408(54)	4540(50)	728(70)

Table 2.8.2 Molecular Dimensions - Distances (\AA), Angles ($^\circ$) for $\text{SnBr}_4 \cdot 10\text{H}_2\text{O}$

MOLECULE A

SN(1)	-	BR(1)	2.528(11)		
SN(1)	-	BR(2)	2.566(12)		
SN(1)	-	BR(3)	2.624(13)		
SN(1)	-	BR(4)	2.543(12)		
SN(1)	-	S(1)	2.569(28)		
SN(1)	-	S(8)	2.552(24)		
BR(1)	-	SN(1)	-	BR(2)	92.1(4)
BR(1)	-	SN(1)	-	BR(3)	88.7(3)
BR(2)	-	SN(1)	-	BR(3)	178.5(4)
BR(1)	-	SN(1)	-	BR(4)	101.8(4)
BR(2)	-	SN(1)	-	BR(4)	89.8(4)
BR(3)	-	SN(1)	-	BR(4)	91.3(4)
BR(1)	-	SN(1)	-	S(1)	88.0(5)
BR(2)	-	SN(1)	-	S(1)	87.5(7)
BR(3)	-	SN(1)	-	S(1)	91.3(7)
BR(4)	-	SN(1)	-	S(1)	170.0(6)
BR(1)	-	SN(1)	-	S(8)	171.1(6)
BR(2)	-	SN(1)	-	S(8)	90.5(7)
BR(3)	-	SN(1)	-	S(8)	88.5(7)
BR(4)	-	SN(1)	-	S(8)	86.7(5)
S(1)	-	SN(1)	-	S(8)	83.7(7)
S(1)	-	C(2)	1.52(7)		
C(2)	-	N(3)	1.41(4)		
C(2)	-	C(9)	1.52(8)		
N(3)	-	C(4)	1.47(5)		
C(4)	-	C(5)	1.57(5)		
C(5)	-	C(6)	1.62(8)		
C(6)	-	C(7)	1.60(7)		
S(8)	-	C(9)	1.70(6)		
C(9)	-	N(10)	1.41(4)		
N(10)	-	C(11)	1.48(5)		
C(11)	-	C(12)	1.54(4)		
C(12)	-	C(13)	1.54(4)		
C(13)	-	C(14)	1.53(4)		
SN(1)	-	S(1)	-	C(2)	102.2(28)
S(1)	-	C(2)	-	N(3)	126 (5)
S(1)	-	C(2)	-	C(9)	122 (5)
N(3)	-	C(2)	-	C(9)	110 (5)
C(2)	-	N(3)	-	C(4)	115 (4)
N(3)	-	C(4)	-	C(5)	104 (4)

Table 2.8.2 Continued

C(4)	-	C(5)	-	C(6)	115 (5)
C(5)	-	C(6)	-	C(7)	110 (6)
SN(1)	-	S(8)	-	C(9)	97.9(20)
C(2)	-	C(9)	-	S(8)	122 (4)
C(2)	-	C(9)	-	N(10)	113 (5)
S(8)	-	C(9)	-	N(10)	124 (4)
C(9)	-	N(10)	-	C(11)	114 (4)
N(10)	-	C(11)	-	C(12)	105 (4)
C(11)	-	C(12)	-	C(13)	119 (5)
C(12)	-	C(13)	-	C(14)	118 (5)
MOLECULE B					
SN(1)	-	S(1)		2.606(26)	
SN(1)	-	BR(1)		2.606(11)	
SN(2)	-	BR(1)		2.544(12)	
BR(1)	-	SN(1)	-	BR(2)	89.9(4)
BR(1)	-	SN(1)	-	BR(2*)	91.9(4)
BR(2)	-	SN(1)	-	BR(2*)	102.7(5)
BR(1)	-	SN(1)	-	BR(1*)	177.1(5)
BR(1)	-	SN(1)	-	S(1)	85.7(6)
BR(2)	-	SN(1)	-	S(1)	169.0(7)
BR(1*)	-	SN(1)	-	S(1)	92.2(6)
BR(2*)	-	SN(1)	-	S(1)	87.5(6)
S(1)	-	SN(1)	-	S(1*)	82.6(6)
S(1)	-	C(2)		1.57(6)	
C(2)	-	N(3)		1.43(4)	
C(2*)	-	C(2)		1.74(11)	
N(3)	-	C(4)		1.45(5)	
C(4)	-	C(5)		1.59(4)	
C(5)	-	C(6)		1.55(4)	
C(6)	-	C(7)		1.55(4)	
SN(1)	-	S(1)	-	C(2)	103.6(27)
S(1)	-	C(2)	-	N(3)	129 (4)
S(1)	-	C(2)	-	C(2*)	119.9(4)
C(2*)	-	C(2)	-	N(3)	110 (5)
C(2)	-	N(3)	-	C(4)	115 (5)
N(3)	-	C(4)	-	C(5)	103 (4)
C(4)	-	C(5)	-	C(6)	114 (4)
C(5)	-	C(6)	-	C(7)	114 (4)

Table 2.8.2 Continued

SOLVENT

C(41)	-	C(43)		1.64(12)	
C(42)		C(43)		1.65(17)	
C(42)		C(41**)		1.67(23)	
C(41)	-	C(43)	-	C(42)	113 (9)
C(43)	-	C(41)	-	C(42**)	107 (10)
C(41**)	-	C(42)	-	C(43)	134 (12)

SYMMETRY ELEMENTS *1.5-X,Y,.5-Z

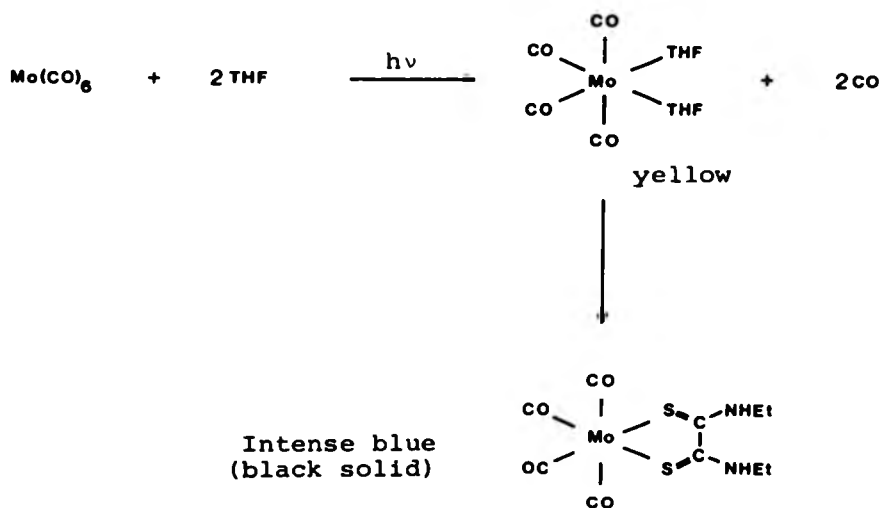
**1-X,1-Y,-Z

2.9 REACTIONS OF DITHIOOXAMIDES WITH Mo(CO) SPECIES

In an effort to form more chelate complexes with dithiooxamide ligands, *cis* Mo(CO)₄(THF)₂ was selected as a suitable reactant. This choice was influenced by the following considerations.

- (a) In Mo(CO)₄(THF)₂ the metal centre is a soft centre in HSAB terms and so it should form stable compounds with sulphur (soft) donating ligands.
- (b) Mo has a small enough atomic radius to fit into the dithiooxamide ligand bite.
- (c) The two oxygen donating (hard) THF substituents are very labile, leaving the *cis* octahedral positions vacant for the sulphur donating dithiooxamide to form a chelate.

As a preliminary experiment molybdenum hexacarbonyl solution in THF under nitrogen was irradiated with u.v. light to give the yellow bis THF adduct. When N,N'-diethyl dithiooxamide was introduced, a colour change to an intense blue solution was observed. The black solid that was obtained was partially characterised by its i.r. and ¹H n.m.r. spectra.



Relevant i.r. peaks: (cm^{-1})

3194 (νNH), 1984, 1900 (broad) (νCO), 1524 (νCN), 800, 835 (νCS)
(the ligand bands do not appear to have shifted at all)

N.m.r. data: δ_{H} (100 MHz; solvent CDCl_3 ; standard Me_4Si)
1.37 (6H, t, $-\text{CH}_3$), 3.74 (4H, m, CH_2), 10.24 (2H, s br, NH).

The results of this preliminary investigation are only an indication that the system is worth investigating further. It is not possible to say at this stage what the products are.

A similar preliminary survey was done with $\text{Fe}_2(\text{CO})_9$. The products of these reactions were extremely air/moisture sensitive and they were not isolated.

2.10 EXPERIMENTAL

Crystal Structure Determination

In the crystal structure determinations of DEDTO, DIPDTO, $\text{SbCl}_3 \cdot \text{DEDTO}_{1.5}$, $\text{SbCl}_3 \cdot \text{DIPDTO}_{1.5}$, $\text{BiCl}_3 \cdot \text{DEDTO}_2$ and $\text{SnBr}_4 \cdot \text{DBDTO}$. Crystals were placed in Lindeman tubes along their most prominent axes. Their crystalline quality was checked under the polarising microscope. Preliminary cell constants and space groups were obtained from precession photographs. The crystals were then transferred to a Stoe STADI-2 diffractometer equipped with a graphite monochromator. The crystals were adjusted more accurately by X-ray counter methods and precise determinations of lattice constants were carried out from the accurate setting angles of a number of axial reflections. Data were taken via ω scans of width $(2.0 + 0.5 \sin \mu / \tan \theta)$. The scan speed was $0.033^\circ \text{ s}^{-1}$ and the background measured at the ends of the ω scan for 20 s. Measurement of standard reflections showed no deterioration.

This is only a summary - a more detailed description of the process of X-ray structure determination is outlined in Section 1.4.

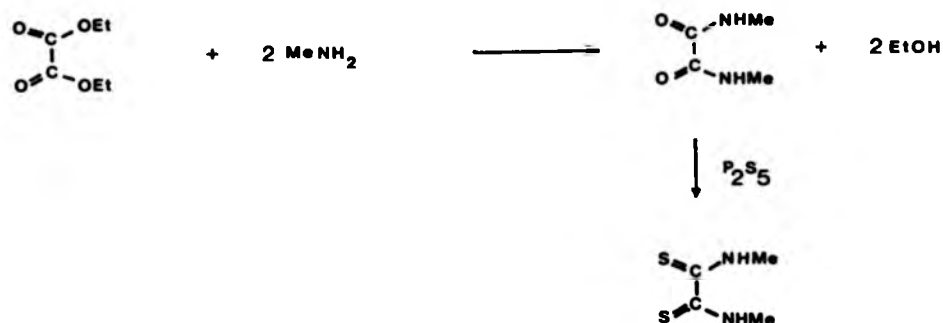
Preparation of Dithiooxamide Ligands

Method (I)

N,N'-Dimethyl Dithiooxamide (DMDTO)

N,N'-Dimethyloxamide was prepared by direct

addition of three-fold excess of aqueous 25% MeNH₂ to a cold solution of diethyloxalate in ethanol. The resulting solid was recrystallised in high yield from methylated spirit



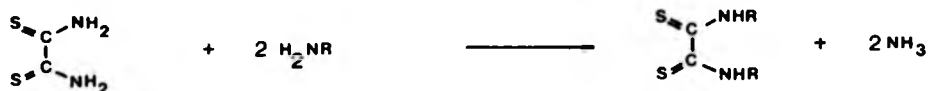
N,N'-Dimethyl dithiooxamide (DMDTO) was prepared from N,N'-dimethyloxamide (DMO) following a slightly modified route from that of Hurd *et al.*¹⁰⁶. To a refluxing suspension of DMO (2.9 g, 25 mmol) in xylene was added excess P₄S₁₀ (25 g, 56 mmol) powder in small portions. The mixture was allowed to reflux for 12 hours producing an orange solution and a very dark brown solid. Most of the xylene was distilled off. The last traces were pumped off *in vacuo*. The resulting solid was dissolved in methanol and refluxed with activated charcoal for five minutes. Filtration through Celite afforded an orange solution which was treated with activated charcoal again. Filtration and concentration of the resulting orange solution gave crystals of DMDTO, which were recrystallised from hot methanol as orange needles.

m.p. 136-137° (litt. 139°) yield 20%.

Method (II)

Preparation of DEDTO, DIPDTO, DBDTO, DCXDTO and DBZDTO

These ligands were prepared by the modified Wallach reaction¹⁰⁷ as described by Woodburn and Scroog¹⁰⁸. In this case the starting material was dithiooxamide and the R-group was inserted by amine exchange with a primary amine.



General Procedure

An aqueous solution of the appropriate amine (0.04 moles) was added to solid dithiooxamide (2.0 g 0.01 moles). The mixture was heated under reflux until all the colour of dithiooxamide had disappeared and evolution of ammonia ceased (15 minutes). The mixture was heated for another five minutes and then cooled and filtered. The resulting yellow to deep orange N,N'-disubstituted dithiooxamides were recrystallised in high yields from methanol.

Advantages of this Method:

- (i) no smell
- (ii) straightforward 'one pot' synthesis
(moderate conditions as well)
- (iii) yields are much better than Method I.

Disadvantages:

- (i) tetrasubstituted dithiooxamides
cannot be prepared in this way.

Complexes of SbX_3 ($\text{X} = \text{Cl}, \text{Br}$) with DMDTO, DEDTO, DIPDTO, DBDTO, DCXDTO, DBZDTO

Complexes were prepared by addition of the appropriate ligand to the metal halide both being in benzene solution. To illustrate the procedure, a typical reaction is described below.

N,N'-Diethyldithiooxamide (1.0 g, 5.7 mmol) in benzene (150 cm³) was added dropwise to a stirred solution of antimony trichloride (1.24 g, 5.4 mmol) in benzene (100 cm³) maintained at 0°C under an atmosphere of nitrogen. The resulting solution was stirred for a further eight hours. Benzene was slowly removed from the reaction mixture until the first appearance of crystalline material. The solution was allowed to stand to facilitate crystal formation. The resultant solid was filtered off, washed with hexane (3 x 100 ml portions) and dried *in vacuo*. Yield 0.9 g, 40%, m.p. 69°.

Complexes of BiCl_3 with DMDTO, DEDTO, DIPDTO, DBDTO, DCXDTO, DBZDTO

For bismuth complexes the procedure is typified by the preparation of $\text{BiCl}_3 \cdot \text{DEDTO}_2 \cdot (\text{CH}_3)_2\text{CO}$ as described below.

Bismuth trichloride (1.72 g, 5.45 mmol) was refluxed with stirring in anhydrous acetone for thirty minutes in an atmosphere of nitrogen. To the warm suspension was added dropwise, a solution of DEDTO (0.96 g, 5.45 mmol). After several hours of magnetic stirring, the solution was filtered and acetone slowly removed until the onset of crystal growth. (Uncontrolled removal of acetone always

resulted in the formation of a frothy solid.) The resulting solution was allowed to stand to facilitate crystal growth. The resulting crystalline product was collected, pumped *in vacuo* at room temperature for several hours and stored in sealed glass ampoules under vacuum. yield 1.0 g, 54%. Found: C 24.81, H 4.17, N 7.70, Calc. for $C_{15}H_{30}N_4Cl_3$ Bi C 24.81, H 4.13, N 7.72.

All $BiCl_3$ dithiooxamide complexes were very unstable in acetone solution. Decomposition to a dark brown solid was evident within a few days. In the solid state, $BiCl_3$ complexes decomposed to a black mass within a few weeks even when sealed under vacuum. Complexes with smaller alkyl substituents (R = Me, Et) were less stable in this respect than those with larger substituents.

Complexes of $SnCl_4$, $SnBr_4$ and $TiCl_4$ with DMDTO, DEDTO, DIPDTO, DBDTO, DCXDTO, DBZDTO

The 1:1 adducts were prepared by direct addition of a benzene solution of the ligand to an equimolar amount of the metal halide in benzene. In a typical reaction, a solution of DIPDTO (0.88 g, 4.3 mmol) in benzene (100 cm³) was added dropwise to a stirred solution of $SnCl_4$ (0.5 cm³, 4.3 mmol) maintained at 0°C in an atmosphere of dry oxygen-free nitrogen. A yellow precipitate was immediately formed. The system was allowed to stir for several hours. The mother liquor was decanted off and the solid washed at the vacuum line with redistilled benzene (4 x 100 ml portions) and then dried *in vacuo* m.p. 228°C, d. Yields were quantitative in all cases.

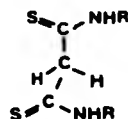
CHAPTER 3
DITHIOMALONAMIDES

CHAPTER 3

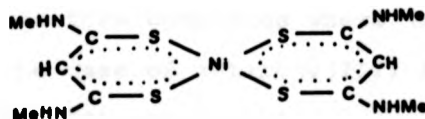
DITHIOMALONAMIDES

3.1 INTRODUCTION

Looking at the structure of dithiomalonamides, one important variation with previous dithiooxamide systems is that we have a tetrahedral $-\text{CH}_2-$ 'hinge' between the two $\text{R}_2\text{N}-\text{C}=\text{S}$ groups:



We still have donor sites at S, and N, hence dithiomalonamide chemistry forms a natural sequel to dithiooxamide chemistry. The coordination chemistry of dithiomalonamide and its N,N'-disubstituted derivatives has received considerable attention in the last twenty years¹³⁵⁻¹⁴⁰. Most of the work done so far involved divalent transition metals. One prominent feature in the formation of dithiomalonamide complexes in neutral aqueous conditions is the deprotonation of the backbone $-\text{CH}_2-$ ¹³⁵. A neutral complex, NiL_2 , is formed for $\text{L} = \text{N,N}'$ -dimethyldithiomalonamide¹³⁶. Here deprotonation results in the formation of two pseudo-aromatic six-membered rings. In these complexes,



(S,S)-coordination is assigned on the basis of i.r. evidence and a *cis*-structure is proposed by analogy with the structures of metal complexes with β -diketones. Similar reactions are observed with Pd(II)^{137,138} and Zn¹³⁹. In acid conditions there is no deprotonation, cationic coordination complexes are formed with M:L stoichiometries 1:2, and 1:3 (M = Ni(II), Pd(II), Zn(II)). (S,N)-coordination has been assigned on the basis of i.r. spectroscopy to feature either *cis*-(S,N)-chelate square planar or octahedral geometries.

Very little work has been done on complexes of dithiomalonamides in non-aqueous conditions. For SbX₃ and BiX₃ (X = halogen), complexes with N,N'-dimethyldithiomalonamide and N,N'-dipenyldithiomalonamide have been prepared in dichloromethane¹⁴⁰. There is no evidence for deprotonation in this case and (S,S)-chelation has been assigned on the basis of i.r. data.

When dithiomalonamide ligands form complexes, the plausible bonding modes include (S,S)-, (S,N)-, (N,N)-chelation; (S,S)-, (S,N)-, (N,N)-bridging and (S,N)-*endo*-chelation. In the absence of structural data, it is very difficult to establish unambiguously whether the preferred bonding mode is (S,S)-chelation or (S,S)-bridging even when there is conclusive evidence for S-donation. The analogous dithiooxamide ligands have been shown to form complexes where (S,S)-bridging is favoured in the case of antimony(III) and (S,S)-chelation in the case of Bi(III) and Sn(IV).

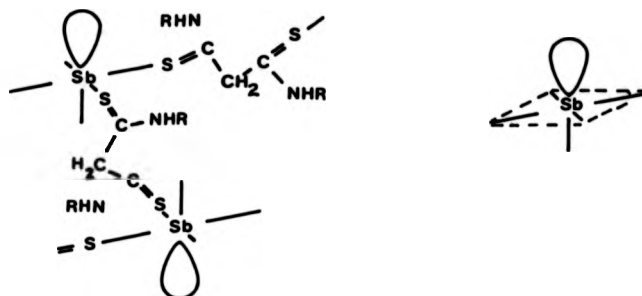
Antimony Trichloride Complexes with Dithioamide Ligands

One interesting observation from the X-ray crystallographic investigation of dithiooxamide Group(VB) complexes is the apparent lack of stereochemical activity of the lone pair. Dithiooxamide ligands are (S,S)-*trans* in the free state and remain so in the complexes $\text{SbCl}_3 \cdot \text{DEDTO}_{1.5}$ and $\text{SbCl}_3 \cdot \text{DIPDTO}_{1.5}$ where antimony is bound to three chlorines and three sulphur atoms each of which comes from a different ligand, resulting in a polymeric structure. This encouraged us to investigate the coordination behaviour of the corresponding dithiomalonamides where the introduction of a $-\text{CH}_2-$ hinge to the C-C backbone not only adds a useful spectroscopic 'flag' but, more importantly provides a more amenable 'bite' angle and increased skeletal flexibility on the part of the ligand.

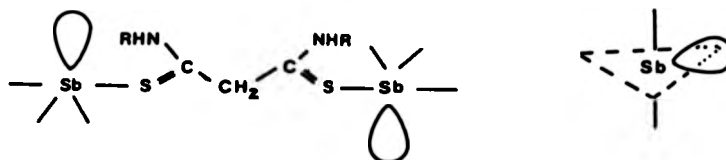
(S,S)-Coordination has been assigned in the Sb(III) and Bi(III) complexes with N,N'-dimethyl- and N,N'-diphenyldithiomalonamide complexes that have been reported¹⁴⁰. This is in accord with HSAB expectations. Interest in dithiomalonamide complexes therefore centres on:

- (a) Whether the sulphur atoms in the free ligand are *trans* to one another and whether they remain so in the complexes formed.
- (b) Whether the apparent lack of stereochemical activity of the lone pair is due to the size of the ligand bite. This assumes that we can only have a stereochemically active lone pair

if a *cis*-chelate is formed (which is not necessarily true). It is not too difficult to envisage an antimony complex with, say, dithiomalonamides where two Sb-S bonds are formed and the ligands are (S,S)-*trans*, leaving room for a lone pair of electrons on one of the coordination sites:



Another interesting possibility is the situation where only one ligand forms a bridge between two SbCl_3 centres to give *tbp* geometry with a lone pair in the equatorial position:



To investigate these several possibilities, we have prepared a series of antimony(III) complexes with N,N'-disubstituted dithiomalonamides. In addition to general spectral data, a structure determination by single crystal X-ray diffraction of one of the complexes, $\text{SbCl}_3 \cdot \text{DEDTM}$ has proved to be the most informative in considerations of metal-ligand binding

Tin Tetrachloride Complexes with Dithioamide Ligands

To complete our current comparison of Lewis acid properties, we now turn to SnCl_4 . With (N)-, (O)-, (P)-, and (S)-donors, monomeric octahedral adducts have been the rule in 1:2 (M:L) complex formation of SnCl_4 adducts^{60,141-144}. Some unidentate ligands have been reported to form 1:1 complexes presumably with trigonal bipyramidal geometries¹⁴⁵⁻¹⁴⁷. Bidentate ligands are expected to form 1:1 octahedral complexes.

Tin Tetrachloride Complexes with Dithioamide Ligands

To complete our current comparison of Lewis acid properties, we now turn to SnCl_4 . With (N)-, (O)-, (P)-, and (S)-donors, monomeric octahedral adducts have been the rule in 1:2 (M:L) complex formation of SnCl_4 adducts^{60,141-144}. Some unidentate ligands have been reported to form 1:1 complexes presumably with trigonal bipyramidal geometries¹⁴⁵⁻¹⁴⁷. Bidentate ligands are expected to form 1:1 octahedral complexes.

Tin Tetrachloride Complexes with Dithioamide Ligands

To complete our current comparison of Lewis acid properties, we now turn to SnCl_4 . With (N)-, (O)-, (P)-, and (S)-donors, monomeric octahedral adducts have been the rule in 1:2 (M:L) complex formation of SnCl_4 adducts^{60,141-144}. Some unidentate ligands have been reported to form 1:1 complexes presumably with trigonal bipyramidal geometries¹⁴⁵⁻¹⁴⁷. Bidentate ligands are expected to form 1:1 octahedral complexes.

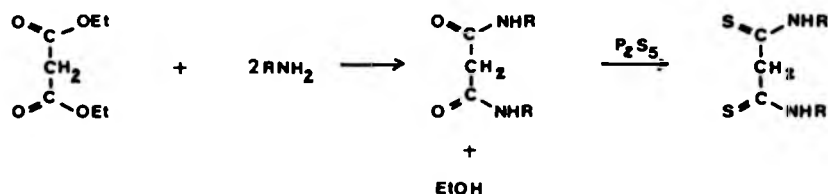
Tin Tetrachloride Complexes with Dithioamide Ligands

To complete our current comparison of Lewis acid properties, we now turn to SnCl_4 . With (N)-, (O)-, (P)-, and (S)-donors, monomeric octahedral adducts have been the rule in 1:2 (M:L) complex formation of SnCl_4 adducts^{60,141-144}. Some unidentate ligands have been reported to form 1:1 complexes presumably with trigonal bipyramidal geometries¹⁴⁵⁻¹⁴⁷. Bidentate ligands are expected to form 1:1 octahedral complexes.

3.2 SYNTHESIS AND CHARACTERISATION OF DITHIO-MALONAMIDES

A variety of synthetic procedures has been followed for the preparation of dithiomalonamides.

- (a) Sulphurisation of malonamides with P_2S_5 :
All malonamides were prepared by the reaction between diethylmalonate and the relevant primary amine.



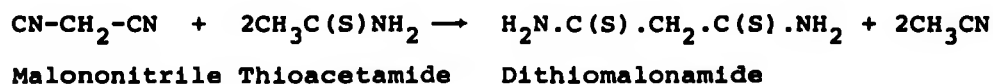
R = $-\text{CH}_3$ (DMDTM), $-\text{C}_2\text{H}_5$ (DEDTM), $-\text{C}_3\text{H}_7$ (DPDTM),
 $-\text{C}_4\text{H}_9$ (DBDTM), $-\text{C}_6\text{H}_{11}$ (DCXDTM).

All five N,N'-disubstituted dithiomalonamides were prepared this way. This reaction has a few drawbacks, *viz.*

- (i) the reaction is very smelly
- (ii) the yields are low, 40% is the norm
- (iii) the products are very difficult to isolate.

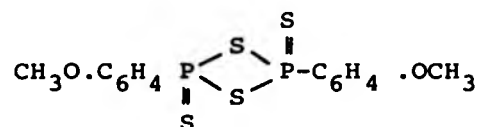
Other avenues to the desired dithiomalonamides were sought.

- (b) An attempt was made to synthesise dithiomalonamide by the method of Taylor *et al.*¹⁴⁸.

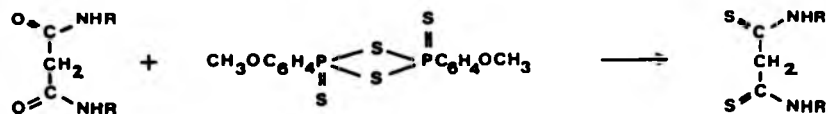


If dithiomalonamide had been isolated, then the synthesis of N,N'-disubstituted dithiomalonamides would follow the Wallach reaction^{107,108}. However, dithiomalonamide was not realised from the thioacetamide reaction.

(c) An attempt was made to replace P_4S_{10} with



and sulphurise the amide following the method of Raucher *et al.*¹⁴⁹.



Unfortunately no substituted dithiomalonamides were isolated from this reaction.

N,N'-Disubstituted Dithiosuccinamides

Methods (a), (b) and (c) above were also used in an attempt to synthesise N,N'-disubstituted dithiosuccinamides but all three methods proved unsuccessful (see Experimental Section).

3.3 REACTIONS OF DITHIOMALONAMIDES WITH SbCl_3

Dropwise addition of the appropriate N,N'-disubstituted dithiomalonamide solution in benzene to an equimolar solution of SbCl_3 in benzene gave rise to yellow/orange precipitates of the 1:1 adducts $\text{SbCl}_3 \cdot \text{L}$ (L = DMDTM, DEDTM, DPDTM, DBDTM, DCXDTM) in high yield. The adducts were purified by washing with benzene and pumping *in vacuo*. The adducts were extremely air/moisture sensitive hence they were handled in strict anaerobic conditions. The complexes are listed in Table 3.3.1 and their solubility is limited to the more polar solvents such as acetonitrile, dichloromethane and acetone.

Principal i.r. vibrational bands of the ligands and adducts are presented in Table 3.3.2. Assignments follow those of Jensen and Nielsen¹⁵⁰. The observed high energy shift ($+32 \text{ cm}^{-1}$ on average) of the $\nu(\text{CN})$ absorption (*ca.* 1540 cm^{-1}) accompanied by the low energy shift (-90 cm^{-1} on average) of the $\nu(\text{CS})$ band (*ca.* 870 cm^{-1}) are in accord with (S)-donation¹³⁵⁻¹⁴¹. The $\nu(\text{NH})$ vibrations remain essentially unchanged. In the $\nu(\text{Sb-Cl})$ stretching region, we find two broad and intense bands at *ca.* 320 and 250 cm^{-1} which no doubt have $\nu(\text{Sb-S})$ components.

¹H n.m.r. data are presented in Table 3.3.3. Due to poor solubility in CDCl_3 , ¹H n.m.r. spectra of the adducts were obtained from $(\text{CD}_3)_2\text{CO}$ solutions wherever possible. The ¹H n.m.r. data of the complexes simply reinforce the non-coordination of the NH sites and are without controversy. Integral values show the presence

3.3 REACTIONS OF DITHIOMALONAMIDES WITH SbCl_3

Dropwise addition of the appropriate N,N'-disubstituted dithiomalonamide solution in benzene to an equimolar solution of SbCl_3 in benzene gave rise to yellow/orange precipitates of the 1:1 adducts $\text{SbCl}_3 \cdot \text{L}$ (L = DMDTM, DEDTM, DPDTM, DBDTM, DCXDTM) in high yield. The adducts were purified by washing with benzene and pumping *in vacuo*. The adducts were extremely air/moisture sensitive hence they were handled in strict anaerobic conditions. The complexes are listed in Table 3.3.1 and their solubility is limited to the more polar solvents such as acetonitrile, dichloromethane and acetone.

Principal i.r. vibrational bands of the ligands and adducts are presented in Table 3.3.2. Assignments follow those of Jensen and Nielsen¹⁵⁰. The observed high energy shift (+32 cm^{-1} on average) of the $\nu(\text{CN})$ absorption (ca. 1540 cm^{-1}) accompanied by the low energy shift (-90 cm^{-1} on average) of the $\nu(\text{CS})$ band (ca. 870 cm^{-1}) are in accord with (S)-donation¹³⁵⁻¹⁴¹. The $\nu(\text{NH})$ vibrations remain essentially unchanged. In the $\nu(\text{Sb-Cl})$ stretching region, we find two broad and intense bands at ca. 320 and 250 cm^{-1} which no doubt have $\nu(\text{Sb-S})$ components.

¹H n.m.r. data are presented in Table 3.3.3. Due to poor solubility in CDCl_3 , ¹H n.m.r. spectra of the adducts were obtained from $(\text{CD}_3)_2\text{CO}$ solutions wherever possible. The ¹H n.m.r. data of the complexes simply reinforce the non-coordination of the NH sites and are without controversy. Integral values show the presence

Table 3.3.1 Analytical data of complexes

Compound	Microanalyses (%) Observed/Calculated			
	C	H	N	Cl
SbCl ₃ (DMDTM)	16.7/15.4	2.5/2.6	7.0/7.2	27.4/27.3
SbCl ₃ (DEDTM)	20.2/20.1	3.2/3.3	7.0/6.7	26.2/25.5
SbCl ₃ (DPDTM)	24.0/24.2	3.9/4.0	6.2/6.3	24.7/23.9
SbCl ₃ (DBDTM)	26.8/27.8	4.5/4.6	5.2/5.9	21.3/22.5

Table 3.3.2 Principal i.r. bands (cm⁻¹) of ligands and metal complexes

Compound	$\nu(\text{NH})$ (s)	Thioamide I $\nu(\text{CN})_{\text{ts}}$	Thioamide IV $\nu(\text{CS})_{\text{tm}}$	Thioamide V $\nu(\text{NH})_{\text{tm}}$	$\nu(\text{MCL/MS})$ (m)
DEDTM	3186, 3057	1540	875	722	
DPDTM	3194, 3060	1542	874	719	
DBDTM	3191, 3040	1536	890	732	
DCXDTM	3518, 3282 3230, 3050	1541	895	746	
SbCl ₃ (DMDTM)	3206, 3109	1584	785	722	315, 250
SbCl ₃ (DEDTM)	3180, 3060	1572	803	717	320, 276, 240
SbCl ₃ (DPDTM)	3188, 3044	1577	790	721	318, 279
SbCl ₃ (DBDTM)	3264, 3200 3068	1565	782	730	323, 275, 235
SbCl ₃ (DCXDTM)	3260, 3078	1561	790	758	321, 288

Table 3.3.3 ¹H n.m.r. data (δ p.p.m. w.r.t. TMS ($\delta = 0$)) of the ligands and a few complexes

Compound	N-H (s, br)	C(S)-CH ₂ -C(S) (s)	N-CH ₂	CH ₂	CH ₂	CH ₃	C ₆ H ₁₁
(a) CDCl ₃ solution							
DMDTM	8.88	4.15				3.18 d	
DEDTM	9.10	4.17	3.67 m			1.29 t	
DPDTM	9.00	4.15	3.60 q	1.70 m		0.99 t	
DBDTM	8.94	4.17	3.65 q	1.65 m	1.40 m	0.95 t	
DCXDTM	8.92	4.25					1.28-2.00 m
(b) (CD ₃) ₂ CO solution							
SbCl ₃ .DMDTM	9.60	4.10					
DEDTM	9.50	4.01	3.62 m			1.20 t	
SbCl ₃ .DEDTM	9.60	4.09	3.65 m			1.22 t	
DBDTM	9.53	4.01	3.64 q	1.64 m	1.40 m	0.90 t	
SbCl ₃ .DBDTM	9.77	4.23	3.65 q	1.68 m	1.40 m	0.90 t	

of two protons on the backbone $\text{-CH}_2\text{-}$ which is consistent with absence of deprotonation of the backbone $\text{-CH}_2\text{-}$ in non-aqueous systems. The ligands have been fully characterised (^1H n.m.r.) for the first time, chemical shift(s) values are evidently strongly solvent dependent.

3.4 THE CRYSTAL STRUCTURE OF $\text{SbCl}_3\cdot\text{DEDTM}$

Crystals suitable for X-ray crystallography were obtained by recrystallisation of $\text{SbCl}_3\cdot\text{DEDTM}$ from hot benzene under nitrogen. Details of cell constants, data collection and refinement are given in Table 3.4.1. The structure was solved by Patterson and Fourier methods and refined by full matrix least squares. Only Sb, S, and Cl were refined anisotropically. The data for this structure is of poor quality as the crystal diffracted X-rays very weakly. However, the structure could be solved and showed the five-coordinate core with the lone-pair active. The structure of the ligand was disordered and we doubt the accuracy of the light atom positions. However, the positions of the Sb, Cl and S atoms are beyond dispute. In the refinement, it proved impossible to refine the light atoms without constraint. In the event we constrained the S-C, C-N and C-C distances at their usual values. However, it proved impossible to locate the ethyl groups bonded to nitrogen. Atomic positions are given in Table 3.4.2, bond lengths and angles are given in Table 3.4.3.

The coordination geometry of $\text{SbCl}_3\cdot\text{DEDTM}$ (Figure 3.4.1) may be described as square pyramidal with the ligand DEDTM bonding through its (S)-atoms as a *cis*-chelate to two basal positions in the antimony coordination sphere. The observed stereochemistry is consistent with VSEPR predictions for an AB_5E system, a pseudooctahedral system with the lone pair taking up

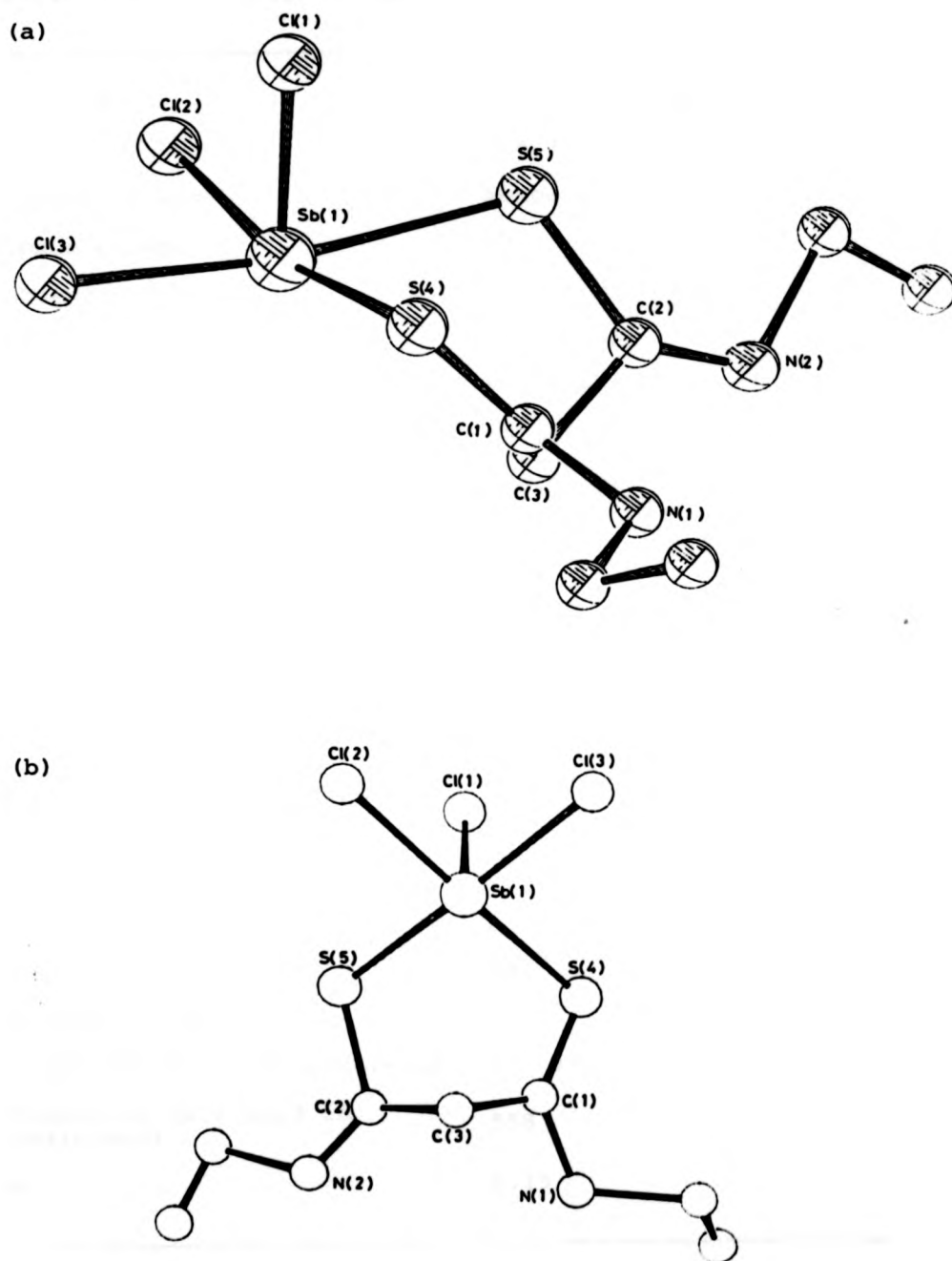
Figure 3.4.1 The Crystal Structure of $\text{SbCl}_3 \cdot \text{DEDTM}$ 

Table 3.4.1 Crystal data for $\text{SbCl}_3\text{DEDTM}$

Formula	$\text{C}_7\text{H}_{14}\text{N}_2\text{S}_2\text{Cl}_3\text{Sb}$
M	418.3
Crystal Class	Monoclinic
Space group	P2_1
Absences	oko, $k = 2n + 1$
$a (\text{\AA})$	10.841(8)
$b (\text{\AA})$	8.276(9)
$c (\text{\AA})$	10.185(11)
$\beta (^\circ)$	120.94(8)
$U (\text{\AA}^3)$	757.7
Z	2
$\mu (\text{Mo K}\alpha) (\text{cm}^{-1})$	23.3
$D_m (\text{g, cm}^{-3})$	1.55
$D_c (\text{g, cm}^{-3})$	1.55
$\lambda (\text{\AA})$	0.7107
$F(000)$	408
Crystal size (mm)	0.5 x 0.5 x 0.1
Rotation axis	b
$2\theta_{\text{max}}$	100°
Number of data	912
Criterion for data inclusion	$I > \sigma(I)$
Number of data used in refinement	558
R	0.15

Table 3.4.2 Atomic Positions for $\text{SbCl}_3 \cdot \text{DEDTM}$

	X	Y	Z
Sb	1723 (14)	2500	-0000 (15)
Cl (1)	3536 (68)	0394 (68)	0037 (72)
Cl (2)	-0167 (65)	0535 (67)	-2059 (63)
Cl (3)	1939 (54)	0557 (67)	2109 (60)
S (4)	4023 (48)	4303 (56)	2007 (59)
S (5)	2098 (57)	4294 (80)	-1978 (53)
C (1)	350 (13)	649 (14)	138 (12)
C (2)	196 (14)	626 (15)	-147 (12)
C (3)	161 (15)	642 (16)	-006 (14)
N (1)	377 (18)	827 (20)	226 (17)
N (2)	175 (21)	834 (24)	-248 (21)

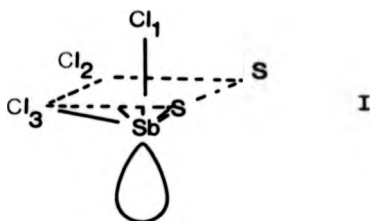
The positions of the remaining atoms are so doubtful that they are not reported here.

Table 3.4.3 Bond lengths (\AA) and angles ($^\circ$) for $\text{SbCl}_3 \cdot \text{DEDTM}$

Sb(1)	-	C1(1)	2.30(6)
Sb(1)	-	C1(2)	2.59(4)
Sb(1)	-	C1(3)	2.60(5)
Sb(1)	-	S(4)	2.67(4)
Sb(1)	-	S(5)	2.69(6)
C1(1)	-	Sb(1) - C1(2)	86.1(21)
C1(1)	-	Sb(1) - C1(3)	84.8(22)
C1(1)	-	Sb(1) - S(4)	84.1(19)
C1(1)	-	Sb(1) - S(5)	83.9(22)
C1(2)	-	Sb(1) - C1(3)	89.2(18)
C1(2)	-	Sb(1) - S(4)	169.7(23)
C1(2)	-	Sb(1) - S(5)	94.9(20)
C1(3)	-	Sb(1) - S(4)	93.0(17)
C1(3)	-	Sb(1) - S(5)	167.6(17)
S(4)	-	Sb(1) - S(5)	81.0(16)

Remaining dimensions were constrained in the refinement and so are not reported here.

one of the octahedral positions on the antimony coordination sphere. The Sb atom is below the Cl_2 , Cl_3 , S, S plane (I) and the angles $\text{Cl}(1)\text{-Sb-Cl}(2)$ $86.1(21)^\circ$, $\text{Cl}(1)\text{-Sb-Cl}(3)$ $84.8(22)^\circ$, $\text{Cl}(1)\text{-Sb-S}(4)$ $84.1(19)^\circ$, $\text{Cl}(1)\text{-Sb-S}(5)$ $83.9(22)^\circ$, all less than 90° by a long way, emphasising the stereochemical influence of the lone pair.



Sb-Cl bond distances (2.60, 2.59 and 2.30 Å) fall into two groups the two *cis* to the lone pair are longer than Sb-Cl distances found in pure crystalline SbCl_3 (2.34, 2.38, 2.38 Å) while the bond *trans* to the lone pair is a little shorter. This lengthening of two Sb-Cl bonds is also attributed to the influence of the lone pair. However, the Sb-S distances in $\text{SbCl}_3\cdot\text{DEDTM}$ (2.67, 2.69 Å) are considerably shorter than Sb-S distances (ca. 3.2 Å) in the ligand bridged polymeric complexes of SbCl_3 with dithiooxamides and cyclic thioethers.

AB_5E geometry where the lone pair acts at one of the octahedral positions resulting in the lengthening of B-A bonds *cis* to the lone pair has been observed in many antimony(III) complexes. The structure of the $[\text{SbCl}_5]^{2-}$ ion in $[\text{NH}_4]_2[\text{SbCl}_5]^{151}$ and $\text{K}_2\text{SbCl}_5^{32}$ shows the antimony in a pseudooctahedral environment with the lone pair presumably occupying one of the positions. In both

these structures, Sb-Cl Bonds *cis* to the lone pair are in the range 2.5-2.8 Å while the shorter Sb-Cl is 2.35-2.39.

Another example is that of the 1:2 adduct of SbCl_3 and pyridine³¹.

The structure of $\text{SbCl}_3 \cdot \text{DEDTM}$ is the first example of an antimony(III) complex with a *cis* chelating ligand resulting in a square pyramidal complex. No chelates were observed between SbCl_3 and the analogous dithiooxamide ligands. It is possible that the ligand bite in dithiooxamides is too small for chelate formation. The bite in malonamides is larger and more flexible. The six-membered ring formed in $\text{SbCl}_3 \cdot \text{DEDTM}$ shows a boat conformation.

The structure of the ligand is not available for comparison since no suitable crystals could be obtained but what is curious is that this complex does not have the *trans*-(S,S)-bridging mode observed in $\text{SbCl}_3 \cdot \text{DEDTO}_{1.5}$ and $\text{SbCl}_3 \cdot \text{DIPDTO}_{1.5}$.

3.5 COMPLEXES OF SnCl_4 WITH DEDTM, DPDTM, DBDTM

Tin tetrachloride reacted with the dithiomalonamide ligands in benzene solution (1:1) forming light coloured precipitates. These were washed with benzene and dried *in vacuo*. Due to the fact that these solids were extremely air/moisture sensitive, all manipulations had to be carried out under an inert atmosphere. The powders were insoluble in common non-coordinating solvents but they dissolved with a colour change to give yellow solutions in acetone and boiling benzene. The complexes are listed in Table 3.5.1 together with their principal i.r. bands.

Table 3.5.1 Principal i.r. bands of the complexes (cm^{-1})

Compound	$\nu(\text{NH})$ (s, br) (s)	$\nu(\text{CN})$ (s)	$\nu(\text{CS})$ (w)	$\pi(\text{NH})$ (s)	$\nu(\text{MX/MS})$ (v.s)
$\text{SnCl}_4\text{DEDTM}$	3260, 3140	1590	800, 773	687	315
DEDTM	3180, 3060	1540	875, 795	645	
$\text{SnCl}_4\text{DPDTM}$	3245, 3130	1580	807	660	309
DPDTM	3200, 3060	1540	875, 750	620	
$\text{SnCl}_4\text{DBDTM}$	3260, 3130	1585	885, 765	660	310
DBDTM	3200, 3040	1535	890, 800	675	

In these complexes the $\nu(\text{CN})$ band moves to higher frequencies and the $\nu(\text{CS})$ moves to lower frequencies on complexation, indicating (S)-donation to the metal. In all previous complexes with dithiooxamides or dithiomalonamides, the $\nu(\text{NH})$ band has remained little

affected by complexation, however in SnCl_4 malonamide complexes, the $\nu(\text{NH})$ region becomes a little more complex on complex-formation being split into up to four bands. The Sn-Cl stretching region of the spectrum is complicated by the possibility of vibrational mixing with Sn-S vibrations. A prominent band at 310-315 is expected to have a major Sn-Cl contribution^{68,152}.

Unfortunately ^1H n.m.r. data are not very informative since δ values remain essentially unchanged on complexation. We favour an (S,S)-chelate ligand attachment to SnCl_4 .

After many attempts at recrystallisation, we were able to isolate crystals from a solution of SnCl_4 /DEDTM in benzene.

I.r. absorptions: (cm^{-1}) (Nujol mull) 3280 $\nu(\text{NH})$, 1545 $\nu(\text{CN})$,
790 $\nu(\text{CS})$, 670 $\pi(\text{NH})$, 514 $\nu(\text{S-S})$,
310,280 $\nu(\text{Sn-Cl})$

(Found: C 23.35, H 3.62, N 8.09 Calculated for
 $\text{C}_{14}\text{H}_{26}\text{S}_4\text{N}_4\text{Cl}_6\text{Sn}$
C 23.67, H 3.66, N 7.89%)

An X-ray crystallographic study has revealed that this product is not the presumed six coordinate neutral adduct but rather the salt-like structure $[\text{EtNHC}(\text{S})\text{CHC}(\text{S})\text{NHEt}]_2[\text{SnCl}_6]$ featuring the hexachlorostannate ion.

SnCl_4 Complexes in Solution

Relatively fewer studies of SnCl_4 complexes and their reactions in solution have been reported. SnCl_4

forms a 1:1 complex with 2,2'-bipyridine with a $\log k > 7$ ¹⁵³, while with acetonitrile, a *cis* 2:1 complex is formed¹⁵⁴. Polarographic studies show that SnCl_4 is essentially a non-electrolyte in acetonitrile but forms the stable SnCl_6^{2-} species upon the addition of chloride ion. The formation of octahedral hexahalogenometallates of the type A_2SnX_6 (A = univalent cation, X = halogen) on addition of excess halide is well documented¹⁵⁵. Structural studies utilising both single crystal X-ray diffraction¹⁵⁶ and halogen n.q.r.¹⁵⁷ techniques show variations of Sn-X bond length within these SnX_6^{2-} species. Evidently the choice of cation is crucial especially where hydrogen bonding may reasonably be expected^{157(d),158}.

Our interest in the solution studies of SnCl_4 complexes stems from the successful isolation of the ionic product $[\text{EtNHC}(\overline{\text{S}})\text{CHC}(\overline{\text{S}})\text{NHET}]_2[\text{SnCl}_6]$ which we proceed to describe in the next section.

3.6 CRYSTAL AND MOLECULAR STRUCTURE OF
 $[\text{EtNHC}(\text{S})\text{CHC}(\text{S})\text{NHET}]_2[\text{SnCl}_6]_2$, AN
UNUSUAL PRODUCT FOLLOWING THE RECRYSTAL-
LISATION OF THE ADDUCT SnCl_4 DEDTM FROM BENZENE

The crystal data and refinement details are given in Table 3.6.1, atomic coordinates in Table 3.6.2, and bond lengths and angles in Table 3.6.3; Figures 3.6.1 and 3.6.2 shows the molecular arrangement. The structure consists of discrete centrosymmetric SnCl_6^{2-} anions and $[\text{EtNHC}(\text{S})\text{CHC}(\text{S})\text{NHET}]^+$ cations in the ration 1:2. The ions are connected *via* N-H...Cl hydrogen bonds. N(11) is involved in a single hydrogen bond *viz.* N(11)...Cl(3) 3.33 Å, N(11)-H...Cl(3) 165°. However, the arrangement around N(31) is more complicated and it forms a bifurcated hydrogen bond to two chlorines from a SnCl_6^{2-} anion. Dimensions are N(31)...Cl(1') 3.46, N(31)...Cl(3') 3.54 with angles N(31)-H...Cl(1') 105 and N(31)-H...Cl(3') 153°.

This hydrogen bond formation is a significant feature in structures of the dithiooxamide complexes $\text{BiCl}_3\text{DEDTO}_2$ and SnBrDBDTO (see Section 2.7 and 2.8) where all the -NH groups are involved in hydrogen bonding. In the present structure, the three Sn-Cl bond lengths are different: Sn-Cl(1) 2.422(1), Sn-Cl(2) 2.405(1), Sn-Cl(3) 2.467(1). It is significant that the longest Sn-Cl bond involves the chlorine atom Cl(3) that forms the strongest hydrogen bond. Indeed all three bonds are consistent with the theory that the formation of hydrogen bonds lengthens the Sn-Cl bond^{158(a)}.

Figure 3.6.1 The Crystal Structure of $[\text{EtNHC}(\text{S})\text{CHC}(\text{S})\text{NHEt}]^+$

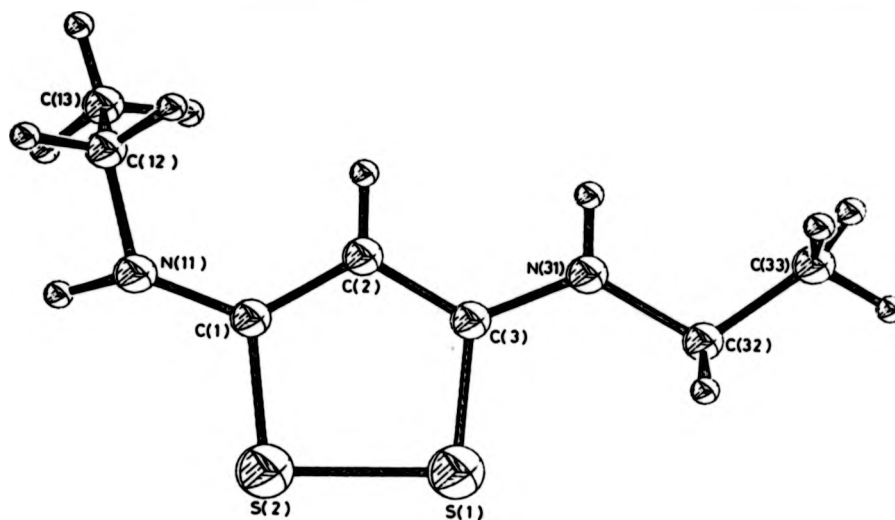


Figure 3.6.2 The Molecular Arrangement in $[\text{EtNHC}(\text{S})\text{CHC}(\text{S})\text{NHEt}]_2[\text{SnCl}_6]$

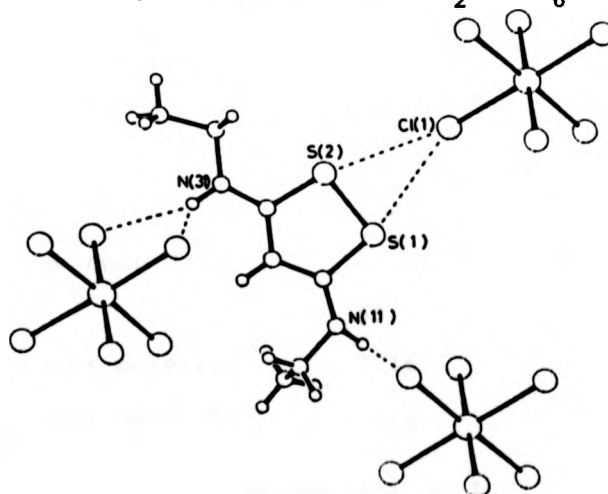


Table 3.6.1 Crystal data and refinement details for
 $[\text{EtNHC}(\bar{S})\text{CHC}(\bar{S})\text{NHET}]_2[\text{SnCl}_6]$

Compound	$[\text{EtNHC}(\bar{S})\text{CHC}(\bar{S})\text{NHET}]_2[\text{SnCl}_6]$
Formula	$\text{C}_{14}\text{H}_{26}\text{S}_4\text{N}_4\text{SnCl}_6$
M	709.8
Crystal class	Triclinic
Space group	$\text{P}\bar{1}$ (from the successful structure analysis)
a (Å)	9.047(7)
b (Å)	9.429(8)
c (Å)	9.935(8)
α (°)	80.4(1)
β (°)	63.0(1)
γ (°)	65.6(1)
U (Å ³)	687.5
Z	1
μ (MoK α) (cm ⁻¹)	18.1
D _m (g, cm ⁻³)	1.71
D _c (g, cm ⁻³)	1.71
λ (Å)	0.7107
F (000)	354
Crystal size (mm)	0.3 x 0.3 x 0.3
Rotation axis	b
2 θ_{max} (°)	50
Number of data measured	3716
Number of data used in refinement	3260
Criterion for data inclusion	$I > 3\sigma I$
Final R value	0.064

Table 3.6.2 Atomic Coordinates ($\times 10^4$) for
 $[\text{EtNHC}(\text{S})\text{CHC}(\text{S})\text{NHEt}]_2[\text{SnCl}_6]$
 with Estimated Standard Deviations
 in Parentheses

ATOM	X	Y	Z
SN(1)	0 (0)	0 (0)	0 (0)
CL(1)	-1008 (2)	1692 (2)	2089 (1)
CL(2)	2831 (2)	303 (2)	-1187 (2)
CL(3)	-1297 (2)	2294 (2)	-1304 (2)
S(1)	6943 (3)	3747 (2)	5566 (2)
S(2)	8365 (3)	4974 (2)	3984 (2)
C(1)	7234 (7)	6684 (7)	5098 (6)
C(2)	5908 (7)	6628 (6)	6523 (6)
C(3)	5635 (7)	5251 (5)	6920 (6)
N(11)	7688 (8)	7882 (7)	4509 (6)
C(12)	6959 (9)	9348 (7)	5313 (8)
C(13)	7940 (12)	9255 (9)	6252 (11)
N(31)	4425 (7)	5014 (5)	8237 (6)
C(32)	4115 (11)	3569 (8)	8649 (9)
C(33)	2674 (20)	3698 (12)	10162 (11)

Table 3.6.3 Bond lengths (\AA) and angles ($^\circ$) for $[\text{EtNHC}(\text{S})\text{CHC}(\text{S})\text{NHIEt}]_2[\text{SnCl}_6]$

ANION

SN (1)	-	CL (1)	2.422(1)		
SN (1)	-	CL (2)	2.405(1)		
SN (1)	-	CL (3)	2.467(1)		
CL (1)	-	SN (1)	-	CL (2)	90.59(5)
CL (1)	-	SN (1)	-	CL (3)	89.26(5)
CL (2)	-	SN (1)	-	CL (3)	90.72(6)

CATION

S (1)	-	S (2)	2.063(3)		
S (1)	-	C (3)	1.738(5)		
S (2)	-	C (1)	1.754(6)		
C (1)	-	C (2)	1.390(7)		
C (1)	-	N (11)	1.316(8)		
C (2)	-	C (3)	1.382(7)		
C (3)	-	N (31)	1.329(7)		
N (11)	-	C (12)	1.455(9)		
C (12)	-	C (13)	1.525(11)		
N (31)	-	C (32)	1.459(7)		
C (32)	-	C (33)	1.458(11)		
S (2)	-	S (1)	-	C (3)	94.63(20)
S (1)	-	S (2)	-	C (1)	95.49(20)
S (2)	-	C (1)	-	C (2)	115.3 (4)
S (2)	-	C (1)	-	N (11)	117.9 (4)
C (2)	-	C (1)	-	N (11)	126.8 (5)
C (1)	-	C (2)	-	C (3)	117.6 (4)
S (1)	-	C (3)	-	C (2)	117.0 (4)
S (1)	-	C (3)	-	N (31)	118.3 (3)
C (2)	-	C (3)	-	N (31)	124.8 (4)
C (1)	-	N (11)	-	C (12)	124.7 (5)
N (11)	-	C (12)	-	C (13)	111.5 (5)
C (3)	-	N (31)	-	C (32)	124.8 (5)
N (31)	-	C (32)	-	C (33)	111.2 (5)

The five-membered 1,2-dithiolynium ring in the cation (Figure 3.6.1) is planar within experimental error (see Table 3.6.3). The N-C groups are also coplanar. However, C(13) is twisted well out of the plane but C(33) remains in the plane. It is only the positions of these final carbon atoms of the ethyl group that prevent the cation having C_s symmetry within experimental error.

Compounds with similar heterocyclic rings have been the subject of several structural investigations¹⁵⁹⁻¹⁶². Such rings are planar and within the ring, conjugation also extends over the S-S bond to give a pseudo aromatic system. In our structure, the two C-C bond lengths 1.38, 1.39 Å are as expected but the C-S and S-S distances are longer than might be expected in a planar aromatic ring, the S-S distance being within the usual range (2.059-2.108 Å)¹⁶³ for S-S single bonds. A survey of 21 crystal structures¹⁶⁴ with S-S bonds showed a range of bond lengths from 1.999 to 2.082. A correlation was found between the S-S bond lengths and the X-C-S-S (X = C or N) torsion angle. When X-C-S-S is between -20° and 20° , the average S-S bond is 2.03 Å (15 structures) while between 70° and 90° the distance is 1.08 Å (6 structures). Our distance is 2.063(3) Å and the torsion angles are close to 0° . This fact could be due to the influence of the positive charge on the ion.



However, in structures of the 1,2-dithiolonium halides^{159,160}, the S-S distances are also in the range 2.00 to 2.03. In these halides, it is found that the sulphur atoms have close interaction with the halide anions (S---I *ca.* 3.5 Å).



In the present structure (see Figure 3.6.2) the S,S,Cl triangle formed has a rather similar geometry to that found in the above halides but the S---Cl distances are rather long at 3.55, 3.60, S(1)---Cl(1), S(2)---Cl(1) respectively and these could represent just Van der Waals contacts. However, as is clear from the Figure this Cl(1) atom is approximately coplanar with the ring.

Other than the distances discussed above there are no interactions of note between ions.

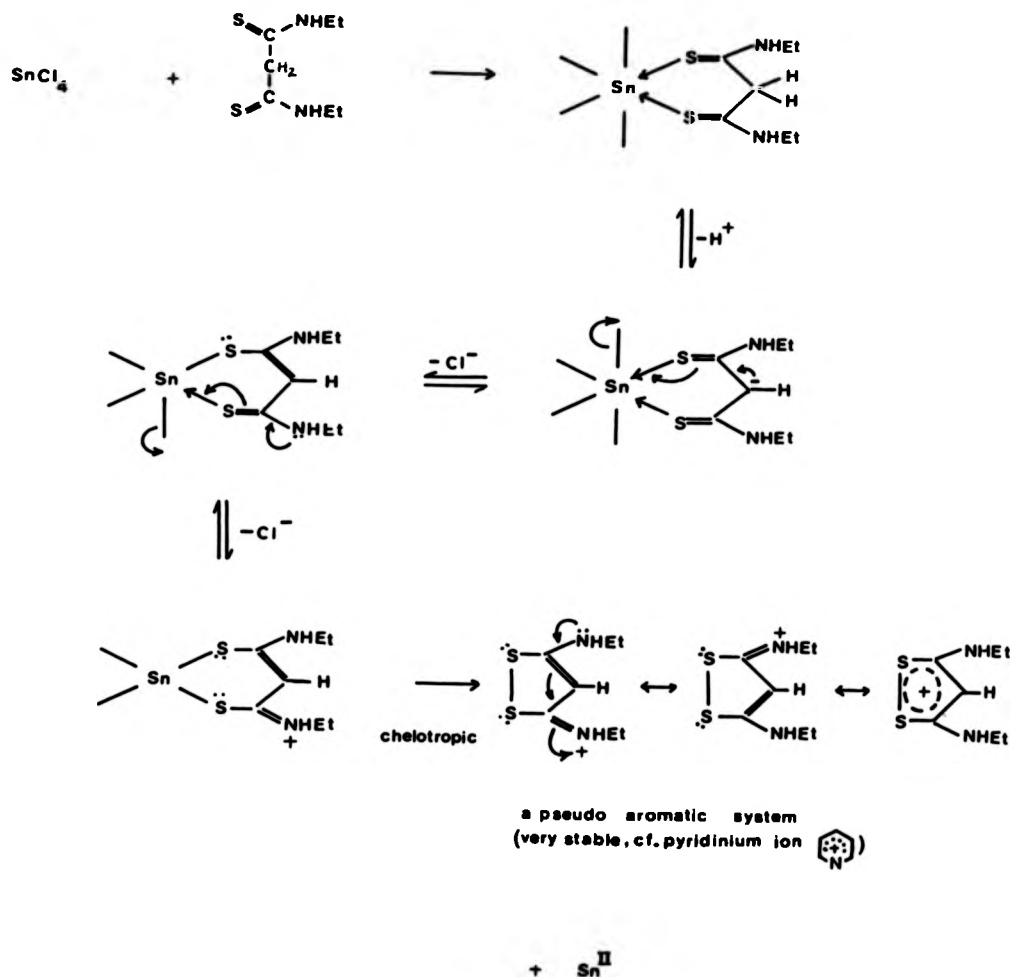
Aside from the structural interest in the dithiolinium ring and SnCl_6^{2-} *vis-a-vis* hydrogen bonding, we are quite interested in the actual formation of such a species from our neutral adduct in benzene solution. The observed pink \rightarrow yellow colour change following dissolution in benzene provided the first hint of a structural reorganisation of the Sn(IV) complex. Frequency values of the $\nu(\text{Sn-Cl})$ i.r. bands observed for the yellow SnCl_6^{2-} complex at 280 and 310 cm^{-1} suggest that the Sn-Cl bonds in SnCl_6^{2-} anion are weaker than the Sn-Cl bond in $\text{Me}_3\text{Sn-Cl}$ (330-336 cm^{-1}) and Me_2SnCl_2 (320-350 cm^{-1}),¹⁶⁵⁻¹⁶⁷. The multiplicity of the bands suggests a deformation in the SnCl_6 octahedron, $\nu(\text{Sn-Cl})$ for SnCl_6^{2-} in $(\text{NH}_4)_2\text{SnCl}_6$ is 312 cm^{-1} . It is possible that this deformation is associated with the link to the cation as well as hydrogen bonding with some of the protons on the ring.

In the high frequency region of the spectrum, $\nu(\text{NH})$ is shifted to higher energy, from 3180 cm^{-1} , in the free ligand, to 3280 cm^{-1} in the complex which suggests an increase in electron density along the N-H bond. It is interesting that νCN (1540 cm^{-1}) is not greatly shifted by dithiolynium ring formation although increased multiplicity of this band is observed. The $\nu(\text{C-S})$ band at 875 cm^{-1} in the ligand is shifted to lower energy (790 cm^{-1}) indicating the expected reduction in C-S double bond character. This is reflected by C-S bond distances of 1.73, 1.75 Å compared with C-S (\sim 1.66 Å).

A new intense band at 514 cm^{-1} is assigned to a $\nu(\text{S-S})$ vibrational mode^{168,169}.

The above spectral assignments are consistent with the isolated product $[\text{EtNHC}(\overline{\text{S}})\text{CHC}(\overline{\text{S}})\text{NHet}]_2[\text{SnCl}_6]$ but throw very little light on the 'reaction pathway' or indeed any of the other products from this reaction. This is a reaction that we have just stumbled on and have not yet set out to do a systematic investigation of. We believe that adduct formation is the initial step of this reaction, then the adduct rearranges on boiling with benzene to give as one of the products, $[\text{EtNHC}(\overline{\text{S}})\text{CHC}(\overline{\text{S}})\text{NHet}]_2[\text{SnCl}_6]$. The ^1H n.m.r. spectrum of the yellow crystals, δ H (220 MHz, solvent $(\text{CD}_3)_2\text{CO}$, standard Me_4Si) 1.28 (6H, t, $-\text{CH}_3$), 3.62 (4H, m, $-\text{CH}_2-$), 7.35 (1H, s, CH), and 9.90 (2H, br.s, $-\text{NH}$) shows only one significant change compared with that of the neat ligand, i.e. the appearance of the methyne ($=\text{CH}-$) singlet (δ 7.35) in place of the original methene ($-\text{CH}_2-$) singlet (δ 6.03).

Proposed Reaction Scheme:



The fate of the H^+ and $\text{Sn}(\text{II})$ species is unknown.

It is unclear whether this reaction is unique to DEDTM or whether other dithiomalonamide ligands would undergo a similar rearrangement. Another point here is the specificity of the metal centre; would $\text{Ti}(\text{IV})$ for example, effect such a rearrangement? One final point: does the solvent participate in this rearrangement? The SbCl_3 complex with DEDTM was recrystallised from benzene

and no similar rearrangement was observed in this case.

3.7 EXPERIMENTALPreparation of the Ligands

The malonamide derivatives - as obtained from the appropriate aminolysis of diethylmalonate - were treated with P_4S_{10} in boiling xylene following a modified route to that described by Hurd *et al.*¹⁰⁶ for N,N'-disubstituted dithiooxamides. (NB: The Wallach reaction involving dithiomalonamide and the appropriate amine as starting materials was not used as the obvious synthetic route due to our inability to prepare dithiomalonamide itself in any reasonable quantities.)

Typically for N,N'-di-n-propyl Dithiomalonamide (DPDTM)

A solution of n-propylamine (44.5 cm^3 , 0.54 mol) in ethanol (50 cm^3) was added to a stirred solution of diethylmalonate (41.0 cm^3 , 0.27 mol) in ethanol (50 cm^3). The mixture was maintained at 50°C for several hours. On cooling, a white crystalline mass slowly precipitated. This was filtered, washed with ether and dried under vacuum. Yield: 20 g, 40%.

A suspension of N,N'-di-n-propylmalonamide (5 g, 26 mmol) in boiling xylene was treated with a large excess of phosphorus pentasulphide powder (40 g, 90 mmol) following incremental additions ($\sim 5 \text{ g}$) over a period of approximately 2 hours. The mixture was stirred mechanically, heated at reflux for 12 hours and then most of the xylene was distilled off. Water ($\sim 300 \text{ cm}^3$) was added to the resulting mixture and the system warmed

over a water bath. The evolved H_2S (sometimes vigorous) was conveniently "trapped out" by bubbling through warm saturated solutions of potassium permanganate. The xylene layer was decanted and the remaining aqueous phase was treated with methanol for extraction of the product. The resulting orange-brown liquid was repeatedly boiled with activated charcoal and filtered until a clear orange solution was obtained. Evaporation gave an orange-brown solid which was recrystallised from ethanol to give orange crystals which were pumped dry at the vacuum line. Yield 3.0 g (51%).

The spectral data for this and other derivatives is given in Tables 3.3.2 and 3.3.3.

Preparation of SbCl_3 Complexes

All manipulations were conducted under an inert atmosphere most often using a dry nitrogen flushed gloved-box. An all glass vacuum line system was used on occasion. To illustrate the procedure, we describe the preparation of the SbCl_3 complex with N,N'-di-n-butyl dithiomalonamide.

A solution of N,N'-di-n-butyl dithiomalonamide (0.97 g, 3.9 mmol) in benzene (150 cm^3) was added dropwise to a stirred solution of antimony trichloride (0.90 g, 3.9 mmol) in benzene (70 cm^3) maintained at 273 K. The resulting solution was stirred overnight. Solvent was slowly removed until the onset of crystallisation. The solution was allowed to stand to facilitate crystal growth. The yellow solid which deposited was recrystallised from benzene to give yellow needles. The solid was pumped

dry at the vacuum line and sealed, under nitrogen, in glass tubes.

Analytical data for this and other products are collected in Table 3.3.1.

Preparation of SnCl_4 Complexes

We choose to illustrate the preparation of SnCl_4 complexes by the procedure that led to the unexpected cyclisation product.

A solution of DEDTM (0.635 g, 3.3 mmol) in benzene (70 cm^3) was added dropwise to a stirred solution of SnCl_4 (0.4 cm^3 , 3.47 mmol) in benzene (100 cm^3). The pink precipitate that formed was stirred for 12 hours. The solvent was decanted off and the powder washed with redistilled benzene (2 x 100 cm^3) at the vacuum line before being dried *in vacuo* and sealed under nitrogen in glass tubes.

I.r. spectrum (Nujol mull) cm^{-1} , ν_{max} : 3260, 3140, 3040
(selected bands) (NH); 1590 (CN); 800, 773 (CS);
315 (MX/MS)

The pink powdery $\text{SnCl}_4\text{DEDTM}$ dissolved in boiling benzene to give a yellow solution. Slow evaporation of this benzene solution at room temperature under nitrogen yielded well formed yellow needle-shaped crystals suitable for crystallographic study, i.r. spectrum is presented here for comparison.

Selected bands (cm^{-1}), ν_{max} : 3280, 3060 (NH); 1545 (CN);
790 (CS); 310, 280 (MX).

CHAPTER 4

OXAMIDES, MALONAMIDES, SUCCINAMIDES AND
THEIR COMPLEXES WITH SbCl_3 AND SnCl_4

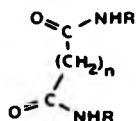
CHAPTER 4

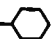
OXAMIDES, MALONAMIDES, SUCCINAMIDES AND
THEIR COMPLEXES WITH SbCl_3 AND SnCl_4

4.1

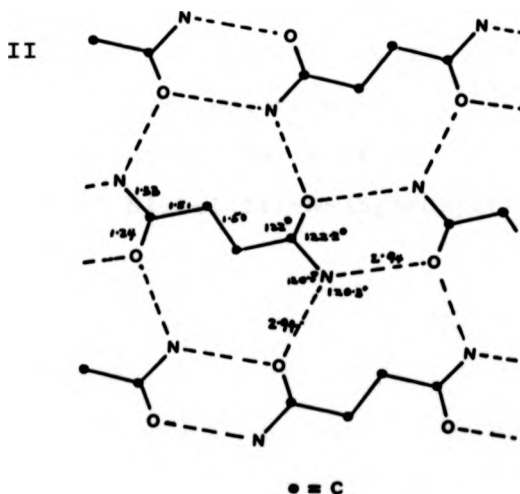
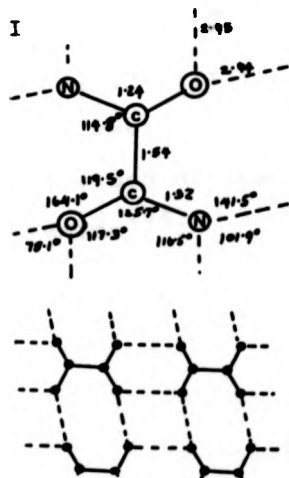
INTRODUCTION

In this Chapter, reactions of various amide ligands are considered; the types of ligand used are shown below together with their abbreviation as referred to in the text.



	R =	$-\text{CH}_3$	$-\text{C}_2\text{H}_5$	$-\text{C}_3\text{H}_7$	${}^n\text{C}_4\text{H}_9$	${}^t\text{C}_4\text{H}_9$	
Oxamides (n = 0)		DMO	DEO	DPO	DBO	DTBO	DCXO
Malonamides (n = 1)		DMM	DEM	DPM	DBM	DTBM	DCXM
Succinamides (n = 2)			DES				

These oxo-species can act as bidentate ligands coordinating through both oxygen atoms, or both nitrogen atoms, or one oxygen and one nitrogen. As potential (O,N) ligands, they have attracted much attention and have been characterised spectroscopically and crystallographically. The crystal structures of oxamide(I)¹⁷⁰ and succinamide¹⁷¹ (II) are shown below.

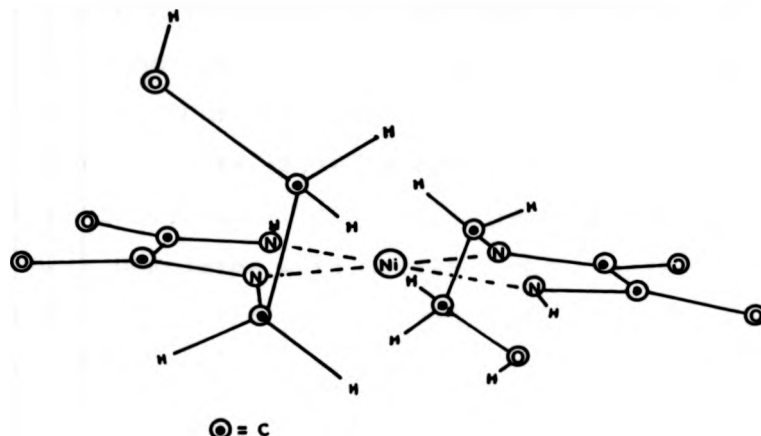


Oxamide molecules are planar in the solid state being held in sheets by hydrogen bonds. Succinamide molecules also feature strong hydrogen bonds. Values for C-N and C-O bond lengths are intermediate between those of formal single and double bonds as a result of delocalisation of electron density in the NCO unit. As with dithiooxamides, skeletal C-C bond distances for oxamides are in agreement with a single bond formulation hence only minimal delocalisation may be expected between the two NCO moieties.

The crystal structure of succinamide shows well resolved hydrogen atoms and bond angles of $\sim 120^\circ$ around the N atom to confirm sp_2 type hybridisation required for a delocalised system. A *trans* O,O arrangement observed in these ligands is analogous to the *trans* S,S arrangement in dithio-ligands.

Coordination Chemistry of the Various Amides

Many transition metal complexes with oxamides and their N-substituted derivatives have been prepared. In alkali conditions, deprotonation of the N-sites results in N,N' chelation to Cu(II), Cu(III), Ni(II), Ni(III), Pd(II), Co(III) as supported by i.r. spectroscopy^{172,173}. This assignment has been confirmed by the crystal structure of the sodium salt of Nickel(II)-N-(hydroxyethyl)-oxamide¹⁷⁴:



Here, square planar Ni(II) is surrounded by four nitrogen atoms of two substituted oxamide ligands following deprotonation at amine sites. Nickel complexes with stoichiometries: Ni.L , Ni.L_2 and Ni.L_3 ($\text{L} = \text{N-monosubstituted}$ or $\text{N,N'-disubstituted oxamide}$) have been isolated and characterised by their vibrational data¹⁷⁵. The donor behaviour of $\text{N,N'-disubstituted oxamides}$ and malonamides in non-aqueous conditions towards some Group (IV) halides has been investigated by Wade and Willey^{93(g)}. They isolated complexes of DMO and DEO with SnCl_4 and TiCl_4 and characterised them by their i.r., ^1H n.m.r., ^{13}C n.m.r. and conductivity data. They found the complexes to be non-conducting and discussed their i.r. data in terms of (O,O) donation to the metal. *Cis* octahedral structures C_{2v} were proposed and a comparative study of SnCl_4 and TiCl_4 oxamides *versus* dithiooxamides showed that for these Group (IV) (A and B) metals, (S)-donors are more strongly bound to the metal than the corresponding (O)-donors.

As with dithiooxamide complexes, X-ray structural evidence is really needed to confirm the predicted (O,O) chelation.

Our interest in such complexes stems from the success of the (S,S) systems where dithiooxamide ligands were found to be (S,S)-*trans* in both the free ligand and their complexes with Sb(III), and *cis*-(S,S) chelates with Sn(IV) and Bi(III) halides. The object of this study is two fold.

- (a) The preparation and characterisation of more oxamide and malonamide complexes in non-aqueous systems as a reference data-bank to decide the relative donor order $O \sim S \sim N$ towards reference Lewis acids.
- (b) Possible structural confirmation of the favourable bonding modes.

The list of complexes reported in this thesis is by no means exhaustive, only a few selected Sb(III) complexes have been studied. What is really needed is a similar range of O-systems to that of S-systems, from which comparisons would follow. Efforts to this end are currently under way. Unfortunately, we have not been able to obtain suitable crystalline samples for X-ray crystallography to date.

4.2 COMPLEXES OF SbCl_3 AND SnCl_4 WITH
N,N'-DISUBSTITUTED OXAMIDES AND MALONAMIDES

The complexes selected for study (see Table 4.2.1) were prepared by direct addition of a benzene solution of the appropriate ligand to an equimolar benzene solution of antimony trichloride. These ligands were much less soluble in benzene than their "thio" counterparts hence larger volumes of solvent were used and in some cases the ligand was dissolved in dry dichloromethane. If addition resulted in immediate precipitation of the white adduct, then the adduct was washed with benzene, otherwise slow evaporation was employed to facilitate crystal formation. The adducts were extremely air/moisture sensitive; most of them were insoluble in non-coordinating solvents but a few were sufficiently soluble in CDCl_3 to permit a limited study of their ^1H n.m.r. spectra.

Principal i.r. vibrational bands of the ligands and adducts are presented in Table 4.2.2. Assignments follow those of Desseyn and coworkers^{173(b), 175, 176}. The direction of frequency shift of the $\nu(\text{CO})$ band can be used to distinguish between oxygen bound and nitrogen bound amide, *viz.* a decrease in frequency accompanies oxygen coordination whereas nitrogen bonding should lead to a frequency increase. SbCl_3 complexes with DEO, DPO, DBO show the low energy shift of $\nu(\text{CO})$ but the $\nu(\text{CN})$ is little affected. Appreciable high energy $\nu(\text{CN})$ shifts are observed however for SbCl_3 complexes with DTBO and DCXO. All SbCl_3 complexes show the intense $\nu(\text{NH})$ band at $\sim 3300 \text{ cm}^{-1}$, sometimes with multiplet character, which may be attributed to solid

Table 4.2.1 Microanalytical data for selected complexes

Compound	C	H	N	(Elemental * Observed/Calculated)
SbCl ₃ .DEO _{1.5}	22.15/24.31	3.70/4.05	8.65/9.45	
SbCl ₃ .DPO _{1.5}	34.02/29.62	5.81/4.93	10.04/8.63	
SbCl ₃ .DBO _{1.5}	33.71/34.03	5.72/5.68	7.90/7.95	
SnCl ₄ .DEO	17.48/17.80	2.89/2.97	7.18/6.92	
SbCl ₃ .DEM	21.66/21.76	3.67/3.62	7.25/7.25	(Cl: 27.46/27.56)

Table 4.2.2 Principal i.r. bands (cm⁻¹) for complexes

Compound	ν (N-H) (s)	ν (C-O) (s, w)	ν (C-N) (s, w)	ν (N-Cl) (m)
DMO	3315	1660	1535	
DEO	3298	1652	1525	
SbCl ₃ .DEO _{1.5}	3328	1632	1512	305
SnCl ₄ .DEO	3340, 3280	1650	1595	338, 285
	3230, 3139		1575	230
DPO	3301, 3060	1654	1530	
SbCl ₃ .DPO _{1.5}	3295, 3060	1615	1528	337, 307
DBO	3300	1650	1532	
SbCl ₃ .DBO _{1.5}	3310, 3072	1650	1528	330, 285
DTBO	3330	1665	1500	
SbCl ₃ .DTBO _{1.5}	3358, 3310 3200, 3143	1638	1520	340, 281
DCXO	3288	1648	1520	
SbCl ₃ .DCXO _{1.5}	3330	1616	1528	350, 328, 299, 264
DMM	3290, 3080	1650	1550	
SbCl ₃ .DMM	3320, 3180	1615	1570	310
DEM	3290, 3079	1630	1550	
SbCl ₃ .DEM	3292, 3095	1610	1580	280, 335, 376
SnCl ₄ .DEM	3390, 3355	1635	1576	325
DPM	3290, 3090	1651	1562	
DBM	3290, 3090	1631	1562	
DTBM	3440, 3300	1650	1580, 1550	
DCXM	3292	1661	1543	

Table 4.2.3 ^1H n.m.r. spectral data for the complexes (δ p.p.m.)

Compound	NH (s, br)	CH ₂	CH ₂	CH ₂	CH ₃
DEO	7.57	3.38 m			1.23 t
SbCl ₃ .DEO _{1.5}	7.74	3.38 m			1.22 t
DPO	7.68	3.31 q	1.62 m		0.96 t
SbCl ₃ .DPO _{1.5}	7.73	3.31 q	1.63 m		0.96 t
DBO	7.78	3.32 q	1.55 m	1.38 m	0.92 t
SbCl ₃ .DBO _{1.5}	7.76	3.35 q	1.57 m	1.39 m	0.93 t
DTBO	7.45				1.38 s
SbCl ₃ .DTBO _{1.5}	7.74				1.46 s
DCXTO	7.38				1.95-1.30 m
SbCl ₃ .DCXTO _{1.5}	7.41				1.96-1.28 m

Compound	NH (s, br)	C \equiv C-CH ₂ -C \equiv O	CH ₂	CH ₃
DNM	7.64	3.22 s		2.83 d
SbCl ₃ .DNM	7.30	3.35 s		2.88 d
DEM	7.25	3.16 s	3.29 m	1.16 t
SbCl ₃ .DEM	7.55	3.49 s	3.37 m	1.20 t

Table 4.2.3 ^1H n.m.r. spectral data for the complexes (δ p.p.m.)

Compound	-NH (s,br)	CH ₂	CH ₂	CH ₂	CH ₃
DEO	7.57	3.38 m			1.23 t
SbCl ₃ .DEO _{1.5}	7.74	3.38 m			1.22 t
DPO	7.68	3.31 q	1.62 m		0.96 t
SbCl ₃ .DPO _{1.5}	7.73	3.31 q	1.63 m		0.96 t
DBO	7.78	3.32 q	1.55 m	1.38 m	0.92 t
SbCl ₃ .DBO _{1.5}	7.76	3.35 q	1.57 m	1.39 m	0.93 t
DTBO	7.45				1.38 s
SbCl ₃ .DTBO _{1.5}	7.74				1.46 s
DCXTO	7.38				1.95-1.30 m
SbCl ₃ .DCXTO _{1.5}	7.41				1.96-1.28 m

Compound	NH (s,br)	C ₆ H ₅ -CH ₂ -C=O	CH ₂	CH ₃
DMM	7.64	3.22 s		2.83 d
SbCl ₃ .DMM	7.30	3.35 s		2.88 d
DEN	7.25	3.16 s	3.29 m	1.16 t
SbCl ₃ .DEN	7.55	3.49 s	3.37 m	1.20 t

state/lattice effects. The complexes also show strong, multiplet $\nu(\text{M-Cl})$ bands ($\sim 330 \text{ cm}^{-1}$) which no doubt have contributions from internal ligand vibrational and also $\nu(\text{M-O})$ modes.

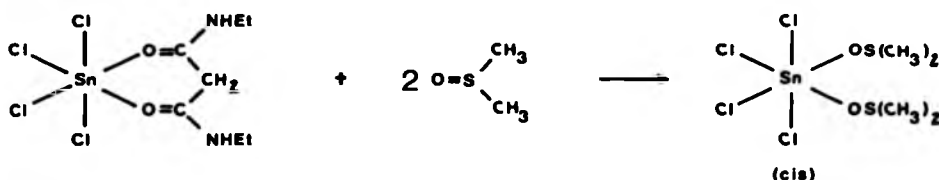
I.r. spectra of $\text{SbCl}_3\cdot\text{DMM}$ and $\text{SbCl}_3\cdot\text{DEM}$ conform to O,O-bonding expectations. The spectrum of $\text{SbCl}_3\cdot\text{DEM}$ shows a broad band between $1610\text{--}1580 \text{ cm}^{-1}$ which has almost certainly both $\nu(\text{CN})$ and $\nu(\text{CO})$ contributions. The ligand DEM shows bands at 1550 cm^{-1} ($\nu(\text{C-N})$) and 1630 cm^{-1} ($\nu(\text{C-O})$).

A spectrum of SbCl_3 (Nujol mull) shows two $\nu(\text{Sb-Cl})$ bands: a weak band at 350 cm^{-1} and a stronger broad band at $330\text{--}310 \text{ cm}^{-1}$. Changes in these bands on complexation reflect the redistribution of electron density within the Sb-Cl bonds. In most cases multiple strong bands are located below 400 cm^{-1} but no obvious pattern can be established yet, presumably charge transfer from the C=O group to the vacant d-orbitals of Sb can bring about a net decrease of the Sb-Cl bond order.

^1H n.m.r. spectra of SbCl_3 complexes are presented in Table 4.2.3. A broad N-H signal at δ 7.4-7.8 is a persistent feature in all the complexes indicating that no deprotonation takes place on complexation. These signals represent a slight downfield shift, w.r.t. δNH for the uncomplexed ligand, in agreement with a deshielding effect of oxygen coordination to the metal. No such transfer of electron density from the alkyl groups onto the OCN group is expected and δ values for R-substituents remain essentially unchanged following complexation.

In the case of SbCl_3 complexes with DMM and DEM, the backbone $-\text{CH}_2-$ shifts downfield again indicating a transfer of electron density to the coordinating oxygen atom. This shift is greater for O-donors (e.g. for SbCl_3DEM , $\Delta\delta(-\text{CH}_2-)$ is -0.33) than for the corresponding S-donors ($\text{SbCl}_3\text{DEDTM}$, $\Delta\delta(-\text{CH}_2-)$ is -0.08).

It would appear that for these oxamide complexes in general, the oxygen atom is only loosely bound to the metal making the ligand reasonably labile. As an example, an attempt to recrystallise SnCl_4DEM resulted in a ligand exchange reaction:



Colourless crystals were isolated from the reaction and subsequently characterised by X-ray crystallography as *cis*- $\text{SnCl}_4(\text{DMSO})_2$ (see Fig. 4.2.1).

Although it is recognised that this result in no way establishes the geometry of the malonamide in SnCl_4DEM reactant, we believe that a *cis*-arrangement is similarly present there. For the complexes $\text{SbCl}_3\text{DEO}_{1.5}$, $\text{SbCl}_3\text{DPO}_{1.5}$, $\text{SbCl}_3\text{DBO}_{1.5}$, an octahedral structure with bridging ligands analogous to the structures of $\text{SbCl}_3\text{DEDTO}_{1.5}$ and $\text{SbCl}_3\text{DPDTO}_{1.5}$ as established by X-ray crystallography¹⁷⁷ is proposed. Correspondingly, no stereochemical activity of the lone pair is expected.

Proposed Structure for SbCl_3 Complexes with Oxamides

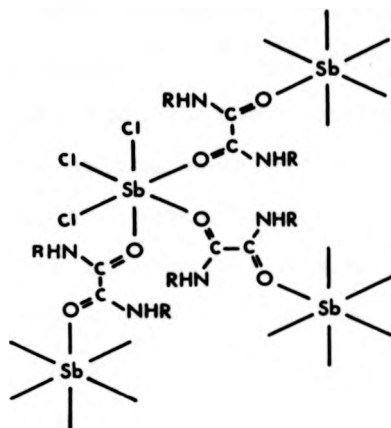
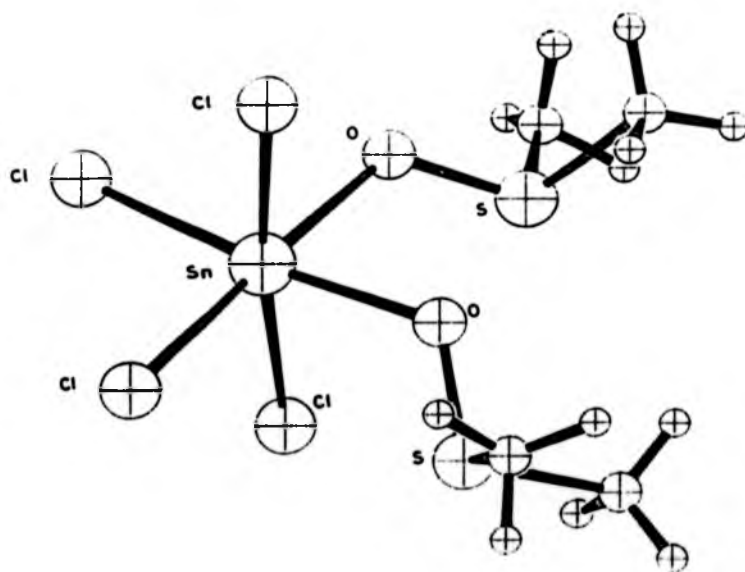
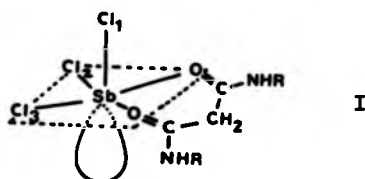


Figure 4.2.1 The Crystal Structure of $\text{SnCl}_4(\text{DMSO})_2$



Five coordinate halo-Sb(III) species usually exist as a distorted square pyramid with a stereochemically active lone pair occupying a sixth position, e.g. $\text{SbCl}_3 \cdot \text{DEDTM}$, SbCl_5^{2-} ¹⁷⁸ and $\text{SbCl}_3 \cdot 2(\text{C}_6\text{H}_5)_3\text{AsO}$ ⁷³. In the $(\text{C}_6\text{H}_5)_3\text{AsO}$ adduct, the oxygen atoms occupy *cis*-positions at the base of the square pyramid. Judging from this, an analogous structure is proposed for $\text{SbCl}_3 \cdot \text{DEM}$ with an implicit stereochemically active lone pair. In this structure (I) the $\text{Sb}-\text{Cl}_1$ distance is expected to be shorter than either $\text{Sb}-\text{Cl}_2$ or $\text{Sb}-\text{Cl}_3$ which suffer greater lone pair-bonding pair repulsion.



A *cis* (O,O)-octahedral structure is proposed for $\text{SnCl}_4 \cdot \text{DEO}$, analogous to the structure of $\text{SnBr}_4 \cdot \text{DBDTO}$.

4.3 EXPERIMENTAL

Preparation of the Ligands

The methyl substituted ligands were prepared by treatment of the appropriate ethyl ester with a two fold excess of aqueous 25% MeNH₂. For the ethyl derivatives, a 2:1 excess of anhydrous EtNH₂ was distilled onto a solution of diethyloxalate in methanol at 77°K *in vacuo*. The resulting mixture was allowed to warm up to room temperature and left to stand for several hours. A white solid precipitated out. The propyl-, butyl-, tertiary butyl-, and cyclohexyl- derivatives were prepared in an analogous manner to the methyl derivatives. The white microcrystalline solids were recrystallised from methanol/ethanol solutions and dried *in vacuo*.

Complexes of SbCl₃ with N,N'-Disubstituted-Oxamides and Malonamides

The complexes were prepared by reactions between SbCl₃ and the appropriate ligand in benzene solutions as illustrated by the preparation of SbCl₃.DBO.

A solution of DBO (0.987 g, 4.8 mmol) in benzene (200 cm³) was added dropwise to a magnetically stirred solution of SbCl₃ (1.10 g, 4.8 mmol) in benzene (100 cm³). The resulting solution was allowed to stir for 12 hours after which, removal of benzene gave a white precipitate which was washed (3 x 100 cm³) with re-distilled n-hexane and finally pumped for several hours at room temperature. M.p. 52-54°

Found: C, 33.71; H, 5.72; N, 7.90 Calculated for
 $C_{10}H_{20}N_2O_2Cl_3Sb$: C, 34.03; H, 5.68; N,
7.95.

In most cases, the yields were quantitative and the products were stored in glass ampoules under a nitrogen atmosphere. Analytical data are summarised in Table 4.2.1.

A Final Comment

The impetus to work on oxamide systems originates from the structural and spectroscopic results obtained for S-systems. When we embarked on the corresponding O-systems, rather than the blanket approach, we were more selective, i.e. smaller set of results. Preliminary set of results showed no controversy, so instead of going through the whole lot, we sought to investigate other systems (see Chapters 5 and 6) involving charged ligands.

CHAPTER 5
REACTIONS OF GROUP (VB) HALIDES
WITH TOLUENE-3,4-DITHIOL



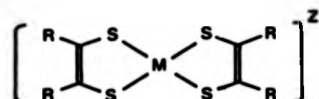
CHAPTER FIVE

REACTIONS OF GROUP (VB) HALIDES WITH TOLUENE 3,4-DITHIOL

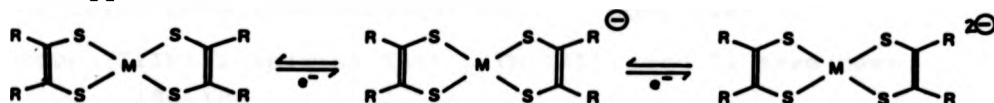
5.1 INTRODUCTION

General Chemistry of 1,2-Dithiolene Systems

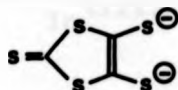
Complexes of the general type,



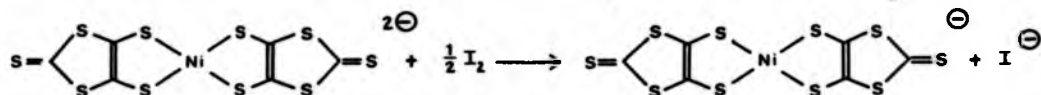
(R = CN, C₆H₅, CF₃ and M = generally a transition metal) undergo reversible and usually facile one-electron transfer reactions which may be effected chemically or electrochemically. These reactions have permitted the synthesis of a wide range of complexes with total charge, Z = 0, -1, -2. There has been an extensive study of 1,2-dithiolene complexes of transition metals¹⁷⁹ leading to a substantial amount of polarographic data to support the redox processes:



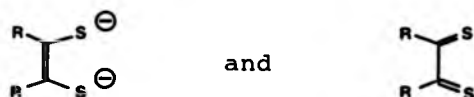
Polarographic studies have also shown that the ease of reduction in solution follows the sequence of R substituents $CN > C_6H_5 > CH_3$. Underhill and co-workers¹⁸⁰ have initiated a study of one-dimensional complexes of Ni, Pd, Pt, in order to investigate their optical properties as well as electrical conductivities. The nickel(II) complex with



which was recently prepared and characterised by X-ray crystallography¹⁸¹, can be oxidised with iodine to the corresponding nickel(III) complex¹⁸². A similar example

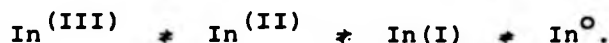


where a nickel(III) complex is prepared from a 1,2-dithiolene ligand and nickel(II) chloride is that of the bis(*cis*-1,2-dicarbomethoxy ethylenedithiolato)nickelate(III) ion¹⁸³. Here there is no 'obvious' oxidising agent and aerial oxidation is presumed. 1,2-Dithiolene complexes also feature extensive ground state π -electron delocalisation and this aspect has received much structural attention^{184,185}. Argument continues as to the nature of dithiolato ligands in metal complexes; two extreme structures can be drawn, *viz.*,

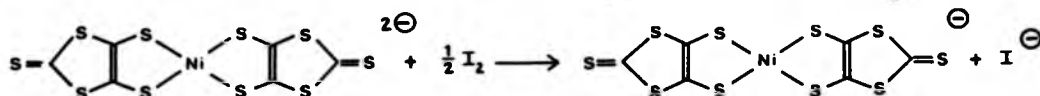


with reality somewhere between the two.

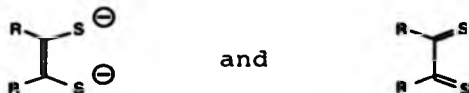
Interest in post-transition metal dithiolate complexes developed somewhat later. Complexes of Group (IIIB) involving In(I), In(III), and Tl have been isolated¹⁸⁶⁻¹⁸⁸. Some of these complexes exhibit the characteristic stepwise one-electron transfer¹⁸⁹, e.g. polarographic reduction of $\text{In}(\text{S}_2\text{C}_2(\text{CN})_2)_3^{3-}$ in aqueous or absolute methanol solution showed in each case a series of reversible one-electron changes formally represented as:



which was recently prepared and characterised by X-ray crystallography¹⁸¹, can be oxidised with iodine to the corresponding nickel(III) complex¹⁸². A similar example

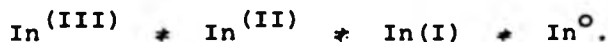


where a nickel(III) complex is prepared from a 1,2-dithiolene ligand and nickel(II) chloride is that of the bis(*cis*-1,2-dicarbomethoxy ethylenedithiolato)nickelate(III) ion¹⁸³. Here there is no 'obvious' oxidising agent and aerial oxidation is presumed. 1,2-Dithiolene complexes also feature extensive ground state π -electron delocalisation and this aspect has received much structural attention^{184,185}. Argument continues as to the nature of dithiolato ligands in metal complexes; two extreme structures can be drawn, viz.,

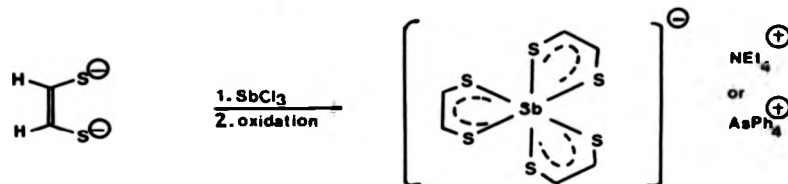


with reality somewhere between the two.

Interest in post-transition metal dithiolate complexes developed somewhat later. Complexes of Group (IIIB) involving In(I), In(III), and Tl have been isolated¹⁸⁶⁻¹⁸⁸. Some of these complexes exhibit the characteristic stepwise one-electron transfer¹⁸⁹, e.g. polarographic reduction of $\text{In}(\text{S}_2\text{C}_2(\text{CN})_2)_3^{3-}$ in aqueous or absolute methanol solution showed in each case a series of reversible one-electron changes formally represented as:



The structures of 1,2-dithiolene complexes with In(III) and Tl(III) have also been reported¹⁹⁰. With Group (IVB) elements, dicyanoethylene-1,2-dithiolato complexes having the general formula $[M(S_2C_2(CN)_2)_3]^{2-}$ ($M = Si, Ge$ and Sn) have been prepared presumably with a distorted octahedral geometry¹⁹¹. 1,2-Dithiolene complexes of Group (VB) elements also exhibit the characteristic redox behaviour; the violet Sb(V) complex obtained from $SbCl_3$ and 1,2-dithiolene was first isolated by Hoyer and co-workers¹⁹².



Hunter¹⁹³ has reported the synthesis of 1,2-dithiolate complexes of antimony(III) and bismuth(III) with varying stoichiometries, e.g. $[Sb(mn)_2]^-$, $Sb_2(td)_3$, $[Bi_2(mn)_2X_4]^-$, $[Bi_2(mn)_3X_2]^{2-}$, $[Bi_2(mn)_5]^{4-}$ and $Bi_2(td)_3$

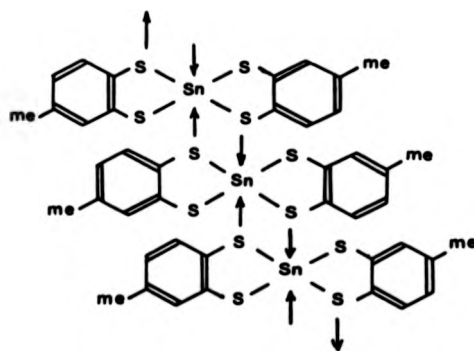


with polymeric ligand-bridged structures. A polarographic study of these complexes provides an explanation for the instability of $[Sb(mn)_2]^-$ towards aerial oxidation.

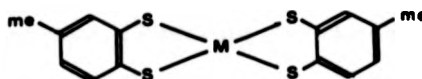
5.2 REACTIONS OF TOLUENE-3,4-DITHIOL WITH POST TRANSITION METALS

Toluene-3,4-dithiol (td) is an attractive choice as a potential (S,S) bidentate chelating ligand. Reactions of td with trimethylaluminium, dimethyl aluminiumchloride and with adducts of trimethylaluminium have been investigated, yield three coordinate Al(III) complexes involving one toluene-3,4-dithiol ligand¹⁹⁴.

Group (IVB) complexes with td were first prepared by Clark in 1936¹⁹⁵. Poller and Spillman¹⁹⁶ have pointed out that the red insoluble bis(toluene-3,4-dithiolato)-tin(IV) used in the colorimetric determination of tin is a coordination polymer:



A series of optically active compounds of the general formula:



(M = Si, Ge, Sn and Pb) has been synthesised and partially resolved¹⁹⁷ by chromatographic techniques.

With Group (VB) elements, the 2:3 complexes $\text{Sb}_2(\text{td})_3$ and $\text{Bi}_2(\text{td})_3$ prepared by Hunter¹⁹³ have already been mentioned. Toluene-3,4-dithiol also forms a 1:1 complex with bismuth(III), e.g. $\text{Bi}(\text{td})\text{Cl}$, which has been reported to form 1:2 adducts with pyridine and 1:1 adducts with 2,2-bipyridyl and 1,10-phenanthroline¹⁹⁸. A whole variety of td complexes with Sn, Pb, Sb and Bi have been described by Gagliardi and Durst¹⁹⁹ to include $[\text{Et}_4\text{N}][\text{M}(\text{td})_2]$ ($\text{M} = \text{As}, \text{Sb}, \text{Bi}$), $[\text{Et}_4\text{N}][\text{Sb}(\text{td})_3]$ and $[\text{Et}_4\text{N}]_2[\text{Sn}(\text{td})_3]$. Conductivity data of the Group (VB) complexes show that they are all 1:1 electrolytes while the Sn(IV) complex is a 1:2 electrolyte.

Because of their possible therapeutic potential, the 1:1 and 1:2 complexes of td with Group (VB) metals have been synthesised¹ and characterised as part of a programme concerned with possible agents in the chemotherapeutic treatment of bilharzia.

Despite all this interest in toluene-3,4-dithiol complexes X-ray crystallographic structural information is minimal. We have therefore mounted a structural investigation with the following points in view:

- (1) To establish unambiguously the structures of complexes with MCl_3 ($\text{M} = \text{As}, \text{Sb}, \text{Bi}$) and assemble a databank.
- (2) To compare the ligand bonding modes, and the metal geometries observed in these td complexes, with similar parameters observed in dithiooxamide complexes. In dithiooxamide complexes, the coordinating sulphur atoms may be either *cis* or *trans* whereas in toluene-3,4-

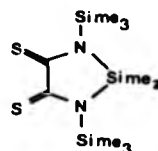
dithiolate complexes they are 'locked' in the *cis*-formation. Consequently, formation of monomeric *cis*-chelates would be expected and would demonstrate that the



'bite' is amenable for $M(\text{III}) = \text{As}, \text{Sb}$ and Bi . [While this work was in progress, the preparation of the cyclic dithiooxamides (A) and (B) was published²⁰⁰.



A



B

Although these could be used to investigate the 'bite' effect(s), their preparation was not pursued because the reported yields were quite low (11%).¹

(3) To compare the strengths of $M-S$ bonds in these toluene-3,4-dithiol complexes with those of $M-S$ bonds in the corresponding dithiooxamides and indeed dithiomalonamides (see Chapters 2 and 3).

(4) To investigate the stereochemical and chemical significance of the formal lone pair present in these $M(\text{III})$ complexes.

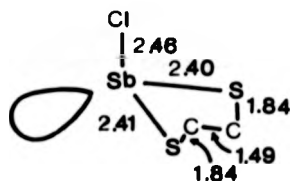
5.3 1:1 COMPLEXES OF MCl_3 ($M = As, Sb, Bi$)
WITH TOLUENE-3,4-DITHIOL

The 1:1 compounds were prepared by equimolar addition of a solution of the metal chloride in methanol to a solution of toluene-3,4-dithiol in methanol. Chelation formation results following expulsion of two chlorines as HCl gas.



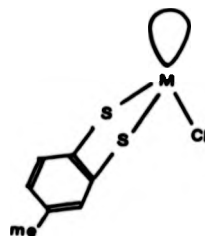
All three compounds are crystalline solids. The yellow arsenic and antimony compounds are soluble in methanol while the brown bismuth compound will only dissolve in methanol solutions doped with dimethyl sulfoxide. The compounds slowly decompose on exposure to air for long periods.

Several preparative²⁰¹ and structural²⁰² studies of related dithiolato complexes of As(III) and Sb(III) have been reported in the literature. The crystal structure of 2-chloro-1,3-dithia-2-stibacyclopentane(I)²⁰² shows three coordinate antimony(III) with a stereochemically active lone pair of electrons. The SbS_2C_2 ring is not planar.



I

Angles $\text{ClSbS}_1 - 94.9^\circ$
 $\text{ClSbS}_2 - 98^\circ$
 $\text{S}_1\text{SbS}_2 - 89.2^\circ$



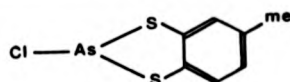
II

We would therefore favour a similar AB_2CE tetrahedral structure (II) for the $M(td)Cl$ complexes ($M = As, Sb, Bi$) with the lone pair taking up one of the tetrahedral positions. Certainly the spectral data are consistent with an $M(td)Cl$ formulation based on tetrahedral $M(III)$. X-ray structural confirmation follows in Section 5.4.

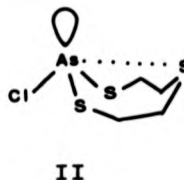
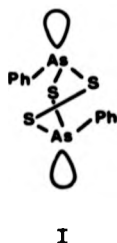
The 1H n.m.r. spectrum of toluene-3,4-dithiol (220 MHz; solvent $CDCl_3$; standard Me_4Si) consists of a (3H) singlet at δ 2.23 for the methyl protons, two (1H) singlets at δ 3.56 and 3.74 for the -S-H protons and a (3H) set of multiplets at δ 6.85 and δ 7.21 for the aromatic protons. The spectra of the $M(td)Cl$ complexes ($M = As, Sb, Bi$) confirm the loss of the S-H protons and there is a general downfield shift of the methyl and aromatic proton signals consistent with complex formation.

The i.r. spectra of the complexes also confirm the removal of SH protons, *viz.* the absence of a sharp $\nu(S-H)$ band located at 2550 cm^{-1} in the ligand. The $400\text{--}200\text{ cm}^{-1}$ region of the $Sb(td)Cl$ i.r. spectrum shows a prominent $\nu(SbCl)$ peak at 282 cm^{-1} with a few smaller peaks probably resulting from a mixture of $\nu(Sb-Cl)$ and $\nu(Sb-S)$ vibrations. The prominent $\nu(As-Cl)$ peak for $As(td)Cl$ is found at 304 cm^{-1} again with many smaller $\nu(As-Cl)$ and $\nu(As-S)$ modes.

5.4 THE CRYSTAL STRUCTURE OF As(td)Cl



The light yellow crystals belong to the $P2_1/c$ space group. A description of the structure determination has already been outlined in Section 1.4. Crystal data and refinement details are given in Table 5.4.1. Atomic positions, bond lengths and angles are listed in Table 5.4.2 and Table 5.4.3 respectively while anisotropic thermal parameters and the calculated hydrogen-atom positions are given in Table 5.4.4. Within the unit cell, there are four monomeric As(td)Cl units. Fig. 5.4.1 shows one such unit. The geometry around each As is pseudo-tetrahedral with the lone pair of electrons occupying an apex of the tetrahedron. The geometry therefore conforms to a four-electron-pair AX_3E type of complex. Bond angles around the As of 92.62° , 99.43° and 100.34° are much less than the regular tetrahedral angle (109.5°) emphasising the stereochemical activity of the lone pair of electrons. A similar AX_3E system which exhibits tetrahedral arsenic(III) geometry with a stereochemically active lone pair is the structure of diphenyldiarsenictrisulphide(I)²⁰³.



Here, two arsenic atoms form part of an As-S five membered ring with As-S distances of 2.252 and 2.253 Å and hardly any π -electron delocalisation. Another comparable system is the eight-membered ring 2-chloro-1,3,6,2-trithiaarsocane(II)^{65(a)} with no π -electron delocalisation. Here As-S distances are 2.26 and 2.25 Å and the As-Cl distance is 2.356 Å. The major difference, of course, is that (II) is a ψ trigonal bipyramidal structure. In As(td)Cl, As-S distances are significantly shorter (2.226 and 2.209) which may be seen to represent some degree of π -delocalisation around the five-membered SbS₂C₂ ring. The S-C distances (1.77 Å) are also shorter than the corresponding distances in the eight-membered ring structure. The As-Cl distance (2.23 Å) is comparable with those found in other AsCl₃ adducts^{25,33} (2.18-2.54 Å). Angles close to 120° around all the aromatic carbons indicate the retention of sp₂ hybridisation within the aromatic system. The packing diagram (Fig. 5.4.2) shows the monomeric units related by a screw axis through the As atoms.

Figure 5.4.1 The Crystal Structure of $\text{As}(\text{td})\text{Cl}$

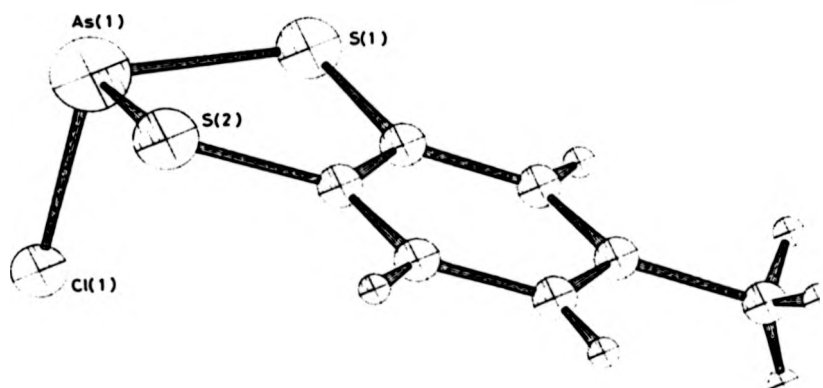


Figure 5.4.2 The Molecular Arrangement in $\text{As}(\text{td})\text{Cl}$

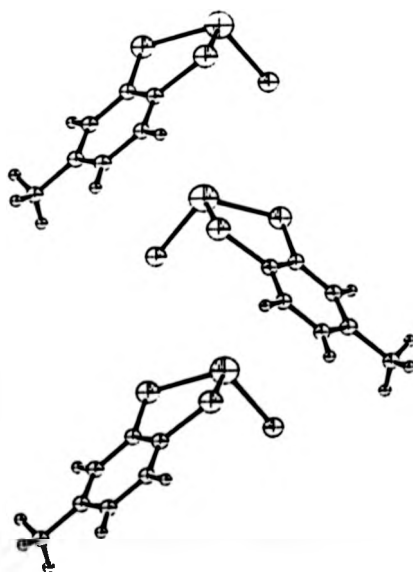


Table 5.4.1 Crystal data and refinement details for As(td)Cl

Formula	$C_7H_6S_2ClAs$
M.W.	264.5
Crystal class	Monoclinic
Space group	$P2_1/c$
Absences	hol $l = 2n + 1$, oko $k = 2n + 1$
a (\AA)	6.127
b (\AA)	15.773
c (\AA)	9.768
α ($^\circ$)	(90)
β ($^\circ$)	91
γ ($^\circ$)	(90)
U (\AA^3)	943.85
F (000)	520
D_m	1.84
D_c	1.86
Z	4
ν (cm^{-1})	44.3
λ	0.7107
Crystal size	1.25 x 0.10 x 0.40
Rotation axis	a
$2\theta_{\text{max}}$	50°
Number of data measured	1480
Number of data used in refinement	1113
Criterion for data inclusion	$I > 3\sigma(I)$
Final R value	0.0588
R_w value	0.0606

Table 5.4.2 Atomic co-ordinates ($\times 10^4$) for As(td)Cl with estimated standard deviations in parentheses

Atom	X	Y	Z	U($\times 1000$)
AS(1)	2363(2)	2348(1)	3415(1)	55(1)
S(2)	-892(4)	2584(1)	4320(3)	55(2)
S(1)	3587(4)	3614(1)	4018(2)	60(2)
CL(1)	3859(4)	1554(2)	5080(2)	84(3)
C(1)	1685(13)	3874(5)	5305(8)	56(8)
C(2)	-251(13)	3430(5)	5441(8)	50(8)
C(3)	-1715(14)	3653(6)	6442(8)	62(9)
C(4)	-1205(13)	4313(6)	7344(8)	63(9)
C(5)	716(15)	4753(5)	7226(8)	59(9)
C(6)	2199(14)	4519(5)	6226(8)	54(8)
C(7)	1328(23)	5455(7)	8222(11)	82(13)

Table 5.4.3 Molecular dimensions for As(td)Cl Distances (\AA), Angles ($^\circ$)

AS (1)	-	S (2)		2.226 (3)	
AS (1)	-	S (1)		2.209 (2)	
AS (1)	-	CL (1)		2.236 (3)	
S (2)	-	C (2)		1.767 (8)	
S (1)	-	C (1)		1.777 (8)	
C (1)	-	C (2)		1.386 (11)	
C (1)	-	C (6)		1.390 (12)	
C (2)	-	C (3)		1.384 (11)	
C (3)	-	C (4)		1.397 (13)	
C (4)	-	C (5)		1.373 (13)	
C (5)	-	C (6)		1.396 (12)	
C (5)	-	C (7)		1.516 (13)	
S (2)	-	AS (1)	-	S (1)	92.62 (9)
S (2)	-	AS (1)	-	CL (1)	99.43 (10)
S (1)	-	AS (1)	-	CL (1)	100.34 (10)
AS (1)	-	S (2)	-	C (2)	100.45 (29)
AS (1)	-	S (1)	-	C (1)	99.97 (28)
S (1)	-	C (1)	-	C (2)	121.6 (6)
S (1)	-	C (1)	-	C (6)	118.8 (6)
C (2)	-	C (1)	-	C (6)	119.5 (7)
S (2)	-	C (2)	-	C (1)	120.2 (6)
S (2)	-	C (2)	-	C (3)	119.4 (6)
C (1)	-	C (2)	-	C (3)	120.4 (4)
C (2)	-	C (3)	-	C (4)	119.7 (8)
C (3)	-	C (4)	-	C (5)	120.4 (8)
C (4)	-	C (5)	-	C (6)	119.6 (7)
C (4)	-	C (5)	-	C (7)	121.2 (8)
C (6)	-	C (5)	-	C (7)	119.0 (8)
C (1)	-	C (6)	-	C (5)	120.2 (8)

Table 5.4.4

(a) ANISOTROPIC AND ISOTROPIC THERMAL PARAMETERS

ANISOTROPIC IN THE FORM $\exp(-2\pi^2 \mathbf{U} \cdot \mathbf{h}^2)$ +
 ... $U_{23}^2 \mathbf{b}^* \mathbf{c}^* \mathbf{k}^* \mathbf{l} + \dots$)

ISOTROPIC $\exp(-8\pi^2 \mathbf{U} \cdot (\sin(\theta)/\lambda)^2)$

ALL VALUES *1000

ATOM	U11(OR U)	U22	U33	U23	U13	U12
AS(1)	55(1)	62(1)	61(1)	-7(0)	0(0)	-2(0)
S(2)	44(1)	67(2)	80(2)	-10(1)	-7(1)	-5(1)
S(1)	54(1)	60(1)	70(1)	-2(1)	9(1)	-10(1)
CL(1)	64(2)	76(2)	100(2)	17(1)	-7(1)	2(1)
C(1)	56(5)	48(4)	54(4)	4(3)	4(3)	3(4)
C(2)	56(5)	54(5)	55(4)	3(3)	-11(3)	-4(4)
C(3)	48(5)	67(6)	64(5)	8(4)	1(4)	0(4)
C(4)	51(5)	68(6)	62(5)	1(4)	-4(4)	12(4)
C(5)	75(6)	52(5)	49(4)	1(3)	-8(4)	9(5)
C(6)	61(5)	45(5)	62(5)	6(4)	-4(4)	-6(4)
C(7)	114(9)	64(7)	73(6)	-4(5)	3(6)	0(6)

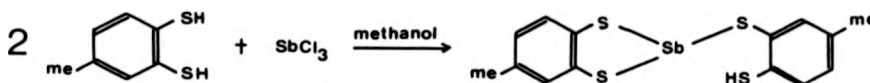
(b) ATOMIC CO-ORDINATES (*10**4) WITH ESTIMATED STANDARD

DEVIATIONS IN PARENTHESES

ATOM	X	Y	Z
H(1)	-3061	3359	6515
H(1)	-2192	4459	8046
H(1)	3565	4801	6174
H(71)	-90	5643	8454
H(72)	2034	5881	7703
H(73)	2155	5346	9034

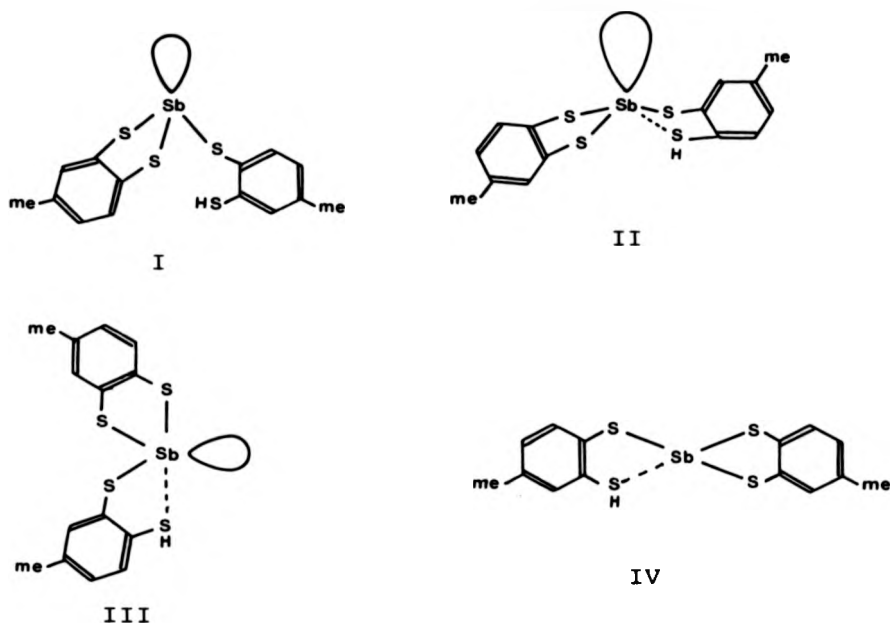
5.5 1:2 COMPLEXES OF Sb, AND Bi WITH TOLUENE-3,4-DITHIOL

These complexes have been prepared by direct addition of the metal chloride and toluene-3,4-dithiol in methanol in a 1:2 molar ratio. The antimony compound has been made previously¹ and reported as a four coordinate antimony(III) system based on $\text{H[Sb(td)}_2\text{]} \cdot \text{OH}_2$.



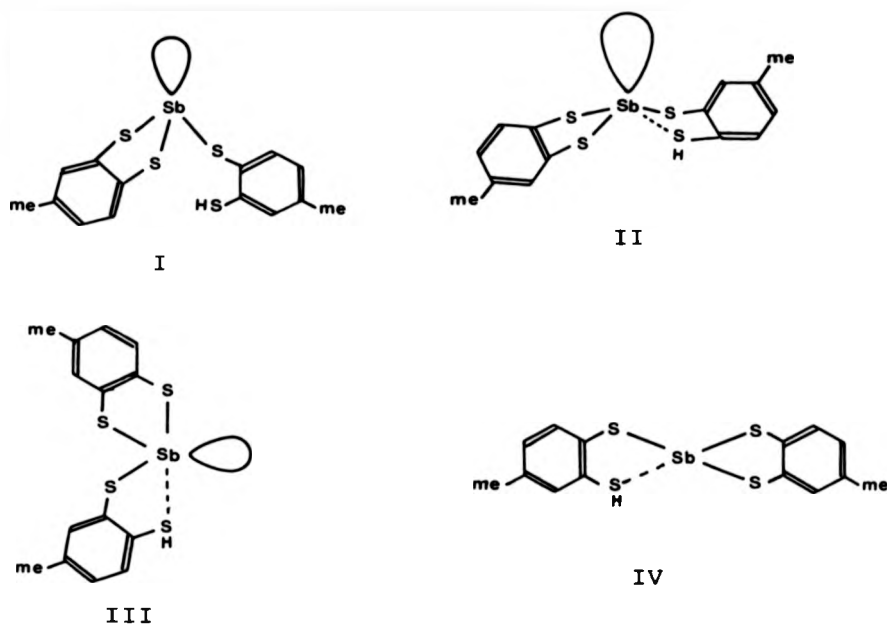
The i.r. spectrum of the yellow Sb(III) complex shows a prominent $\nu(\text{SH})$ band at 2338 cm^{-1} . This observation coupled with the already reported negligible conductivity (S.O.W) suggests a neutral complex formation in which one of the ligands has retained a thiol proton. The fact that $\nu(\text{S-H})$ has shifted (-212 cm^{-1}) to lower energy rather suggests that one consequence of Sb-S bond formation is an appreciable charge drain from the aromatic ring. Again this low energy shift of the $\nu(\text{S-H})$ mode could be the result of a weak $\text{Sb} \cdots \text{S} \begin{smallmatrix} \text{C} \\ \text{H} \end{smallmatrix}$ interaction thus increasing further the effective charge drain from the S-H bond towards the metal. The ^1H n.m.r. spectrum of this complex shows only one S-H resonance at δ 3.48 as a singlet and a slight downfield shift of the methyl singlet to δ 2.28. The aromatic signals are relatively unaffected.

There are many possibilities for the preferred shape of this complex. If there is no $\text{Sb} \cdots \text{S} \begin{smallmatrix} \text{C} \\ \text{H} \end{smallmatrix}$ interaction then a tetrahedral structure (I) featuring a stereochemically active lone pair would be predicted.



However, if there is an Sb...(H)S- interaction then a square pyramidal geometry (II) is possible with the lone pair occupying the apical position. Alternatively, a trigonal bipyramidal structure (III) with the lone pair at one of the equatorial positions is feasible. Finally, but less likely, there is the possibility of a square planar structure (IV) with no lone pair activity. These examples represent monomeric possibilities but polymeric structures are equally conceivable.

Attempts to eliminate the remaining S-H proton from this complex have been made by the addition of a base. Unfortunately this has always resulted in the formation of the antimony(V) product (see later Section 5.6). This phenomenon has been observed in another Sb(III) 1,2-dithiolene compound, $\text{Sb}(\text{mn})_2^-$, as mentioned in Section 5.1. So we have not been able

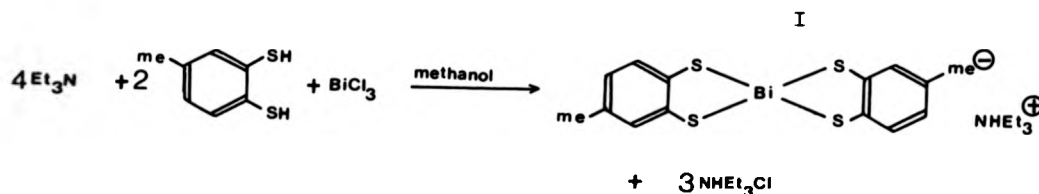


However, if there is an Sb...(H)S- interaction then a square pyramidal geometry (II) is possible with the lone pair occupying the apical position. Alternatively, a trigonal bipyramidal structure (III) with the lone pair at one of the equatorial positions is feasible. Finally, but less likely, there is the possibility of a square planar structure (IV) with no lone pair activity. These examples represent monomeric possibilities but polymeric structures are equally conceivable.

Attempts to eliminate the remaining S-H proton from this complex have been made by the addition of a base. Unfortunately this has always resulted in the formation of the antimony(V) product (see later Section 5.6). This phenomenon has been observed in another Sb(III) 1,2-dithiolene compound, $\text{Sb}(\text{mn})_2^-$, as mentioned in Section 5.1. So we have not been able

to establish the existence of a one-sided, four coordinate, sulphur-bound antimony(III) compound analogous to the oxygen-bound arsenic(III) compound $K[As(C_6H_4O_2)_2]$ reported by Skapski³⁰ (see page 29).

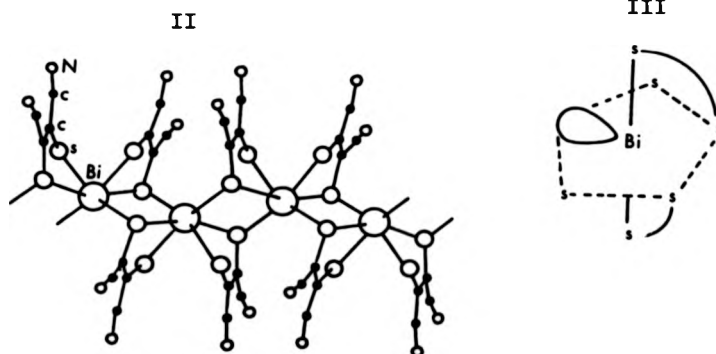
Although considerable effort was made, we were unable to isolate a 1:2 arsenic(III) complex with toluene-3,4-dithiol, based on the $[As(td)_2]^-$ anion. However, with bismuth, such a species (I) has been isolated following the addition of stoichiometric quantities of triethylamine to toluene-3,4-dithiol prior to the addition of a methanol solution of $BiCl_3$.



The i.r. spectrum of (I) does not show an $\nu(S-H)$ band. The 1H n.m.r. spectrum shows a (3H) triplet at δ 1.25 (\underline{CH}_3-CH_2-) and a (2H) quartet at δ 3.05 ($CH_3-\underline{CH}_2-$) but there is no S-H resonance. The (6H) singlet at δ 2.20 indicates magnetic equivalence of the methyl protons of the two ligands in the complex. The N-H resonance for $[Et_3NH]^+$ is not observed probably because this proton is in fast exchange.

Although the complex (I) has been represented as a monomeric, four coordinate complex, the predicted molecular geometry is greatly influenced by a very recent crystal structure determination of tetraphenyl-arsonium bis(1,2-dicyanoethylene-1,2-dithiolato)-

bismuthate(III) (II)²⁰⁴ which consists of an infinite linear polymeric chain in which successive bismuth atoms are bridged by two dithiolene ligands, each ligand providing one bridging sulphur atom. Although the geometry could be described as a greatly distorted octahedron with no stereochemically active lone pair, a description in terms of a pentagonal bipyramidal array with one of the equatorial positions occupied by a stereochemically active lone pair, i.e. a seven-electron-pair AX_6E system with 1:5:1 stereochemistry (III), is much more attractive.



We would favour a similar bonding geometry in our bis(toluene-3,4-dithiolato)bismuthate(III) complex.

5.6 1:3 COMPLEXES OF Sb(V) WITH TOLUENE-3,4-DITHIOL

The instability of the 1:2 Sb(III) toluene-3,4-dithiol compound towards aerial oxidation in the presence of base, has led to a novel one-pot synthesis of the tris(toluene-3,4-dithiolato) antimonate(V) anion. Addition of base to a solution of the yellow $[\text{Sb}(\text{td})_2\text{H}]$ in methanol resulted in the formation of a deep violet-red solution which in the case of NaOH and KOH yielded thick red oils. However, when Et_4NCl was added to the red solution, crystalline $[\text{Et}_4\text{N}][\text{Sb}(\text{td})_3]$ was isolated on slow evaporation. Unfortunately, the material was unsuitable for X-ray crystallographic purposes. Subsequent preparations were carried out by adding stoichiometric quantities of the organic base, triethylamine, to a methanol solution of toluene-3,4-dithiol, followed by the addition of SbCl_3 in a metal:ligand mole ratio of 1:2. This gave the red methanolic solution containing the anion which was isolated in crystalline form by addition of large cations such as $[\text{PPh}_4]^+$ or $[\text{NEt}_4]^+$. Conductivity measurements on these compounds show little dissociation in dichloromethane solution, e.g. for 2.2×10^{-3} M solutions, conductivities are in the range $30\text{--}40 \Omega^{-1}\text{mol}^{-1}\text{cm}^2$ (compared to $139 \Omega^{-1}\text{mol}^{-1}\text{cm}^2$ as found for $\text{Et}_4\text{N}^+\text{Cl}^-$).

ligands. The aromatic multiplet has shifted slightly upfield to δ 6.71 compared to δ 6.85 in the free ligand.

The ^1H n.m.r. spectrum of $\text{Ph}_4\text{PSb}(\text{td})_3$ shows a prominent (9H) singlet for the CH_3 protons at δ 2.13, a (9H) set of multiplets for (td) aromatic protons at δ 6.59 and 7.10 and a (20H) multiplet between δ 7.5 and 7.8 for the aromatic PPh_4 protons.

The observed spectral patterns are consistent with the $[\text{Sb}(\text{td})_3]^-$ formulation for the complex. We predict an octahedral geometry around the Sb centre similar to that found in the tris(benzene-1,2-diolato)-arsenate(V) anion⁵⁹ (see page 38).

5.7 THE CRYSTAL STRUCTURE OF TETRAPHENYLPHOSPHONIUM
TRIS (TOLUENE-3,4-DITHIOLATO) ANTIMONY (V) ,
 $[\text{Ph}_4\text{P}][\text{Sb}(\text{td})_3]$

$[\text{Ph}_4\text{P}][\text{Sb}(\text{td})_3]$ crystallises in the $\text{P}2_1$ space group. The structure was solved by the heavy atom method. The Patterson function was utilised to locate the antimony position. The positions of the remaining atoms were located from Fourier maps and refined by full matrix least squares wherever possible. The data from this crystal was not very good quality and it has only refined to a final R value of 0.14. Crystal data and refinement details are given in Table 5.7.1. Atomic coordinates are given in Tables 5.7.2; bond lengths and angles are given in Table 5.7.3.

The $[\text{Sb}(\text{td})_3]^-$ ion has a tris-chelate structure (Figure 5.7.1) with approximate D_3 symmetry. Each ligand is (S,S)-bonded to the central Sb atom with the sulphurs forming a distorted octahedron around the antimony. The average Sb-S bond length (2.446 Å) is a bit longer than Sb-S distances observed in the Sb(III) compound $\text{SbClS}_2(\text{CH}_2)_2^{202}$ but shorter than Sb-S distances observed in dithiooxamides. The C-S bond distances of 1.86-1.89 Å are a bit longer than those in the $\text{As}(\text{td})\text{Cl}$ structure (1.77 Å). The angles around Sb reveal distortions within the octahedron but these distortions do not appear to be related to the 'bite' of the ligand. The structure of $[\text{Sb}(\text{td})_3]^-$ is very similar to that of the tris(benzene-1,2-diotato)arsenate(V) anion⁵⁹ (see page 38).

The cation $[\text{Ph}_4\text{P}]^+$ has the expected slightly distorted tetrahedral structure with angles close to the tetrahedral angle (109.5°) around the phosphorous.

Figure 5.7.1 The Crystal Structure of the $[\text{Sb}(\text{td})_3]^-$ ion

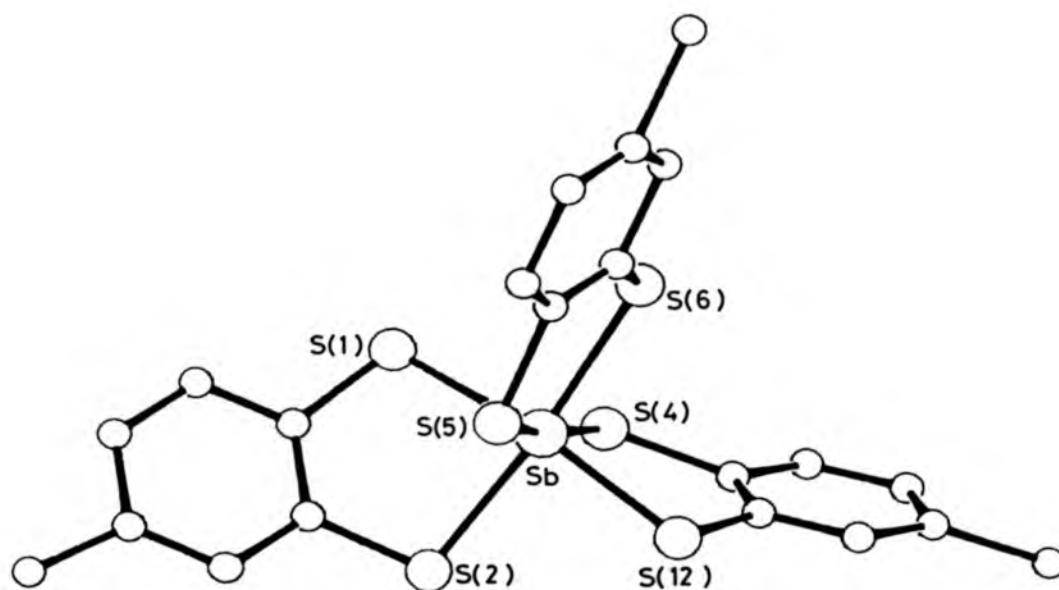


Table 5.7.1 Crystal Data and Refinement Details for
 $\text{Sb}(\text{td})_3\text{PPh}_4$

Formula	$\text{C}_{45}\text{H}_{38}\text{S}_6\text{SbP}$
M.W.	923.384
Crystal class	Monoclinic
Space group	P2_1
Absences	oko $k = 2n + 1$
a (\AA)	10.464
b (\AA)	12.825
c (\AA)	16.433
α ($^\circ$)	(90)
β ($^\circ$)	102.5
γ ($^\circ$)	(90)
U (\AA^3)	2152.9
F(000)	940
D_m	1.43
D_c	1.42
Z	2
μ (MoK_α) cm^{-1}	9.97
λ (\AA)	0.7107
Crystal size (mm)	1.6 x 0.6 x 0.05
Rotation axis	b
$2\theta_{\text{max}}$ ($^\circ$)	40
Number of data measured	2290
Number of data used in refinement	884
Criterion for data inclusion	$I > 3\sigma(I)$
Final R value	0.14
R_w value	0.14

Table 5.7.2 Atomic Coordinates ($\times 10^4$) for $[\text{Ph}_4\text{P}][\text{Sb}(\text{td})]$ with Estimated Standard Deviations in Parentheses

ATOM	X	Y	Z
SB(1)	730(7)	2500(0)	2799(5)
S(1)	3011(27)	3042(24)	3406(21)
S(2)	293(28)	4310(18)	2167(23)
S(5)	1515(45)	1887(23)	1590(23)
P(1)	5586(25)	2008(16)	7407(16)
S(4)	378(29)	2875(20)	4121(20)
S(6)	956(40)	690(20)	3226(20)
S(12)	-1607(38)	2212(17)	2198(23)
C(61)	2893(99)	3728(68)	4361(68)
C(62)	3894(98)	4478(85)	4546(89)
C(63)	3468(93)	5045(69)	5424(73)
C(64)	2497(88)	5065(84)	5585(80)
C(65)	1694(87)	4284(95)	5126(97)
C(66)	1855(93)	3671(78)	4554(73)
C(71)	-1445(97)	4331(71)	1679(69)
C(72)	-1683(99)	5297(72)	1213(70)
C(73)	-3105(99)	5364(87)	640(69)
C(74)	-3772(96)	4499(79)	609(76)
C(75)	-3582(94)	3479(75)	1105(75)
C(76)	-2167(94)	3460(55)	1612(60)
C(11)	6321(73)	1341(55)	8272(44)
C(12)	6720(73)	1825(55)	9046(44)
C(13)	7309(73)	1241(55)	9742(44)
C(14)	7501(73)	172(55)	9665(44)
C(15)	7102(73)	-313(55)	8892(44)
C(16)	6513(73)	272(55)	8195(44)
C(21)	4153(62)	1386(48)	6848(50)
C(22)	3453(62)	642(48)	7192(50)
C(23)	2454(62)	78(48)	6678(50)
C(24)	2155(62)	258(48)	5820(50)
C(25)	2855(62)	1003(48)	5477(50)
C(26)	3854(62)	1567(48)	5990(50)
C(31)	4964(77)	3240(39)	7680(43)
C(32)	3630(77)	3336(39)	7659(43)
C(33)	3133(77)	4273(39)	7892(43)
C(34)	3970(77)	5113(39)	8145(43)
C(35)	5305(77)	5017(39)	8166(43)
C(36)	5802(77)	4080(39)	7933(43)
C(41)	6683(73)	2259(55)	6805(46)
C(42)	7644(73)	1522(55)	6757(46)
C(43)	8489(73)	1681(55)	6218(46)
C(44)	8373(73)	2578(55)	5727(46)
C(45)	7412(73)	3315(55)	5775(46)
C(46)	6567(73)	3156(55)	6313(46)

Table 5.7.3 Bond lengths (\AA) and angles ($^\circ$) for $[\text{Ph}_4\text{P}][\text{Sb}(\text{td})_3]$

SB(1)	-	S(1)	2.48(3)		
SB(1)	-	S(2)	2.544(27)		
SB(1)	-	S(5)	2.44(3)		
SB(1)	-	S(4)	2.33(3)		
SB(1)	-	S(6)	2.422(26)		
SB(1)	-	S(12)	2.46(3)		
S(1)		SB(1)	S(2)	88.9(8)	
S(1)	-	SB(1)	-	S(5)	87.3(12)
S(2)	-	SB(1)	-	S(5)	91.3(11)
S(1)	-	SB(1)	-	S(4)	84.2(10)
S(2)	-	SB(1)	-	S(4)	98.1(10)
S(5)	-	SB(1)	-	S(4)	167.2(13)
S(1)	-	SB(1)	-	S(6)	97.3(11)
S(2)	-	SB(1)	-	S(6)	172.2(12)
S(5)	-	SB(1)	-	S(6)	84.2(11)
S(4)	-	SB(1)	-	S(6)	87.3(9)
S(1)	-	SB(1)	-	S(12)	172.3(9)
S(2)	-	SB(1)	-	S(12)	84.1(8)
S(5)	-	SB(1)	-	S(12)	96.0(13)
S(4)	-	SB(1)	-	S(12)	93.5(11)
S(6)	-	SB(1)	-	S(12)	89.9(11)
S(1)	-	C(61)	1.83(10)		
S(2)	-	C(71)	1.82(11)		
P(1)	-	C(11)	1.70(6)		
P(1)	-	C(21)	1.77(5)		
P(1)	-	C(31)	1.80(5)		
P(1)	-	C(41)	1.70(6)		
S(4)	-	C(66)	1.86(12)		
S(12)	-	C(76)	1.89(8)		
C(61)	-	C(62)	1.41(15)		
C(61)	-	C(66)	1.20(13)		
C(62)	-	C(63)	1.76(16)		
C(63)	-	C(64)	1.10(13)		
C(64)	-	C(65)	1.41(17)		
C(65)	-	C(66)	1.26(15)		
C(71)	-	C(72)	1.45(13)		
C(71)	-	C(76)	1.34(11)		
C(72)	-	C(73)	1.58(14)		
C(73)	-	C(74)	1.31(13)		
C(74)	-	C(75)	1.53(14)		
C(75)	-	C(76)	1.53(13)		

Table 3.7.3 Bond lengths (\AA) and angles ($^\circ$) for $[\text{Ph}_4\text{P}][\text{Sb}(\text{td})_3]$ (Continued)

SB(1)	-	S(1)	-	C(61)	104.1(4)
SB(1)	-	S(2)	-	C(71)	105.1(3)
C(11)	-	P(1)	-	C(21)	111.1(4)
C(11)	-	P(1)	-	C(31)	111.1(4)
C(21)	-	P(1)	-	C(31)	102.1(3)
C(11)	-	P(1)	-	C(41)	110.1(3)
C(21)	-	P(1)	-	C(41)	113.1(4)
C(31)	-	P(1)	-	C(41)	108.1(3)
SB(1)	-	S(4)	-	C(66)	101.1(4)
SB(1)	-	S(12)	-	C(76)	104.4(29)
S(1)	-	C(61)	-	C(62)	109.1(8)
S(1)	-	C(61)	-	C(66)	116.1(10)
C(62)	-	C(61)	-	C(66)	131.1(11)
C(61)	-	C(62)	-	C(63)	99.1(10)
C(62)	-	C(63)	-	C(64)	128.1(14)
C(63)	-	C(64)	-	C(65)	109.1(14)
C(64)	-	C(65)	-	C(66)	113.1(17)
S(4)	-	C(66)	-	C(61)	131.1(10)
S(4)	-	C(66)	-	C(65)	113.1(12)
C(61)	-	C(66)	-	C(65)	116.1(14)
S(2)	-	C(71)	-	C(72)	107.1(7)
S(2)	-	C(71)	-	C(76)	121.1(7)
C(72)	-	C(71)	-	C(76)	130.1(10)
C(71)	-	C(72)	-	C(73)	113.1(9)
C(72)	-	C(73)	-	C(74)	114.1(11)
C(73)	-	C(74)	-	C(75)	134.1(13)
C(74)	-	C(75)	-	C(76)	108.1(9)
S(12)	-	C(76)	-	C(71)	124.1(7)
S(12)	-	C(76)	-	C(75)	116.1(6)
C(71)	-	C(76)	-	C(75)	120.1(8)
P(1)	-	C(11)	-	C(12)	122.2(27)
P(1)	-	C(11)	-	C(16)	117.8(27)
P(1)	-	C(21)	-	C(22)	124.0(29)
P(1)	-	C(21)	-	C(26)	115.1(3)
P(1)	-	C(31)	-	C(32)	119.0(26)
P(1)	-	C(31)	-	C(36)	121.0(26)
P(1)	-	C(41)	-	C(42)	119.4(26)
P(1)	-	C(41)	-	C(46)	120.5(26)

5.8 EXPERIMENTAL

All chemicals were of reagent grade and were used without further purification. Solvents were stored over $\text{CaH}_2/\text{P}_2\text{O}_5$ and distilled under a nitrogen atmosphere prior to use. Because of the air-moisture sensitivity of many of the reactants and products, manipulations and synthetic work on these systems required the use either of vacuum-line techniques or of a N_2 -filled gloved box, or both. I.r. spectra were recorded on a Perkin-Elmer 580B spectrophotometer with samples between CsI plates as Nujol mulls or in solution. ^1H n.m.r. spectra were recorded on a Perkin Elmer R34 instrument (220 MHz) for CDCl_3 solutions doped with tetramethylsilane as internal reference. Elemental analyses were carried out by Butterworth Laboratories Ltd., Teddington, Middlesex. Chloride was determined by the Volhard titration.

Preparation of the ComplexesChloro(toluene-3,4-dithiolato)arsenic(III)

Arsenic trichloride (0.54 cm^3 , 6.4 mmol) was added to a solution of toluene-3,4-dithiol (1.0 g, 6.9 mmol) in chloroform (50 cm^3). The resulting mixture was heated under reflux for twenty minutes when a yellow solution was obtained. Chloroform was slowly removed *in vacuo* leaving the *product* as a yellow solid. Recrystallisation from methanol gave long yellow needles (yield 1.5 g, (85%).

5.8 EXPERIMENTAL

All chemicals were of reagent grade and were used without further purification. Solvents were stored over $\text{CaH}_2/\text{P}_2\text{O}_5$ and distilled under a nitrogen atmosphere prior to use. Because of the air-moisture sensitivity of many of the reactants and products, manipulations and synthetic work on these systems required the use either of vacuum-line techniques or of a N_2 -filled gloved box, or both. I.r. spectra were recorded on a Perkin-Elmer 580B spectrophotometer with samples between CsI plates as Nujol mulls or in solution. ^1H n.m.r. spectra were recorded on a Perkin Elmer R34 instrument (220 MHz) for CDCl_3 solutions doped with tetramethylsilane as internal reference. Elemental analyses were carried out by Butterworth Laboratories Ltd., Teddington, Middlesex. Chloride was determined by the Volhard titration.

Preparation of the ComplexesChloro(toluene-3,4-dithiolato)arsenic(III)

Arsenic trichloride (0.54 cm^3 , 6.4 mmol) was added to a solution of toluene-3,4-dithiol (1.0 g, 6.9 mmol) in chloroform (50 cm^3). The resulting mixture was heated under reflux for twenty minutes when a yellow solution was obtained. Chloroform was slowly removed *in vacuo* leaving the *product* as a yellow solid. Recrystallisation from methanol gave long yellow needles (yield 1.5 g, (85%).

Found: C, 31.7; H, 2.2; Cl, 13.4
 $C_7H_6S_2ClAs$ requires C, 31.8; H, 2.3; Cl, 13.4
 I.r. bands (ν_{max}): 1252, 1112, 1035, 871, 866, 804,
 683, 631, 537, 482, 441, 427, 398,
 304, 251 cm^{-1} (Nujol)
 N.m.r. data: δH (220 MHz; solvent $CDCl_3$;
 standard Me_4Si) 2.35 (3H, s, CH_3),
 7.05 and 7.41-7.48 (3H, m, aromatic
 C_6H_3).

Chloro(toluene-3,4-dithiolato)antimony(III)

Toluene-3,4-dithiol (1.05 g, 6.7 mmol) was added to a hot solution of $SbCl_3$ (1.53 g, 6.7 mmol) in chloroform (50 cm^3) to give a deep yellow solution. This was cooled in ice when a yellow solid precipitated out. The product was recrystallised from a methanol solution doped with DMSO to give fine yellow needles. (Yield 0.6 g, 25%), m.p. 141-142°C.

Found: C, 27.0; H, 1.9; Cl, 11.6; S, 20.9
 $C_7H_6S_2$ requires C, 27.0; H, 1.9; Cl, 11.4; S, 20.6
 I.r. bands (ν_{max}): 1254, 1108, 810, 679, 628, 538, 475, 431,
 371, 334, 282 cm^{-1} (Nujol)
 N.m.r. data: δH (220 MHz; solvent $CDCl_3$; standard
 Me_4Si) 2.33 (3H, s, CH_3), 6.93 and
 7.38-7.46 (3H, m, aromatic C_6H_3).

Chloro(toluene-3,4-dithiolato)bismuth(III)

Chloroform (50 cm^3) was distilled onto a mixture of $BiCl_3$ (2.0 g, 6.4 mmol) and toluene-3,4-dithiol (1.03 g,

6.5 mmol) and the resulting mixture was heated at reflux for two hours under an atmosphere of dry nitrogen. The brown suspension that resulted was allowed to settle and the colourless solution was decanted off. The remaining brown solid was collected and pumped dry. Recrystallisation of the *product* from methanol/DMSO gave very dark brown needles, m.p. 252-254°C (dec.).

Found: C, 21.7; H, 1.7; S, 16.2

$C_7H_6S_2ClBi$ requires C, 21.1; H, 1.5; S, 16.1

I.r. bands (ν_{max}): 1252, 1143, 1106, 866, 799, 680, 533, 431, 372, 328 cm^{-1} (Nujol).

N.m.r. data: δH (220 MHz; solvent $CDCl_3$; standard Me_4Si) 2.28 (3H, s, CH_3), 6.87 and 7.36 (3H, m, aromatic C_6H_3).

Bis(toluene-3,4-dithiolato)antimony(III)

Toluene-3,4-dithiol (2.4 g, 15 mmol) was added to a hot solution of $SbCl_3$ (1.6 g, 7 mmol) in methanol (50 cm^3). A deep yellow solution immediately formed. This solution was allowed to cool slowly to give the *product* as a microcrystalline yellow solid. Recrystallisation from methanol gave chunky yellow crystals (yield 10.1 g, 30%).

Found: C, 39.7; H, 2.8; S, 30.2

$C_{14}H_{13}S_4Sb$ requires C, 39.0; H, 3.0; S, 29.7

I.r. bands (ν_{max}): 3040-2860, 2335, 1584, 1458, 1379, 1256, 1112, 1031, 863, 807, 680, 631, 540, 438, 365, 331, 290 cm^{-1} ($CHCl_3$ solution)

6.5 mmol) and the resulting mixture was heated at reflux for two hours under an atmosphere of dry nitrogen. The brown suspension that resulted was allowed to settle and the colourless solution was decanted off. The remaining brown solid was collected and pumped dry. Recrystallisation of the *product* from methanol/DMSO gave very dark brown needles, m.p. 252-254°C (dec.).

Found: C, 21.7; H, 1.7; S, 16.2

$C_7H_6S_2ClBi$ requires C, 21.1; H, 1.5; S, 16.1

I.r. bands (ν_{max}): 1252, 1143, 1106, 866, 799, 680, 533, 431, 372, 328 cm^{-1} (Nujol).

N.m.r. data: δH (220 MHz; solvent $CDCl_3$; standard Me_4Si) 2.28 (3H, s, CH_3), 6.87 and 7.36 (3H, m, aromatic C_6H_3).

Bis(toluene-3,4-dithiolato)antimony(III)

Toluene-3,4-dithiol (2.4 g, 15 mmol) was added to a hot solution of $SbCl_3$ (1.6 g, 7 mmol) in methanol (50 cm^3). A deep yellow solution immediately formed. This solution was allowed to cool slowly to give the *product* as a microcrystalline yellow solid. Recrystallisation from methanol gave chunky yellow crystals (yield 10.1 g, 10%).

Found: C, 39.7; H, 2.8; S, 30.2

$C_{14}H_{13}S_4Sb$ requires C, 39.0; H, 3.0; S, 29.7

I.r. bands (ν_{max}): 3040-2860, 2335, 1584, 1458, 1379, 1256, 1112, 1031, 863, 807, 680, 631, 540, 438, 365, 331, 290 cm^{-1} ($CHCl_3$ solution)

N.m.r. data: δ H (220 MHz; solvent CDCl_3 ;
standard Me_4Si) 2.28 (6H, s, 2CH_3),
3.49 (H, s, S-H), 6.87 and 7.25-7.35
(3H, m, aromatic C_6H_3).

Triethyl ammonium bis(toluene-3,4-dithiolato)bismuth(III)

Bismuth trichloride (0.92 g, 2.9 mmol) was added to a solution of toluene-3,4-dithiol (0.92 g, 5.8 mmol) and triethylamine (1.63 cm^3 , 11.7 mmol) in methanol (50 cm^3). The mixture was gently heated at reflux with magnetic stirring under an atmosphere of dry nitrogen for thirty minutes. On cooling, the *product* separated as a brown solid which was filtered off and collected. After several washings with water, recrystallisation from acetone provided deep brown platelets.

Found: C, 39.3; H, 4.6; N, 2.6; S, 20.1
 $\text{C}_{20}\text{H}_{28}\text{NS}_4\text{Bi}$ requires C, 38.7; H, 4.5; N, 2.3; S, 20.7
i.r. bands (ν_{max}): 1581, 1246, 1104, 1030, 863, 807,
681, 631, 542, 470, 437, 304, 271 cm^{-1}
(Nujol)

N.m.r. data: δ H (220 MHz; solvent CDCl_3 ;
standard Me_4Si) 1.25 (9H, t, $3\text{CH}_3\text{-CH}_2\text{-}$),
2.20 (6H, s, 2CH_3 (aromatic ring)),
3.05 (6H, q, $3\text{CH}_3\text{-CH}_2\text{-}$), 7.02 and 7.48 (6H,
m, 2 aromatic C_6H_3).

Tetraethylammonium tris(toluene-3,4-dithiolato)antimony(V)

A solution of antimony trichloride (0.69 g, 3 mmol) in methanol (20 cm^3) was added to a solution containing toluene-3,4-dithiol, (0.96 g, 6 mmol),

triethylamine (1.7 cm^3 , 12 mmol), and tetraethylammonium chloride (0.56 g, 3 mmol) dissolved in methanol (40 cm^3). A vigorous reaction ensued to give a deep red solution. On standing overnight a dark purple-red solid separated from solution. This was collected and washed with warm water ($3 \times 25 \text{ cm}^3$) until the washings gave a negative test for chloride. The purple-violet *product* was further washed with boiling water ($2 \times 25 \text{ cm}^3$) and ether ($3 \times 25 \text{ cm}^3$) and finally recrystallised from a 1:10 chloroform:methanol solution as almost black crystals, m.p. $149\text{--}150^\circ\text{C}$.

Found: C, 47.5; H, 5.4; N, 2.5; S, 27.0

$\text{C}_{29}\text{H}_{38}\text{NS}_6\text{Sb}$ requires C, 48.7; H, 5.3; N, 2.0; S, 26.9

I.r. bands (ν_{max}): 2860–3041, 1585, 1449, 1390, 1367, 1250, 1169, 1105, 1037, 999, 869, 807, 681, 636, 546, 476, 437, 351, 317 cm^{-1}

(CH_2Cl_2 solution)

N.m.r. data: δH (220 MHz; solvent CDCl_3 ; standard Me_4Si) 1.07 (12H, t, $4\text{CH}_3\text{--CH}_2\text{--}$), 2.22 (9H, s, CH_3 (aromatic ring)), 2.93 (8H, q, $4\text{CH}_3\text{--CH}_2\text{--}$), 6.71 and 7.25 (9H, m, 3 aromatic C_6H_3)

Tetraphenyl phosphonium tris(toluene-3,4-dithiolato)-antimony(V)

Antimony trichloride (0.44 g, 1.9 mmol) was added to a solution containing toluene-3,4-dithiol (0.59 g, 3.8 mmol) and triethylamine (1.1 cm^3 , 7.6 mmol) in methanol (40 cm^3). The resulting red solution

was heated at reflux for twenty minutes. Addition of tetraphenyl phosphonium bromide (0.80 g, 1.9 mmol) to this solution resulted in immediate precipitation of the *product* as a purple solid. Recrystallisation from a 1:10 chloroform:methanol solution provided very dark purple platelets, m.p. 192-193°C.

Found: C, 58.5; H, 3.8

$C_{45}H_{38}S_6PSb$ requires C, 58.5; H, 4.1

I.r. bands (ν_{max}): 1587, 1260, 1108, 1042, 1000, 874, 803, 691, 637, 540, 480, 442, 355, 321 cm^{-1} (Nujol)

N.m.r. data: δH (220MHz, solvent $CDCl_3$, standard Me_4Si) 2.13 (9H, s, \underline{CH}_3 (aromatic ring)), 6.58 and 7.11 (9H, m, 3 aromatic \underline{C}_6H_3), and 7.5-7.8 (20H, m, $4C_6H_5$).

CHAPTER 6

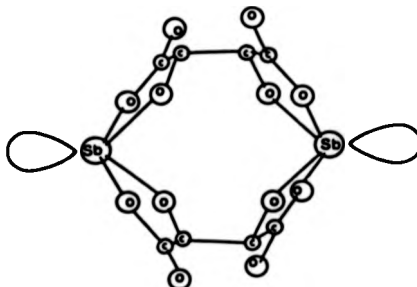
COMPLEXES OF PENICILLAMINE AND DIMERCAPTOSUCCINIC ACID WITH GROUP (VB) ELEMENTS

CHAPTER 6

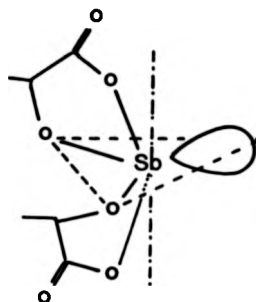
COMPLEXES OF PENICILLAMINE AND
DIMERCAPTOSUCCINIC ACID WITH
GROUP (VB) ELEMENTS6.1 INTRODUCTIONChemotherapeutic Agents used in the Treatment of
Bilharzia

The main chemotherapeutic agent has been potassium (sodium) antimonyl tartrate or tartar emetic $[\text{Sb}^{(\text{III})}(\text{OOC}.\text{CH}(\text{O}).\text{CH}(\text{O}).\text{COO})]_2\text{K}^+(\text{Na}^+)$, but there is an accompanying high level of toxicity. However, recent work has suggested that simultaneous administration of *d*-penicillamine and tartar emetic reduces the toxicity of the latter without affecting its parasitic activity.

Because tartaric acid exhibits three isomeric forms (*d*, *l*, and *meso*), the 2:2 bridged complex formed between antimony(III) and tartaric acid can have six isomers (*dd*, *ll*, *d-meso*, *l-meso*, *dl*, and *meso-meso*). For this reason, the complex has been the subject of numerous crystallographic investigations²⁰⁵⁻²¹². In tartar emetic, the complex exists as antimony tartrate dimers:

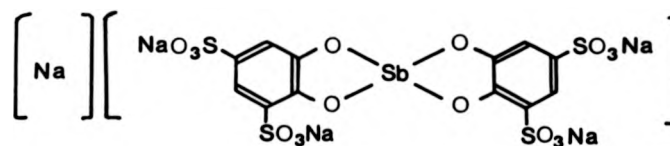


The environment around the antimony approximates to a distorted trigonal bipyramid with the stereochemically active lone pair occupying an equatorial position.

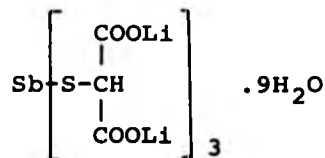


Other chemotherapeutic agents include:

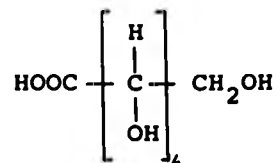
- (a) Sodium antimony bis(pyrocatechol-3,5-sodium-disulphonate) known as *Stibophen* (*Fuadin*)



- (b) Lithium antimony thiomalate (*Anthiomaline*)



- (c) Sodium antimony gluconate (*Triostam Tsag*)
gluconic acid:



- (d) Antimony thioglycolamide

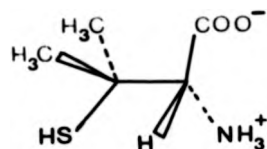
$$\text{Sb}(\text{S}-\text{CH}_2-\text{CONH}_2)_3$$
- (e) Antimony sodium thioglycolate

$$\text{Sb}(\text{S}-\text{CH}_2-\text{COONa})_3$$
- (f) Sodium antimony dimercaptosuccinate
(Astiban Stibocaptate, TWSb)
- (g) Piperazine diantimonytartrate (*Bilharoid*)

Our attempts to prepare a sulphur-bound antimony(III) compound similar to *Fuadin* have been described in the preceding chapter. In this chapter we describe the reactions of antimony(III) and (a) dimercaptosuccinic acid (b) *d,l* penicillamine.

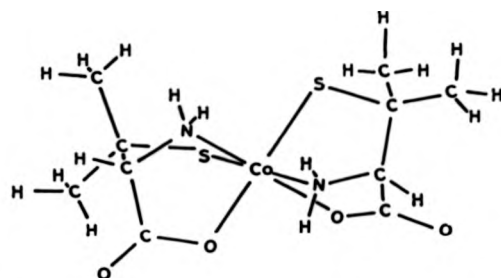
Penicillamine

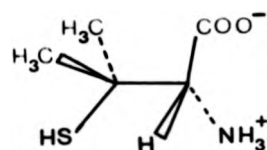
Reactions of penicillamine (I) and other sulphur containing amino acids with both transition and non-transition metal elements have been of great interest mainly because of the potential of these ligands as chelation therapeutic agents in the treatment of heavy metal poisoning. *d*-Penicillamine already finds use in the treatment of heavy metal poisoning²¹³. Structural studies of Hg(II)²¹⁴⁻²¹⁶, Mo(V)²¹⁷, Pb(II)²¹⁸, Cd(II)^{219,220}, Cu(I) and Cu(II)^{221,222}, Pd(II)²²³, Co(III)²²⁴⁻²²⁷, Cr(III)²²⁸, Tc(IV)²²⁹, Pt(II)²³⁰, Au(I) and Ni(II)²³¹, as well as spectroscopic studies of Sn(IV)^{232,233} with penicillamine and related ligands, have provided much information regarding the chelation properties of such systems.



I

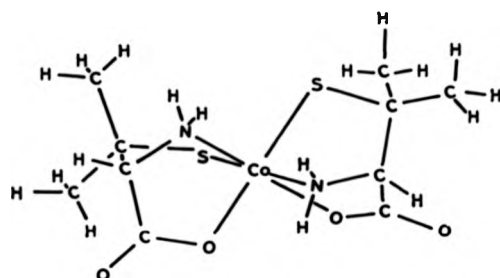
The ligand penicillamine (I) can coordinate to a metal via (N)-, (S)- and (O)-sites as seen in the structure of $K[\text{Co(III)}d\text{-pen}, l\text{-pen}]\cdot 2\text{H}_2\text{O}^{227}$:

*l*-penicillamine*d*-penicillamine



I

The ligand penicillamine (I) can coordinate to a metal via (N)-, (S)- and (O)-sites as seen in the structure of $K[\text{Co(III)}d\text{-pen}, l\text{-pen}]\cdot 2\text{H}_2\text{O}$ ²²⁷:

*l*-penicillamine*d*-penicillamine

6.2 REACTIONS INVOLVING PENICILLAMINE

Consideration of Ligand Sites

The electrochemical titration of penicillamine shows the presence of three ionisable centres with pKa values 1.8 (carboxyl), 7.9 (amino) and 10.5 (thiol)²³⁴. We have investigated the effect of pH on the ¹H n.m.r. spectrum of *d*-penicillamine. The natural pH of a solution of *d*-penicillamine in D₂O is *ca.*, 5.4, hence the -COOH proton was completely ionised at this stage. An increase in pH over the range 5.4-10.8 resulted in further deprotonation of the -NH₃⁺ and -SH centres as shown by the ¹H n.m.r. spectrum (see Table 6.5.1).

Both sets of -CH₃ protons as well as the -C-H proton showed increased shielding (upfield shift) with increasing pH of solution. The -C-H was more affected because of its closeness to the region of increased electron density. Both *d*- and *l*-penicillamine showed similar ¹H n.m.r. behaviour with varying pH.

Reactions with Sb(III) and As(III) Compounds

(a) Antimony potassium(+)-tartrate with *d*-penicillamine:

No reaction was found between antimony potassium(+)-tartrate and *d*-penicillamine in aqueous solutions.

(b) Antimony(III)oxide with *d*-penicillamine:

The treatment of aqueous solutions of antimony(III) oxide with *d*-penicillamine at pH 7.9 resulted in an insoluble yellowish-brown solid after two days of heating at reflux. The i.r. spectrum identified this solid as Sb₂S₃ (by comparison

Table 6.5.1 Effect of pH on ^1H n.m.r. spectrum of *d*-penicillamine
 δH p.p.m. (220 MHz, Solvent D_2O , standard $(\text{CH}_3)_3\text{Si}(\text{CH}_2)_3\text{SO}_3\text{Na} \cdot x\text{H}_2\text{O}$)

pH	$-\text{CH}_3$	$-\text{CH}_3$	$-\text{CH}$
5.4	1.47	1.56	3.69
8.4	1.32	1.55	3.42
10.8	1.21	1.47	3.13

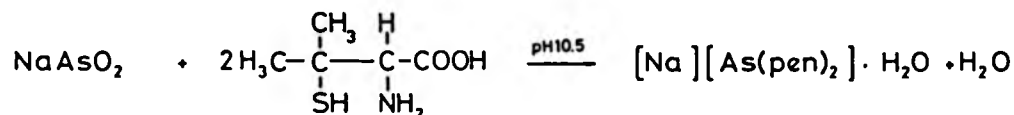
Table 6.5.2 ^1H n.m.r. spectra of a penicillamine solution treated with successive quantities of NaAsO_2 . δH p.p.m. (220 MHz, Solvent D_2O , Standard $(\text{CH}_3)_3\text{Si}(\text{CH}_2)_3\text{SO}_3\text{Na} \cdot x\text{H}_2\text{O}$)

Starting with <i>d</i> -penicillamine at pH 10.8			
	$-\text{CH}_3$	$-\text{CH}_3$	$-\text{CH}$
First addition of NaAsO_2	1.31	1.54	3.38
Second	1.35, 1.33, 1.28	1.50, 1.56	3.41, 3.34
Third	1.35, 1.33, 1.27	1.50, 1.57	3.33, 3.25
Saturation	1.35, 1.31, 1.25	1.48, 1.55	3.30, 3.20
After 10 weeks	1.35, 1.33, 1.27	1.49, 1.56	3.35, 3.25
Starting with <i>l</i> -penicillamine at pH 12.5			
First addition	1.19	1.42	3.02
Second and Third	1.22	1.33	3.05
Saturated	1.35, 1.29	1.52	3.24, 3.28
After 8 weeks	1.35, 1.31, 1.27	1.50, 1.55	3.32, 3.25

with the i.r. spectrum of an authentic sample).

(c) Sodium arsenite with *d*-penicillamine:

Direct addition of aqueous NaAsO₂ and *d*-penicillamine at pH 10.5 gave a solution which, on evaporation, yielded the arsenic(III) complex [Na][As.Pen₂] · H₂O as a glassy solid. The complex was recrystallised from methanol.



The ¹H n.m.r. spectrum of the product shows major singlets at δ 1.46, 1.62 and 3.52 for the two -CH₃ groups and H-C(NH₂)-COO⁻ respectively. Along with these, there are much smaller singlets (~ 10% the height) at δ 1.35, 1.56 and 3.35. At first it was thought that *d*-penicillamine had isomerised to give partly *d*- and partly *l*-penicillamine complexes as observed for cobalt(III)²²⁷. The treatment of either *d*- or *l*-penicillamine with successive quantities of NaAsO₂ (see Table 6.5.2) showed similar ¹H n.m.r. developments. No satisfactory explanation of these small peaks has been obtained.

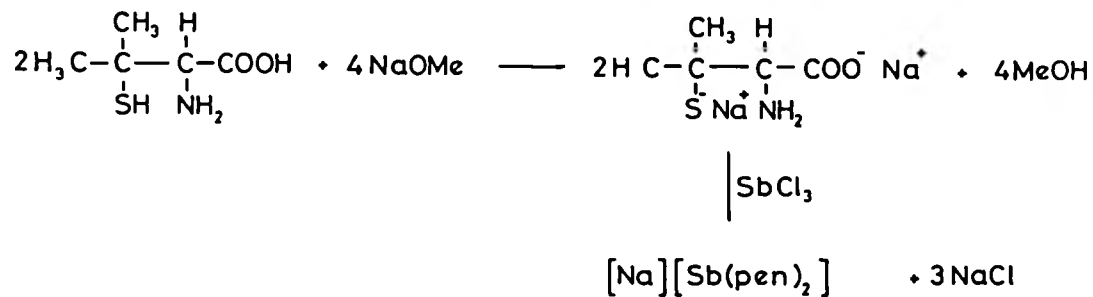
The i.r. spectrum of the complex shows a strong, broad, band at 3500-3100 cm⁻¹ with contributions from H₂O present in the lattice as well as contributions from ν(N-H) bands of *d*-penicillamine. Other assignments follow those of Franklin, Howard-Lock and Lock²²⁹ (see Experimental).

(d) Antimony trichloride with *d*-penicillamine:

D-penicillamine in methanol was treated with stoichiometric quantities of sodium methoxide prior to the addition of antimony trichloride. A homogeneous solution was

obtained which on evaporation gave a water soluble solid. An aqueous solution of this solid gave a positive test for halogen but the expected $[\text{Na}][\text{Sb}(\text{pen})_2]$ could not be isolated from the mixture.

Proposed reaction:

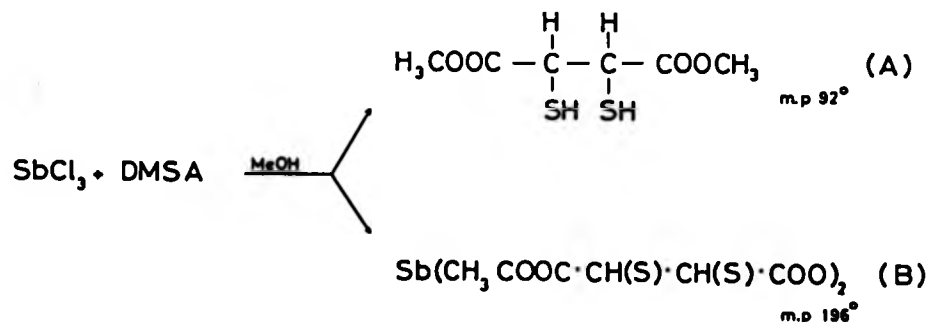


6.3 REACTIONS INVOLVING DIMERCAPTOSUCCINIC ACID
(DMSA) HOOC·CH(SH)·CH(SH)COOH

DMSA bears a close resemblance with tartaric acid in that the two -SH groups in DMSA are replaced by -OH groups in tartaric acid; hence reactions observed with tartaric acid might be expected to take place with DMSA. In the first place the preparation of antimony(III) tartrate is achieved by heating at reflux an aqueous suspension of Sb_2O_3 with $\text{KHC}_4\text{H}_4\text{O}_6$ in an acidic medium (oxalic acid)²³⁵. Under analogous conditions, the reaction between DMSA and Sb_2O_3 gave a yellow solid which was characterised by infrared spectroscopy as Sb_2S_3 . The same product was also isolated from the reaction between Sb_2O_3 and DMSA under alkaline conditions.

The Reaction between DMSA and Antimony trichloride

Two products were isolated from the reaction between DMSA and SbCl_3 in methanol:

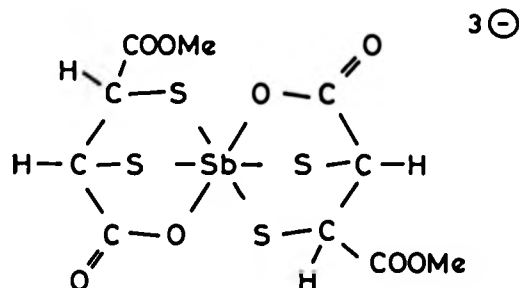


Product (A) is a colourless crystalline solid, readily soluble in CHCl_3 and CH_2Cl_2 and has been characterised as the methyl ester of DMSA. The ^1H n.m.r.

spectrum shows a methyl singlet at δ 3.8, a multiplet at δ 3.65 (H-C), and another multiplet at δ 2.38 due to the S-H protons. In a spin-decoupling experiment, irradiating at δ 2.38 gave a singlet at 3.65 and irradiating at δ 3.65 gave a singlet at δ 2.38 showing that the splitting patterns of these two sets of protons are due to mutual coupling with one another. The proton integral ratio suggests diester formation in agreement with mass spectral data (see Experimental). Shaking the CDCl_3 solution of product (A) with a drop of D_2O resulted in the diminishing of the resonances at δ 2.38 and a much simpler pattern at δ 3.65 showing that the resonance at δ 2.38 is indeed due to S-H protons. The i.r. spectrum shows a prominent, sharp $\nu(\text{S-H})$ band at 2550 cm^{-1} and a fairly broad carbonyl band $\nu(\text{C-O})$ at $1730\text{--}1715\text{ cm}^{-1}$.

Product (B) (m.p. 196°) analyses as a 1:2 antimony: methyl ester derivative. It was insoluble in all the common organic solvents and we were unable to obtain any solution spectra. The i.r. spectrum (Nujol mull) shows no $\nu(\text{S-H})$ bands but there are two strong well-resolved bands in the carbonyl region ($1690, 1735\text{ cm}^{-1}$).

Proposed structure:



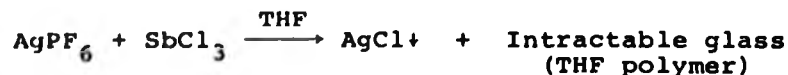
6.4

REACTIONS INVOLVING THE 'NAKED' CATIONIC SPECIES
Sb³⁺ SOLVATE

Kellog and Matwiyoff²³⁶ have reported the removal of all chloride from MCl_3 ($\text{M} = \text{As}, \text{Sb}$) by the treatment of MCl_3 with AgClO_4 in a coordinating solvent such as N,N -dimethylformamide (DMF). This resulted in the formation of the simple cations Sb^{3+} and As^{3+} solvated by DMF which were isolated as the anhydrous salts $[\text{As}(\text{DMF})_6][(\text{ClO}_4)_3]$ and $[\text{Sb}(\text{DMF})_6][(\text{ClO}_4)_3]$. These results suggested to us that such species might turn out to be suitable precursors in the synthesis of both antimony(III)-penicillamine and antimony(III)-DMSA complexes. Rather than be exposed to the dangers of perchlorate, other non-coordinating counter-ions were favoured.

(a) Reaction of SbCl_3 with Silver Hexafluorophosphate, AgPF_6

The addition of a solution of SbCl_3 in tetrahydrofuran (THF) to a THF solution of AgPF_6 caused the immediate precipitation of AgCl . The Sb^{3+} product could not be isolated because the whole solution formed a colourless jelly-like solid which was not soluble in any common organic solvents, (possibly a THF polymer).



(b) Reaction of SbCl_3 with Silver Tetra-fluoroborate, AgBF_4

The addition of a THF solution of SbCl_3 to a

The precipitate that was isolated from this reaction was recrystallised from DMSO. Much to our embarrassment an X-ray crystal structural determination has revealed that the precipitate is in fact Ph_4PBF_4 and not the expected $[\text{Ph}_4\text{P}][\text{Sb}(\text{pen})_2]$.

6.5 EXPERIMENTAL1. The Reaction of NaAsO₂ with *d*-Penicillamine

An aqueous solution of NaAsO₂ (0.29 g, 2.2 mmol) was added to an aqueous solution of *d*-penicillamine (0.67 g, 4.49 mmol). A clear solution with a slight red tinge was obtained. The solution was slowly evaporated to give a glassy solid which was recrystallised from methanol to give colourless needle-shaped, crystals of Na(AsPen₂).H₂O.

Found: C, 28.56; H, 4.69; N, 6.48, C₁₀H₂₀N₂O₅S₂AsNa requires C, 29.27; H, 4.87; N, 6.83%

N.m.r. data δ H (220 MHz; solvent CD₃OD; Standard Me₄Si) 1.46 (3H, s, Me), 1.62 (3H, s, Me), 3.52 (1H, s, $\underline{\text{H}}\text{-C}(\text{NH}_2)\text{-COO}^-$)

Selected i.r. absorptions: (Nujol mull) ν_{max} 3500-3100 s,br (H₂O, N-H), 1612 (-COO) 1588 (δ NH₂) 425 (As-N), 395 (S-C-CN), 270 (As-S) cm⁻¹.

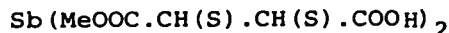
2. The Reaction between SbCl₃ and *d*-Penicillamine

A methanol solution of SbCl₃ (0.37 g, 1.6 mmol) was added to a methanol solution of sodium methoxide (0.355 g, 6.5 mmol) and *d*-penicillamine (0.489 g, 3.2 mmol). The clear colourless solution that resulted was allowed to stand for 15 hours. Some of the methanol was evaporated off *in vacuo*. The white precipitate that came out gave a positive test for chloride (AgNO₃). Further evaporation gave another white solid.

I.r. absorptions: (Nujol mull) ν_{max} ; 3350-3440 (H₂O), 3195 (N-H), 1600 (s,br, -COO), 382, 353 (Sb-s, C-C-S) cm⁻¹.

3. The Reaction between SbCl_3 and *meso*-2,3-Dimercaptosuccinic Acid (DMSA)

A solution of SbCl_3 (0.364 g, 1.6 mmol) in dry methanol ($\sim 50 \text{ cm}^3$) was added to solid DMSA (0.437 g, 2.4 mmol) and the mixture was magnetically stirred until a homogeneous solution was obtained. The solution was gently refluxed for 10 hours and then allowed to cool. A white microcrystalline solid precipitated out. This solid was recrystallised from chloroform m.p. 196-198.



Found: C, 24.41; H, 2.16; Sb (A.A), 23.88

$\text{C}_{10}\text{H}_{12}\text{O}_8\text{S}_4\text{Sb}$ requires C, 23.53; H, 2.54; Sb, 23.73

I.r. absorptions: (Nujol mull) ν_{max} 1738, 1690, 1325, 1207, 1070, 1020, 980, 885, 800, 641, 497, 404, 381, 360, 349, 330, 270 cm^{-1} .

The remaining solution was slowly evaporated to yield a crystalline colourless solid. Chromatography on silica gel with chloroform as eluant yielded the pure crystalline methyl ester ($\text{CH}_3\text{OOC}-\underset{\text{I}}{\text{CH}}-\text{SH}$)₂.

Found: C, 34.60; H, 4.80%, M (mass spectrum), 210

$\text{C}_6\text{H}_{10}\text{O}_4\text{S}_2$ requires: C, 34.28; H, 4.76; M, 210.

I.r. absorptions: (Nujol mull) ν_{max} 2550, 1730-1710, 1313, 1255, 999, 929, 874, 790, 710, 618, 528, 387, 339, 250 cm^{-1} .

N.m.r. data: δ_{H} (220 MHz; Solvent CDCl_3 ; Standard Me_4Si)
2.38 (2H, m, -S-H), 3.65 (2H, m, -C-H),
3.81 (6H, s, -O- CH_3).

4. The Reaction of SbCl_3 + AgPF_6 in THF

A solution of SbCl_3 (0.29 g, 1.27 mmol) in THF ($\sim 30 \text{ cm}^3$) was added to a solution of AgPF_6 (0.965 g, 3.8 mmol). The white solid that immediately precipitated out was filtered off, dried and weighed. The solution was allowed to stand for 12 hours after which it had become a clear colourless jelly-like solid. This solid was insoluble in most solvents.

5. The Reaction of SbCl_3 with AgBF_4

A solution of SbCl_3 (0.31 g, 1.36 mmol) in THF ($\sim 10 \text{ cm}^3$) was added to a solution of AgBF_4 (0.796 g, 4.09 mmol) in THF ($\sim 20 \text{ cm}^3$). AgCl which precipitated out was immediately filtered off, dried and weighed (0.516 g, 3.6 mmol). DMSO (0.58 cm^3 , 8.1 mmol) was added to the solution. Boiling resulted in the separation of two colourless layers. Slow evaporation of THF *in vacuo* resulted in a colourless oil which was allowed to stand and crystals started to grow in the oil over several days. The crystals were extremely hygroscopic and decomposed to a black mass on exposure to air.

6. The Reaction of *d*-Penicillamine with Sb^{3+}

A solution of SbCl_3 (0.3151 g, 1.38 mmol) in THF ($\sim 30 \text{ cm}^3$) was added to a solution of AgBF_4 (0.808 g, 4.1 mmol) in THF ($\sim 20 \text{ cm}^3$). AgCl was filtered off the resulting solution and *d*-penicillamine (0.4122 g, 2.76 mmol) was added to it. The solution was left to stand for 12 hours before Ph_4PBr (0.579 g, 1.38 mmol) was added to the solution.

A white solid precipitated out immediately. This solid was not soluble in non-coordinating solvents. However, a crystalline product was obtained on recrystallisation from DMSO. A partial determination of the crystal structure of this solid shows that it is in fact $\text{Ph}_4\text{PAgBF}_4$.

APPENDIX

APPENDIX
STARTING MATERIALS AND ANALYTICAL METHODS

(a) Starting Materials

Acetonitrile was obtained from Fisons Scientific Apparatus Ltd., Loughborough and prior to use, refluxed over CaH_2 and distilled under a normal pressure of dry nitrogen.

Antimony trichloride (AR grade) was obtained from BDH Chemicals Ltd., Poole, and purified by sublimation *in vacuo*.

Antimony tribromide was obtained from BDH Chemicals Ltd., Poole, and recrystallised from benzene prior to use.

Arsenic trichloride was used as supplied from Hopkin and Williams Ltd., Essex.

Benzene (AR grade) was obtained from Koch Light Laboratories Ltd., Colnbrook Bucks. Prior to use, it was refluxed over CaH_2 and distilled under a normal pressure of dry nitrogen.

Carbon tetrachloride was obtained from BDH Chemicals Ltd., Poole, and distilled from CaH_2 under a normal pressure of nitrogen prior to use.

Chloroform and Dichloromethane were obtained from BDH Chemicals Ltd., Poole, and refluxed over P_2O_5 for two hours before distilling under a normal pressure of dry nitrogen.

Diethyl ether was obtained from BDH Chemicals Ltd., Poole, and stored over Na wire.

Dimethyl sulphoxide (DMSO) was obtained from Fisons Scientific Apparatus Ltd., Loughborough and stored over Linde-type 4A molecular sieves. Prior to use, it was distilled at reduced pressure over CaH_2 , discarding the first fraction.

Dithiooxamide was used as supplied from The Aldrich Chemical Co. Ltd., Gillingham, Dorset, SP8 4JL.

All deuterated solvents were used as supplied by The Aldrich Chemical Co. Ltd., The Old brickyard, New Road, Gillingham, Dorset, SP8 4JL.

n-Hexane was obtained from May and Baker Ltd., Dagenham and distilled from CaH_2 under a normal pressure of dry nitrogen prior to use.

Pyridine was obtained from Fisons Scientific Apparatus Ltd., Loughborough and prior to use distilled over KOH under an N_2 atmosphere.

Tetrahydrofuran was obtained from Koch-Light Laboratories Ltd., Colnbrook, Bucks. It was refluxed for several hours over CaH_2 and then distilled over Na metal doped with Benzophenone prior to use.

Tin tetrachloride, *Tin tetrabromide* and *Titanium tetrachloride* were all obtained from Fisons Scientific Apparatus Ltd., Loughborough and used as supplied.

(b) Analytical Methods

Chlorine and Bromine were determined by the Volhard method . A small quantity of the test sample (0.1-0.3 g) was hydrolysed in concentrated HNO_3 and the solution made up to 100 ml. Determinations were carried out on 25 cm^3 aliquots of the test solution which were titrated against standard KSCN with $\text{NH}_4\text{Fe}(\text{SO}_4)_2$ as indicator. The formation of blood-red $\text{Fe}(\text{III})(\text{SCN})_6^{3-}$ indicated the end point. In chloride determinations, nitrobenzene ($\sim 3 \text{ cm}^3$) was added to each test aliquot to coagulate the AgCl precipitate.

Antimony was determined by Atomic Absorption. Typically 0.07-0.15 g of sample were dissolved in dilute HCl , a little 1% tartaric acid solution was added to the flask and the solution made up to 100 cm^3 . The solution was run on a Varian AA6 spectrophotometer using an air acetylene flame at 217.8 nm. The spectrophotometer was standardised before each determination with standard

solutions of antimony potassium tartrate (SpectrosoL grade, BDH Chemicals Ltd., Poole).

Tin was also determined by atomic absorption. In this case 0.2-0.3 g of sample were dissolved in dilute HCl and made up to 100 cm³. This was used as the stock solution from which solutions of lower concentration ($50-100 \times 10^{-6} \text{ g cm}^{-3}$) were prepared and determined on a Varian AA6 spectrophotometer using an Acetylene-Nitrous oxide flame at 286.3 nm. The spectrophotometer was standardised before each determination with standard solutions of stannous chloride (SpectrosoL grade, BDH Chemicals Ltd., Poole).

Carbon, Hydrogen, Nitrogen and Sulphur were determined professionally by either Elemental Micro-Analysis Ltd., Bedworthy, Devon, or Butterworth Laboratories Ltd., Teddington, Middlesex.

Experimental Techniques

The majority of compounds described in this thesis were air/moisture sensitive and therefore necessitated handling under an inert atmosphere (N₂) or in high vacuum.

The Dry Box

The loading of reaction vessels, and the preparation of samples for spectroscopic analysis was carried out in a steel gloved-box with a perspex front. The box was constantly flushed with dry nitrogen and the pressure

inside the box was kept at a little higher than atmospheric. The internal atmosphere of the box was dessicated by P_2O_5 in open dishes. Entrance to the box was achieved *via* an 'air lock' entry port, which was flushed with an independent supply of dry nitrogen. The box was equipped with electrical contacts for recrystallisation and distillation purposes.

The Vacuum Line

Purification and isolation of products was carried out using a standard all glass vacuum line. The vacuum was produced and maintained with a Genevac double stage rotary pump, type G.R.D.2 and an electrically heated mercury diffusion pump. With this system, a vacuum of 10^{-3} mmHg was obtainable (Figure A.1).

Solvent Drying

Solvents were dried in specially designed solvent still (Figure A.2) which allowed a rapid reflux, collection and removal of solvents under a dry nitrogen atmosphere. Solvents were refluxed *ca.* 1 hour over the appropriate desiccant and then collected on the sintered frit. Solvents were degassed either by applying a positive pressure of dry nitrogen at the solvent collection point or by freeze-pump-thaw cycles on the vacuum line or by merely pumping off a small fraction of the solvent *in vacuo*.

Product Storage

When satisfactory purity and dryness of a

Figure A.1 The Vacuum Line

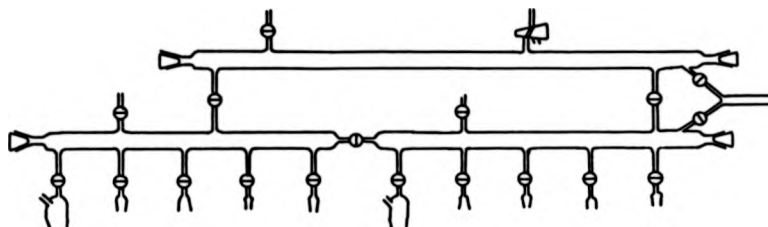


Figure A.2 Solvent Still

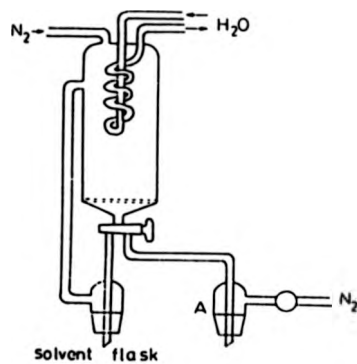


Figure A.3 A "Pig"

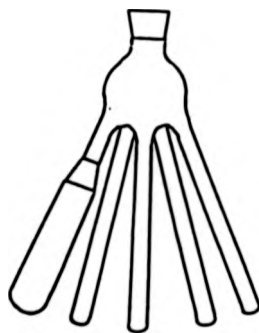


Figure A.4

Washing at the Vacuum Line

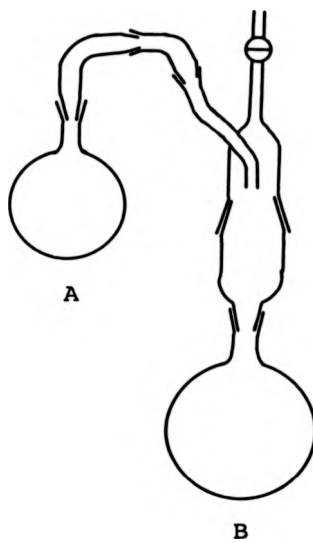
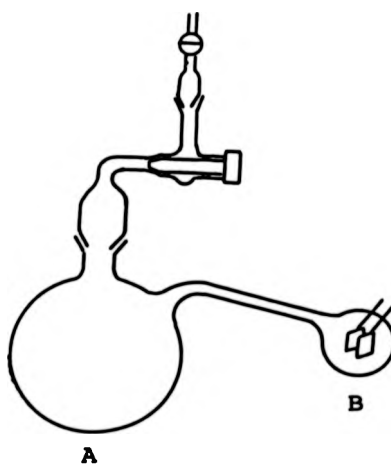


Figure A.5

Conductivity Cell



product had been achieved, the product was introduced into a pre-flamed glass "pig" (Figure A.3). The pig was then transferred to the vacuum line, evacuated and the atmosphere replaced with dry nitrogen. Each "leg" was then sealed under a normal pressure of nitrogen thus encapsulating the sample.

Reactions of Complexes

Reactions involving AsCl_3 , SbCl_3 , SbBr_3 , SnCl_4 , SnBr_4 , and TiCl_4

Complexes were prepared by dropwise addition of a solution of the ligand in a non-coordinating solvent (normally benzene, n-hexane, CCl_4 , etc.) to a well stirred solution of the metal chloride in the same solvent, under a constant head of dry nitrogen. The resulting system was then transferred to the vacuum line and some of the solvent removed *in vacuo*. The product, if solid, was successively washed at the vacuum line (Figure A.4).

'Washing' at the Vacuum Line (Figure A.4)

The crude products are placed in flask A and dry solvent placed in flask B and the system evacuated. The solvent is distilled into flask A at 77 K, and when the flask has warmed to room temperature, the flask and contents are swirled around to extract any soluble impurities. After the contents of the flask have settled, the solvent is carefully decanted into flask B. This process is repeated until a satisfactory degree of purity has been attained. The insoluble product is then pumped *in vacuo* for several hours.

Instrumentation and Physical Measurements

Infrared Spectra

Infrared spectra ($4000\text{--}200\text{ cm}^{-1}$) were recorded on Perkin-Elmer 580B Grating Infrared Spectrophotometer. Solid samples were investigated as Nujol or hexachlorobutadiene mulls sandwiched between CsI plates. Solutions were investigated using CsI solution cells. Spectra in the $400\text{--}50\text{ cm}^{-1}$ region were recorded on a RIIC FS-720 spectrophotometer as Nujol mulls held between polythene plates.

Nuclear Magnetic Resonance Spectra

Proton n.m.r. spectra were recorded on Perkin Elmer R34 (220 MHz) spectrometer. Tetramethylsilane (TMS) was used as the internal standard for organic n.m.r. solvents while the water-soluble, hydrated, sodium salt of 3-(trimethyl silyl)-1-propanesulphonic acid (TSS) was the internal standard for D_2O solutions.

Conductivity Measurements

The apparatus used is shown in Figure A.5. It consists of a large reservoir bulb A connected by a glass tube to a much smaller reservoir bulb B which contains the electrodes. Typically the whole cell was weighed and then an accurately weighed small amount of sample was placed in bulb A, and the apparatus evacuated. The appropriate solvent was then distilled into A at 77 K and the weight of solvent determined by difference. The apparatus was allowed to warm up to room temperature before sufficient solution was

poured into cell B to cover the platinum electrodes. The resistance was measured using a Phillips PR9500 bridge. Further readings of resistance at different concentrations were taken by removing some of the solvent *in vacuo* and repeating the above procedure. The conductivity can now be calculated by

$$\Lambda_m = \frac{1000 C}{C_m R}$$

where Λ = molar conductivity

C = cell constant, calculated as 0.28 cm^{-1}
using standard 0.1 M KCl solution

C_m = molar concentration of solute

R = resistance

The obtained conductivity values were compared with those for non-conducting, 1:1 and 1:2 electrolytes in the same solvent.

REFERENCES

REFERENCES

1. S. O. Wandiga, *J. Chem. Soc., Dalton Trans.*, 1975, 1894
2. L. Pauling, "The nature of the chemical bond", 3rd edn. Cornell University Press, 1960
- 3.(a) H. Bethe, *Ann. Physik.* [5], 1929, 3, 135
(b) J. H. van Vleck, *Phys. Rev.*, 1932, 41, 208
(c) J. H. van Vleck, *J. Chem. Phys.*, 1935, 3, 803; 807
4. C. J. Ballhausen and H. B. Gray, "Molecular Orbital Theory", Benjamin, 1964
- 5.(a) N. V. Sidgwick and H. M. Powell, *Proc. Roy. Soc. (London)*, 1940, A176, 153
(b) R. J. Gillespie and R. S. Nyholm, *Quart. Rev. (London)*, 1957, 11, 339
(c) R. J. Gillespie, *J. Chem. Educ.*, 1963, 40, 295
(d) R. J. Gillespie, *J. Am. Chem. Soc.*, 1963, 85, 467
(e) R. J. Gillespie, *Inorg. Chem.*, 1966, 5, 1634
(f) R. J. Gillespie, *J. Chem. Educ.*, 1970, 47, 18
(g) R. J. Gillespie, *J. Chem. Educ.*, 1974, 51, 367
(h) R. J. Gillespie, "Molecular Geometry", Van Nostrand Reinhold Co., London (1972)
- 6.(a) W. J. Adams, H. B. Thompson, Jr., and L. S. Bartell, *J. Chem. Phys.*, 1970, 53, 4040
(b) E. J. Jacob and L. S. Bartell, *J. Chem. Phys.*, 1970, 53, 2235
- 7.(a) J. L. Hoard, *J. Am. Chem. Soc.*, 1939, 61, 1252
(b) G. M. Brown and L. A. Walker, *Acta Crystallogr.*, 1966, 20, 220

- 8.(a) L. S. Bartell, R. M. Gavin, Jr., H. B. Thompson,
and C. L. Chernick, *J. Chem. Phys.*, 1965, 43,
2547
- (b) R. M. Gavin and L. S. Bartell, *J. Chem. Phys.*,
1968, 48, 2466
- (c) R. D. Burbank and G. R. Jones, *J. Am. Chem. Soc.*,
1974, 96, 43
- (d) K. S. Pitzer and L. S. Bernstein, *J. Chem. Phys.*,
1975, 63, 3849
- 9.(a) G. N. Lewis, "Valence and Structure of Atoms and
Molecules", The Chemical Catalog Co. Inc.,
New York, 1923
- (b) G. N. Lewis, *J. Franklin Inst.*, 1938, 226, 293
- 10.(a) J. N. Brønsted, *Recl. Trav. Chim. Pays-Bas*,
1923, 42, 718
- (b) T. M. Lowry, *Chem. Ind. (London)*, 1923, 42, 43
11. M. Usanovich, *Zh. Obshch. Khim.*, 1939, 9, 182
12. J. Bjerrum, *Chem. Rev.*, 1950, 46, 381
13. G. Swarzenbach, *Experientia*, 1956, 5, 162
14. S. Ahrland, J. Chatt, and N. R. Davies,
Chem. Soc., Quart. Rev., 1958, 12, 265
- 15.(a) R. G. Pearson, *J. Am. Chem. Soc.*, 1963, 85, 3533
- (b) R. G. Pearson, *J. Chem. Educ.*, 1965, 45, 581; 643
- 16.(a) R. F. Hudson and G. Klopman, *Tetrahedron Lett.*,
1967, 12, 1103
- (b) R. F. Hudson and G. Klopman, *Theor. Chim. Acta*,
1967, 8, 165
- (c) G. Klopman, "Chemical reactivity and reaction
paths", ed. G. Klopman, John Wiley, 1974, p55-165

17. C. K. Jørgensen, *Inorg. Chem.*, 1964, 3, 1201
18. R. G. Pearson, *Inorg. Chem.*, 1973, 12, 712
19. J. A. Davies and F. R. Hartley, *Chem. Rev.*, 1981, 81, 79
20. (a) R. F. Schramm and B. B. Wayland, *J. Chem. Soc., Chem. Commun.*, 1968, 898
- (b) B. B. Wayland and R. F. Schramm, *Inorg. Chem.*, 1969, 8, 971
21. G. R. Clark and G. J. Palenik, *Inorg. Chem.*, 1970, 9, 2754
22. A good review of the chelate effect is by A. E. Martell in "Advances in Chemistry Series", No. 62, American Chemical Society, Washington, D.C. 1967, p.272
23. (a) D. K. Cabbiness and D. W. Margerum, *J. Am. Chem. Soc.*, 1969, 91, 6540
- (b) F. P. Hinz and D. W. Margerum, *Inorg. Chem.*, 1974, 13, 2941
- (c) F. P. Hinz and D. W. Margerum, *J. Am. Chem. Soc.*, 1974, 96, 4993
24. R. Hulme and J. C. Scrutton, *J. Chem. Soc. (A)*, 1968, 2448
25. M. Webster and S. Keats, *J. Chem. Soc. (A)*, 1971, 836
26. B. Rubin, F. J. Heldrich, W. K. Dean, D. J. Williams, and A. Viebeck, *Inorg. Chem.*, 1981, 20, 4434
27. A. Demalde, A. Mangia, M. Nardelli, G. Pelizzi, and M. E. Vidoni Tani, *Acta Crystallogr., Sect. B*, 1972, 28, 147

28. R. Hulme and J. T. Szymanski, *Acta Crystallogr., Sect. B*, 1969, 25, 753
29. R. Hulme and D. J. E. Mullen, *J. Chem. Soc., Dalton Trans.*, 1976, 802
30. A. C. Skapski, *J. Chem. Soc., Chem. Commun.*, 1966, 1, 10
31. R. Hulme, D. Mullen, and J. C. Scrutton, *Acta Crystallogr., Sect. A*, 1969, 25, S171
32. R. K. Wismer and R. A. Jacobson, *Inorg. Chem.*, 1974, 13, 1678
33. D. J. Williams, C. O. Quicksall, and K. J. Wayne, *Inorg. Chem.*, 1978, 17, 2071
34. P. W. Dehaven and R. A. Jacobson, *Cryst. Struct. Comm.*, 1976, 5, 31
35. W. G. McPherson and E. A. Meyers, *J. Phys. Chem.*, 1968, 72, 3117
36. W. G. McPherson and E. A. Meyers, *J. Phys. Chem.*, 1968, 72, 532
37. B. K. Robertson, W. G. McPherson and E. A. Meyers, *J. Phys. Chem.*, 1967, 71, 3531
38. M. Colapietro, A. Domeniciano, L. Scaramuzza, and A. Vaciago, *J. Chem. Soc., Chem. Commun.*, 1968, 302
39. C. L. Raston and A. H. White, *J. Chem. Soc., Dalton Trans.*, 1976, 791
40. D. B. Sowerby, I. Haiduc, A. Barbul-Rusu, and M. Salajan, *Inorg. Chim. Acta*, 1983, 68, 87
41. M. C. Poore and D. R. Russel, *J. Chem. Soc., Chem. Commun.*, 1971, 18

42. A. Hyman and A. Perloff, *Acta Crystallogr., Sect. B*, 1972, 28, 2007
43. G. Chapuis, Ch. Gnehm and V. Krämer, *Acta Crystallogr., Sect. B*, 1972, 28, 3128
44. D. Fenske, N. Mrona, and K. Dehnicke, *Z. Anorg. Allg. Chem.*, 1938, 498, 131
45. M. Webster, *Chem. Rev.*, 1966, 66, 87
46. (a) P. A. W. Dean and R. J. Gillespie, *J. Am. Chem. Soc.*, 1969, 91, 7260
- (b) R. J. Gillespie, K. Ouchi, and G. P. Pez, *Inorg. Chem.*, 1969, 8, 63
- (c) M. Brownstein and R. J. Gillespie, *J. Am. Chem. Soc.*, 1970, 92, 2718
- (d) G. S. H. Chen and J. Passmore, *J. Chem. Soc., Dalton Trans.*, 1979, 1251
- (e) W. A. S. Nandana, J. Passmore, D. C. N. Swindells, P. Taylor, P. S. White and J. E. Verkis, *J. Chem. Soc., Dalton Trans.*, 1983, 619
47. A. J. Edwards and R. J. C. Sills, *J. Chem. Soc., Dalton Trans.*, 1974, 1726
48. J. G. Ballard, T. Birchall, and D. R. Slim, *J. Chem. Soc., Chem. Commun.*, 1976, 653
49. (a) A. J. Edwards and P. Taylor, *J. Chem. Soc., Dalton Trans.*, 1975, 2174
- (b) H. W. Baird and H. F. Giles, *Acta Crystallogr., Section A*, 1969, 25, S115
50. R. Ortwein and A. Schmidt, *Z. Anorg. Allg. Chem.*, 1976, 420, 240
51. S. P. Bone and D. B. Sowerby, *J. Chem. Soc., Dalton Trans.*, 1979, 718

52. M. Hall and D. B. Sowerby, *J. Am. Chem. Soc.*, 1980, 102, 628
53. N. Kanehisa, Y. Kai, and N. Kasai, *Inorg. Nucl. Chem. Lett.*, 1972, 8, 375
54. K. Onuma, Y. Kai, and N. Kasai, *Inorg. Chem. Lett.*, 1972, 8, 143
55. W. Klein, D. Krauss and H. P. Latscha, *Z. Anorg. Allg. Chem.*, 1973, 401, 85
56. B. Kruss and M. L. Zeigler, *Z. Anorg. Allg. Chem.*, 1973, 401, 89
57. R.-A. Laber and A. Schmidt, *Z. Anorg. Allg. Chem.*, 1975, 416, 32
58. R.-A. Laber and A. Schmidt, *Chem. Ber.*, 1975, 108, 1125
59. A. Kobayishi, T. Ito, F. Marumo, and Y. Saito, *Acta Crystallogr., Sect. B*, 1972, 28, 3446
60. I. R. Beattie, *Chem. Soc., Quart. Rev.*, 1963, 17, 382
61. M. Antler and A. W. Laubengayer, *J. Am. Chem. Soc.*, 1955, 77, 5250
62. G. W. A. Fowles and R. A. Hoodless, *J. Chem. Soc.*, 1963, 33
63. H. J. Emeleus and G. S. Rao, *J. Chem. Soc.*, 1958, 4245
64. (a) M. Dräger and R. Engler, *Z. Anorg. Allg. Chem.*, 1975, 413, 229
- (b) M. Dräger and R. Engler, *Chem. Ber.*, 1975, 108, 17
65. (a) M. Dräger, *Chem. Ber.*, 1974, 107, 2601
- (b) M. Dräger, *Z. Anorg. Allg. Chem.*, 1975, 411, 79

65. (c) M. Dräger and R. Engler, *Z. Anorg. Allg. Chem.*, 1974, 405, 183
66. R. F. Bryan, *J. Am. Chem. Soc.*, 1964, 86, 733
67. M. Nardelli, C. Pelizzi and G. Pelizzi, *J. Organomet. Chem.*, 1976, 112, 263
68. I. R. Beattie, M. Milne, W. Webster, H. E. Blayden, P. J. Jones, R. C. G. Kilean, and J. L. Lawrence, *J. Chem. Soc. (A)*, 1969, 482
69. I. R. Beattie, R. Hulme, and L. Rule, *J. Chem. Soc.*, 1965, 1581
70. G. G. Mather, G. M. McLaughlin, and A. Pidcock, *J. Chem. Soc., Dalton Trans.*, 1973, 1823
71. Y. Hermodsson, *Acta Crystallogr.*, 1960, 13, 656
72. C. I. Bränden, *Acta Chem. Scand.*, 1963, 17, 759
73. I. Lindquist, "Inorganic adduct molecules of oxo-compounds" Academic Press, New York, 1963
74. M. Webster and H. E. Blayden, *J. Chem. Soc. (A)*, 1969, 2443
75. D. M. Barnhart, C. N. Caughlan and M. Ul-Haque, *Inorg. Chem.*, 1968, 7, 1135
76. P. G. Hugget, R. J. Lynch, T. C. Waddington, and K. Wade, *J. Chem. Soc., Dalton Trans.*, 1980, 1164
77. P. G. Harrison, B. C. Lane, and J. J. Zuckerman, *Inorg. Chem.*, 1972, 11, 1537
78. N. Ohkaku and K. Nakamoto, *Inorg. Chem.*, 1973, 12, 2446
79. C. I. Bränden and I. Lindqvist, *Acta Chem. Scand.*, 1960, 14, 726

65. (c) M. Dräger and R. Engler, *Z. Anorg. Allg. Chem.*, 1974, 405, 183
66. R. F. Bryan, *J. Am. Chem. Soc.*, 1964, 86, 733
67. M. Nardelli, C. Pelizzi and G. Pelizzi, *J. Organomet. Chem.*, 1976, 112, 263
68. I. R. Beattie, M. Milne, W. Webster, H. E. Blayden, P. J. Jones, R. C. G. Kilean, and J. L. Lawrence, *J. Chem. Soc. (A)*, 1969, 482
69. I. R. Beattie, R. Hulme, and L. Rule, *J. Chem. Soc.*, 1965, 1581
70. G. G. Mather, G. M. McLaughlin, and A. Pidcock, *J. Chem. Soc., Dalton Trans.*, 1973, 1823
71. Y. Hermodsson, *Acta Crystallogr.*, 1960, 13, 656
72. C. I. Bränden, *Acta Chem. Scand.*, 1963, 17, 759
73. I. Lindquist, "Inorganic adduct molecules of oxo-compounds" Academic Press, New York, 1963
74. M. Webster and H. E. Blayden, *J. Chem. Soc. (A)*, 1969, 2443
75. D. M. Barnhart, C. N. Caughlan and M. Ul-Haque, *Inorg. Chem.*, 1968, 7, 1135
76. P. G. Hugget, R. J. Lynch, T. C. Waddington, and K. Wade, *J. Chem. Soc., Dalton Trans.*, 1980, 1164
77. P. G. Harrison, B. C. Lane, and J. J. Zuckerman, *Inorg. Chem.*, 1972, 11, 1537
78. N. Ohkaku and K. Nakamoto, *Inorg. Chem.*, 1973, 12, 2446
79. C. I. Bränden and I. Lindqvist, *Acta Chem. Scand.*, 1960, 14, 726

80. L. Brun, *Acta Crystallogr.*, 1966, 20, 739
81. M. Boyer, Y. Jeannin, C. Rocchccioli-Deltcheff and R. Thovenof, *J. Coord. Chem.*, 1978, 4, 219
82. C. I. Bränden, *Acta Chem. Scand.*, 1962, 16, 1806
83. (a) R. J. H. Clark, D. L. Kepert, R. S. Nyholm and J. Lewis, *Nature*, 1963, 99, 559
- (b) W. P. Crisp, R. L. Deutscher, and D. L. Kepert, *J. Chem. Soc. (A)*, 1970, 2199
84. "International Tables for X-ray Crystallography", Vol. I, Kynoch Press, Birmingham
85. "International Tables for X-ray Crystallography", Vol. IV, Kynoch Press, Birmingham
86. G. M. Sheldrick, University of Cambridge, 1976, M. G. B. Drew's personal communication
87. R. W. Raston and C. M. Loane, (to the standard Oil Co. of Indiana) U.S. Patent 2,484,257 October, 11, 1949
88. R. A. Naylor and E. O. Hook (to the American Cyanamid Co.) U.S. Patent 2,723,969 November, 15, 1955
89. (a) K. Liebermeister, *Z. Naturforsch.*, 1950, 5B, 79
- (b) G. Hagelloch and K. Liebermeister, *Z. Naturforsch.*, 1951, 6B, 147
90. P. Karrer and H. C. Sanz, *Helv. Chim. Acta*, 1944, 27, 219
91. (a) C. S. Miller and B. L. Clark (to the Minnesota Mining and Manufacturing Co.) U.S. Patent 2,663,656, December, 22, 1953
- (b) W. F. Amon, Jr., and M. W. Kane (to the

- Polaroid Corp.) U.S. Patent 2,505,085
April, 25, 1950
92. J. J. Girerd, S. Jeannin, Y. Jeannin, and
O. Kahn, *Inorg. Chem.*, 1978, 17, 3034
93. See for example: (a) G. Peyronel, G. C. Pellacani,
and A. Pignedoli, *Inorg. Chim. Acta*, 1971, 5,
627; (b) G. Peyronel, A. C. Fabretti, and
G. C. Pellacani, *J. Inorg. Nucl. Chem.*, 1973,
35, 973; (c) A. J. Aarts, H. O. Desseyn, and
M. A. Herman, *Inorg. Chim. Acta*, 1978, 29, L197;
(d) G. Peyronel, G. C. Pellacani, A. Pignedoli,
and G. Benetti, *Inorg. Chim. Acta*, 1971, 5, 263;
(e) A. C. Fabretti, G. C. Pellacani, and
G. Peyronel, *J. Inorg. Nucl. Chem.*, 1971, 33,
4247; (f) G. Peyronel, A. C. Fabretti, and
G. C. Pellacani, *Spectrochim. Acta, Part A*,
1974, 30, 1723; (g) S. R. Wade and G. R. Willey,
Inorg. Chim. Acta, 1980, 43, 1973 and references
therein.
94. B. Persson and J. Sandström, *Acta Chem. Scand.*,
1964, 18, 1099
95. G. C. Pellacani, G. Peyronel, and A. C. Fabretti,
Gazz. Chim. Ital., 1972, 102, 11
96. S. O. Wandiga, L. S. Jenkins, and G. R. Willey,
J. Inorg. Nucl. Chem., 1979, 41, 941
97. A. C. Fabretti, G. C. Pellacani, and G. Peyronel,
Gazz. Chim. Ital., 1973, 103, 397
98. H. O. Desseyn, W. A. Jacob, and M. A. Herman,
Spectrochim. Acta, Part A, 1969, 25, 1685

99. C. R. Kanekar and A. J. Casey, *J. Inorg. Nucl. Chem.*, 1969, 31, 3105
100. R. N. Hurd, G. De La Mater, G. C. McElheny, and L. V. Peiffer, *J. Am. Chem. Soc.*, 1960, 82, 4454
101. G. C. Pellacani and G. Peyronel, *Inorg. Chim. Acta*, 1974, 9, 189
102. H. Hofman, s H. O. Desseyn, J. Shamir, and R. Dommissie, *Inorg. Chim. Acta*, 1981, 54, L227
103. G. Kiel and R. Engler, *Chem. Ber.*, 1974, 107, 3444
104. S. C. Jain and R. Rivest, *J. Inorg. Nucl. Chem.*, 1967, 29, 2787
105. G. W. A. Fowles and R. A. Walton, *J. Chem. Soc.*, 1964, 4331
106. R. N. Hurd, G. De La Mater, G. C. McElheny, R. J. Turner, and V. H. Wallingford, *J. Org. Chem.*, 1961, 26, 3980
107. O. Wallach, *Ann.*, 1891, 262, 357
108. H. M. Woodburn and C. E. Scroog, *J. Org. Chem.*, 1952, 17, 371
109. P. J. Wheatley, *J. Chem. Soc.*, 1965, 396
110. D. Rinne and U. Thewalt, *Z. Anorg. Allg. Chem.*, 1978, 443, 185
111. A. Christensen, H. J. Geise, and B. S. Van der Veken, *Bull. Soc. Chim. Belg.*, 1975, 84, 1173
112. N. R. Kunchur and M. R. Truter, *J. Chem. Soc.*, 1958, 2551
113. P. J. Wheatley, *Acta Crystallogr.*, 1953, 6, 369
114. M. R. Truter, *J. Chem. Soc.*, 1960, 997

115. H. O. Desseyn and M. A. Herman, *Spectrochim. Acta, Part A*, 1967, 23, 2457
116. H. Hofmans, H. O. Desseyn, R. Dommissie, and M. A. Herman, *Bull. Soc. Chim. Belg.*, 1982, 91, 175
117. H. Hofmans, H. O. Desseyn, A. J. Aarts, and M. A. Herman, *Bull. Soc. Chim. Belg.*, 1982, 91, 19
118. J. I. Jones, W. Kynaston, and J. L. Hales, *J. Chem. Soc.*, 1957, 617
119. S. R. Wade, Ph.D. Thesis, University of Warwick, 1980
120. E. Hough and D. G. Nicholson, *J. Chem. Soc., Dalton Trans.*, 1981, 2083
121. W. Lindemann, R. Wögerbauer and P. Berger, *Z. Anorg. Allg. Chem.*, 1977, 437, 155
122. M. Schmidt, R. Bender, and Ch. Burschka, *Z. Anorg. Allg. Chem.*, 1979, 454, 160
123. G. C. Pellacani and G. Peyronel, *Inorg. Nucl. Chem. Lett.*, 1972, 8, 299
124. H. Hofmans, H. O. Desseyn, and M. A. Herman, *Spectrochim. Acta, Part A*, 1982, 38, 1213
125. T. Halder, W. Schwarz, J. Weidlein, and P. Fischer, *J. Organomet. Chem.*, 1983, 246, 29
126. M. G. B. Drew, *Progr. Inorg. Chem.*, 1977, 23, 67
127. D. J. Williams, C. O. Quicksall, and K. M. Barkigia, *Inorg. Chem.*, 1982, 21, 2097

128. S. L. Lawton, C. J. Fuhrmeister, R. G. Haas, C. S. Jarman, Jr., and F. G. Lohmeyer, *Inorg. Chem.*, 1974, 13, 135
129. S. L. Lawton and G. T. Kokotailo, *Inorg. Chem.*, 1972, 11, 363
130. L. P. Battaglia, A. B. Corradi, N. Nardeli, and M. E. Vidoni Tani, *J. Chem. Soc., Dalton Trans.*, 1978, 583
131. L. P. Battaglia, A. B. Corradi, G. Pelizzi and M. E. Vidoni Tani, *J. Chem. Soc., Dalton Trans.*, 1977, 1141
132. K. J. Wyne, *J. Chem. Educ.*, 1973, 50, 328
133. S. Calogero, U. Russo, G. Valle, P. W. C. Barnard, and J. D. Donaldson, *Inorg. Chim. Acta*, 1982, 59, 111
134. P. P. Singh and I. M. Pande, *J. Inorg. Nucl. Chem.*, 1972, 34, 591, 1131
135. G. Peyronel, G. C. Pellacani, G. Benetti, and G. Pollaci, *J. Chem. Soc., Dalton Trans.*, 1973, 879
136. G. C. Pellacani, G. Peyronel, and W. Malavasi, *Inorg. Chim. Acta*, 1974, 8, 49
137. G. C. Pellacani, *Can. J. Chem.*, 1974, 52, 3454
138. G. C. Pellacani, and W. D. D. Malavasi, *J. Inorg. Nucl. Chem.*, 1975, 37, 477
139. G. C. Pellacani, G. Peyronel, G. Pollaci and R. Coronati, *J. Inorg. Nucl. Chem.*, 1976, 38, 1619
140. G. C. Pellacani, G. Peyronel, W. Malavasi, and L. Menabue, *J. Inorg. Nucl. Chem.*, 1977, 39, 1855

128. S. L. Lawton, C. J. Fuhrmeister, R. G. Haas, C. S. Jarman, Jr., and F. G. Lohmeyer, *Inorg. Chem.*, 1974, 13, 135
129. S. L. Lawton and G. T. Kokotailo, *Inorg. Chem.*, 1972, 11, 363
130. L. P. Battaglia, A. B. Corradi, N. Nardeli, and M. E. Vidoni Tani, *J. Chem. Soc., Dalton Trans.*, 1978, 583
131. L. P. Battaglia, A. B. Corradi, G. Pelizzi and M. E. Vidoni Tani, *J. Chem. Soc., Dalton Trans.*, 1977, 1141
132. K. J. Wyne, *J. Chem. Educ.*, 1973, 50, 328
133. S. Calogero, U. Russo, G. Valle, P. W. C. Barnard, and J. D. Donaldson, *Inorg. Chim. Acta*, 1982, 59, 111
134. P. P. Singh and I. M. Pande, *J. Inorg. Nucl. Chem.*, 1972, 34, 591, 1131
135. G. Peyronel, G. C. Pellacani, G. Benetti, and G. Pollaci, *J. Chem. Soc., Dalton Trans.*, 1973, 879
136. G. C. Pellacani, G. Peyronel, and W. Malavasi, *Inorg. Chim. Acta*, 1974, 8, 49
137. G. C. Pellacani, *Can. J. Chem.*, 1974, 52, 3454
138. G. C. Pellacani, and W. D. D. Malavasi, *J. Inorg. Nucl. Chem.*, 1975, 37, 477
139. G. C. Pellacani, G. Peyronel, G. Pollaci and R. Coronati, *J. Inorg. Nucl. Chem.*, 1976, 38, 1619
140. G. C. Pellacani, G. Peyronel, W. Malavasi, and L. Menabue, *J. Inorg. Nucl. Chem.*, 1977, 39, 1855

141. W. H. Nelson, *Inorg. Chem.*, 1967, 6, 1509
142. P. G. Harrison, B. C. Lane, and J. J. Zuckerman, *Inorg. Chem.*, 1972, 11, 1537
143. N. Ohkaku and K. Nakamoto, *Inorg. Chem.*, 1973, 12, 2440
144. P. P. Singh, O. P. Agrawaal, and A. K. Gupta, *Inorg. Chim. Acta*, 1976, 18, 19
145. S. C. Jain and R. Rivest, *Inorg. Chem.*, 1967, 6, 467
146. R. A. Slavinskaya, T. N. Sumarokova, M. Nurakhynova, and A. Dolgova, *Z. Obshch. Khim.*, 1980, 50, 406
147. Sh. Sh. Bashkirov, I. Ya. Kuramshin, A. S. Khromov, and A. N. Purdovik, *Koord. Khim.*, 1980, 6, 386
148. E. C. Taylor and J. A. Zoltewicz, *J. Am. Chem. Soc.*, 1960, 82, 2656
149. S. Raucher and P. Klein, *Tetrahedron Lett.*, 1980, 21, 4061
150. K. Jensen and P. H. Nielsen, *Acta Chem. Scand.*, 1966, 20, 597
151. M. Webster and S. Keats, *J. Chem. Soc. (A)*, 1971, 298
152. I. R. Beattie, T. R. Gilson, and G. A. Ozin, *J. Chem. Soc. (A)*, 1968, 2772
153. G. Matsubayashi, Y. Kawasaki, T. Tanaka, and R. Okawara, *J. Inorg. Nucl. Chem.*, 1966, 28, 2937
154. C. L. Wild, M. Spahis, D. R. Blankenship, J. W. Rogers, and R. J. Williams, *Polyhedron*, 1983, 2, 379

155. J. A. Zubieta and J. J. Zuckerman,
Progr. Inorg. Chem., 1978, 24, 251
156. See, e.g.
- (a) P. A. Cusak, P. J. Smith, J. D. Donaldson,
and S. M. Grimes, "A bibliography of X-ray
crystal structures of tin compounds",
International Tin Research Institute, publication
No. 588, 1981
- (b) T. Higashi, S. Syoyama, and K. Osaki,
Acta Crystallogr., Section B, 1979, 35, 144
- (c) K. Nielsen and R. W. Berg, *Acta Chem. Scand.*,
Ser. A, 1980, 34, 153
157. (a) A Sasane, D. Nakamura and M. Kubo,
J. Magn. Reson., 1970, 3, 76
- (b) T. B. Brill, R. C. Gearhart, and W. A. Welsh,
J. Magn. Reson., 1974, 13, 27
- (c) M. Sutton and R. L. Armstrong, *J. Magn. Reson.*,
1982, 47, 68
- (d) K. B. Dillon, J. Halfpenny, and A. Marshall,
J. Chem. Soc., Dalton Trans., 1983, 1091
- (e) P. G. Huggett, R. L. Lynch, T. C. Waddington,
and K. Wade, *J. Chem. Soc., Dalton Trans.*,
1980, 1164
158. (a) R. C. Gearhart, T. B. Brill, W. A. Welsh, and
R. H. Wood, *J. Chem. Soc., Dalton Trans.*, 1973,
359
- (b) T. B. Brill, and W. A. Welsh, *J. Chem. Soc.*,
Dalton Trans., 1973, 357
- (c) M. H. Ben Ghazlen, A. Daoud, and J. W. Bats,
Acta Crystallogr., Sect. B, 1981, 37, 1415

158. (d) O. Knop, T. S. Cameron, M. A. James, and
M. Falk, *Canad. J. Chem.*, 1981, 59, 2550
- (e) O. Knop, T. S. Cameron, M. A. James, and
M. Falk, *Canad. J. Chem.*, 1983, 61, 1620
159. A. Hordvic and H. M. Kjødge, *Acta Chem. Scand.*,
1965, 19, 935
160. A. Hordvic and E. Sletten, *Acta Chem. Scand.*,
1966, 20, 1874
161. A. Hordvic and H. M. Kjødge, *Acta Chem. Scand.*,
1966, 20, 1923
162. A. Hordvic, K. Jynge, and I. Pedersen, *Acta
Chem. Scand.*, 1981, A35, 607
163. M. B. Ferrari, G. G. Fara, and C. Pelizzi,
Inorg. Chim. Acta, 1981, 55, 167
164. L. S. Higashi, M. Lundeen, and K. Seff, *J. Am.
Chem. Soc.*, 1978, 100, 8101
165. I. R. Beattie and G. P. McQuillan, *J. Chem. Soc.*,
1963, 1519
166. I. R. Beattie, G. P. McQuillan, L. Rule, and
M. Webster, *J. Chem. Soc.*, 1963, 1514
167. R. Hulme, *J. Chem. Soc.*, 1963, 1524
168. C. Perrin-Billot, A. Perrin, and J. Pringent,
J. Chem. Soc., Chem. Commun., 1970, 676
169. N. V. U'lko and V. L. Kolenichenko, *Russ. J.
Inorg. Chem. (Engl. Transl.)*, 1980, 25, 1418
170. E. M. Ayerst and J. R. Duke, *Acta Crystallogr.*,
1954, 7, 588
171. D. R. Davies and R. Pasternak, *Acta Crystallogr.*,
1956, 9, 334

172. P. X. Armendarez and K. Nakamoto, *Inorg. Chem.*, 1966, 5, 796
173. (a) J. J. Bour, P. J. M. W. L. Birker, and J. J. Steggerda, *Inorg. Chem.*, 1971, 10, 1202
- (b) H. O. Desseyn, W. Van Riel, L. Van Heverbeke, and A. Goeminne, *Transition Met. Chem.*, 1980, 5, 88
174. W. Van Riel, H. O. Desseyn, W. Van de Mieroop, and A. T. H. Lenstra, *Transition Met. Chem.*, 1980, 5, 330
175. G. Schoeters and H. O. Desseyn, *Transition Met. Chem.*, 1981, 6, 305
176. H. O. Desseyn, B. J. Van der Veken, and M. A. Herman, *Spectrochim. Acta*, 1977, 33A, 633
177. M. G. B. Drew, J. M. Kisenyi, and G. R. Willey, *J. Chem. Soc., Dalton Trans.*, 1982, 1729
178. M. Edstrand, M. Inge, and N. Ingri, *Acta Chem. Scand.*, 1955, 9, 122
179. (a) J. A. McCleverty, *Progr. Inorg. Chem.*, 1968, 10, 49
- (b) A. Davison and R. Holm, *Inorg. Synth.*, 1967, 10, 8
- (c) A. Davison, N. Edelstein, R. Holm, and A. H. Maki, *Inorg. Chem.*, 1964, 3, 814 and references therein
180. M. M. Ahmad and A. E. Underhill, *J. Chem. Soc., Dalton Trans.*, 1983, 165 and references therein
181. O. Lindqvist, L. Sjölin, J. Sieler, G. Steimecke, and E. Hoyer, *Acta Chem. Scand.*, 1979, A33, 445
182. O. Lindqvist, L. Andersen, J. Sieler, G. Steimecke, and E. Hoyer, *Acta Chem. Scand.*, 1982, A36, 855

183. R. K. Brown, R. J. Bergendahl, J. S. Wood,
and J. H. Waters, *Inorg. Chim. Acta*, 1983,
68, 79
184. R. Eisenberg, *Progr. Inorg. Chem.*, 1970, 12, 295
185. O. Lindqvist, L. Sjölin, J. Sieler, G. Steimecke,
and E. Hoyer, *Acta Chem. Scand.*, 1982, A36,
853
186. A. F. Berniaz, G. Hunter, and D. G. Tuck,
J. Chem. Soc. (A), 1971, 3254
187. D. G. Tuck and M. K. Yang, *J. Chem. Soc. (A)*,
1971, 214
188. G. Hunter and B. C. Williams, *J. Chem. Soc. (A)*,
1971, 2554
189. F. W. B. Einstein, G. Hunter, D. G. Tuck, and
M. K. Yang, *J. Chem. Soc., Chem. Commun.*, 1968,
6, 423
190. R. O. Day and R. R. Holmes, *Inorg. Chem.*, 1982, 21,
2379
191. E. S. Bretschneider, C. W. Allen, and J. H. Waters,
J. Chem. Soc. (A), 1971, 500
192. E. Hoyer, W. Dietzsch, H. Hennig, and W. Schroth,
Chem. Ber., 1969, 102, 603
193. G. Hunter, *J. Chem. Soc., Dalton Trans.*, 1972,
1496
194. A. A. Carey and E. A. Schram, *Inorg. Chim. Acta*,
1982, 59, 75; 79; 83
195. R. E. D. Clark, *Analyst*, 1936, 61, 242; 1937, 62,
661
196. R. E. Poller and J. A. Spillman, *J. Chem. Soc. (A)*,
1966, 958; 1024

197. F. H. Fink, J. A. Turner, and D. A. Payne, Jr.,
J. Am. Chem. Soc., 1966, 88, 1571
198. P. Powell, *J. Chem. Soc. (A)*, 1968, 2587
199. E. Gagliardi and A. Durst, *Monatsh.*, 1971, 102,
308; 1972, 103, 292
200. H. W. Roesky, H. Hofman, W. Clegg, M. Noltemeyer,
and G. M. Sheldrick, *Inorg. Chem.*, 1982, 21,
3798
201. (a) A. Cohen, H. King, and W. I. Strangeways,
J. Chem. Soc., 1931, 3043
(b) R. E. D. Clark, *J. Chem. Soc.*, 1932, 1826
(c) E. W. Abel, D. A. Armitage, and R. P. Bush,
J. Chem. Soc., 1965, 7098
202. (a) M. A. Bush, P. F. Lindley, and P. Woodward,
J. Chem. Soc., Chem. Commun., 1966, 149
(b) M. A. Bush, P. F. Lindley, and P. Woodward,
J. Chem. Soc. (A), 1967, 221
203. A. W. Cordes, P. D. Gwinup, and M. C. Malmstrom,
Inorg. Chem., 1972, 11, 836
204. G. Hunter and T. J. R. Weakley, *J. Chem. Soc.,
Dalton Trans.*, 1983, 1067
205. G. A. Kiosse, N. I. Golovaskikov, A. V. Ablov,
and N. V. Belov, *Doklady Akad. Nauk. S.S.S.R.*,
1967, 177, 329
206. B. Kamenar, D. Grdenic, and C. K. Prout,
Acta Crystallogr., Sect. B, 1970, 26, 181
207. A. Zaklin, D. H. Templeton, and T. Ueki,
Inorg. Chem., 1973, 12, 1641
208. M. E. Gress and R. A. Jacobson, *Inorg. Chim. Acta*,
1974, 8, 209

209. K. Yokoho, K. Matsumoto, S. Ooi, and H. Kuroya,
Bull. Chem. Soc. Jpn., 1976, 49, 1864
210. K. Matsumoto, S. Ooi, M. Sakuma, and H. Kuroya,
Bull. Chem. Soc. Jpn., 1976, 49, 2129
211. Y. Nakayama, K. Matsumoto, S. Ooi, and H. Kuroya,
Bull. Chem. Soc. Jpn., 1977, 50, 2304
212. L. Bohaty, R. Frohlich, and K. F. Tebbe,
Acta Crystallogr., Sect. C, 1983, 39, 59
213. J. J. Chisolm, Jr., *J. Pediatrics*, 1968, 73, 1
214. A. J. Carty and N. J. Taylor, *J. Chem. Soc.,
Chem. Commun.*, 1976, 214
215. Y. S. Wong, P. C. Chieh and A. J. Carty,
J. Chem. Soc., Chem. Commun., 1973, 741
216. N. J. Taylor, Y. S. Wong, P. C. Chieh,
and A. J. Carty, *J. Chem. Soc., Dalton Trans.*,
1975, 438
217. M. G. B. Drew and A. Kay, *J. Chem. Soc. (A)*,
1976, 1846, and 1851
218. H. C. Freeman, G. N. Stevens, and I. F. Taylor,
J. Chem. Soc., Chem. Commun., 1974, 366
219. H. C. Freeman, F. Huq, and G. N. Stevens,
J. Chem. Soc., Chem. Commun., 1976, 90
220. P. de Mester and D. J. Hodgson, *J. Am. Chem. Soc.*,
1977, 99, 6884
221. P. J. M. W. L. Birker and H. C. Freeman,
J. Chem. Soc., Chem. Commun., 1976, 312
222. P. J. M. W. L. Birker and H. C. Freeman,
J. Am. Chem. Soc., 1977, 99, 6892
223. L. P. Battaglia, A. B. Corradi, C. G. Palmieri,
M. Nardelli, and M. E. V. Tani, *Acta Crystallogr.*,

- Sect. B*, 1973, 29, 762
224. P. de Mester and D. J. Hodgson, *J. Chem. Soc., Chem. Commun.*, 1976, 8, 280
225. P. de Mester, and D. J. Hodgson, *J. Chem. Soc., Dalton Trans.*, 1976, 618
226. P. de Mester and D. J. Hodgson, *J. Am. Chem. Soc.*, 1977, 99, 101
227. H. M. Helis, P. de Mester, and D. J. Hodgson, *J. Am. Chem. Soc.*, 1977, 99, 3309
228. P. de Mester, D. J. Hodgson, H. C. Freeman, and C. J. Moore, *Inorg. Chem.*, 1977, 16, 1494
229. K. J. Franklin, H. E. Howard-Lock, and C. J. L. Lock, *Inorg. Chem.*, 1982, 21, 1941
230. V. Theodorou, I. Photaki, N. Hadjiliadis, R. W. Gilbert, and R. Bau, *Inorg. Chim. Acta*, 1982, 60, 1
231. P. M. W. L. Birker and G. C. Verschoor, *Inorg. Chem.*, 1982, 21, 990
232. K. C. Molloy, J. J. Zuckerman, G. Domazetis, and B. D. James, *Inorg. Chim. Acta*, 1981, 54, L217
233. A. Saxena, J. P. Tandon, K. C. Molloy, and J. J. Zuckerman, *Inorg. Chim. Acta*, 1982, 63, 71
234. E. Chain, *Ann. Rev. Biochem.*, 1948, 17, 657
235. F. Chemnitz, *Chem. Abs.*, 1930, 24, 2832
236. F. D. Kellogg, and N. A. Matwiyoff, *Inorg. Nucl. Chem. Letters*, 1968, 4, 47